The University of Manitoba

The Separation and Isolation of Metals Using Polyurethane Materials

by

Richard David Oleschuk

A thesis submitted to the Faculty of Graduate Studies in partial fulfillment of the requirements for the degree of

DOCTOR OF PHILOSOPHY

Department of Chemistry

1998

Winnipeg, Manitoba

THE UNIVERSITY OF MANITOBA

FACULTY OF GRADUATE STUDIES

*****

COPYRIGHT PERMISSION PAGE

THE SEPARATION AND ISOLATION OF METALS USING POLYURETHANE MATERIALS

BY

RICHARD DAVID OLESCHUK

A Thesis/Practicum submitted to the Faculty of Graduate Studies of The University of Manitoba in partial fulfillment of the requirements of the degree of

DOCTOR OF PHILOSOPHY

Dedicated to:

Grandma and Grandpa,

Mom, Dad, Chantal and Curt

Acknowledgments

I wish to express my gratitude to my supervisor Dr. Art Chow for his encouragement, guidance and patience during the course of my thesis work. Special thanks are also due to Dr. Gesser for his enlightening consultations and frequently loaned materials and equipment. I would also like to thank my Ph.D. committee Dr. Martin King, Dr. Hélène Perreault and Dr. George Baldwin for their guidance and consultations throughout the course of this work. Also thanks are due to a number of summer students that have helped contribute towards my thesis research including Michael Rybak, Connie Tosberg, Poly Mavroudis and Shaheen Shojania.

I would like to thank my wife Chantal who tolerated my late nights and sometimes erratic behavior during the writing of the thesis, my current and former labmates, Kathy Rzeszutek, Marta Pecuch, Rob Werbowski and the "coffee crowd", Darren Manley, Mark McComb and Kevin Richardson for their many insightful discussions which led to a number of important ideas and concepts.

Many thanks are also due to NSERC (National Research Council of Canada) and to the University of Manitoba for financial assistance in the form of grants and scholarships.

Throughout the course of my thesis work I have been fortunate to have been able to work with a number of excellent people. Regretfully, they are far too numerous to name but are no less appreciated.

Table of Contents

List of Tables

Table of Figures

Abstract

Membranes made of polyurethane have shown the ability to quantitatively extract and transport certain metal complexes from one solution to another. The transport of the metals can be controlled using appropriate solution conditions to form the extractable metal species. Initial studies performed using iron as a probe suggested that the $HFeCl_4$ and $HFeBr_4$ complexes are responsible for the extraction and transport processes.

Analogous to iron, gold forms the $HAuCl_4$ and $HAuBr_4$ complexes that are both quantitatively extracted and transported through the membrane. Several separations of gold from binary metal mixtures and gold ore have been performed with complete and quantitative separation of gold from the other metals.

There are several factors that effect the rate of the separation including: membrane thickness; the temperature of the system; the type of metal complex; and the concentration of the extractable metal complex in solution.

A detailed study was performed on the membrane to elucidate its chemical structure and characterize degradation taking place throughout a separation experiment..

Using a porous fluorocarbon filter impregnated with polytetramethylene glycol (polyTHF), we have found that gold, platinum and palladium can be extracted as the $HAuBr_4$, H_2PtSCN_6, H_2PdSCN_4 complexes respectively from solution and isolated from other metals.This extraction has been shown to be dependant on the solution flow rate, filter pore size, filter porosity and the concentration of the metal complex in solution.

Chapter 1: Introduction

The isolation of selected metals from solution has been a problem in both industry and analysis. For sample preparation and in actual analysis, separation is an important aspect of analytical chemistry, but in most cases the separations are neither quick nor quantitative. When measurement techniques are used to determine a species or compound in a sample, interferences from extraneous substances in that sample can cause significant problems. Thus, the removal of interferences, or the isolation of the analytical species, is of considerable importance. In industry, separations are needed to produce purer materials and cleaner effluents.

There have been many techniques developed to separate and concentrate metal species. These have included traditional methods such as solvent extraction, precipitation, formation of volatile compounds, ion-exchange methods and mechanical methods, in addition to more modern techniques such as membrane separation and solid phase extraction.

1.1 Membrane Separation

Membranes used for separation act as barriers separating two phases, yet are permeable and are often selective toward a particular species present in one of the phases. Several materials have been used as membranes ranging from bi-layers that surround living cells to thin semi-permeable polymeric barriers. A membrane in its broadest sense is a region of discontinuity interposed between two phases. A more applicable definition for chemistry is that it is a thin sheet of natural or synthetic material, that is permeable to substances in

solution. Membranes have been studied since 1861 when membrane dialysis was first investigated by Graham[1] and have continued to be developed, with millions of dollars spent annually on further research and development.

One function of a membrane is to act as a selective barrier that permits the passage or transport of certain components in a mixture while rejecting others. Ideally, analytical membranes would provide a quantitative separation of a permeating species, however in most cases they are limited to a partial enrichment of one of the phases. In separation processes involving large particles, membranes behave similarly to a filter and the membrane composition is less important than the actual pore size. Conversely, processes on the molecular level are due to interactions between the membrane and analyte. Therefore the composition of the membrane assumes a greater role in the separation process. Depending on the affinity of a species for the membrane material, the rate of transport or transmission is expected to be different for each component of the mixture. In the development of a separation, one would look for a membrane that has a higher selectivity for the preferred component allowing it to be transported through while other components are rejected. The selectivity of a membrane separation process can be based on:

i) Size of the species

ii) Charge of the species

iii) Hydrophobicity/ hydrophilicity of the species

iv) Solubility of the species in the membrane

v) Diffusivity within the membrane

Several different types of membranes have been developed for the separation and

isolation of different chemical species. Membranes used for the separation of large particles are classified based on the pore size. Table 1-1 shows different membrane pore sizes and their associated process.

In any membrane system there are three different phases: the feed or starting phase that contains the particular analyte of interest at the beginning of the separation; the membrane phase; and the receiving phase. These are shown below in Figure 1-1. Regardless of the type of membrane or membrane mechanism there are several equations that can be used to determine permeability data of a membrane system. Alluding to Figure 1-2 the following equation can be derived to represent the permeability of a membrane system[2]:

$$J_a = P_a \cdot A \frac{C_{1_a} - C_{2_a}}{l}$$

where:

J_a	-	flux for penetrant "a"
P_a	-	permeability of penetrant "a"
A	-	surface area of membrane
C_1	-	concentration of penetrant "a" starting phase
C_2	-	concentration of penetrant "a" receiving phase
l	-	thickness of membrane

In this model, it is assumed that both sides of the membrane are covered by thin layers of an immobile fluid called the boundary layer. In its most simplified sense, the equation can be

reduced to:

$$J = D \cdot S_a$$

where:

J - flux for penetrant

D - diffusivity constant

S_a - solubility in membrane

The overall mass transport process through a membrane involves five steps.

i) Diffusion through the boundary layer

ii) Sorption into the membrane

iii) Diffusion through the membrane

iv) Desorption out of the membrane

v) Diffusion through the boundary layer

Each step in the membrane separation process presents a resistance to the permeating species although for some systems the resistance due to some of these steps is considered negligible. For example, in a gas phase membrane system the boundary layer effects can be omitted, while in liquid phase membrane systems large boundary resistances may result, reducing the driving forces for diffusion inside the membrane.

Table 1-1. Membrane processes related to membrane pore size[3]

Membrane Process	Pore Size
Conventional filtration	10-100μm
Microfiltration	100Å-10μm
Ultrafiltration	25Å-100Å
Reverse Osmosis	1Å-25Å
Non-Porous	--

Figure 1-1. Schematic diagram of a generic membrane system

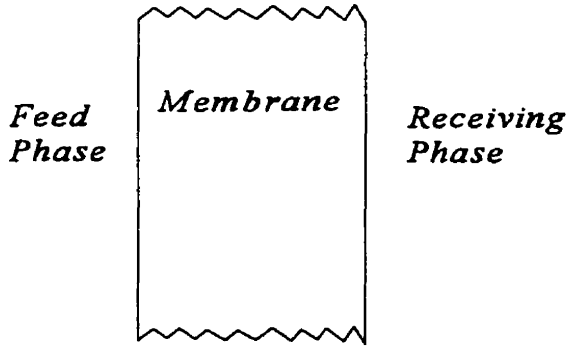

Figure 1-2. Schematic diagram of the membrane process

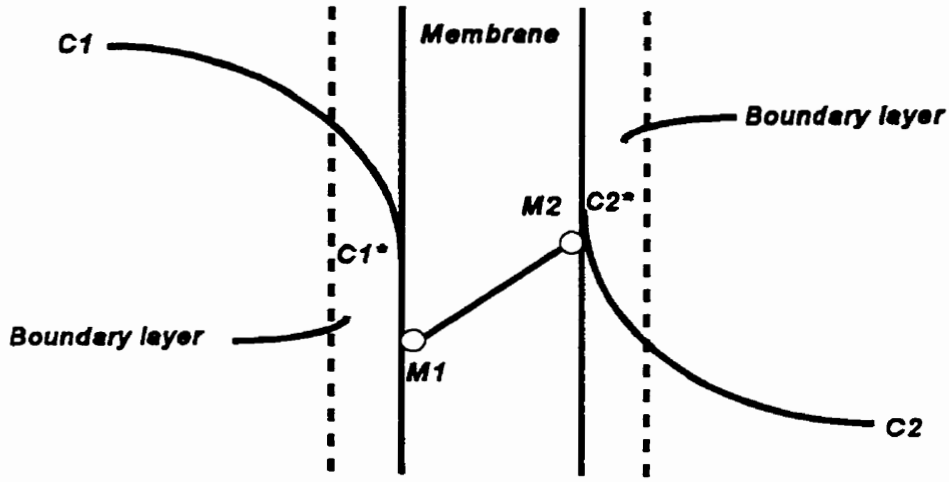

Where: C1, C2 - concentrations in fluid
M1, M2 - concentrations in membrane
C1,C2* - concentrations at membrane/surface boundary layer*

Porous membrane systems can be used for metal removal when the metal is a colloid or is precipitated, while metals in ionic form can be removed using non-porous membrane processes. In the case of non-porous membrane systems, the factors most effecting the separation and transport ability of a membrane are the solubility of a species and the diffusivity of a species in the membrane. These two factors ultimately determine the permeability of a species. The non-porous type membranes are divided into two sub-groups consisting of the liquid membranes and polymeric membranes.

1.1.1 Liquid Membranes

Liquid membranes involve relatively new technologies that have attracted interest from both engineers and scientists because of their inherent advantages over solid membranes. Research on the use of liquid membrane systems for metal removal is currently being undertaken at more than 100 laboratories throughout the world. Liquid membranes have many synonymous names in the literature including: liquid pertraction, carrier-mediated extraction, facilitated transport, two stage extraction etc. The most suitable name that has emerged has been liquid pertraction. The name liquid pertraction was developed out of the nature of the liquid membrane process. Liquid refers to the phase of the membrane itself. The "per" refers to permeation of the component through the membrane material and "traction" refers to the name of the closest established separation process (ie. liquid-liquid extraction).

Liquid membranes have commanded increasing interest due to the significant advantages of having a liquid membrane phase rather than a solid membrane phase. The main advantage of a liquid phase over solid phase is that diffusion within a liquid is

Figure 1-3. Schematic diagram of a liquid membrane system

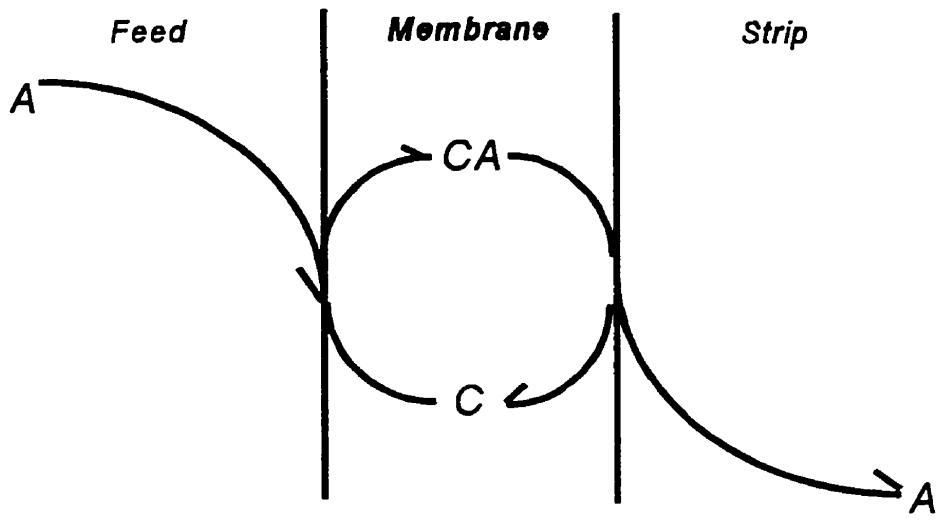

Where: ***A*** ***- metal in solution***
C ***- carrier dissolved within the membrane***
CA ***- carrier/ metal complex***

substantially faster than within a solid, translating into much larger fluxes for liquid membranes. In addition, a mobile carrier[4,5,6] can be placed within the liquid membrane, acting as a selective "shuttle" to transport the metal of interest from the feed phase/membrane interface to the membrane/stripping phase interface. A schematic diagram of the liquid membrane system is shown in Figure 1-3.

The use of pure liquid membranes has the drawback of providing only limited surface area and a limited number of membrane configurations. In addition liquid membrane systems are usually quite thin (25- 250μm) and are thus fragile. This has led to the utilization of a solid supporting "mesh" to make them more robust. A solid-supported liquid membrane (SLM) is composed of microporous support made usually of porous polyethylene with pore sizes ranging from 0.2 - 5μm and thicknesses of 50 - 250μm. An organic "membrane" phase is then inserted into the pores of the membrane material shown in Figure 1-4. One of the expected disadvantages to this type of membrane system is the instability of the membrane. If the feed or stripping phase is too turbulent, loss of membrane material to either of these solutions may result. In addition, the membrane phase and the dissolved carrier cannot be soluble in either the feed phase or strip phase, because this solubility would eventually lead to the failure of the membrane. In addition to SLM systems, emulsion liquid membrane systems[7] (ELM) have also been developed, utilizing a double emulsion to form microscopic "membrane modules" shown in Figure 1-5. ELM systems also suffer from the solubility of the membrane phase in either of the feed or strip phases and require a stable emulsion throughout the separation process.

Figure 1-4. Schematic Diagram of a Supported Liquid Membrane (SLM)

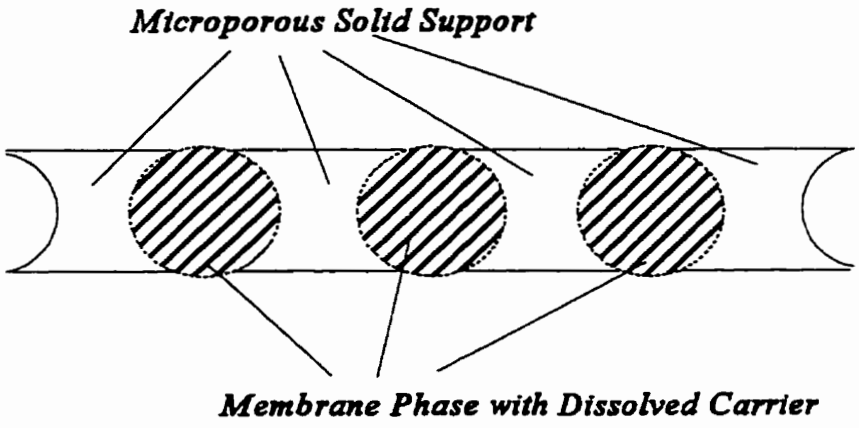

Figure 1-5. Schematic Diagram of a Emulsion Liquid Membrane

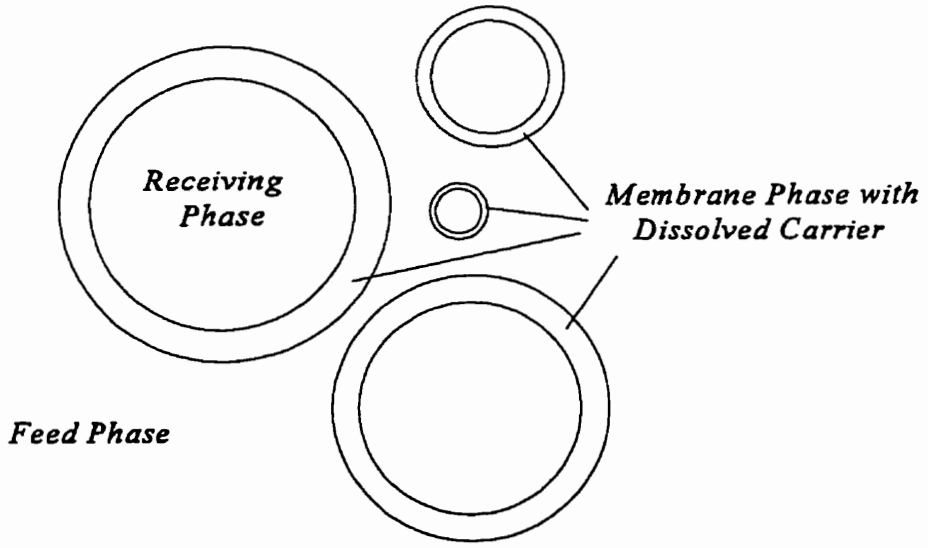

The emulsion must eventually be separated from the feed phase and then broken, in order to separate the membrane phase from the strip phase. The main advantage of an ELM system is the tremendous surface area (10^6 m^2/m^3)[8] that can be generated in a relatively small volume, translating into high fluxes and rapid separation times.

The permeation of metal species through the liquid membrane can be described as a combination of both extraction and elution under non-equilibrium conditions[9]. Both extraction and diffusion coefficients are important in the ELM process. The combination of these two processes was simplified by Danesi[10] to the form:

$$\frac{J}{C} = \frac{K_D}{K_D \Delta_a + \Delta_o}$$

where:

K_D - Distribution coefficient of the permeating species

J - Flux of permeating species

C - Concentration of permeate in feed phase

Δ_a - d_a/D_a thickness of aqueous diffusion layer/diffusion coefficient

Δ_o - membrane thickness/apparent diffusion coefficient of permeating species

The tremendous interest in liquid membrane technology has led to several extensive investigations into the mechanism of transport[11,12,13,14] of the metal species within the liquid

membrane. The mechanistic studies have in turn led to the development of a number of applications of these membrane materials for metal ion removal.

More recently, liquid membrane systems have been developed for the separation and isolation of gold[15,16,17,18], copper[19,20,21], silver[22], uranium[23,24,25], lead[26] and cadmium[27]. In each separation one metal has been preferentially extracted based on the increased affinity of the carrier molecule for the analyte of interest. Until recently only the carriers developed were able to selectively transport a metal cation across the membrane alone. A bi-functional carrier, that possesses both a site to chelate an anion and a site to chelate a cation, has been developed. The carrier has both a crown ether component to selectively bind Cs^+ which is covalently linked to an anion chelating group that displays selectivity between Cl^- and NO_3^- anions[28]. Several reviews have been written outlining the ongoing research in the development of liquid membrane systems.[29,30,31]

In liquid membrane systems, it is the carrier molecule that provides the selectivity rather than the membrane solvent. This directly contrasts with separations involving non-porous polymeric membranes where the bulk membrane phase provides the selectivity.

1.1.2 Polymeric membranes

Although the majority of the polymeric membrane systems have been used for the separation and the enrichment of gases and volatile organic species, applications of polymeric membranes to metal separations have also been investigated. The first realization that a non-porous polymer membrane could be used for the removal of metal species was by Vofsi and co-workers[32,33], who showed that an uranyl-nitrate complex could permeate through a

polyvinylchloride membrane. Gesser et al[34] later showed that by complexing both Fe(III) and Ga(III) with chloride ligands, forming the $FeCl_4^-$ and $GaCl_4^-$ respectively, these metals could be transported through a membrane composed of polyurethane. The transport process for iron and gallium was driven by an acid chloride gradient of >2.0 M HCl on the feed side to 0.1 M HCl on the receiving side.

Similarly, Kamizawa showed that several metal species, when complexed with ligands such as NH_3 and citric acid, were able to permeate through a dense cellulose acetate membrane[35]. The first use of a non-porous polymer material for the separation of a binary metal mixture was by Kobayashi and Sumitomo[36]. They investigated the use of a 0.01mm membrane made of poly(sodium 3-0 vinylbenzyl gluconate-co-acrylonitrile) for the adsorption permeation of a metal ion mixture of Cu/Cd, Ca/Mg, Cu/Zn and Cd/Ca with sorption differentials of 3.9:1, 4.2:1, 4.0:1, 1.5:1 respectively demonstrating that the membrane could be used to enrich and preconcentrate metal species when in the presence of other metals.

Polymeric membranes possess excellent physical properties and stability compared to their liquid membrane analogues. The high molecular weights of the polymer materials makes them virtually insoluble in aqueous systems. The majority of the work using polymeric membranes for metal removal in our laboratory has focussed on polyurethane membrane materials because of their unique ability to extract certain metal complexes from solution. The term "membrane" in polyurethane chemistry has been applied to two separate solid physical forms, those which are non-porous polymer film membranes as used in this investigation, and those which are porous, made of polyurethane foam that allows solutions to percolate through the membrane. The non-porous membranes, although providing a lower

surface area, separate the two solutions and prevent them from mixing.

Polyurethane foams were first shown by Bowen[37] to selectively extract metals from aqueous solution. Since then polyurethane foams have been extensively investigated for the sorption of both metals and organic solvents from solution and several reviews of the subject have been published[38,39,40,41,42,43]. Initially metals such as Hg(II) and Au(III) were shown to be readily extractable from 0.2 M HCl while metals such as Fe(III), Sb(V), Tl(III), Mo(VI) and Re(III) required 6.0 M HCl to produce appreciable distribution coefficients. In addition Bowen[44] showed that gold and silver could be preconcentrated from liquid mineral waste. Later Lo and Chow[45] studied the sorption of Sn(II), Sn(IV), Sb(III)and Sb(V) from acid chloride solutions with both polyether and ester-type polyurethane foams (see discussion on polyurethane chemistry). It was suggested that the foam behaved as an organic solvent and the extractable species were considered to be protonated forms of various tin and antimony chloride complexes. The solvent extraction-like behaviour of the polyurethane foam was also suggested by Gesser et al.[46], for the extraction of iron and gallium from acidic chloride solutions. A mechanistic study of the Fe(III) extraction[47] suggested that the extractable species was either the $FeCl_3$ or $HFeCl_4$ neutral complex and the polyurethane foam was regarded as a "liquid extractant".

In addition to extracting metal species from acid chloride media, many metals have been shown to be extractable from thiocyanate media. Initially, Maloney et al.[48] demonstrated that Co(II), Fe(III), Zn(II), Cd(II) and Hg(II) could be extracted by polyether-type polyurethane foam. In addition, Al-Bazi extensively investigated both the extraction of platinum and palladium from acidic thiocyanate solutions, showing that the $Pd(SCN)_4^{2-}$ and

the $Pt(SCN)_6^{2-}$ complexes could be readily[49,50] extracted with unloaded polyurethane foam. It was also demonstrated that the two metals could be separated[51] based on the relative rates at which the extractable complexes were formed.

The mechanism by which the sorption occurs has been investigated by several authors. The first to be developed was the solvent extraction mechanism, which showed that compounds extracted by ether-type polyurethane foams were analogous to those that are extracted by diethyl ether. From this, it was proposed that polyurethane foams could be used as solid substitute for diethyl ether. Although this mechanism accounted for the extraction of the individual metal complexes, it did not explain why distribution coefficients for diethyl ether and ether-type polyurethane foam differ greatly for a metal under identical conditions.

An ion exchange mechanism was later suggested where the sorption was explained by the interaction of ions and the weak or strong anion exchange sites of the polyurethane foam.

Figure 1-6. Anion exchange sites for ether-type polyurethane.

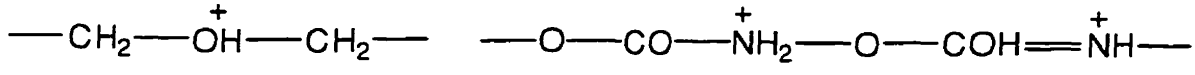

Later, the cation chelation[52] mechanism was suggested for the sorption of anionic metal complexes. The sorption of the complexes was shown to be dependent upon the radius of the cation associated with the anionic complex. The polyalkenoxy chains of the foam

sorbent are arranged in a helical structure. The helical structure forms a clathrate with suitible cations. The order of extraction of anionic complexes with differing cations was found to be ($Li^+<Na^+<Cs^+<K^+$) which is similar to the crown ether dicyclohexyl-18-crown-6. The mechanism and many uses of polyurethane sorption have been reviewed by several authors[53,54,55,56]. The mechanistic studies of the sorption of hydrophobic metal complexes indicate that, due to the complex nature of polyurethane materials several mechanisms may be involved simultaneously[57]

1.1.3 Metal Extraction and Separation Using a Polyurethane Membrane

When performing extractions with "foam-like" sorbents, it is often necessary to perform an additional extraction step to obtain the isolated species from the foam. In addition, once the foam is saturated with a species, it is no longer an efficient sorbent and performance deteriorates. These two problems can be overcome by using polyurethane in the form of a membrane. Since the species is only in the membrane for a short period of time and is then isolated on the other side, it eliminates the additional extraction step required when using the foam. The membrane can also become saturated like the foam, but as the saturated species is transported from the feed phase/ membrane interface the membrane will continue to function as a separatory device until the feed phase has been depleted of the target analyte.

It has previously been shown that cobalt thiocyanate complexes[58], as well as iron and gallium chloride complexes, can be extracted and transported through polyurethane membranes. The extent and rate of transport are dependent on the temperature, the affinity of the complex for the membrane, and the amount of extracting species present in solution.

The amount of extractable species in solution is then dependent on the individual stability constants of the metal complexes, and the relative concentrations of the complexing species present in solution. For gallium(III) and iron(III) the extracting species were shown to be $GaCl_4^-$ and FeX_4^- (where: X = Cl, Br) respectively.

Gold(III) is a softer acid than Ga(III) and Fe(III) in a Pearson[59] sense, so it prefers to form complexes with the larger halides at lower halide concentrations. Gold(III) forms halide complexes with chloride, bromide, and iodide[60]. The iodide complex is less stable than the chloride and bromide, and extremely difficult to prepare in pure form. The gold(III) halide complexes are analogous to those of iron(III) and gallium (III), all of which possess the formula MX_4^-.

Several researchers[61,62,63,64] have investigated the extraction of gold by polyurethane foams from aqueous media. Gold was observed to be extractable using an unloaded polyurethane ether-type foam from extremely acidic aqueous media (>1 M HCl). The extraction was found to be due to the presence of the $AuCl_4^-$ complex formed at high HCl concentrations.

The overall objectives of the research described in this thesis were to obtain an understanding of the extraction, transport, and recovery of the metal species during the polyurethane membrane separation process. The identity of the metal complex responsible for the extraction and separation was determined by studying the effects of different ligand concentrations. In addition different halide complexes were examined to provide evidence as to why some complexes are transported preferentially over others while some are not transported at all. Several factors affecting the rate of transport were investigated including,

temperature of the system, receiving cell composition, concentration of complexing ligand, acidity of starting and receiving cell solutions, and nature of the metal complex.

The chemical structure of the polyurethane membrane we have acquired is presently unknown. We have attempted to characterize the membrane material by using a variety of analytical techniques such as gas chromatography/mass spectrometry, X-ray photo-electron spectroscopy, Fourier transform infra-red spectroscopy and scanning electron microscopy. The characterization of the membrane is important to enable meaningful mechanistic information to be derived from experimentation. We also examined the ability of the polyurethane membrane to separate metals from one another in solution based on the stability constants of various metal halide complexes and the extractability/permeability of those complexes.

1.2 Solid Phase Extraction (SPE)

Solid phase extraction (SPE) is a technique utilizing the selective partitioning of one or more species between either a liquid or gas phase and a solid phase. A sample containing the analyte of interest is passed over a solid extractant and the analyte is extracted. Once an equilibrium has been established the two phases are physically separated. The analytes can then be removed from the sorbent material using an appropriate solvent that elutes the analyte from the sorbent.

Extractants that complex with metal species facilitating the extraction of the metal generally possess O, N, S or P moieties. These atoms each have lone pairs of electrons that can be used to chelate metal species. A virtual myriad of anionic, cationic and neutral

extractants are available for the preconcentration of trace elements.

Effective separation by SPE depends on the proper choice of sorbent material to selectively bind the target analyte, and eluting solvents to quantitatively elute the extracted species. The sorbent material can be tailor-made for a specific analyte[65] or analytes in order to extract only certain components in a mixture, or it can be modified so that only the compounds of interest are not sorbed on the solid phase material. The extraction of metals is performed using either a chelating sorbent or by employing solution conditions to form complexes that are extractable onto the solid sorbent. For example, the crown ethers are noted for their ability to selectively extract only certain metal species based on the molecular size or ionic radii. Only those metal complexes that "fit" within the crown ether are able to be extracted and others are left behind[66,67,68,69].

During SPE an equilibrium is developed between the surface of the sorbent material and the solution. The equilibrium of the system can be represented using a distribution coefficient K_D where:

$$K_D = \frac{concentration\ of\ solute\ sorbent\ phase}{concentration\ of\ solute\ solvent\ phase}$$

The larger the distribution coefficient the greater the affinity the sorbent phase has for a particular analyte.

Analytes can be extracted based on a number of interactions. These include hydrophobic, hydrophillic and ion exchange interactions. Based on the differential ability of a component to participate in these interactions it can be separated from other components. Typical numbers of theoretical plates for SPE processes are between 10-50[70]. Although the

number of theoretical plates for SPE is much lower than for other analytical techniques SPE is an extremely rapid and inexpensive technique. In addition SPE has a relatively low usage of organic solvent making it attractive from both an environmental and cost standpoint.

Initially solid phase extraction devices were prepared by coating a small particles with the designated stationary phase followed by the packing these materials into a column. The analyte-containing sample was passed through the column material where the analyte of interest was extracted from solution or gas. The use of columns is somewhat problematic because of relatively low flow rates, loss of material on the column, and a high cost per column. More recently, there has been a shift away from the use of SPE in the form of a column or as foam to a small circular disk. The disk has the advantage of being small, compact and ultimately disposable after a single use. The disks have been marketed by manufacturers under names like EMPORE™, Sartobind™ and SPEC™.

In this thesis we describe the rapid extraction and isolation of gold from solutions of HBr and HCl (Chapter 5) and platinum(IV) and palladium(II) from acidic thiocyanate solutions (Chapter 6) using a fluorocarbon filter impregnated with α-hydro-ω hydroxypoly(oxy -1,4 -butanediyl), which we will call "polyTHF". The structure is shown in Figure 1-7.

Figure 1-7. Structure of Poly-THF

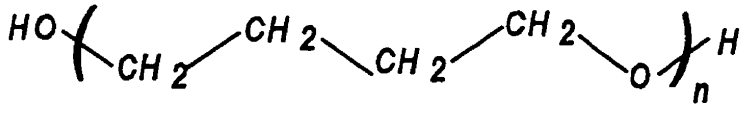

This device is termed an organic-impregnated filter (OIF)[71]. The extraction of the metal complexes is highly dependent on the solution flow rate, ligand concentration and acidity of the solution. We have shown that the OIF can be used to selectively extract gold from binary metal mixtures and more complex matrices such as gold ore. In addition platinum and palladium can be removed from solution either by being extracted simultaneously or sequentially with appropriate solution conditions.

1.3 Chemistry of Polyurethanes

The name "polyurethane" sometimes causes confusion with the organic compound urethane.

Figure 1-8. Urethane

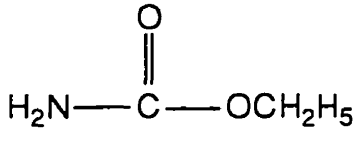

Urethane does not possess the ability to be polymerized, nor does the degradation or depolymerization of polyurethane yield the compound. Instead, the term polyurethane suggests any polymer that contains a large number of urethane groups. A urethane group/linkage is defined as:

Figure 1-9. A urethane linkage

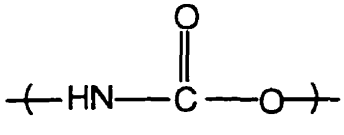

This naming scheme is quite ambiguous because of the several types of polymers classified under the polyurethane name. A polyurethane is normally comprised of and prepared from several classes of compounds. These include, diisocyanates, polyols and chain extenders as well as minor amounts of catalysts and additives. The large variety of these compounds available leads to the diversity in polyurethane chemistry.

1.3.1 Diisocyanates

The isocyanate group forms the basis for polyurethane synthesis and can be represented by three distinct resonance structures.

Figure 1-10. Resonance Structures of Isocyanate Group

The presence of three resonance structures for the isocyanate group leads to a variety of possible reactions that include: insertion, oligomerization, cycloaddition, and the formation of adducts. Insertion and oligomerization are the most important reactions in polyurethane preparation. The principle reaction is insertion between an isocyanate and an alcohol. The two compounds react to yield a carbamate ester linkage more commonly known as a "urethane" linkage.

Figure 1-11. Reaction of an Isocyanate with an Alcohol

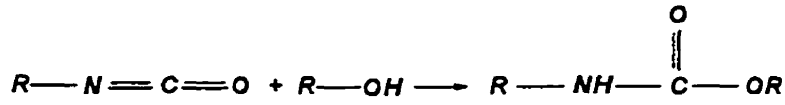

Isocyanates can also participate in reactions involving amines to form what are known as urea linkages. This reaction is commonly used when incorporating chain extenders into the polymer backbone.

In most cases, when preparing a polyurethane elastomer, the presence of water is to be avoided. The addition of water induces the following side reaction:

Figure 1-12. The Reaction of Isocyanate and Water

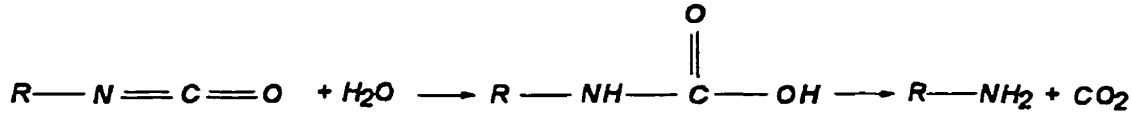

In certain cases, where polyurethane foam is the desired product, water is added to the polyurethane reaction mixture. The carbon dioxide released as a result of the reaction, is trapped in the forming polyurethane elastomer leading to the production of a polyurethane foam.

There are several undesirable side reactions that isocyanates can undergo during polyurethane synthesis. Often steps are taken to impede these reactions by closely controlling temperature and reactant concentrations, and when applicable, eliminating water.

The two most commonly used isocyanates in polyurethane synthesis are toluene diisocyanate, (TDI), and methylene bis(p-phenyl isocyanate), (MDI) shown in Figure 1-13.

Figure 1-13. Commonly Used Isocyanates

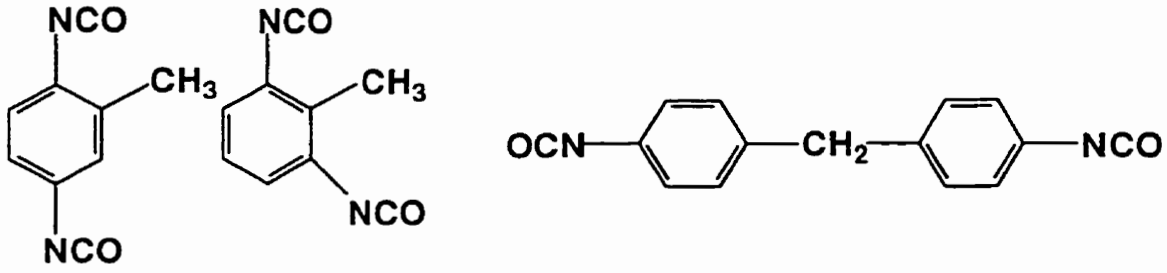

TDI **MDI**

These isocyanates are generally used because they are relatively inexpensive and lead to polymers that exhibit good physical and mechanical properties. In addition, there are a variety of aliphatic-based isocyanates used in polyurethane synthesis. Aliphatic-based isocyanates are important because they exhibit an increased resistance to hydrolysis and are more thermally and photolytically stable than their aromatic analogues but generally possess poorer mechanical and physical properties.

1.3.2 Polyols

Polyols are a class of compounds having two or more hydroxyl functional groups in their structure, as shown in Figure. 1-14.

Figure 1-14. Structure of Polyols

These compounds comprise the "soft" segments of the polyurethane molecules. The R groups have been traditionally polyester and polyether-types (Figure 1-15) but the polyalkyls and poly di-methyl siloxanes types are also used.

Figure 1-15. Polyether and Polyester Polyols

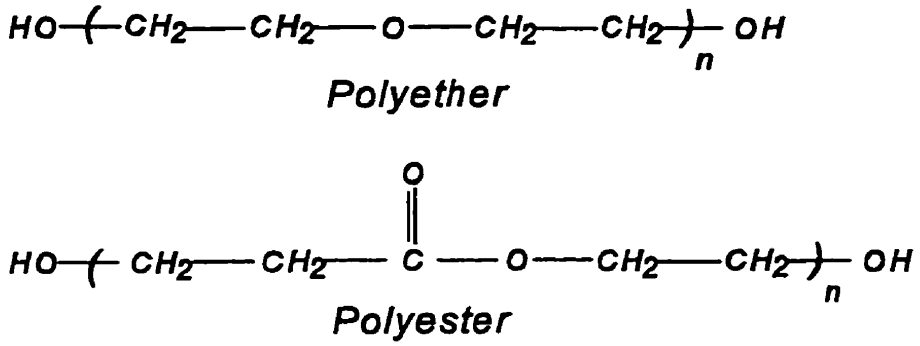

Polyester-based polyurethanes have a low resistance to hydrolysis due to the susceptibility of the ester functionality to acid catalysed hydrolysis[72] but possess the superior mechanical properties of the polyether types. The polyols react with the diisocyanate to form urethane linkages and ultimately a pre-polymer.

1.3.3 Chain Extenders

Polyurethanes having different ratios of hard and soft segments consequently exhibit differing physical and mechanical characteristics. It is therefore important to be able to adjust the hard/soft ratio. These ratios can be controlled using compounds called chain extenders. Chain extenders are low molecular weight polymers usually made of either a combination of diisocyanates and diols or diisocyanates and diamines shown in Figure 1-16.

Figure 1-16. Two Types of Chain Extenders

$$-(I - D)_n- \qquad\qquad -(I - A)_n-$$

I= Isocyanate, D= Diol, A= Diamine

Chain extenders are used to control the physical and mechanical properties of a polymer. In general, chain extenders of aliphatic diols or diamines combined with diisocyanates lead to a polymer that is relatively soft exhibiting good elasticity, while aromatic-based chain extenders generally lead to a polymer that is quite hard exhibiting good tactile strength.

1.3.4 Hard and Soft Segments

The polyurethane elastomer is comprised of two distinct regions within its bulk structure. The two different regions are classified as hard and soft domains. The hard domains are regions where the hard segments are hydrogen-bonded to one another yielding a small degree of crystallinity while the soft domains are amorphous arrangements of the soft segments. The hard segments are comprised of the isocyanate and chain extenders while the soft segments are comprised of the polyether or polyester portions of the polymer. The hard segments are relatively hydrophilic compared to the hydrophobic soft segment. Figure 1-17 shows a schematic diagram of the domains of a typical polyurethane elastomer.

Figure 1-17. Hard and Soft Domains of a Polyurethane

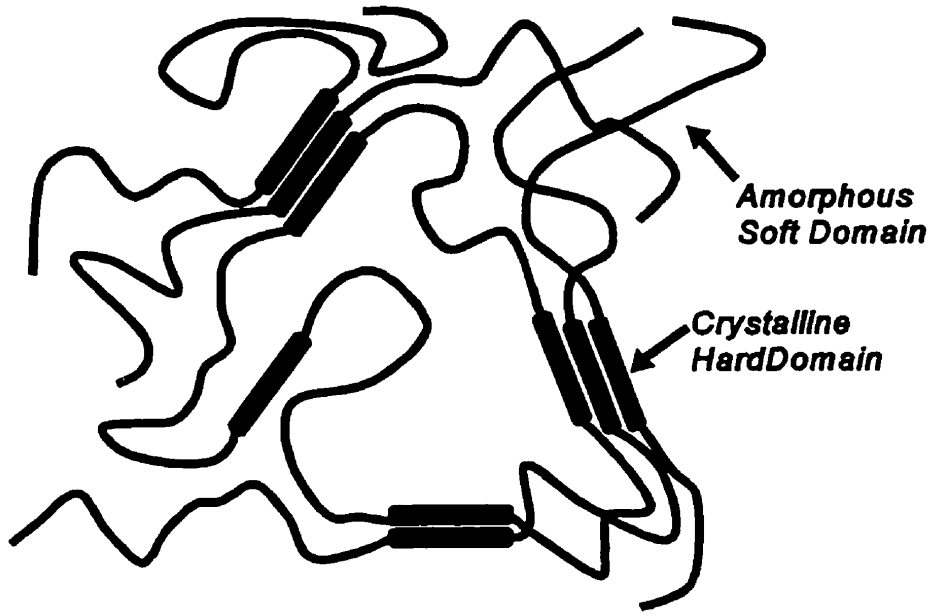

1.3.5 Catalysts and Additives

In the synthesis of polyurethanes, a variety of catalysts are used to increase the rate of polymerization. Catalysts are typically dialkyl compounds of tin and following polymer synthesis these compounds remain within the polymer at low concentrations.

Plasticizers are additives that are often used to extend the range of properties of flexible polymers. The effect of the plasticizer is to swell the amorphous regions of the polymer and lower the cohesive forces (i.e. hydrogen bonds) between the polymer chains. The most commonly used plasticizers[73] are different types of phthalate esters.

Figure 1-18. Summary of Chemical Reactions Used in Polyurethane Synthesis

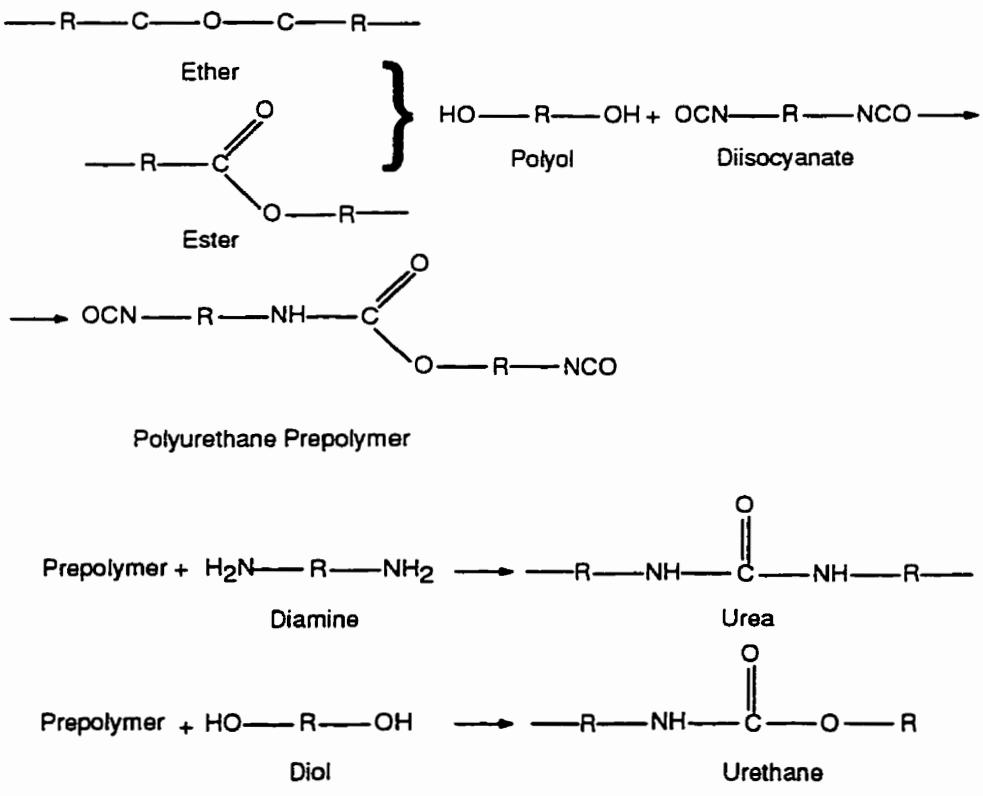

1.4 General Introduction to Aqueous Solution Chemistry of Metal Complexes

Reference to the development of different metal complexes will be made throughout the thesis. In order to understand the different extraction mechanisms that are proposed some knowledge of metal complexes will be described.

Technically speaking, metal ions dissolved simply in water are already complexed because they have formed aqua ions. The process of forming other complexes in aqueous solution is the displacing of one set of ligands with another. In this case that would be the removal of water ligands and their subsequent replacement by ligands of another type.

The extent to which a complex forms is directly related to the thermodynamic stability of a complex, which can be indicated using an equilibrium constant. The equilibrium constant relates the concentration of a complex to the concentration of other species in solution *when the system has reached an equilibrium.* If a solution possesses metal ions, M, and monodentate ligands, L, and only soluble mononuclear complexes are formed, then the equilibrium of the system can be described by the following equations:

$$M + L \rightleftharpoons ML$$

$$ML + L \rightleftharpoons ML_2$$

$$ML_{n-1} + L \rightleftharpoons ML_n$$

where:

$$K_1=\frac{[ML]}{[M]\cdot[L]} \quad \cdots \quad K_2=\frac{[ML_2]}{[ML]\cdot[L]} \quad \cdots \quad K_n=\frac{[ML_n]}{[ML_{n-1}]\cdot[L]}$$

In solution there will be n different equilibria, where n represents the largest coordination number of the metal ion M for the ligand L. The coordination number may vary for different ligands depending on their size and charge.

From the above equations it can be seen that the individual concentrations of each of the complexes in the equilibrium are contingent upon primarily three conditions, the concentration of the metal ion in solution, the concentration of the ligand available in solution, and the individual stability constants of each of the complexes.

Another common way of expressing the equilibrium is using overall formation constants.

$$\beta_1=\frac{[ML]}{[M]\cdot[L]} \quad \cdots \quad \beta_2=\frac{[ML_2]}{[M]\cdot[L]^2} \quad \cdots \quad \beta_n=\frac{[ML_n]}{[M]\cdot[L]^n}$$

Where , M is the concentration of metal that is not complexed with any of the ligands, L is the concentration of free ligand, and β_n are the individual overall formation constants for each of the complexes. The two methods of representing equilibria are of course directly related, according to the relation:

$$\beta_n = K_1 K_2 K_3 \cdots K_n$$

Each of these methods have particular advantages in certain instances, and both are prominently used in the literature. In this paper only the stepwise equilibrium constants will be quoted.

Typically for a complex system, the values of the K_n decrease with increasing values of n. A typical example of this phenomenon is shown in Figure 1-19.

After initially adding the complexing ligand, the first and major complex formed would be ML. After sufficient ligand is added then we would begin to observe a rapid rise in the concentration of the ML_2 complex, where it is the major complex formed, until at high ligand concentrations the ML_4 complex predominates. The reasons for the decreasing values of K_n with increasing n is due primarily to three factors, increased stearic hinderance (if the ligands are bulkier than those they are replacing), coulombic factors (mostly prominent in cases where the ligands are charged) and statistical factors which rely upon the number of sites available for gaining a ligand and those for losing a ligand. It follows that the formation of a complex ML_{max} can be encouraged by the addition of excess ligand.

In the discussion of the complexation of metals it is convenient to relate the ability of a metal to preferentially form complexes with some ligands compared to others using the theory of hard and soft acids and bases (HSAB). This method of classification was originally proposed by Pearson[74].

1.4.1 HSAB

A species in solution can be termed either a Lewis acid or a Lewis base, depending on its ability to either donate electrons (in the case of a base) or accept electrons (in the case

Figure 1-19. Plot of Concentration of Various Iron Chloride Complexes as a Function of Chloride Concentration

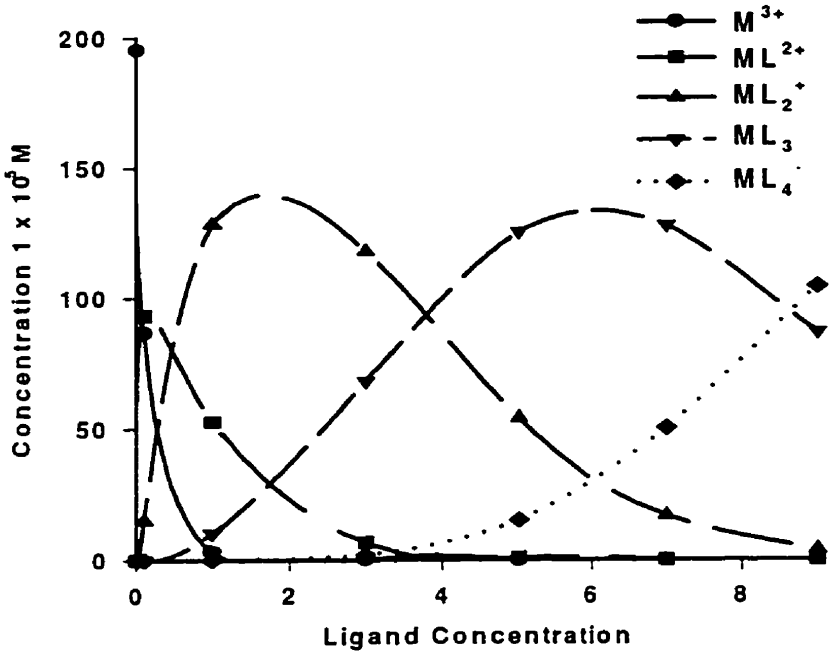

K_1	K_2	K_3	K_4
30	4.5	0.15	0.0068

of an acid). These two groups are further broken down into Lewis acids, class (a) and (b), and Lewis bases, class (a) and (b). If we look at class (a) Lewis acids we find that they are small in size, possess a high positive charge and contain no unshared electron pairs in their valence shell. These properties produce a high electronegativity and a low polarizability. Pearson termed this class of acids as "hard". Class (b) Lewis acids are generally large in size, possess a low positive charge and unshared pairs of electrons (p or d electrons) in the valence shell. Consequently these factors lead to the high polarizability and low electronegativity. This class of acids was termed "soft". The same terminology is also applied to bases. Donor atoms that are of high electronegativity and low polarizability, and are difficult to oxidize are termed as "hard", while those that possess low electronegativity, are highly polarizable and easy to oxidize are termed "soft".

Table 1-2. Example of the Classification of Several Common Lewis Acids and Bases According to Pearson.

Classification of Lewis Bases

Hard	Soft
H_2O, OH^-, F^-, Cl^-	Br^-, SCN^-, H^-, RS^-, CN^-

Classification of Lewis Acids

Hard	Soft
H^+, K^+, Al^{3+}, UO_2^+, Sn^{4+}	Au^+, Ag^+, Pd^{2+}, Pt^{2+}, Pt^{4+}

Through empirical evidence, Pearson showed that soft acids prefer to complex with soft bases and hard acids prefer to react and complex with hard bases.

1.5 The Aqueous Chemistry of Iron, Gold, Platinum and Palladium Halides

1.5.1 Oxidation states and complexes of Iron(III)

Iron(III) is noted for its ability to hydrolyse and form complexes in aqueous solution. A number of these complexes have been well characterized and the stability constants meticulously determined.

Iron(III) can complex with any of the halides including (F, Cl, Br and I). There is abundant literature based on the fluoride and chloride analogues with step-wise stability constants for each of these complexes determined[75]. Information on the bromide and iodide complexes is much less abundant. Each of the complexes when coordinated with the maximum number of ligands are of the form FeX_4^- and the halides each possess a tetrahedral geometry around the iron atom.

Iron(III) is a relatively hard ion by Pearson classification so it favours complexation with the hard F^- ion. With increasing size of the halide ion the stability constants of the iron complexes decrease. In fact the stability constants for the F^- ion are ~ 10^4 greater than those for Cl^-. Even at high Cl^- concentrations the iron is present as a mixture of chloride and/or aqua complexes of the form $Fe(H_2O)_mCl_n^{x-}$.

1.5.2 Oxidation States and Complexes of Gold

Gold can form complexes in a variety of oxidation states[76]. The possible oxidation states include (I), (II), (III) and (V), with (I) and (III) being the most common. The Au^+ ion possesses a closed shell electron configuration, [Xe] $4f^{14}$ $5d^{10}$, thus gold(I) complexes are diamagnetic, and most often develop regular structures. The most common stereochemistry for this oxidation state is linear with a coordination number of 2, with higher numbers being known.

When Au^+ is complexed with halides, complex ions with the formula $(AuX_2)^-$ are formed and the stability of the (AuX_2^-)complex increases with the heavier halides. The fluoride complex is unknown while the iodide complex can be readily prepared as follows.

$$Au^+ + I^- = (AuI_2^-)$$

The gold ion (Au^+) is a soft acid because of the ion's large size and small positive charge. This metal would then prefer to complex with a ligand with a similar "softness". Thus the gold forms a more stable complex with the I^- ion compared to the F^- ion. The existence of $(AuCl_2)^-$ and $(AuBr_2)^-$ has been debated in the literature, but recently Pan and Wood[77,78] showed that $(AuCl_2)^-$ and $(AuBr_2^-)$ can be formed when a solution containing either $(AuCl_4)^-$ or $(AuBr_4)^-$ are heated above 50 °C.

In the oxidation state of (III) the gold is a harder acid than in (I) so it will form stable complexes with harder bases than Au(I) does. The complex halides of gold(III) are perhaps

the most important of all commonly used gold complexes. The halide complexes are all of the formula $(AuX_4)^-$ and all possess a square planar structure. Gold does not dissolve in any one particular mineral acid but readily dissolves in aqua-regia. This leads to the formation of either tetrabromoauric(III) acid $HAuBr_4$ or tetrachloroauric(III) acid $HAuCl_4$ depending whether HBr or HCl is used in conjunction with HNO_3 (nitric acid). Both of these complex acids can be isolated in hydrated forms, and are extremely soluble in organic solvents such as diethyl ether and ethyl acetate. This forms the basis of several processes for the quantitative separation of gold.

The bromide and chloride complexes of Au(III) all possess a square planar geometry. Weak interactions with neighbouring halide atoms also occur to give the complex an overall tetragonal stereochemistry about the metal.

In aqueous solution both the $(AuCl_4)^-$ and $(AuBr_4)^-$ complex ions are hydrolysed to some extent, but much less so than the complex $(AuF_4)^-$ which is hydrolysed completely upon contacting water.

$$(AuX_4)^- + H_2O \rightleftharpoons (AuX_3(OH_2)) + X^-$$

The equilibrium constants for the hydrolysis reactions are $K = 4.6 \times 10^{-5}$ when X = Cl and $K = 3.4 \times 10^{-6}$ when X = Br in 0.4 M perchloric acid solution. This shows that the chloride complex is more prone to hydrolysis than the bromide complex. The AuX_3 complex can then act as a weak acid in dilute aqueous media in the following way.

$$AuX_3(OH_2) \rightleftharpoons (AuCl_3(OH))^- + H^+$$

The halide complexes of gold are not as numerous as those for platinum and palladium. This is due primarily to the high ionization potentials of gold. The halide complexes that gold does form, play an integral part in the chemistry of gold.

1.5.3 Oxidation states and complexes of platinum and palladium

The elements platinum and palladium possess similar aqueous solution chemistry so they will be dealt with in the same section. Platinum and palladium can both be present in number of oxidation states. Platinum forms (I, II, IV, V) where as palladium forms (I, II, IV). Of the possible oxidation states formed, the II state is by far the most common for both of the metals, although several complexes are known where the metals are in the zero and (IV) states. The zero and (IV) states are much more common for platinum than palladium. The larger reluctance of palladium to form the (IV) complex compared with platinum can be attributed to the higher ionisation energy needed to produce Pd^{+4} than the Pt^{+4} ions.

Palladium forms halide complexes with only fluoride, bromide and iodide while platinum forms complexes with all the halides[79,80,81,82]. The fluoride complexes of both palladium and platinum are rapidly hydrolysed upon contacting water. The chloro and bromo complexes of palladium are both stable to hydrolysis and are most commonly used to prepare further platinum and palladium complexes in solution.

References for Chapter 1

1.T. Graham; *Phil. Trans. Inst. Chem. Engr (London)*, 144 (1854) 177.

2. S. Hwang, K. Kammermeyer; Membranes in Separations, Techniques of Chemistry Volume VII, John Wiley & Sons, 1975.

3. R. Noble, S. Stern; Membrane Separations Technology, Principles and Applications, Elsevier, 1995.

4. R. Bloch; Membrane Science and Technology, Plenum Press, New York, 1970.

5. E. L. Cussler; *AIChE. J.*, 17 (1971) 1300.

6. K. Smith, J. Meldon, C. Colton; *AIChE J.*, 19 (1973) 102.

7. R. Izatt, R. Bruening, J. Christensen; Liquid Membranes Theory and Applications, Chapter 7, American Chemical Society, 1987.

8. W. Ho, K. Sirkar; Membrane Handbook, Van Nostrand Reinhold, 1992.

9. R. Chiarizia, E.Horwitz; *Solvent Extr. Ion Exch.*, 8, (1990) 65.

10. P. Danesi; *Sep. Sci. Technol.*, 19, (1985) 857.

11. N. Platé, T. Lebedeva, G. Shandryuk, L. Kardivarenko, V. Bagreev; *J. Memb. Sci.*, 104 (1995) 197.

12. J. Schultz, J. Goddard, S. Suchdeo: *AlChE*, 20 (1974) 417.

13. W. Ho, N. Li; Membrane Handbook, Chapter 37, Van Nostrand Reinhold, 1992.

14. P. Stroeve, P. Varanasi; *Sep. And Purifi. Methods*, 11 (1982) 29.

15. E. Lachowicz, *Analytical Sciences*; 11 (1995) 277.

16. G. Zuo, S. Orecchio, M. Muhammed; *Sep. Sci. Tech.*, 31(1996) 1597.

17. M. Taylor, D. Barnes, G. Marshall; *Anal. Chim. Acta*, 265 (1992) 71.

18. V. Salvado, A. Masana, M. Hidalgo, M. Valiente, M. Muhammed; *Analytical Letters*, 22(1989) 2613.

19. R. Baker, M. Tuttle, D. Kelly, H. Lonsdale; *J. Membr. Sci.*, 2 (1977) 213.

20. N. Parthasarathy, J. Buffle; *Anal. Chim. Acta*, 254 (1991) 1.

21. J. Cox, A. Bhatnagar, R Francis Jr.; *Talanta*, 33 (1986) 713.

22. E. Lachowicz; *Talanta*, 39 (1992) 1031.

23. R. Chiarizia, E. Horwitz; *Solvent Extr. Ion Exch.*, 8 (1990) 65.

24. W. Babcock, R. Baker, E. Lachapelle, K. Smith; *J. Membr. Sci.*, 7 (1980) 71.

25. R. Chiarizia; *J. Membr. Sci.*, 55 (1991) 39.

26. J. van Zantan, D. Chang, I Stanish, H. Monbouquette; *J. Membr. Sci.*, 99 (1995) 49.

27. P. Danesi; *J. Membr. Sci.*, 14 (1983) 161.

28. D. Rudkevich et al.; *J. A. Chem. Soc.*, 117 (1995) 6124.

29. R. Borwankar, D. Wasan, N. Li; Metals Speciation, Separation and Recovery, Lewis Publisher Inc., 1987.

30. R. Chiarizia; Metals Speciation, Separation and Recovery, Lewis Publisher Inc., 1987.

31. L. Boyadzhiev, Z. Lazarova; Membrane Separations Technology, Principles and Applications, Chapter 7,Liquid Membranes(Liquid Pertraction), Elsevier, 1995.

32. R. Bloch, O. Kedem, D. Vosfi; *Nature*, 199 (1963) 802.

33. R.Block, A. Finkelstein, O. Kedem, D. Vosfi; *Ind. Eng. Chem. Process Des. Develop.*, 6 (1967) 231.

34. H. Gesser, G. Horsfall, K. Gough, B. Krawchuk; *Nature*, 268 (1977) 324.

35. C. Kamizawa; *J. Appl. Polym. Sci.*, 22 (1978) 2867.

36. K Kobayashi, H. Sumitomo; *Polymer Bulletin*, 1 (1978) 121.

37. H. Bowen; *J. Chem. Soc. A*, 1082 (1970).

38. Z. B. Alfassi and C. M. Wai; Preconcentration Techniques for Trace Elements, CRC Press, Boca Raton, FL, 1985.

39. T. Braun, J. D. Navratil and A. B. Farag; Polyurethane Foam Sorbents in Separation Science, CRC Press, Boca Raton, FL, 1985.

40. G. J. Moody and J. D. R. Thomas; Chromatographic Separation and Extraction with Foamed Plastics and Rubbers, Marcel Dekker, New York, 1982.

41. T. Braun and A. B. Farag; *Analytica Chimica Acta*, 99 (1978) 1.

42. T. Braun; *Fresenius' Z. Anal. Chem.*, 333 (1989) 1985.

43. Z. Alfassi, C. Wai; Preconcentration Techniques for Trace Elements, CRC Press 1992.

44. H. Bowen; *Radiochem. Radioanal. Lett.*, 7 (1971) 71.

45. V. Lo, A. Chow; *Anal. Chim. Acta*, 106 (1979) 161.

46. H. Gesser, E. Bock, G. Baldwin, A. Chow, D. McBride, D. Lipinski; *Sep. Sci.*, 11 (1976) 317.

47. J. Oren, K. Gough, H. Gesser; *Can. J. Chem.*, 57 (1979) 2032.

48. M. Maloney, G. Moody, J. Thomas; *Proc. Anal. Div. Chem. Soc.*, 14 (1977) 244.

49. Al-Bazi, S. J., Chow, A.; *Talanta*, 29 (1982) 507.

50. Al-Bazi, S. J., Chow, A.; *Talanta*, 30 (1983) 487.

51. Al-Bazi, S. J., Chow, A.; *Anal. Chem.*, 55 (1983) 1094.

52. R. F. Hamon, A. S. Khan and A. Chow; *Talanta*, 29 (1982) 313.

53. Zeev B. Alfassi, Chien M. Wai: Preconcentration Techniques for Trace Elements, CRC Press, 364, 1992.

54. T. Braun, J. D. Navratil and A. B. Farag; Polyurethane Foam Sorbents in Separation Science, CRC Press, Boca Raton, FL, 1985.

55. T. Braun; *Fresenius' Z. Anal Chem*, 333 (1989) 785.

56. G. Moody, J. Thomas;Chromatographic Separation and Extraction with Foamed Plastics and Rubbers, Marcel Dekker, 1982.

57. T. Braun; *Fresenius A. Anal. Chem.*, 333 (1989) 785.

58. R. F. Hamon, PhD. Thesis (University of Manitoba), (1981) 423.

59. R. G. Pearson; *J. Chem. Ed.*, 45 (1968) 581.

60. R. J. Puddephatt; The Chemistry of Gold, Elsevier, New York, 1978.

61. A. S. Khan and A. Chow; *Talanta*, 33 (1986) 182.

62. T. Braun and A. B. Farag; *Anal. Chim. Acta*, 153 (1983) 319.

63. S. Sukiman; *Radiochem. Radioanal. letters*, 18 (1974) 129.

64. P. Schiller, G. B. Cook; *Anal. Chim. Acta*, 54 (1971) 364.

65. R. Izatt, J. Bradshaw, R. Bruening, M. Brueing; *American Laboratory*, December, (1994) 28C.

66. S.Tsurubou; *Anal. Chem.*, 67 (1995) 1465.

67. S. Fang, L. Fu; *Indian J. Chem.*, 33A (1994) 885.

68. Y. Hongwu, Z. Zhixian, Z. Mingrui, Z. Xianxin, R. Boyang; *Polyhedron*, 10 (1991) 1025.

69. R. Izatt, G. Clark, J. Bradshaw, J. Lamb, J. Christensen; *Sep. Purif. Methods*, 15 (1986) 21.

70. P. McDonald, E. Bouvier; Solid Phase Extraction, Applications Guide and Bibliography, 6th ed., Waters, Milford, Massachusetts, 1995.

71. R. Oleschuk, A. Chow; *Talanta*, 44 (1997) 1371.

72. F. Carey, R. Sundberg, Advanced Prganic Chemistry, Part A: Structure and Mechanism, Plenum Press, 1990.

73. H. R. Alcock, F. W. Lampe; Contemporary Polymer Chemistry 2nd Edition, Prentice Hall, 1990.

74. R. Pearson; *J. Chem. Educ.*, 45 (1968) 581.

75. F. Cotton, G. Wilkenson;Advanced Inorganic Chemistry 5th Edition, John Wiley & Sons, 1988.

76. R. Puddephatt; The Chemistry of Gold (Monograph 16), Elsevier, 1978.

77. P. Pan, S. Wood; *Geochim. Cosmochim. Acta*, 55 (1991) 2365.

78. P. Pan, S. Wood; *J. Solution Chem.*, 22 (1993) 163.

79.U. Rao; Platinum Group Metals and Compounds (Advances in chemistry series 98), American Chemical Society, 1971.

80. Gmelin Handbook of Inorganic Chemistry, Platinum, Supplement Vol. A1, Technology, 1986.

81. W. Griffith; The Chemistry of the Rarer Platinum Metals , Interscience Publishers, 1967.

82. F.R. Hartley; The Modern Chemistry of Platinum and Palladium, John Wiley & Sons, 1973.

Chapter 2: Experimental

2.1 Apparatus and Reagents

2.1.1 Commercial Instrumentation

Most metal analyses were performed on a Varian SpectrAA-20 atomic absorption spectrometer, equipped with an air-acetylene flame and Varian Mark VI burner head. Each metal was analysed with an element specific hollow cathode lamp listed in Table 2-1.

A Varian Liberty 200 ICP emission spectrometer located in the Department of Geology, University of Manitoba, was used for the multi-element determinations made when performing the separation of gold from gold ore. Inter-element correction was used when overlapping emission lines from other metals were present in the sample.

Scanning electron microscopy (SEM) and image analysis were performed on a Cambridge Instruments Stereoscan 120 scanning electron microscope and an IBAS Kontron Electronik Image Analyser with accompanying software. Both instruments were located in the Department of Geology, University of Manitoba. Sample coating for SEM analysis was accomplished using an Edwards Sputter Coater #5150B.

High performance liquid chromatography (HPLC)/gel permeation chromatography (GPC) was done using a Spectra Physics SP8700 HPLC system accompanied by a Spectra Physics SP8450 Ultraviolet/ visible detector, Hewlett Packard HP3396A integrator and a Waters™ linear Ultrastyragel Column (7.8 x 300 mm, part # 10681).

X-ray photo electron spectroscopy (XPS)/Electron Scanning for Chemical

Table 2-1. Hollow cathode lamps used for atomic absorption analysis

Element	Wavelength	Band Pass	Lamp Manufacturer
Au	242.8 nm	1.0 nm	Instrumentation Laboratory
Fe	248.3 nm	0.2 nm	Cathodeon
Ni	232.0 nm	0.2 nm	Instrumentation Laboratory
Pd	244.8 nm	0.2 nm	Atomic Spectral Lamps
Pt	266.0 nm	0.2 nm	Atomic Spectral Lamps
Zn	213.9 nm	1.0 nm	Instrumentation Laboratory

Analysis (ESCA) was performed on a Perkin-Elmer PHI model 5600 (Physical Electronic Division) located at the Institut des Biomatériaux, Quebec City, using a monochromatic Al K_{α} X-ray source. The X-ray gun was operated at 14kV and 18 mA with the sample chamber pressure below 10^{-8} Torr.

Differential Scanning Calorimetry (DSC) thermograms were collected over a range of -100 °C to 250 °C using a Perkin-Elmer Model 7 DSC also located at the Institut des Biomatériaux.

Gas Chromatographic/Mass Spectrometric (GC/MS) Analysis was performed on a Varian 3400 gas chromatograph coupled to a Finnigan Mat 800 MS Ion Trap detector accompanied by ITDS software.

Weighing was done with either a Mettler PC440 Delta range balance or on a Mettler AE163 balance when more accurate measurements were required.

The pH measurements were made with an Orion Expandable ion Analyzer EA 940 coupled with a Baxter Canlab dual reference/ working electrode. All water used for experimentation was purified by a Barnsted Nanopure™ II system using reverse osmosis-treated feedstock with a resistance of 18.1- 18.3 megohm-cm.

Fourier Transform Infra-Red (FT-IR) was accomplished on a Bomem MB-series instrument, used with, and without an attenuated total reflectance (ATR) attachment (Spectra tech Horiz ATR part # 0012-482T).

Ultraviolet/ visible spectroscopy was performed using an 8452A Hewlett Packard Diode Array Spectrophotometer and accompanying software.

For OIF experiments an HPLC filtration apparatus was used shown in Figure 2-1.

Figure 2-1. Apparatus Used for OIF extraction/filtration experiments

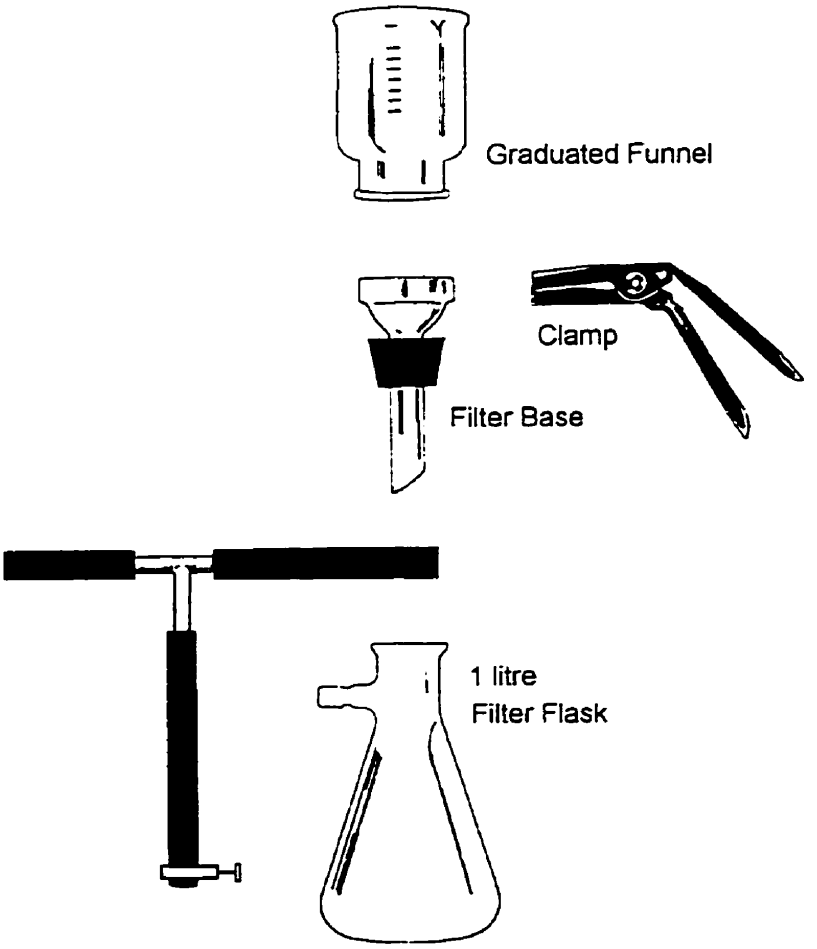

2.1.2 Fabricated/ Custom Apparatus

I) Modified Donnan Dialysis Cell

The apparatus used for most membrane testing consisted of two separate cells (a starting and receiving cell). The starting cell was a Nalgene 125 mL PETG (polyethylene terephthalate copolyester) media bottle (cat# 2015-0125) with a 2.6 cm diameter hole drilled in the screw cap. A small notch was also cut at the side of the drilled hole to prevent air bubbles from being trapped along the membrane surface. The receiving cell consisted of a 100 mL beaker cut to an appropriate height to allow a smaller volume of receiving solution (≈30 mL) to be used. Media bottles are very well suited for the starting cells because they enable a quick easy way of fastening the membrane to the bottle with an air and water- tight seal. For units to be run at elevated temperatures, a small hole was drilled in the edge of this starting cell to prevent any pressure build-up. Membranes were cut in 5 cm x 5 cm squares and placed on top of the open media bottle holding a sample. The cap was placed on the bottle and carefully tightened, yielding a membrane with an active surface area of 5.3 cm^2. The media bottle was then inverted and immersed into the solution held by the receiving cell (shown in Figure 2-2a) and the air bubbles removed through the notch with the membrane separating the two solutions.

Figure 2-2a. Modified Donnan Dialysis Cell

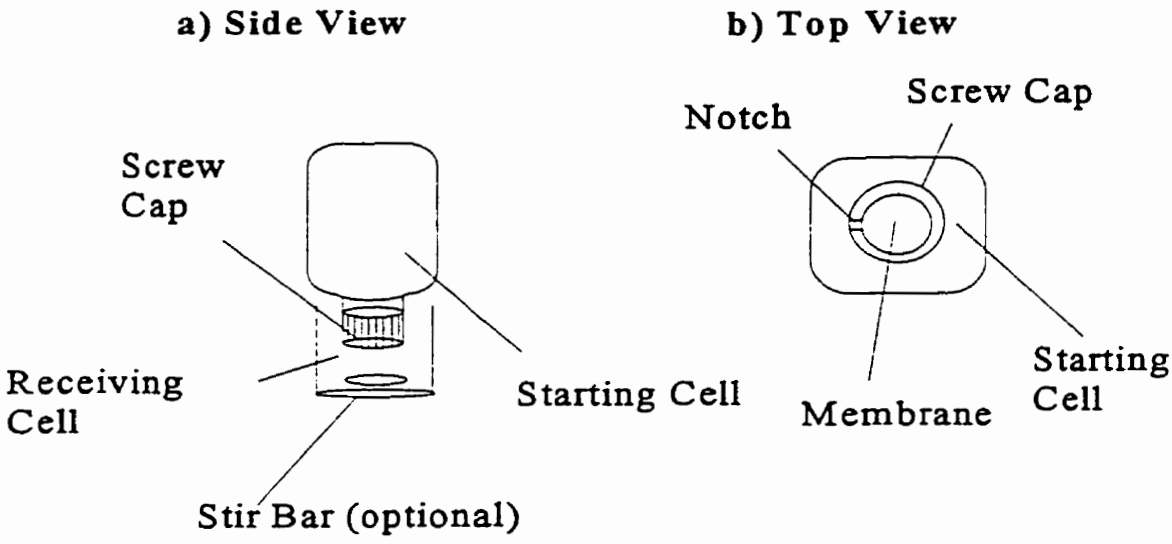

Figure 2-2b. Membrane cells (650 mL starting cell , 650 mL receiving cell) used for preconcentration, pH and membrane degradation studies

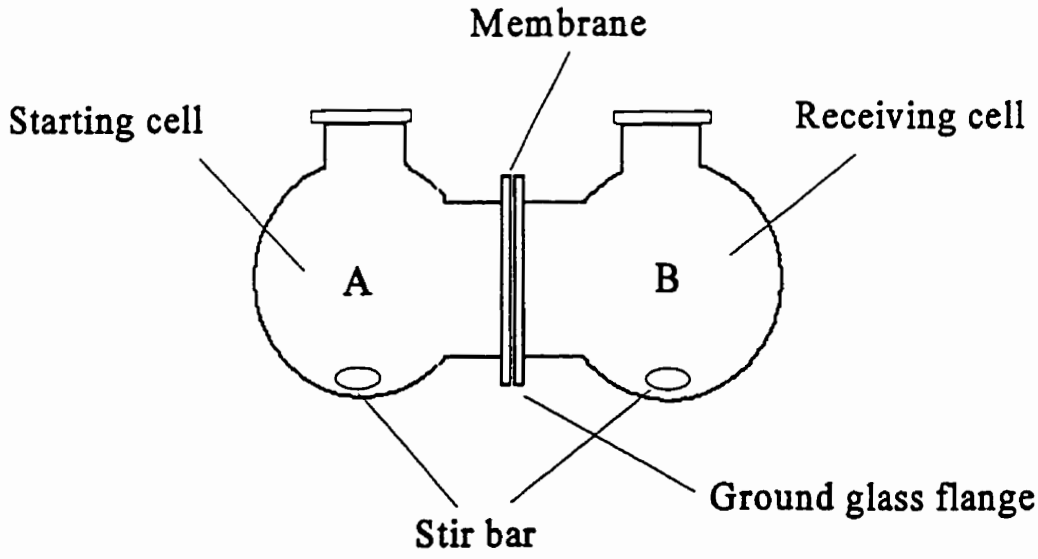

Figure 2-2c. Membrane cells (9000 mL starting cell, 30 mL receiving cell) used for preconcentration studies.

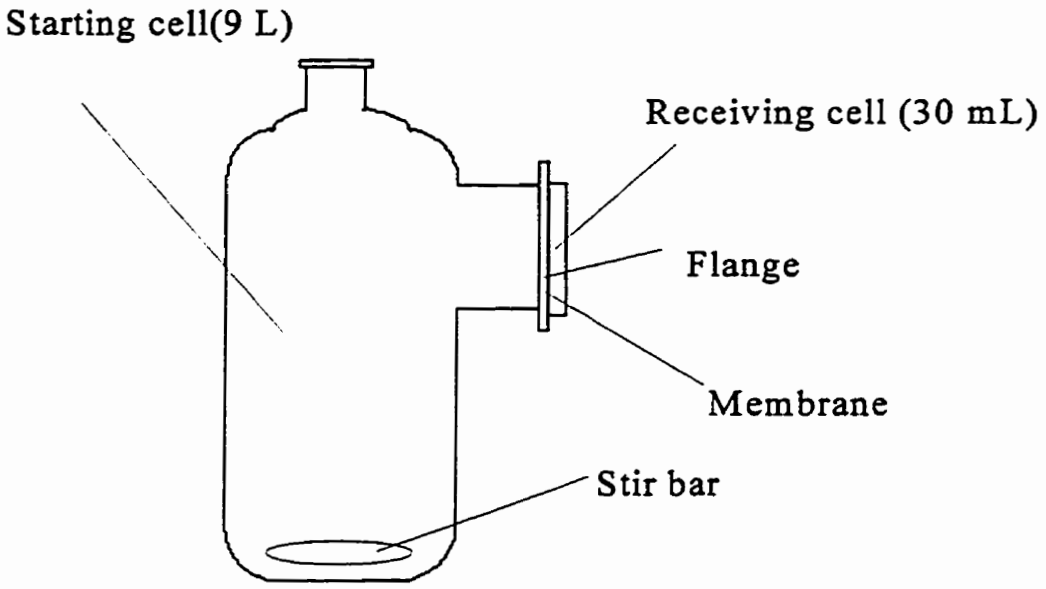

Each unit was then wrapped in Parafilm™ to prevent evaporation of solution. At elevated temperatures Parafilm softened and melted and instead a plastic wrap, Resinite by Borden Chemical, was substituted. For each experiment a number of units were prepared and then stopped after various times during the experiment to obtain a separation profile and establish reproducibility.

II) Larger Membrane Cells

To observe subtle effects of the membrane system two larger membrane testing cells were used shown in Figures 2-2b and 2-2c. These possessed both a larger membrane surface area and greater solution volume for both the starting and receiving cells. Prior to the experiment the membrane was cut to the size of the outside diameter of the glass flange + 2 cm. The flanges were covered with a thin layer of Dow Corning® high vacuum grease to yield an air and water tight seal about the membrane. The membrane was then placed on one of the cell sides and the other cell side fitted to it. After assuring a tight seal around the membrane the flanges were clamped to one another "sandwiching" the membrane between them. The appropriate solutions could then be placed in either of the flasks without leakage.

Subtle effects such as membrane degradation, and a change in cell pH could more easily be monitored over extended periods of time, with this type of apparatus. In addition, the larger cell volumes enabled us to perform experiments yielding larger preconcentration values.

III) Stirring Apparatus

A stirring apparatus was constructed for experiments requiring the Modified Donnan Dialysis Cell to be stirred. The stirring apparatus consisted of 10 water-driven stirrer hooked up in tandem. A piece of rigid foam was placed on each stirrer to insulate the membrane cell from the stirrer. The foam insulation eliminated temperature fluctuations in the membrane cell, caused by fluctuations in the water temperature.

2.1.3 Polyurethane membrane materials

Several different polyurethane membrane materials were used in the course of the thesis. These ranged in thickness, polymeric composition and manufacturer. Table 2-2 lists the membrane materials used. For composition and molecular weight characterization of the membrane materials see Chapter 7.

In addition to the use of flat sheet membrane materials, polyurethane films in the form of both condoms and gloves were used. The condoms and gloves were used as membrane "bags" that once filled with receiving cell solution, could be sealed. The characteristics of the condom and glove materials are presented in Table 2-3.

Table 2-2. Polyurethane membrane materials used in the course of this thesis

Manufacturer	Trade Name/Product Number	Polyurethane Type	Thickness
Stevens Elastomerics Northampton,MA 01060	XPR625-FS	polyether	25 µm
	XPR625-FS	polyether	50 µm
	MP1495-SL	polyester	50 µm
Deerfield Urethane South Deerfield, MA 01373	PT61005	polyether	25 µm
	PT63105	polyether	50 µm

Table 2-3. Polyurethane glove and condom material characteristics

Product	Manufacturer/ Supplier	Polyurethane Type	Thicknesses
Polyurethane Glove	Lab Safety Supply Co. Janesville, WI, 53547	--	40 µm
Polyurethane Condom	U.S. Holdings Inc. Schmid Laboratories, Sarasota, FL 34230-4703	--	Super Thin: 38 µm Normal: 127µm

2.1.4 Uncommon reagents

During the development of the organically-impregnated filter (OIF) process for metal complex removal there were several molecular weights α- Hydro-ω-hydroxypoly(oxy-1,4-butandiyl), known as "polyTHF", used including 250, 650, 1000, 2000, 4500 g/mol. Samples were provided by BASF Corporation, P.O. Box 457, 8404 River Road, Geismar, Louisiana 70734-0457.

Table 2-4. Some uncommon chemicals used in the course of this thesis

Chemical	Supplier/Manufacturer
Sodium tetrachloroaurate ($NaAuCl_4$)	Johnson-Matthey
Hydrobromic acid (HBr)	Anachemia
Sodium hexachloroplatinate(IV) (Na_2PtCl_6)	Johnson-Matthey
Palladium(II) chloride ($PdCl_2$)	Matheson, Coleman and Bell
Ferric Nitrate ($Fe(NO_3)_3 \cdot 9H_2O$	Fisher Scientific
Ammonium Thiocyanate (NH_4SCN)	J.T. Baker

2.2. General Procedures

2.2.1 Membrane Testing Protocol

Membranes were cut into 5 cm x 5 cm squares with a sharp knife and placed on the top of the open media bottle holding the sample. The screw cap was placed on a wetted media bottle and carefully turned until finger tight, yielding a membrane with an active surface area of 5.3 cm^2. The media bottle was then inverted and immersed in the solution held by the receiving cell and then the unit was wrapped in Parafilm™ to minimize evaporation. For each experiment a number of units were prepared and stopped after various time increments to obtain a separation profile and establish reproducibility. After the cells were stopped by removing the starting cell from the receiving cell, each cell was individually weighed and the pH of the receiving cell measured to determine any solution losses due to evaporation or leakage through the membrane. Results from any cells which leaked were not used in subsequent calculations. The volume of solution in each of the cells was calculated using the solution density and the mass of solution.

2.2.2 Standards and Standard Preparation

Standard buffer solutions of pH 4.0, 7.0, and 10.0 obtained from Mallinckrodt were used for pH calibration. Calibration of the gel permeation column was performed with ten molecular weight polystyrene standards obtained from Showa Denko (Shodex Standard, SM-

105, #41201) ranging from 1.28×10^3 to 3.15×10^6 mass units.

All gold solutions were prepared from a 500 mg/L standard prepared by dissolving $NaAuCl_4$ in dilute HCl. A stock 1000 $\mu g\ mL^{-1}$ palladium solution was prepared from palladium(II) chloride in 0.1 M hydrochloric acid. Sodium hexachloroplatinate(IV) dissolved in dilute HCl was used for the preparation of a stock 1000 $\mu g\ mL^{-1}$ platinum solution. Stock 1000 $\mu g\ mL^{-1}$ iron solutions were prepared by dissolving ferric nitrate in dilute HCl.

2.2.3 Dissolving of Gold Ore

The gold ore used for membrane testing is from the Kirkland Lake Mine in eastern Ontario, Canada. Gold ore solutions were prepared by first digesting the ore in aqua regia. The nitric acid portion of the mixture was then evaporated off while adding aliquots of concentrated HCl. The acid content of the mixture was lowered by then boiling this solution while adding aliquots of deionised water. The solution was then filtered using a Whatman™ No.42 filter paper to remove the silicates not dissolved in the acid mixture. When spiking of the gold sample was required, gold standard was added to the gold ore solution. Finally, the solution was made to either 2.0 M HCl or 2.0 M HBr to form the $HAuCl_4$ and $HAuBr_4$ complexes.

2.2.4 OIF Preparation

Two different types of polytetrafluoroethylene filters were used to prepare the OIF's Both filters were supplied by Millipore™ with the following specifications: pore size 5.0 µm, 47 mm diameter, 60% porosity and thickness 125 µm, (catalogue #LSWP04700) and pore

size 3.0 µm, 47 mm diameter, 85% porosity and thickness 200 µm, (catalogue # FGLP04700).

The OIF was prepared by first liquefying the PolyTHF (M.W. 1000) at 65°C in an oven for approximately 15 min. PolyTHF is a waxy solid at room temperature requiring softening to facilitate impregnation. The filter to be impregnated was first weighed and placed in a standard Millipore™ HPLC filtration device. Then 3-5 mL of PolyTHF was poured into the filtering receptacle. Vacuum was applied to the filter flask to pull PolyTHF through the filter until all the polymer in the filtering receptacle had been either passed through, or coated on the filter. The filter was then removed from the HPLC filtering apparatus and any excess PolyTHF beaded on the surface gently removed from the polytetrafluoroethylene filter by pressing with a Kimwipe™. The organic-impregnated filter was weighed and was then ready to be used for extraction. The impregnation process yielded a filter with an active area of 9.6 cm^2 and requires less than ten minutes of preparation time. Scanning electron micrographs of the polytetrafluoroethylene filters prior to and after the impregnation process are shown in Figures 2-3 and 2-4.

Figure 2-3. Scanning electron micrograph of 5.0 µm filter prior to being impregnated

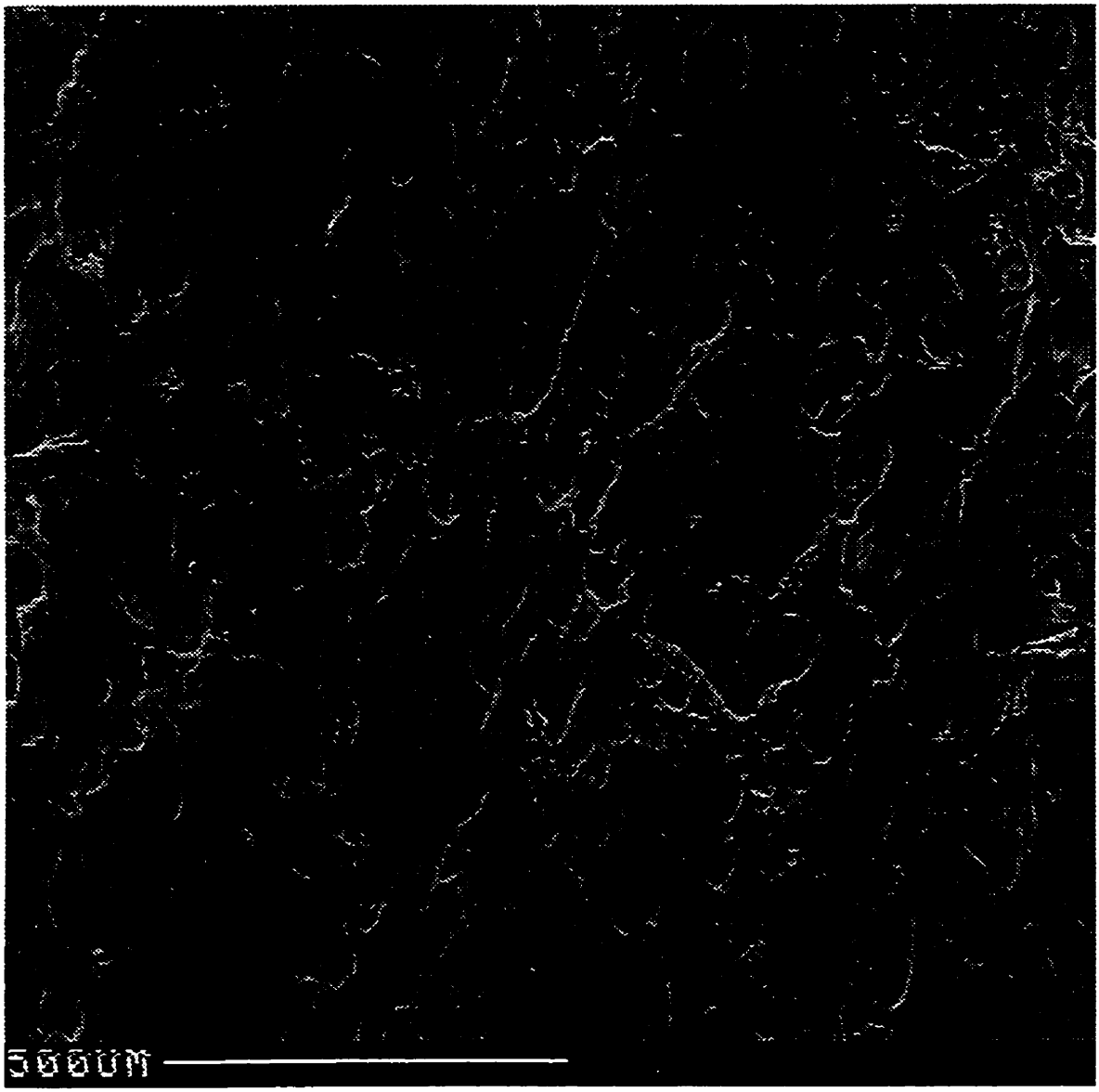

Figure 2-4. Scanning electron micrograph of 5.0 μm filter after impregnation with polyTHF.

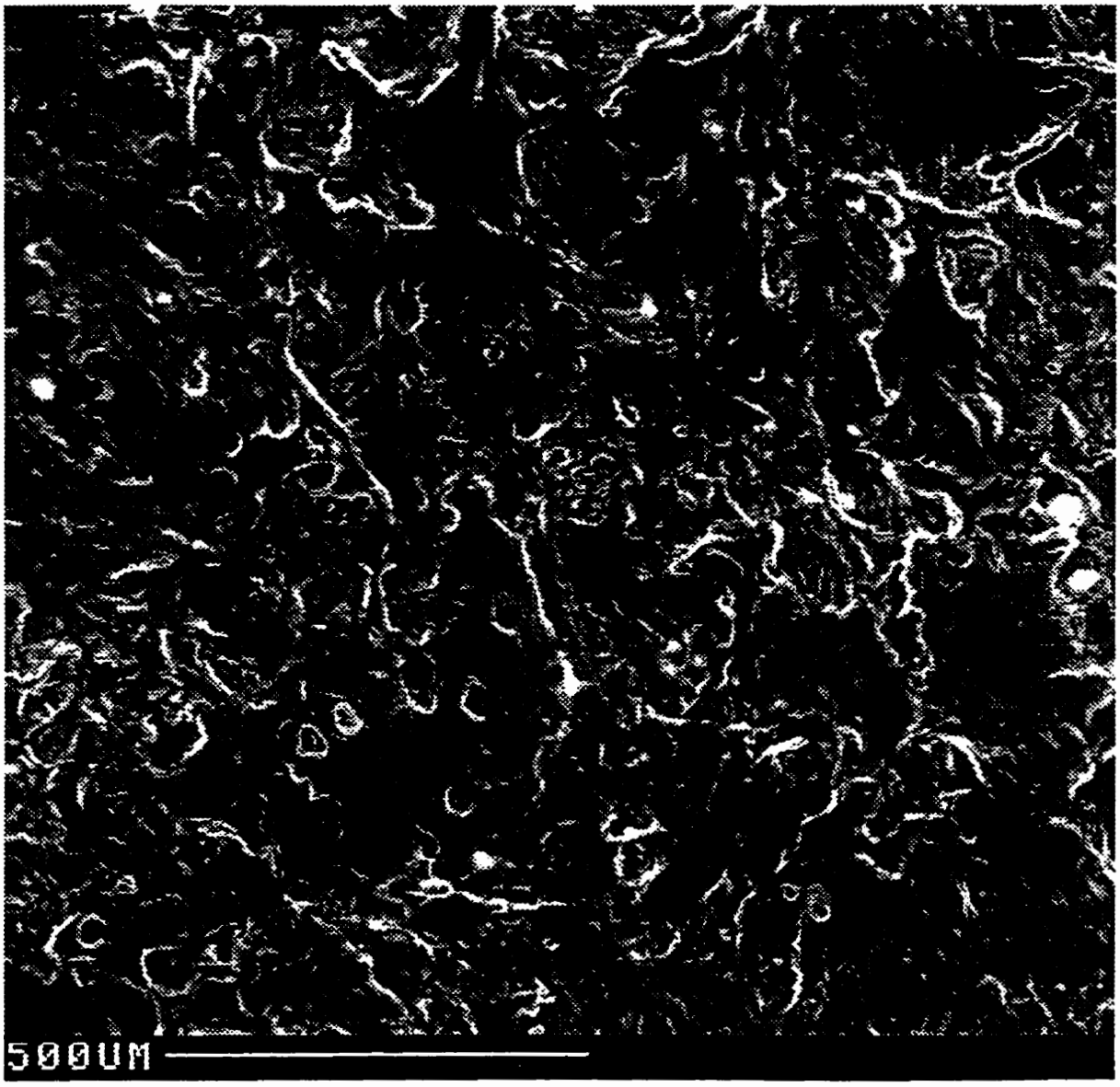

PolyTHF forms the active layer of the OIF in the metal extraction. The preparation process leads to an average loading of 50 mg and 100 mg of PolyTHF on the 5.0 and 3.0 μm pore size material respectively. The larger loading on the 3.0 μm filter is due to the increased thickness and porosity of this filter compared to the 5.0 μm filter. PolyTHF coats the entire surface of the filter, penetrates into the pores of the filter and then solidifies. Scanning electron microscopy revealed that there are still holes visible on the surface of the OIF facilitating the passage of liquid through the filter. The presence of holes after the impregnation is essential for adequate flow through the filter because otherwise the filter would be clogged and unusable. Smaller pore size filters (0.2 and 0.5 μm) were impregnated and tested, but the impregnation step led to clogging of the pores.

2.2.5 OIF Testing Protocol

Once the OIF had been prepared it was placed in a standard HPLC filtration apparatus and clamped into place. The metal complex-containing solution was then placed in the filtering receptacle and a vacuum applied to the bottom filter flask to obtain the desired flow rate of the solution. The average flow rate was then calculated by dividing the time required for filtration by the volume of solution filtered. After the solution had passed through the OIF, an aliquot of the filtrate was taken for further analysis and the solution was placed again in the filtering receptacle, and the filtration/extraction process repeated until the desired number of passes through the OIF had been completed. Once extracted the metal was eluted from the filter by passing an eluting solvent through the filter and collecting the filtrate for analysis.

2.3 Methods of Analysis and Calculations

2.3.1 Metal Content

Atomic absorption spectrophotometry, inductively coupled plasma spectrophotometry and UV-Visible absorption spectrophotometry were used for the quantitation of metals in solution. The wavelengths used for the UV-Visible determination of the various metal complexes are shown in Table 2-5.

Once the concentration of a metal in either the starting or receiving cell had been determined the metal content of an individual cell was then determined by:

$$Metal\ Content_{cell} = \frac{[M^{n+}] \times Mass_{soln}}{\rho_{soln}}$$

where: $[M^{n+}]$ - metal concentration in a cell (μg/mL)

$Mass_{soln}$ - mass of solution in cell (g)

ρ_{soln} - density of solution in cell (g/mL)

Table 2-5.Wavelengths used to determine various metal complexes

Metal Complex	Wavelength (λ_{max})
$AuBr_4^-$	374 nm
$AuCl_4^-$	314
$Pt(SCN)_6^{2-}$	286, 360
$PtCl_6^{2-}$	262
$Pd(SCN)_4^{2-}$	308
$PdCl_4^{2-}$	290

2.3.2 Determination of the thermodynamic constants ΔH, ΔS and E_a

For each of the metals, membrane transport experiments were run at several different temperatures to obtain thermodynamic data about the membrane sorption/ transport process. A membrane transport experiment was performed with each metal at various temperatures. The data was then plotted according to:

$$\ln(\frac{n}{n_0}) \ vs. \ t$$

where: t – time

n – number of moles of non-extracted metal complex at time(t)

n_0 – number of moles of metal complex at t = 0

The resulting curve for each temperature was plotted and fit to the linear equation:

$$y = mx + b$$

where: m – slope of the line

b – y intercept

The slope of the line represents the rate constant (k_{obs}) for that temperature and conditions. For each of the metal complexes the k_{obs} for each temperature are plotted as:

$$\ln\frac{k_{(obs)}}{T} \text{ vs. } \frac{1}{T}$$

From the resulting plots for each of the metals the constants $\Delta H^{\ddagger}$, $\Delta S^{\ddagger}$ and E_a can be calculated.

where: $\Delta H^{\ddagger}$ – enthalpy of activation

$\Delta S^{\ddagger}$ – entropy of activation

E_a – activation energy

In this plot the slope of the line represents $-(\frac{\Delta H^{\ddagger}}{R})$ and the y-intercept represents $\ln\frac{k_B}{h} + \frac{\Delta S^{\ddagger}}{R}$.

where: R – universal gas constant

h – Planck's Constant

k_B – Boltzmann constant

Also, using the Arrhenius equation:

$$k = A\exp(-E_a/RT)$$

and taking the natural logs of both sides of the equation yields the relation

$$\ln k = \ln A - \frac{E_a}{RT}.$$

Plotting the ($\ln k$ vs. $\frac{1}{T}$) yields a straight line with a slope equal to ($-\frac{E_a}{R}$).

2.3.3 Calculation of Concentrations of Metal Complexes vs. Ligand Concentration

The following equilibria relations were used to determine the concentrations of metal complexes that predominate at different ligand concentrations (Note: The equations shown are for the iron(III) chloride equilibrium system:

$$K_1=\frac{[FeCl]}{[Fe]\cdot[Cl]} \quad \ldots \quad K_2=\frac{[FeCl_2]}{[FeCl]\cdot[Cl]} \quad \ldots \quad K_3=\frac{[FeCl_3]}{[FeCl_2]\cdot[Cl]} \quad \ldots \quad K_4=\frac{[FeCl_4]}{[FeCl_3]\cdot[Cl]}$$

$$Total\ Conc_{Fe} = Fe + FeCl + FeCl_2 + FeCl_3 + FeCl_4$$

$$Total\ Conc_{Cl} = Cl + FeCl + 2FeCl_2 + 3FeCl_3 + 4FeCl_4$$

The concentrations of the individual iron chloride complexes can be determined by using the literature values for the constants K_1 - K_4 and combining the above equations. From the resulting equations you have a system of six equations and six unknowns. The unknowns can then be solved for using a mathematical program. A program was written in Mathcad™ that allowed the determination of the concentrations of the individual complexes at various concentrations. Two examples of the programs used are shown on the following two pages. Figure 2-5 displays the program used for iron(III) chloride system.

2.3.4 Determination of ICP Detection Limits

Detection limits for each of the elements analysed were determined by taking ten readings of the blank at the emission line of each element. Blanks used consisted of 0.5 M KBr for the receiving cells and 2.0 M HBr for the starting cells. The standard deviation of the

blank measurements was calculated and both the detection limit and the limit of quantitation determined using the following formula:

$$L.L.D. = 3\delta_b$$

$$L.O.Q. = 10\delta_b$$

where: L.L.D. - lower limit of detection

L.O.Q. - limit of quantitation

δ_b - standard deviation of measurements of blank

Figure 2-5. Mathcad™ program written by Dr. G Baldwin for the calculation of iron chloride complexes at different HCl concentrations using stability constants.

Iron(III)- chloride complexes in aqueous solution;
stability constants taken from Bjerrum&Lukes, Acta Chem Scand., 1986, A40,31-40

Equations for speciation: Fe3+ + Cl- = FeCl2+ with K1 etc

Equilibrium constants:

$K1 := 30 \quad K2 := 4.5 \quad K3 := 0.15 \quad K4 := .0078$

Initial (analytical concentrations) $C_{fe} := .001954 \quad C_{Cl} := 3.87$

Initial guesses for solution

$Cl := 3.87 \quad fe := \frac{C_{fe}}{10000} \quad feCl := fe \cdot .2$

$feCl2 := feCl \quad feCl3 := feCl \quad feCl4 := feCl$

Solve Block

Given

$K1 = \frac{feCl}{fe \cdot Cl} \quad K2 = \frac{feCl2}{feCl \cdot Cl} \quad K3 = \frac{feCl3}{feCl2 \cdot Cl} \quad K4 = \frac{feCl4}{feCl3 \cdot Cl}$

$fe > 0 \quad Cl > 0 \quad feCl > 0 \quad feCl2 > 0 \quad feCl3 > 0 \quad feCl4 > 0$

$C_{fe} = fe + feCl + feCl2 + feCl3 + feCl4$

$C_{Cl} = Cl + feCl + 2 \cdot feCl2 + 3 \cdot feCl3 + 4 \cdot feCl4$

$$\begin{bmatrix} fe \\ Cl \\ feCl \\ feCl2 \\ feCl3 \\ feCl4 \end{bmatrix} := Find(fe, Cl, feCl, feCl2, feCl3, feCl4)$$

$fe = 5.8522369766 \cdot 10^{-7} \quad Cl = 3.8654353112$

$feCl3 = 0.0006844507$

$feCl = 0.0000678643 \quad feCl2 = 0.0011804633$

$feCl4 = 0.0000206365$

Chapter 3: Transport of Iron Through a Polyurethane Ether-Type Membrane

3.1 Introduction

Some iron and gallium chloride[1] complexes and cobalt thiocyanate[2] complexes can be extracted by unloaded polyurethane ether-type membrane material. Furthermore, once extracted these complexes are transported through the polyurethane membrane material where they can be recovered in a receiving solution. The different extraction behaviours of various metal complexes demonstrates the possible use of polyurethane membranes for metal separations. The extraction of a metal complex is contingent upon the formation of the metal complex and the solubility of that complex within the membrane material. It follows that the formation of a metal complex depends on the stability constants of the individual metal complex and the amount of ligand present in solution. Both properties control the amount of a metal complex that is present in solution and can likely be used to facilitate the separation of metals.

The extraction and transport of iron through the polyurethane membrane was studied to obtain a better understanding of the transport mechanism essential to establishing the potential of this process. Iron(III) was used as a probe into the nature of the extraction and transport mechanisms of the membrane process because of its well-known propensity to form $HFeX_4$ (where X = Cl^- and Br^-) complexes. The use of different acids in the starting cell facilitates the formation of different halide complexes which enabled the direct comparison of the transport abilities of each of the metal halide complexes. The use of different iron halide complexes allowed the determination of the effect of the hydrophobicity/ hydrophilicity of a

complex and how the stability constants of the extractable complex affect its rate of transport. The energy of activation associated with the sorption/ transport process was investigated using separations at different temperatures. Different polymer thicknesses were used to determine the effect of membrane thickness on the sorption, transport, and recovery of the metal species. The role that acid plays in the sorption/ transport process was explored using the formation of $FeCl_4^-$ in the presence of salt rather than a high concentration of acid.

3.2 The Extraction and Transport of $HFeCl_4$

The transport of iron was first investigated by Gesser et al.[1] through polyurethane membranes. They showed that iron could be extracted into the membrane as the $HFeCl_4$ complex from high concentrations of mixtures of LiCl and HCl. Initially we chose high HCl concentrations ≥ 5.0 M to investigate the ability of the Stevens Elastomerics (XPR625-FS) polyether-type polyurethane film to extract and transport the iron halide complex. In addition we chose receiving cell conditions that favoured the elution of iron from the membrane, and provide an environment in which the metal does not hydrolyse or precipitate. After obtaining conditions where transport and recovery occurred we examined the effect of the HCl concentration in the starting cell on the extraction and transport of iron.

3.2.1 Effect of HCl Concentration

The stability constants of iron (III) species with chloride ion in an aqueous system can be represented as the following equilibrium:

$$Fe^{3+} \rightharpoonup FeCl^{2+} \rightharpoonup FeCl_2^+ \rightharpoonup FeCl_3 \rightharpoonup FeCl_4^-$$

Both the iron and chloride concentration in solution determine the concentrations of the individual iron chloride complexes. The concentrations of the various iron chloride complexes at different ligand concentrations are shown in Figure 3-1. The concentrations of each of the complexes were calculated using Mathcad™ (program shown in Figure 2-5, Chapter 2) and iron chloride stability constants[3]. For the calculations, the chloride concentration was taken to be equal to the activity of the chloride ion.

Figure 3-1. Plot of the proportions of various iron chloride complexes as a function of ligand and concentration.

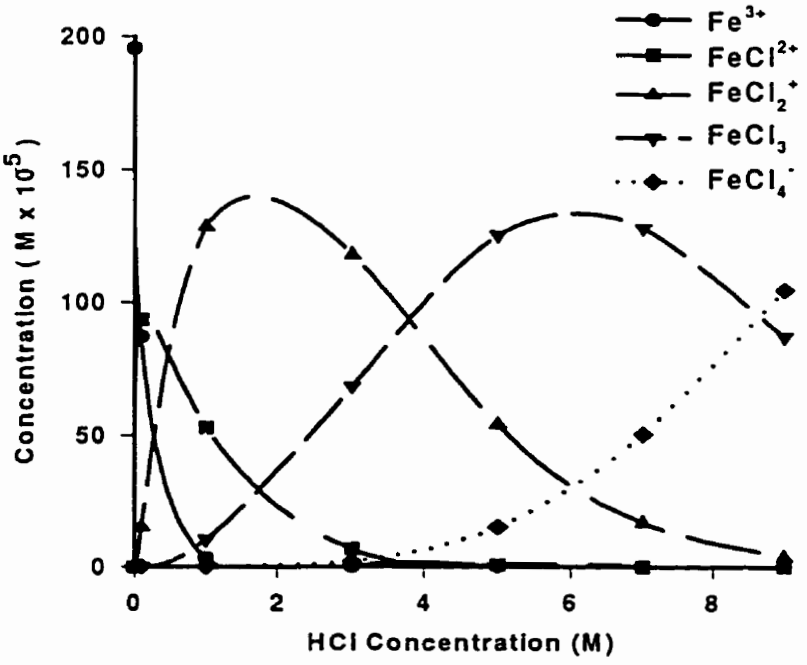

Table 3-1. Percentage of Iron in the $FeCl_4^-$ Complex at Various HCl Concentrations and Time Required for Quantitative Transport

HCl Concentrations (*M*)	**% Fe in $FeCl_4^-$ Complex**	**Time Required for Quantitative Transport**
9	53.4	4 hours
7.0	25.8	7.5
5.0	7.7	48
3	1	--
1.0	0.02	--
0.1	1.15×10^{-5}	--

The amount of iron in a particular complex can be controlled by adjusting the HCl concentration. As the HCl concentration increases, the percentage of iron as the $HFeCl_4$ complex also increases. To study the effects of varying concentrations of HCl, and consequently varying proportions of the $HFeCl_4$ complex in solution on the separation, 15 mg/L iron solutions were prepared with several HCl concentrations (0, 1.0, 3.0, 5.0, 7.0, 9.0 M). A membrane transport experiment was performed with each of the different acid solutions in the starting cell while all the receiving cells contained 0.1 M HCl. At concentrations of zero and 1.0 M HCl there is neither extraction into the membrane nor transport of the iron from the starting to the receiving cell over the running time of the experiment. At 3.0 M acid, only a small amount of iron was transported across the membrane. At HCl concentrations of 5.0 M and greater it was found that the iron is quantitatively extracted and transported to the receiving cell and a smooth separation profile is obtained where the transport rate increases with increasing HCl concentration. This supports a previous suggestion[4] that the transport of iron through the polyurethane membrane may be due to the $FeCl_3$ and $HFeCl_4$ neutral complexes. In Table 3-1 it is shown that for solutions containing less than 3.0 M HCl, less than 1% of the iron is in the $FeCl_4^-$ complex. As the acidity increases, the proportion of iron present as the $HFeCl_4$ complex increases. At higher HCl concentrations there are significant amounts of $HFeCl_4$ present which facilitates the transport across the membrane. Table 3-1 also provides evidence that the $FeCl_3$ complex is probably not responsible for the extraction. If $FeCl_3$ were extractable the process should occur at lower acidities than observed. For example, in Figure 3-1 we see that even at concentrations of 2.0 M HCl there is a significant amount of $FeCl_3$ present. If $FeCl_3$ were

extractable, we would expect the transport of iron to occur at lower HCl concentrations. With an increase in the proportion of the species required for transport, we would expect to see an increase in the rate of transport as well. This rate should continue to increase if more of the extractable $HFeCl_4$ complex is present, or until the membrane becomes saturated, at which point the rate of transport will have reached a maximum. This can be seen in the results; with each increase in HCl concentration there was a corresponding increase in the rate of transport as shown in Figures 3-2a and 3-2b, although no maximum was observed. The quantitative transport of iron to the receiving cell from 5.0 M HCl required 48 hours while only requiring 9 hours when the HCl concentration was increased to 9.0 M. The acid concentrations of the starting and receiving cells were found to change during the experiment. The amount of acid in the receiving cell increased as the length of experiment increased. The transparent membrane gradually became cloudy and translucent and then white, opaque and "puckered". In the experiments run at room temperature over a period of 48 hours, the physical changes did not appear to play a factor in the separation (see Chapter 7).

3.3 Choice of Receiving Cell Solution

The choice of the receiving cell solution is extremely important for metal transport and recovery. If the solution is not able to remove the metal species from the membrane material, the metal concentration within the membrane will continue to increase, lowering the ability of the membrane to further extract more metal species. In addition, if the receiving solution removes a species but causes the metal to precipitate then further complications arise. The precipitation of the metal at the membrane/ receiving cell interface reduces the effective surface area of the membrane by covering it. Experiments were

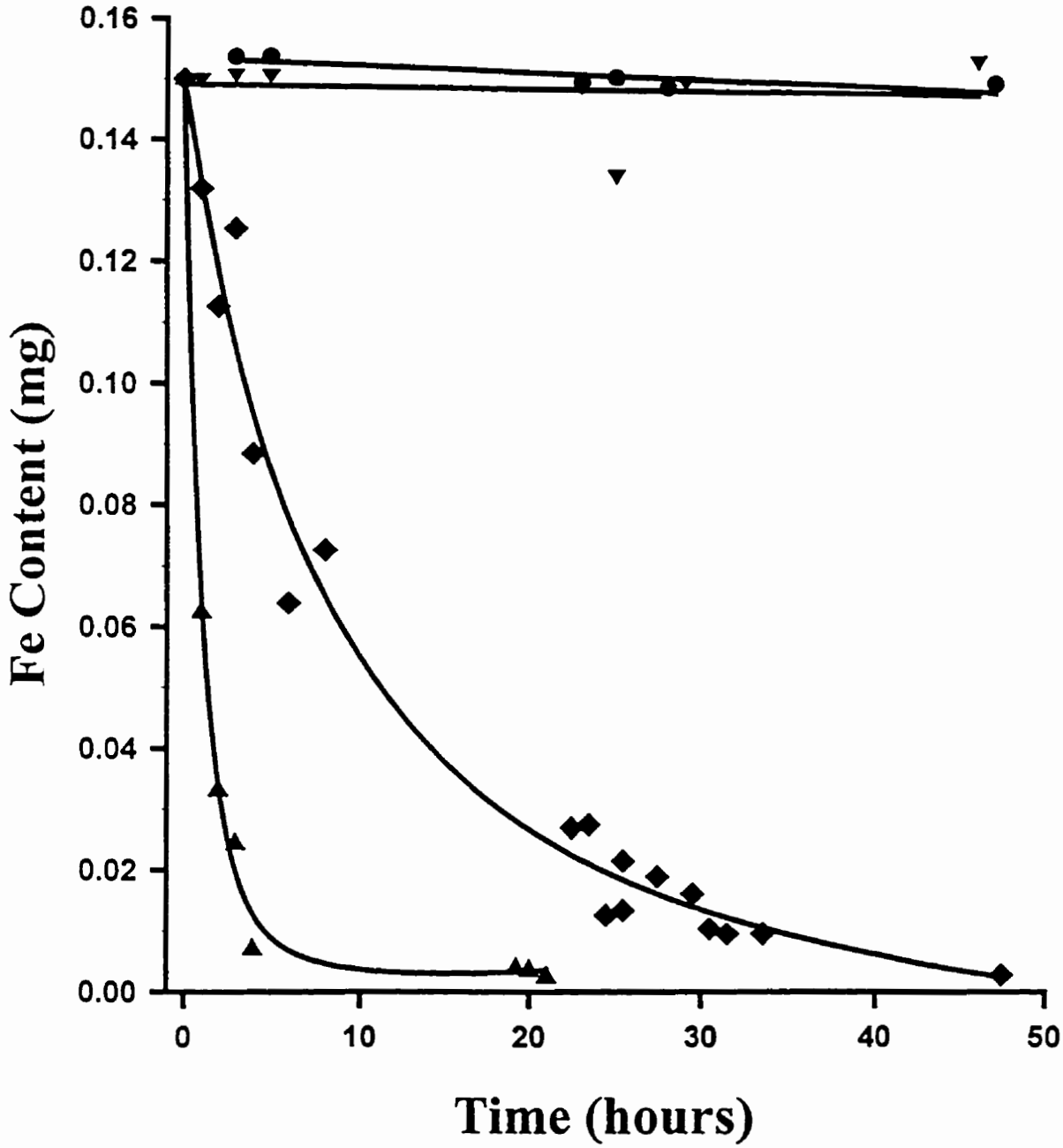

Figure 3-2a. Iron separation profile for starting cells containing 10mL of 15mg/L iron.

—●— no HCl added
—▼— 1.0M HCl
—◆— 5.0M HCl
—▲— 9.0M HCl

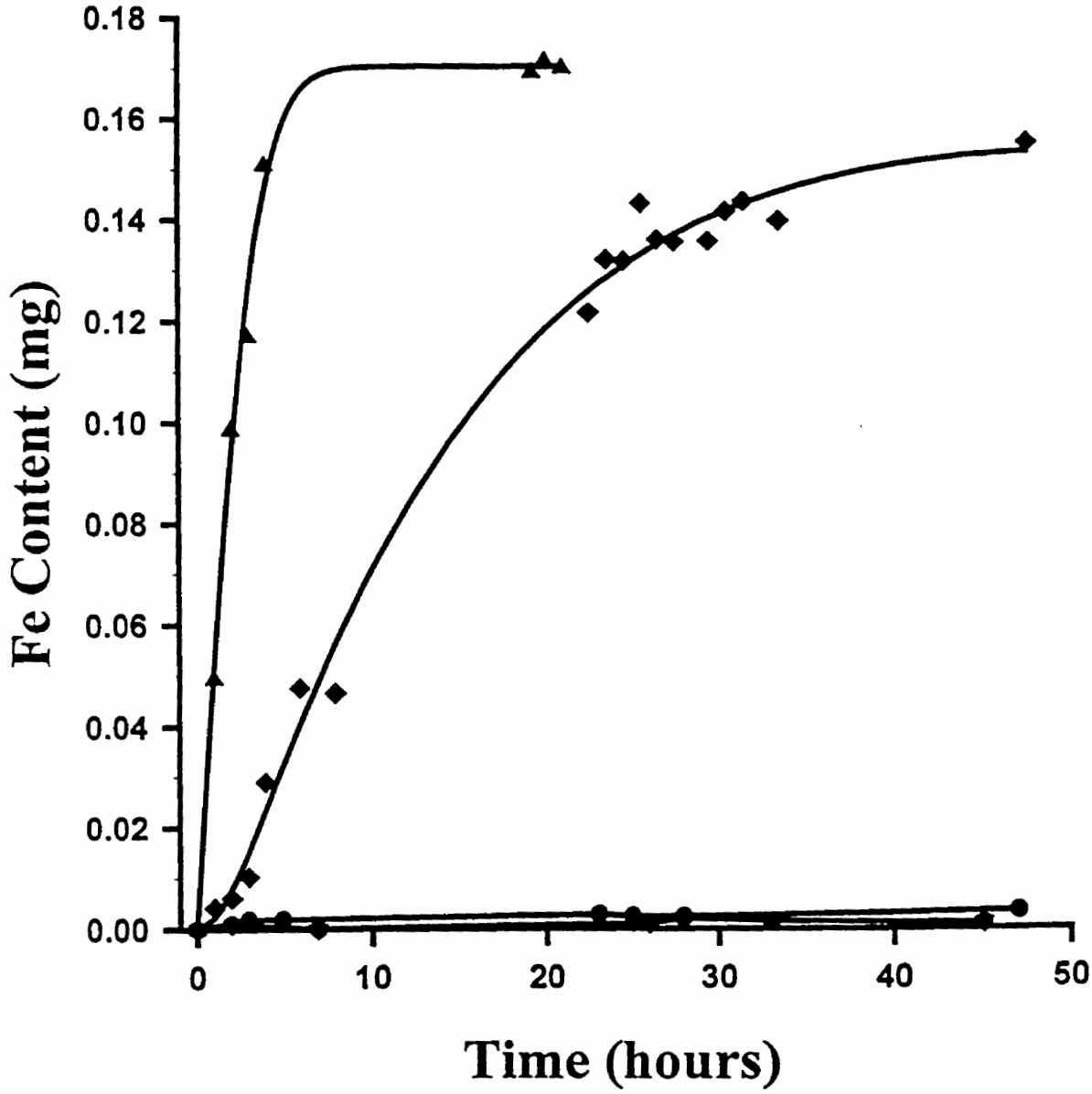

Figure 3-2b. Receiving cell iron contents corresponding to each of the starting cell HCl concentrations in Fig. 3-2a. Each receiving cell initially contained 30 mL of 0.1*M* HCl.

performed that used either 0.1 M HCl or deionised water as the receiving cell solution. The use of the deionised water as a receiving cell solution lead to the precipitation of the iron at the membrane/ receiving solution interface as the $Fe(OH)_3$ complex and was discontinued. The receiving solution that we chose for the remainder of the experiments was 0.1 M HCl because it provided a stable environment for the iron halide complex after elution.

Once the iron complex diffuses to the membrane/ receiving phase interface the iron complex is in an environment that contains less halide than the starting cell. The equilibrium is then shifted from the HMX_4 complex to other species that do not possess the ability to be extracted and transported through the membrane. At a 0.1 M HCl concentration the equilibrium is shifted away from the formation of the $FeCl_4^-$ complex (Figure 3-1). The lower halide concentration within the receiving cell leads to the partial hydrolysis of the iron species to form a mixture of Fe^{3+}, $FeCl^{2+}$, $FeCl_2^+$ metal complexes. None of these complexes are extractable into the membrane material. The iron is therefore trapped in the receiving cell and cannot proceed back through the membrane to the starting cell until sufficient halide is present to re-form the complex, or the membrane develops pores allowing diffusion back into the starting cell solution. The overall mechanism for iron transport through the polyurethane ether-type membrane is shown in Scheme 3-1. The HCl concentration in the receiving cell has large effect on the ability of the membrane to quantitatively extract the iron species. For example, Figure 3-3 shows an experiment where the starting cell contained 15 mg L^{-1} Fe/ 5.0 M HCl and the receiving cell also contained 5.0 M HCl. At the early stages of the experiment the iron complex is extracted from the starting cell solution. Later we see the appearance of iron in the receiving cell solution.

Scheme 3-1. Schematic representation of membrane separation mechanism for iron(III).

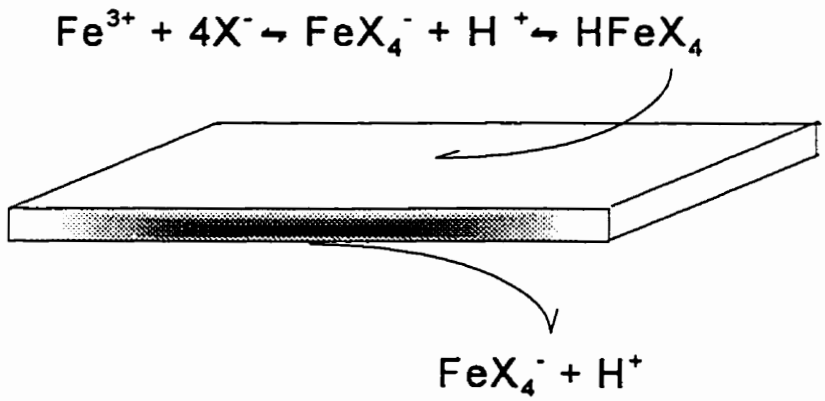

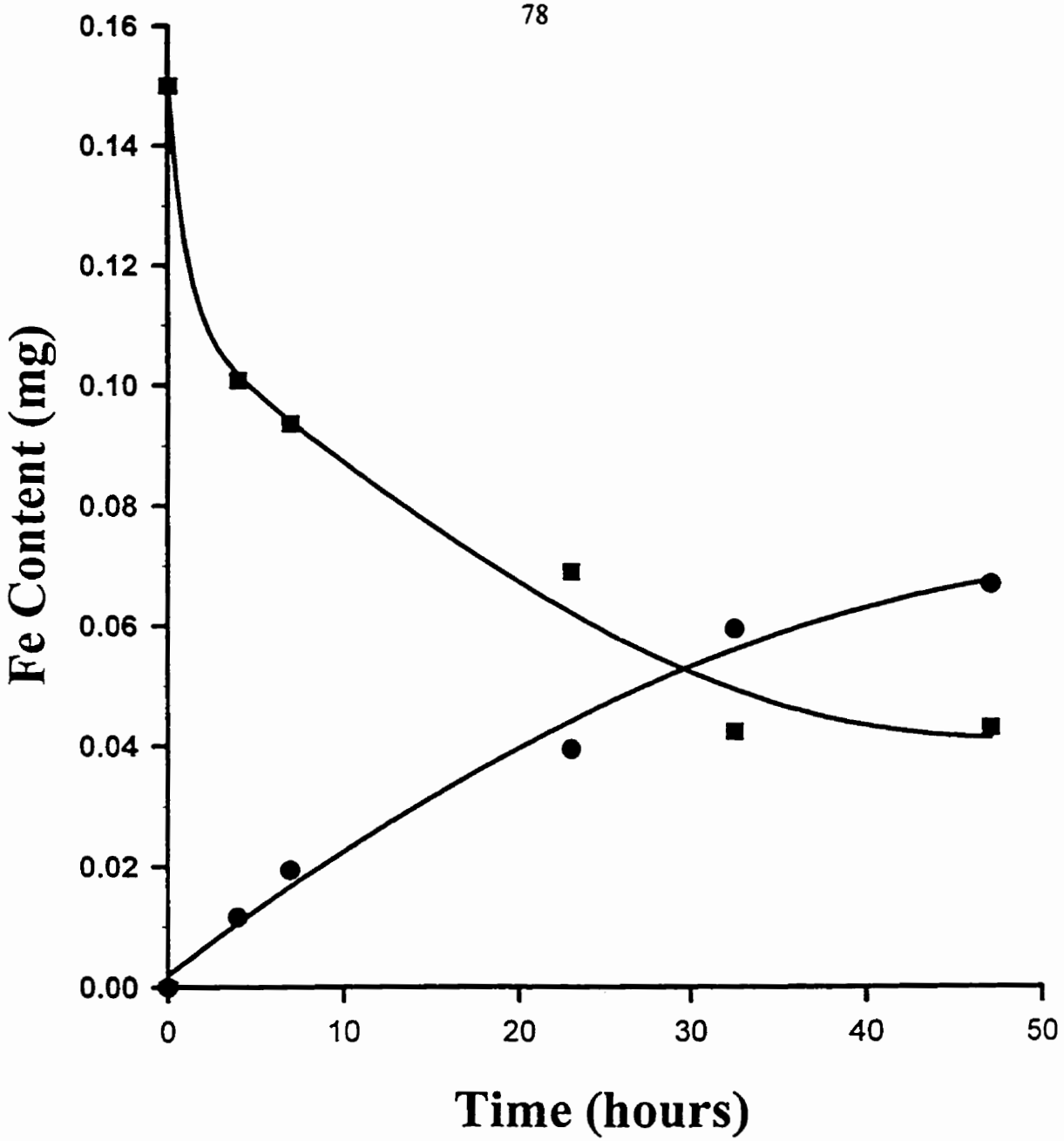

Figure 3-3. Iron separation profile for starting cells containing 10mL of 15mg L^{-1} Fe/ 5.0 M HCl. Receiving Cells contain 30 mL of 5.0 M HCl.

—■— Starting Cell
—●— Receiving Cell

3.4 Effect of Other Halo-acids

Experiments using HBr and HI in place of HCl in both the starting (5.0 M) and receiving flasks (0.1 M) were performed. The use of HBr produced a five-fold increase in transport rate as compared to HCl. If only the stability constants of the complexes are looked at this phenomenon is somewhat unexpected. The trend for the stability of the halide complexes for iron[5] follows the order; $F^- > Cl^- > Br^- > I^-$. If the determining factor for the separation was solely the stability of the complex we would expect the chloride complex to be transported faster than the bromide, while this is actually reversed. This phenomenon can be attributed the increased hydrophobicity of the bromide complex compared to the chloride. The bromide ligands are much larger and bulkier giving the metal complex an increased hydrophobic character that has an increased affinity for the hydrophobic membrane material.

In the early stages of the separation using hydriodic acid no iron is transported through the membrane. After 3 hours the membrane becomes porous so that both iron and acid solution can pass through the membrane. Because it does not form the tetrahedral complex in the presence of iodide ion, iron is not transported through the membrane. The results of the separations performed using the different halo-acids are presented in Figure 3-4.

It is important to note that when HCl and HBr were used the iron was quantitatively (>98%) transported from the starting to the receiving cell and then remains in the receiving cell. Also the phenomenon occurring in our case is not solely diffusion as other authors[6] using polyurethane membranes have reported. Rather the transport process involves the initial extraction of the iron complex followed by diffusion through the nonporous polymer

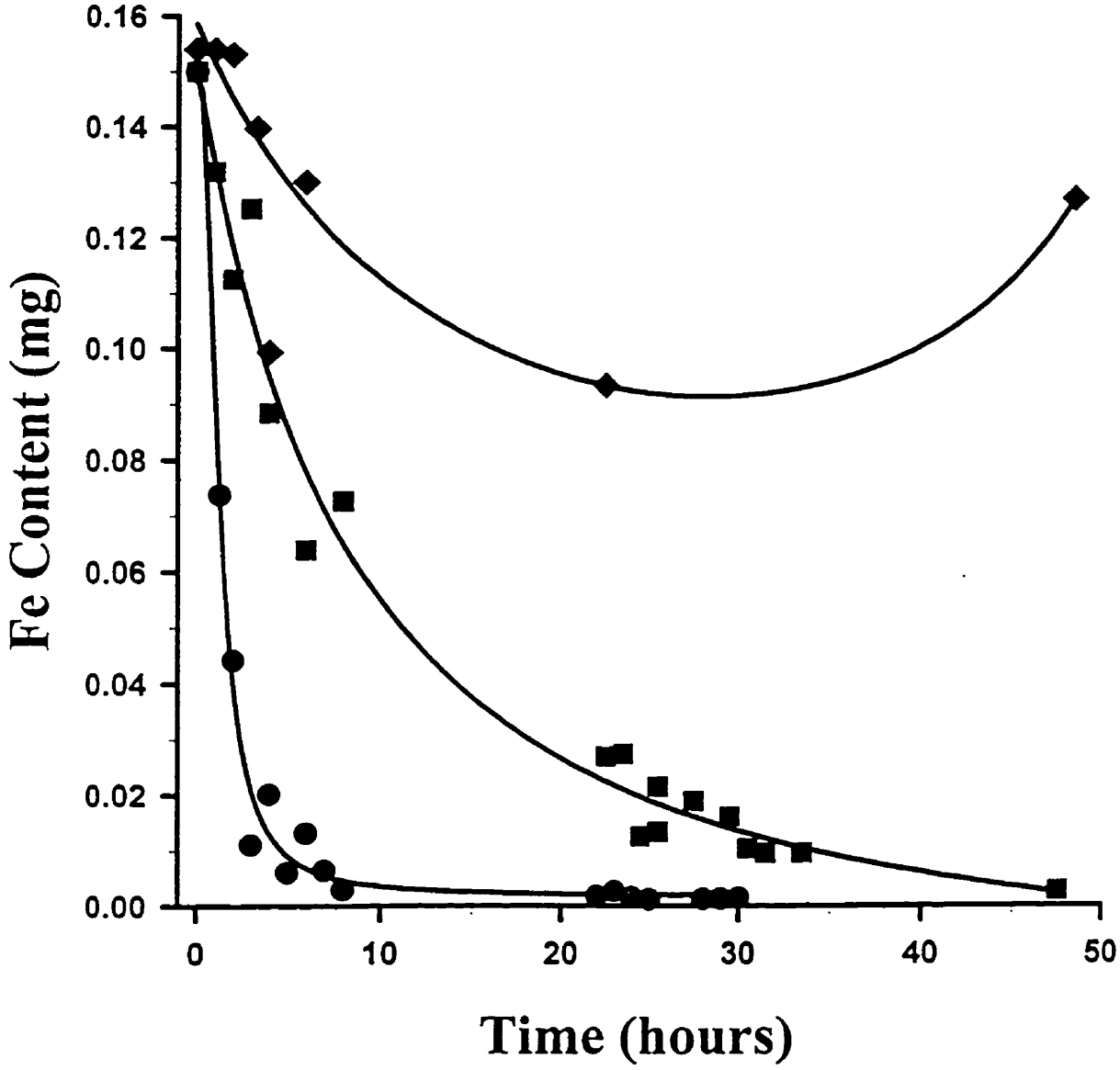

Figure 3-4. Iron Separation profile for starting cells containing 10 mL of 15mg/L iron with a concentration of 5.0*M* acid.

—◆— Hydriodic acid
—■— Hydrochloric acid
—●— Hydrobromic acid

membrane. Our investigation has shown that a quantitative separation of iron is possible with the membrane which would not occur if simple diffusion was the sole process acting on the system. In order to produce uphill transport of the iron complex a driving force is required. In the case of this separation the driving force is the concentration of $HFeX_4$. Initially there is no iron complex in the membrane. After iron complex has been sorbed into the membrane material a concentration gradient with respect to the iron complex is developed within the membrane material. The concentration of iron complex begins to build at the feed phase/membrane interface. Because of the concentration gradient within the membrane the metal complex begins to diffuse through the dense polymer to try to eliminate the gradient within the membrane system. Once the complex reaches the membrane/receiving cell interface the complex becomes deprotonated and eluted, preserving the concentration gradient within the membrane. This continually drives the separation until the concentration of $HFeX_4$ is depleted from the starting cell.

3.5 Membrane Thickness

To determine the effects that the thickness of the membrane has on the rate of transport, a 0.025 mm membrane was used that was half as thick as that used previously. As expected the iron was transported across the thinner membrane twice as fast as through the thicker membrane, as is shown in Figure 3-5. This indicates that the rate-determining step of the separation is the movement of the iron through the polymer rather than the sorption of metal complex onto or recovery from the polymer surface. In addition it provides evidence that diffusion is the process responsible for the transport of the iron species once

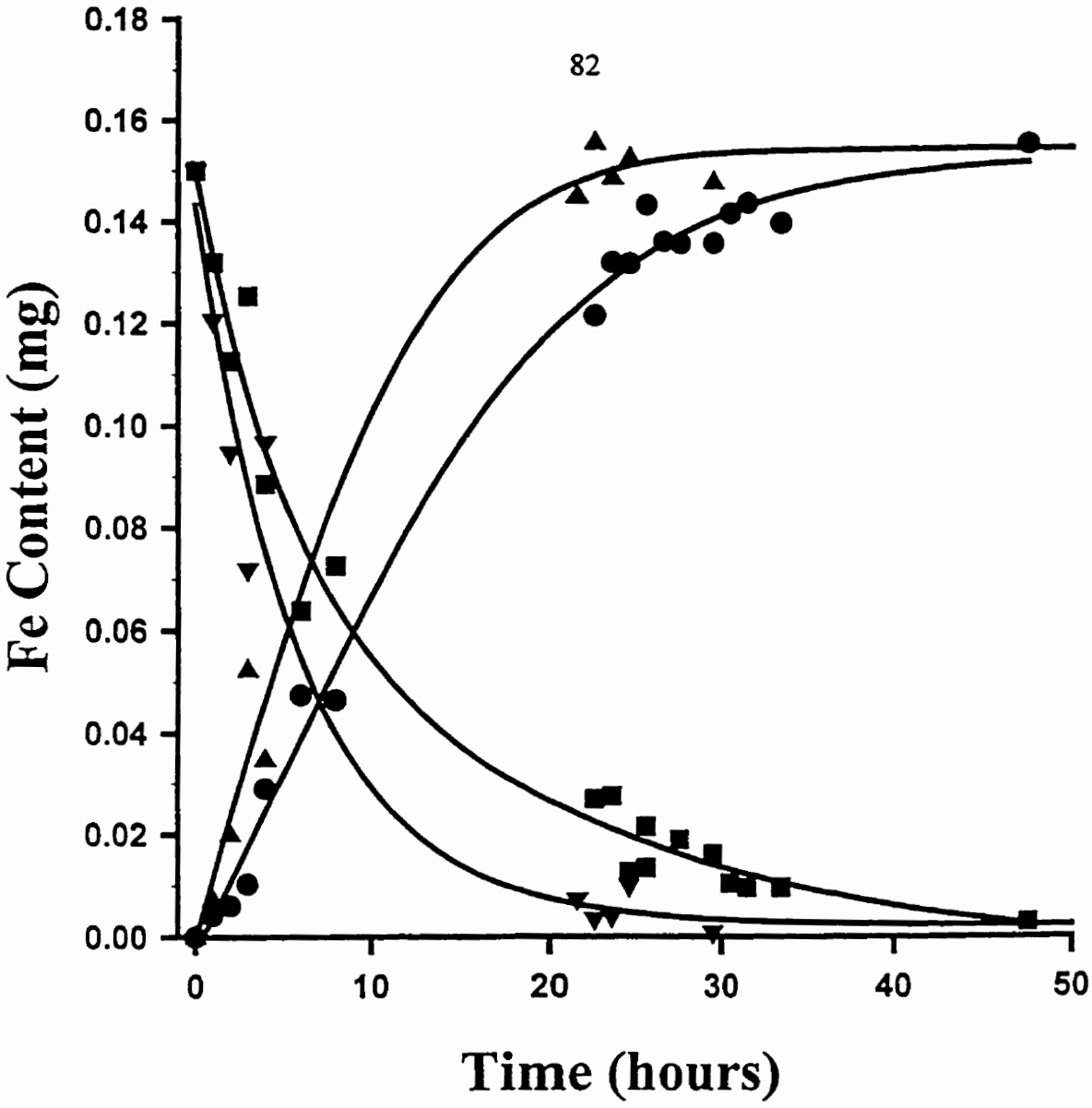

Figure 3-5. Iron separation profile using two different membrane thicknesses. Starting cell contained 10 mL of 15 mg/L iron in 5.0*M* HCl and receiving cell 0.1*M* HCl.

—■— Starting cell using a 0.050 mm thick membrane
—●— Receiving cell using a 0.050 mm thick membrane
—▼— Starting cell using a 0.025 mm thick membrane
—▲— Receiving cell using a 0.025 mm thick membrane

it has entered the membrane material. It follows that the overall process can be represented by Fick's law of diffusion.

$$J_i = \frac{D_i \Delta c_i}{x_i}$$

where:

J_i - flux of penetrant "i"

D_i - diffusivity of penetrant "i"

Δ - the concentration difference between points "x" distance apart in the membrane

x_i - membrane thickness

By changing only the thickness of the membrane material and leaving all other conditions constant we see a twofold increase in the flux of the iron species through the membrane. This increase in rate directly correlates to diffusion law. Examining the equation we can see that by halving the membrane thickness (ie. $\frac{x_i}{2}$) we would expect an increase in the flux by a factor of two. Furthermore, if the polymeric membrane could be made thinner then a faster separation might be possible although this might cause mechanical problems.

3.6 Effect of Temperature

The effect of temperature on the rate of transport was studied with the starting flask containing 10 mL of 15 ppm Fe in 5.0 M HCl and the receiving flask containing 30 mL of 0.1

M HCl. These conditions were chosen because the iron is quantitatively transported through the membrane in a reasonable amount of time (<2 days at room temperature). With these conditions five experiments were run at different temperatures (5, 22, 37, 50, 65°C) to obtain thermodynamic data. As expected, the rate of transport increased markedly with an increase in temperature. The reason for the increase in transport rate may be due to two factors. The increase in temperature allows more molecules to overcome the activation barrier and as well may cause a shift in the equilibrium to favour more $HFeCl_4$ formation. Separation data are presented in Table 3-2. The energy of activation was calculated to be 50 kJ/ Mol using the Arrhenius plot shown in Figure 3-6. This value is consistent with values[7,8] found for the sorption and transport of aqueous salt and acetic acid solutions in polyurethane membrane material.

As in the experiments at room temperature, the membrane became white, opaque and "puckered". This phenomena was shown to be caused by the swelling and "puckering" of the membrane subsequently resulting in the formation of microscopic holes which can be seen by optical or scanning electron microscopy. These holes then allow the restricted, but non-selective passage of acid from the starting to the receiving cell. The formation of holes was observed to be separate from the transport of iron and primarily due to the harsh conditions to which the membrane was subjected. The physical changes

Table 3-2. Time Required for Quantitative Transport of Iron at Various Temperatures

Temperature °C	Time Required for Quantitative Transport (hours)
5	250
22	48
37	22
50	10
65	4

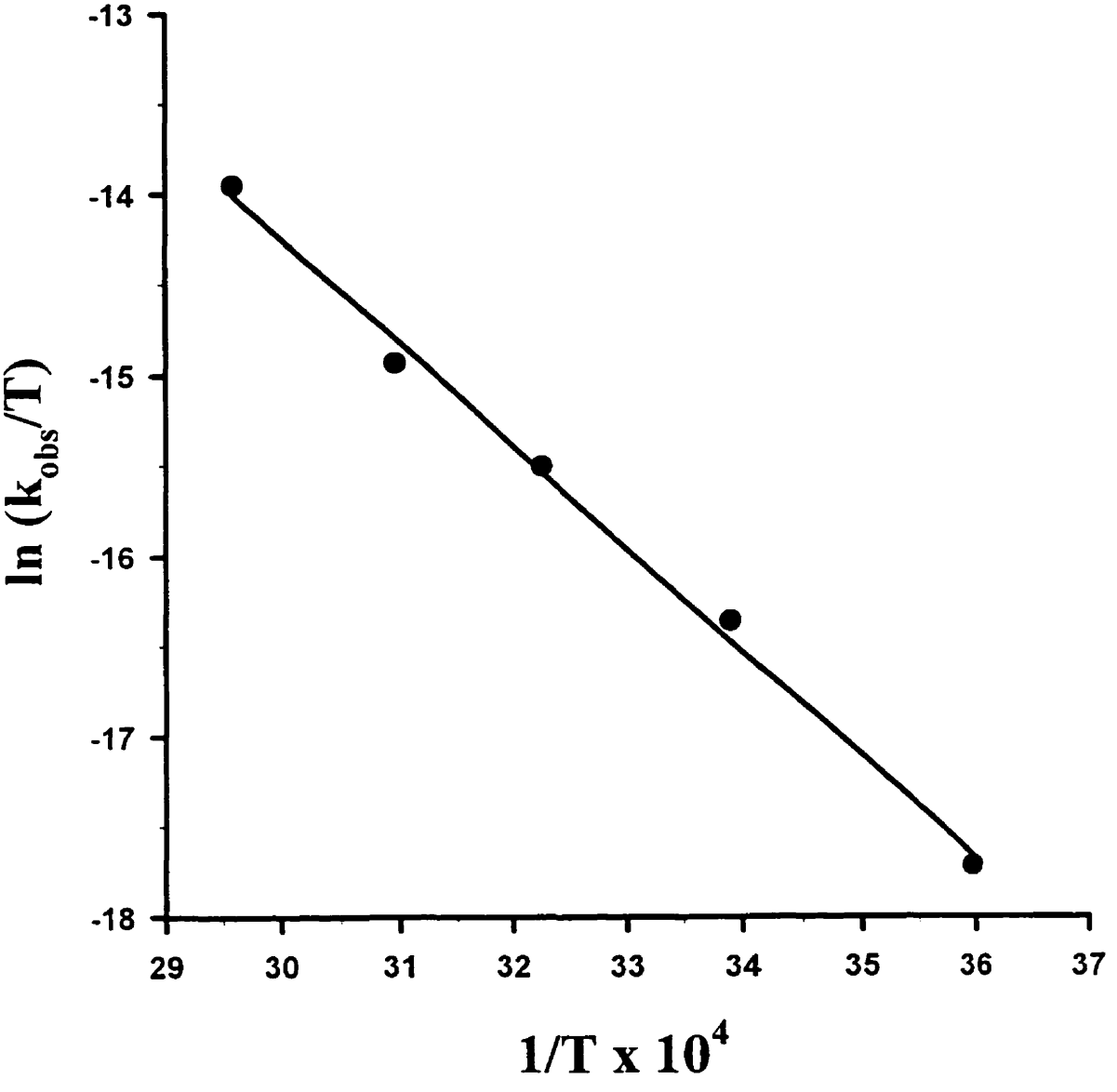

Figure 3-6. Arrhenius plot of 0.050 mm membrane at 5, 22, 37, 50, and 65°C. Starting cells contained 15 mg/L Fe in 5.0*M* HCl. Receiving cells contained 0.1*M* HCl.

associated with the degradation of the membrane in the harsh acid gradient environment are discussed in the Chapter 7.

3.7 Use of Salt to Form $FeCl_4^-$

It is possible to form the $FeCl_4^-$ complex by the addition of chloride salts. Preliminary investigations performed used 5.0 M HCl with 0.5 M salts (NaCl, KCl, LiCl) yielded no difference in transport rate. A further experiment was undertaken where a high concentration of a salt was used in the place of a high concentration of HCl. LiCl was chosen for its high solubility in water. Some acid was needed to keep the iron in solution so the experiment was performed with 60 ppm iron in 4.8 M LiCl and 0.2 M HCl in the starting flask and 0.1 M HCl in the receiving flask. The larger iron concentration was necessary because the salt solutions needed dilution by a factor of four before analysis by atomic absorption spectrophotometry. The results of the separation are presented in Figure 3-7. The separation profile looks quite different when compared to that of the experiment performed with 5.0 M HCl in the starting flask, although the total chloride concentrations are identical. When LiCl was used the separation proceeded much more slowly and was not quantitative within the time of the experiment. Using stability constants[6], the percentage of iron in the iron-tetrachloro complex in this LiCl solution was calculated to be 5.5%. Although this is less than the 7.7% when 5.0 *M* HCl is used, the lower concentration does not fully explain the dramatic change in transport behaviour. This indicates that the acid plays an integral part in the transport process in addition to the chloride concentration. It is probable that ether groups present in the polymer, which we believe participate in the chelation of the iron complex,

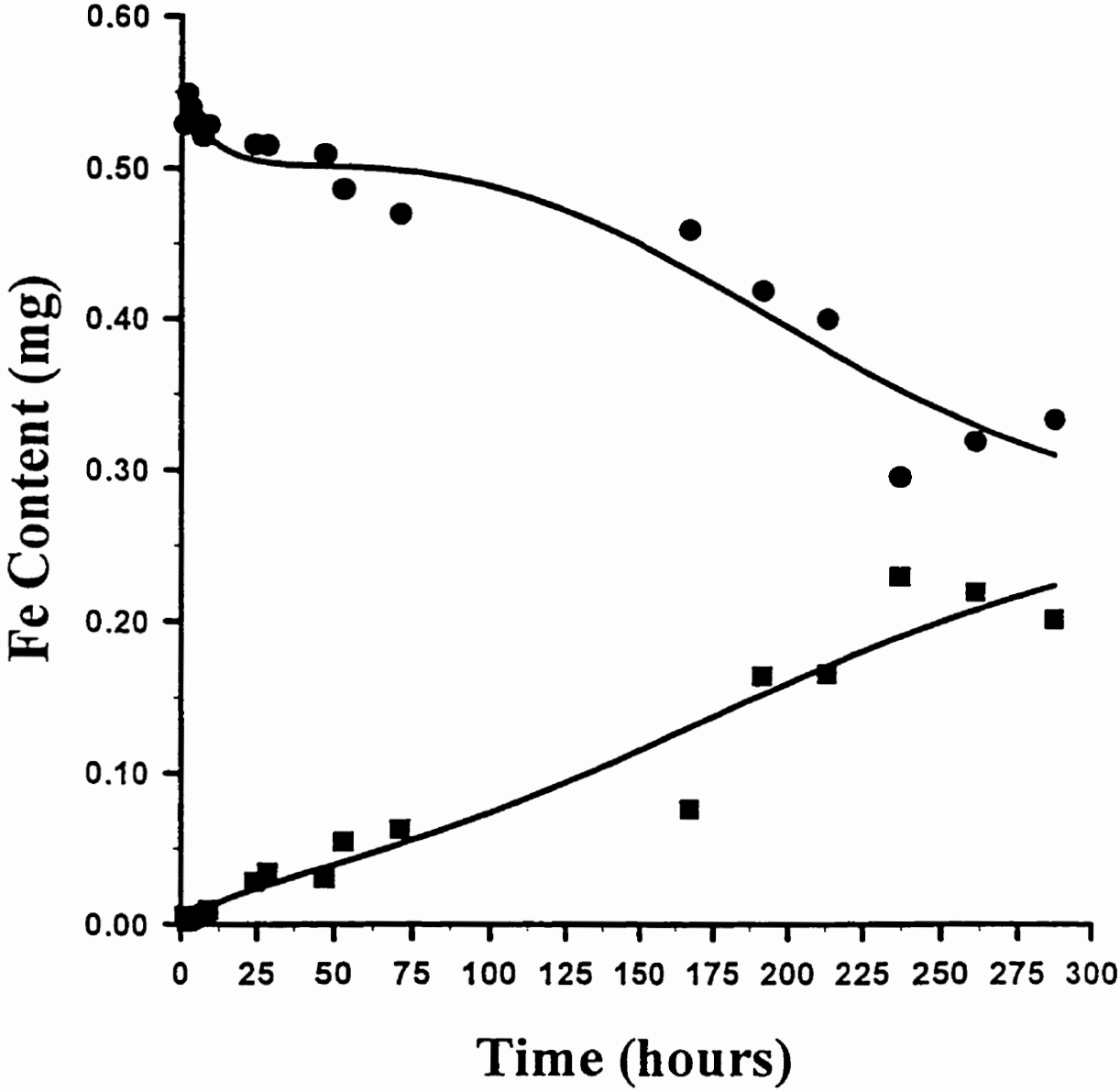

Figure 3-7. Iron separation profile with 10 mL of 60 mg/L Fe in 4.8*M* LiCl and 0.2*M* HCl in the starting cell and 30 mL of 0.1*M* HCl in the receiving cell.

—●— Starting cell
—■— Receiving cell

need to be protonated in order for the iron complex to be sorbed and transported through the membrane. In the LiCl experiment the transporting complex is $LiFeCl_4$, compared with the $HFeCl_4$ in the previous HCl experiments, this highlights the role that the size of the cation plays in the transport of the metal species across the membrane. Previous studies[9] by Hamon et al. indicate that the cation does indeed play a paramount role in the extraction of a metal complex by polyurethane foam. They found that the cation complexes were increasingly extracted in the following order ($Li^+ < Na^+ < Cs^+ < Rb^+ < K^+$) but this phenomenon was not observed in the current investigation. The difference may be due to the fact that although both our membrane material and the one used by Hamon are polyether-type polyurethane they are synthesized with different polyols. The polymer they used was prepared with polyethylene oxide (PEO) polyol see Figure 3-8, while the Stevens elastomer was synthesized with polytetramethylene oxide (PTMO). Therefore, the "sites" available in the membrane may have a different size preference for accepting different-sized cations and thus the complexes will be extracted and transported to differing degrees. The PTMO may not adopt the same helical structure as the PEO polymer favouring to complex cations of a different size.

3.8 Conclusions

The transport of iron from hydrochloric acid solutions less than 1.0 M through polyurethane membrane material does not occur. At 3.0 M HCl iron begins to be transported but this is quite slow and at concentrations of 5.0 M and greater, the transport becomes

Figure 3-8. The structures of polyethylene oxide and polytetramethylene oxide polyols used in polyurethane synthesis.

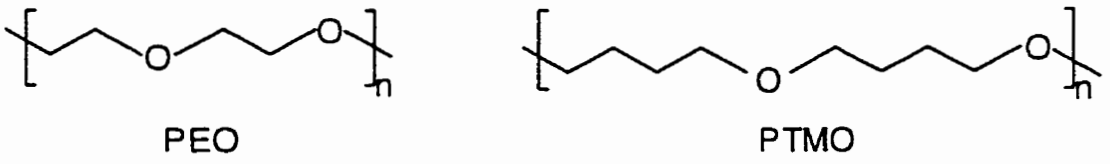

PEO PTMO

quantitative (>99%). This effect is due to the increased formation of the $HFeCl_4$ complex, which is the species extracted into the polyurethane membrane. The higher the HCl concentration, the greater the percentage of iron in the ferric-tetrachloro complex, which results in faster transport rates. Substituting hydrobromic acid, the transport rates quintuple, primarily due to the $HFeBr_4$ being a weaker acid. Thus more of the iron-bromide complex is in the protonated form which leads to a higher extraction rate and a faster transport.

The transport of iron from hydrochloric acid is aided by an increase in temperature. At 5 °C the quantitative transport of iron requires >10 days in comparison to 7 hours at 65 °C. Membrane thickness also plays an important role in the time needed for transport. Quantitative transport through a membrane 0.050 mm thick requires 48 hours as compared to 24 hours with a thickness of 0.025 mm.

The use of salt rather than hydrochloric acid to form the ferric-tetrachloro complex leads to a slower process that does not allow quantitative separation. This is possibly due to two factors, the size of the complex and the need for the ether groups present in the polymer to be protonated in order for transport to occur.

The phenomenon of quantitative transport across an ether-type polyurethane membrane provides evidence that the polymer may be used to separate mixtures of metals based on their ability to form halide complexes. Although the active transport of iron presented in this paper is not presently practical for its separation, it demonstrates the ability of polyurethane membranes to quantitatively transport a metal from one phase to another. The method is inherently simple and inexpensive compared to other available techniques and may prove an interesting alternative to other separation processes presently available for both

analytical and industrial applications.

References for Chapter 3

1. H. D. Gesser, G. A. Horsfall, K. M. Gough and B. Krawchuk, *Nature*, 268 (1977) 323.

2. R. F. Hamon, *PhD. Thesis* (University of Manitoba), 423, 1981.

3. J. Bjerrum, I. Lukes, *Acta Chemica Scand.* , 40 (1986) 31.

4. J. J. Oren, K. M. Gough, and H. D. Gesser, *Can. J. Chem.*, 57 (1978) 2032.

5. F. Cotton, G. Wilkinson; Advanced Inorganic Chemistry, John Wiley & Sons, 1988.

6. William A. Hunke and Lloyd E. Matheson, *J. of Pharmaceutical Sciences*, 70 (1981) 1313.

7. Shivaputrappa B. Harogoppad, Tejraj M. Aminabhavi, and Ramachandra H. Balundgi. *J. Applied Polymer Sci.*, 42 (1991) 1297.

8. S.B. Harogoppad and T.M. Aminabhavi, *Polymer*, 31 (1990) 2346.

9. R. F. Hamon, A. S. Khan and A. Chow, *Talanta*, 29 (1982) 313.

Chapter 4: The Separation and Isolation of Gold by Selective Extraction and Transport Through a Polyurethane Ether-Type Membrane

4.1 Introduction

The amount of extractable metal species in solution is dependent on the individual stability constants of the metal complexes, and the relative concentrations of the complexing species present in solution. For gallium and iron the extracting species were shown to be $GaCl_4^-$ and FeX_4^- (where: X = Cl, Br) respectively. Gold(III) is a softer acid than both Ga(III) and Fe(III) in a Pearson sense, so it prefers to form complexes with the larger halides and at lower halide concentrations. Gold(III) forms halide complexes with chloride, bromide, and iodide. The iodide complex is less stable than the chloride and bromide, and extremely difficult to prepare in pure form[1]. The gold(III) halide complexes are analogous to those of iron(III) and gallium (III), all of which possess the formula MX_4^- but possess different stereochemistry. Both $FeCl_4^-$ and $GaCl_4^-$ have tetrahedral structures about the metal atom, while the $AuCl_4^-$ complex is square planar.

Several researchers[2,3,4,5] have investigated the extraction of gold by polyurethane foam from aqueous media. Gold was observed to be extractable using an unloaded polyurethane ether-type foam from extremely acidic aqueous media (>1 M HCl). The extraction was found to be due to the presence of the $AuCl_4^-$ complex formed at sufficiently high HCl concentrations.

Figure 4-1. Structure of $FeCl_4^-$ and $AuCl_4^-$

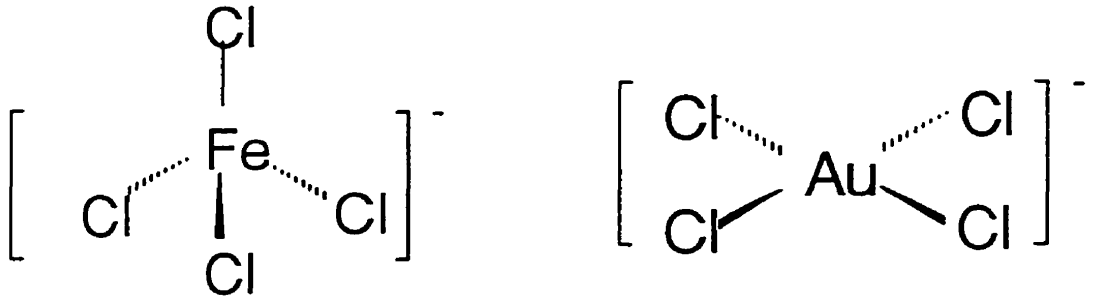

The objective of the investigation into the extraction and transport of gold through the polyurethane membrane was to demonstrate that gold can be quantitatively and selectively extracted from a starting cell solution and then transported and recovered in a receiving cell solution. The effect of the hydrophobicity/ hydrophilicity of the complex on the rate of extraction and transport were tested by using both the chloride ($HAuCl_4$) and bromide ($HAuBr_4$) complexes. In addition two membrane thicknesses were investigated to determine if the metal complex transport could be accelerated using a thinner membrane material. Also, the ability of the membrane material to concentrate gold was investigated utilizing different volumes of solution on either side of the membrane. The ability of the polyurethane membrane material to separate gold from other metals in solution was tested by attempting to separate

gold from a number of binary metal mixtures and from gold ore. The separation of gold from various matrices was used to demonstrate the ability of the membrane to separate and isolate gold from a complex mixture and show possible practical applications. The investigation into the extraction, transport and elution of gold from the membrane was undertaken to determine the viability of the separation, as well as to obtain a better understanding of the overall extraction and transport processes.

4.2 Extraction and transport of $HAuCl_4$ and $HAuBr_4$

Gold in the presence of suitable HCl and HBr concentrations forms either the $AuCl_4^-$ or $AuBr_4^-$ complexes[6,7,8,9] respectively. Characterization of the complexes has included the reporting of hydrolysis[10,11,12] constants for both the chloride and bromide complexes. The hydrolysis constants are shown in Table 4-1. The hydrolysis of either of the complexes can be represented by the following equations:

$$AuX_4^- + H_2O \rightleftharpoons AuX_3OH^- + X^- + H^+$$

$$AuX_3OH^- + H_2O \rightleftharpoons AuX_2(OH)_2^- + X^- + H^+$$

$$AuX_2(OH)_2^- + H_2O \rightleftharpoons AuX(OH)_3^- + X^- + H^+$$

$$AuX(OH)_3^- + H_2O \rightleftharpoons Au(OH)_4^- + X^- + H^+$$

where for example:

$$K_{3-4} = \frac{[AuX_3OH^-]\ [X^-]\ [H^-]}{[AuX_4^-]}$$

The hydrolysis equilibrium constants (K) can be used to determine the concentrations of each of the individual gold complexes at various halide concentrations. The concentrations of the gold chloride and gold bromide complexes as a function of ligand concentration were calculated using an algorithm similar to that shown in Chapter 2, Figures 2-5. The data for the gold chloride and gold bromide complexes is shown in Figures 4-2a and 4-2b respectively. The data obtained for the gold chloride complexes shows that above 4 x 10^{-4} M HCl the overwhelmingly predominant species is $AuCl_4^-$. Below 4 x10^{-4} M HCl we begin to see other gold chloride complexes forming. In comparison, Figure 4-2b showing the gold bromide complexes indicates a similar trend where above an HBr concentration of 3.5 x 10^{-4} the overwhelmingly predominant species is $AuBr_4^-$.

We investigated the use of both these complexes for the extraction and transport of gold through a polyurethane ether-type membrane. An experiment with a starting cell

Table 4-1. Hydrolysis constants of the gold chloride and gold bromide complexes[13]

Complex	K_{3-4}	K_{2-3}	K_{1-2}	K_{0-1}
gold chloride	7.1×10^{-7}	7.1×10^{-8}	1.1×10^{-8}	$\sim 2.1 \times 10^{-9}$
gold bromide	3.1×10^{-9}	1.1×10^{-9}	not determined	not determined

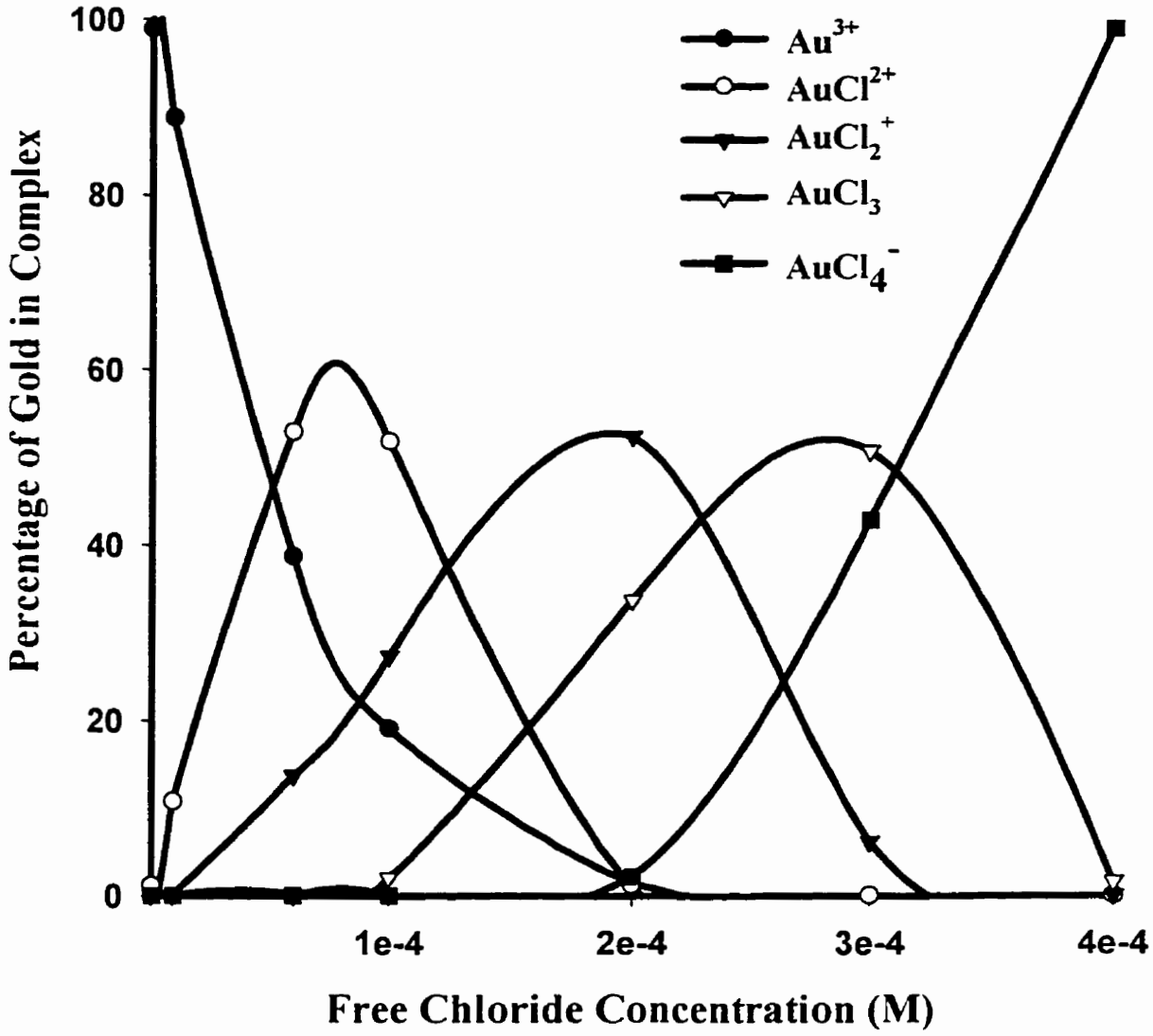

Figure 4-2a. The percentage of gold in various gold chloride complexes at different chloride concentrations.

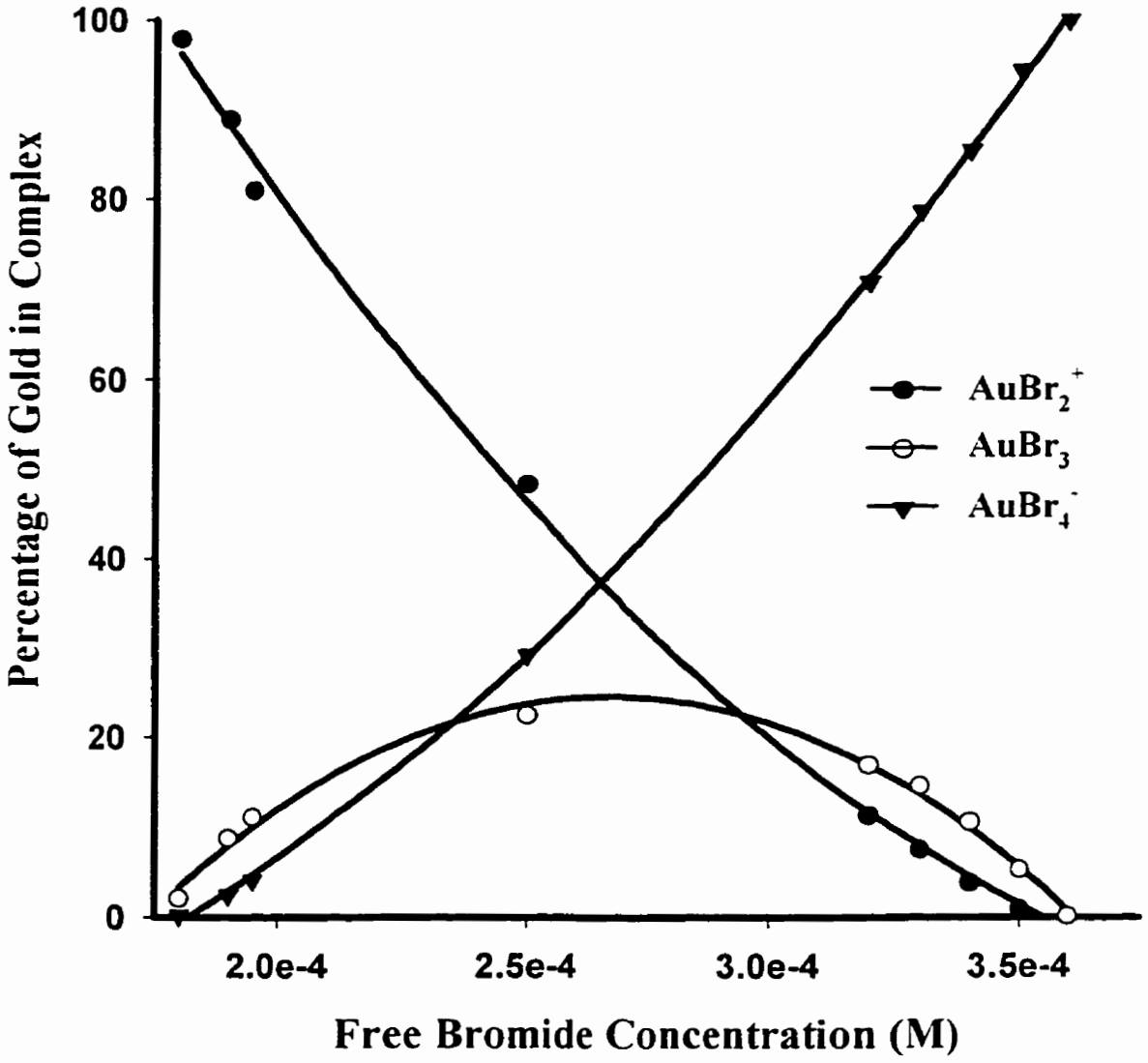

Figure 4-2b. The percentage of gold in various gold bromide complexes at different bromide concentrations

solution of 2.0 M HCl and 16 mg/L Au combined with 0.5 M KCl in the receiving cell was performed with the result shown in Figure 4-3. The amount of gold in the starting cell is shown to decrease to the point where it is quantitatively extracted into the membrane after 50 hours. Conversely, we see the appearance of gold in the receiving cell after just 2 hours, which increases to the point where quantitative recovery of the gold (>97%) is achieved after 50 hours. This experiment was also performed with 2.0 M HBr/ 16 mg L^{-1} Au in the starting cell combined with 0.5 M KBr in the receiving cell. These conditions were chosen to allow a direct comparison between the two gold halide complexes. The results of this experiment are also shown in Figure 4-3. The quantitative extraction of gold under these conditions takes place in under 20 hours, while the quantitative recovery of the gold in the receiving cell occurs in approximately 40 hours. The difference in extraction and transport rates of these two complexes can be explained by the relative hydrophobicity of each of the complexes. The $HAuBr_4$ complex, possessing the larger bromide ligands, is more hydrophobic than its chloride analogue. Thus, the bromide complex will be more readily extracted into the hydrophobic membrane material. One would also expect that the stability constants of the gold complexes would play a factor in the extraction rate as shown by Oleschuk and Chow[14] and as shown in Chapter 3 for iron halide complexes. Pan and Wood[15,16] have performed detailed laser Raman spectroscopy studies on gold (III) chloride and bromide complexes in the concentration ranges in which we are working and found that the overwhelmingly predominant species present under these conditions were the $AuCl_4^-$ and $AuBr_4^-$ complexes. This explains the reason for the extraction into the membrane material but not the transport of the metal species through the membrane and recovery of the gold in the receiving cell.

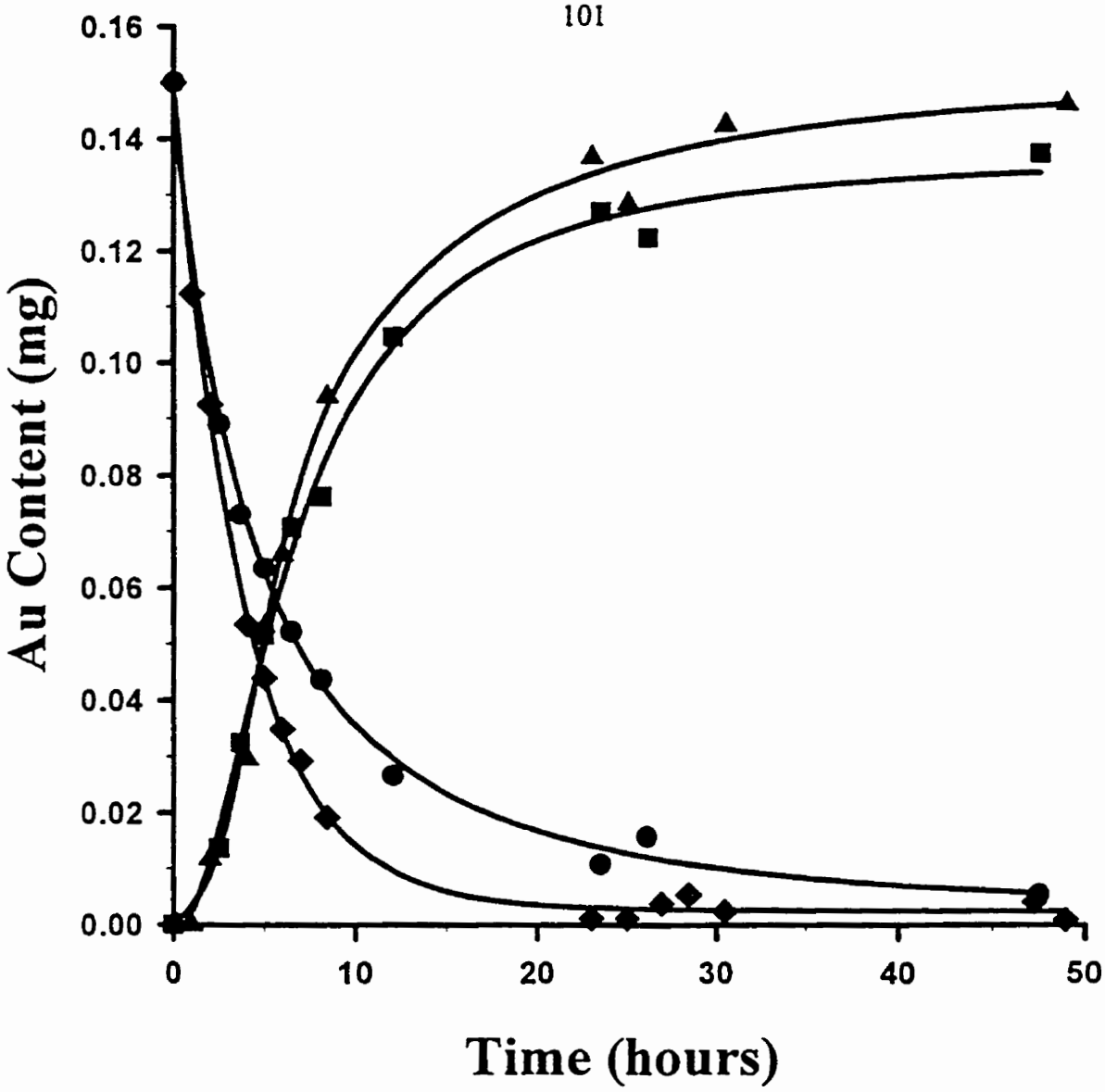

Figure 4-3. Extraction and transport of $HAuCl_4$ and $HAuBr_4$ through a polyurethane membrane. Starting cell contains 10 mL of 15 mg/L Au in 2.0 M HCl or HBr. Receiving cell contains 0.5 M KCl or KBr.

- -●- Starting cell, $HAuCl_4$
- -■- Receiving cell, $HAuCl_4$
- -◆- Starting cell, $HAuBr_4$
- -▲- Receiving cell, $HAuBr_4$

Transport in the membrane material after extraction appears to follow Fick's law of diffusion and is concentration independent. During the extraction of the gold species, the membrane took on the same golden yellow colour as the aqueous phase. This indicates that the state of gold is identical in the two phases (i.e. $HAuBr_4$). This same phenomenon has been observed by Fang et al[17] for the extraction of $KAuCl_4$ with benzo-15-crown-5.

The gold complex diffuses through the membrane to the membrane/receiving cell interface and is then eluted into the receiving cell solution. The conditions used in the receiving cell (0.5 M KCl and 0.5 M KBr respectively) favour the formation of the deprotonated $AuCl_4^-$ and $AuBr_4^-$ complexes once they have come in contact with the receiving cell solution (Scheme 4-1). This phenomenon has been verified by Ultraviolet/ visible spectra of the receiving cell solutions. Both starting and receiving cell solutions possessed identical spectra with λ_{max} at 374 nm and 314 nm for the $AuBr_4^-$ and $AuCl_4^-$ complexes respectively.

In addition to using high acid concentrations in the starting cells to form the gold halide complexes, high salt concentrations were also investigated. Three experiments were performed using 2.0 M HCl, 2.0 M NaCl and 2.0 M KCl in the starting cells with all the receiving cells containing 0.05 M HCl.

Scheme 4-1. Schematic representation of the proposed mechanism for gold transport.

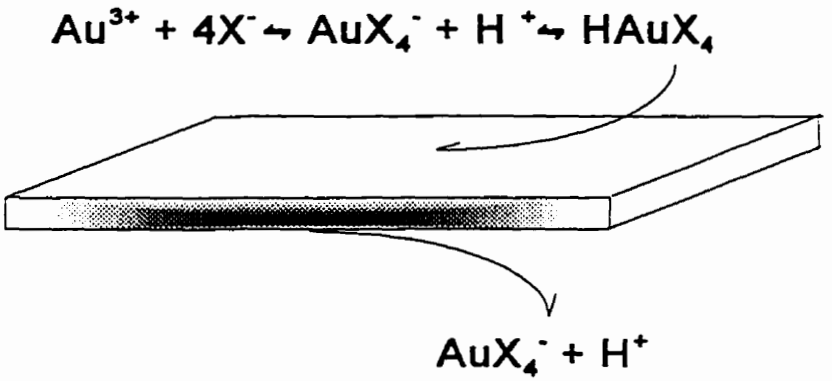

These conditions lead to the formation of the $HAuCl_4$, $NaAuCl_4$ and $KAuCl_4$ ion pairs respectively. Results of the three experiments are presented in Figures 4-4a, 4-4b and 4-4c respectively. The results of using each starting cell condition show gold transport, but the rate of gold transport is quite different. The gold transport for experiments using HCl in the starting cell is faster by an order of magnitude than when using either NaCl or KCl. Comparing the rates of extraction and transport, the ion pairs display the following trend for extraction and transport rate:

$$HAuBr_4 > NaAuBr_4 > KAuBr_4$$

The overall difference in rates of extraction may be due to several factors including: the relative hydrophobicities of each of these complexes; the individual stability constants of the complexes; and the ability of the cation to form an ion pair with the gold complex. The nature of the cation has been shown by Hamon et al.[18] to strongly effect the rate and extent of extraction into a polyurethane foam sorbent material. The rates of extraction for the gold complexes into the membrane material are faster for complexes with a smaller cation while other polyurethane elastomers have preferred the larger cation for enhanced extraction. The different extraction behaviours exhibited by different polyurethane materials can be explained by the type of polyol material used for the chemical synthesis of the polyurethane material. For example the polymer used by Hamon et al. was prepared using a polyethylene glycol polyol while the Stevens elastomer (used in this investigation) was prepared with a

polytetramethylene glycol polyol. In addition, the use of polyurethane foams prepared from polyester polyols produces different extraction characteristics[19]. The different polyols lead to drastically different extraction behaviours.

Using the extraction data presented in Figures 4-4a, 4-4b and 4-4c we can see that the smaller cations are extracted preferentially over complexes incorporating larger cations in the ion pair.

In addition to using HBr alone to form the $HAuBr_4$ complex, we have shown that a combination of salt and acid is effective for the formation of the $HAuBr_4$. Experiments using starting cell conditions of 2.0 M KBr/1.0 M HCl were effective for the transport of the gold species. The success of this experiment shows that HCl can be used to protonate the $AuBr_4^-$ complex formed by the addition of KBr and demonstrates that the extremely high acid concentrations that we have used for the bulk of our experiments (i.e. 2.0 M) may not be required. The use of lower acid concentrations has two intrinsic advantages. The high acid concentrations are responsible for membrane degradation and eventual membrane failure. The use of lower acid concentrations would lead to prolonged membrane life. Also, the KCl and KBr salts are less expensive than the corresponding acids making the separation more cost effective. This is also less harmful from an environmental standpoint.

4.2.1 Choice of Receiving Cell Composition

The choice for the solution in the receiving cell is extremely important to the overall separation process. The receiving cell solution must allow the elution of the metal complex from the membrane material and provide a stable environment to prevent the hydrolysis and

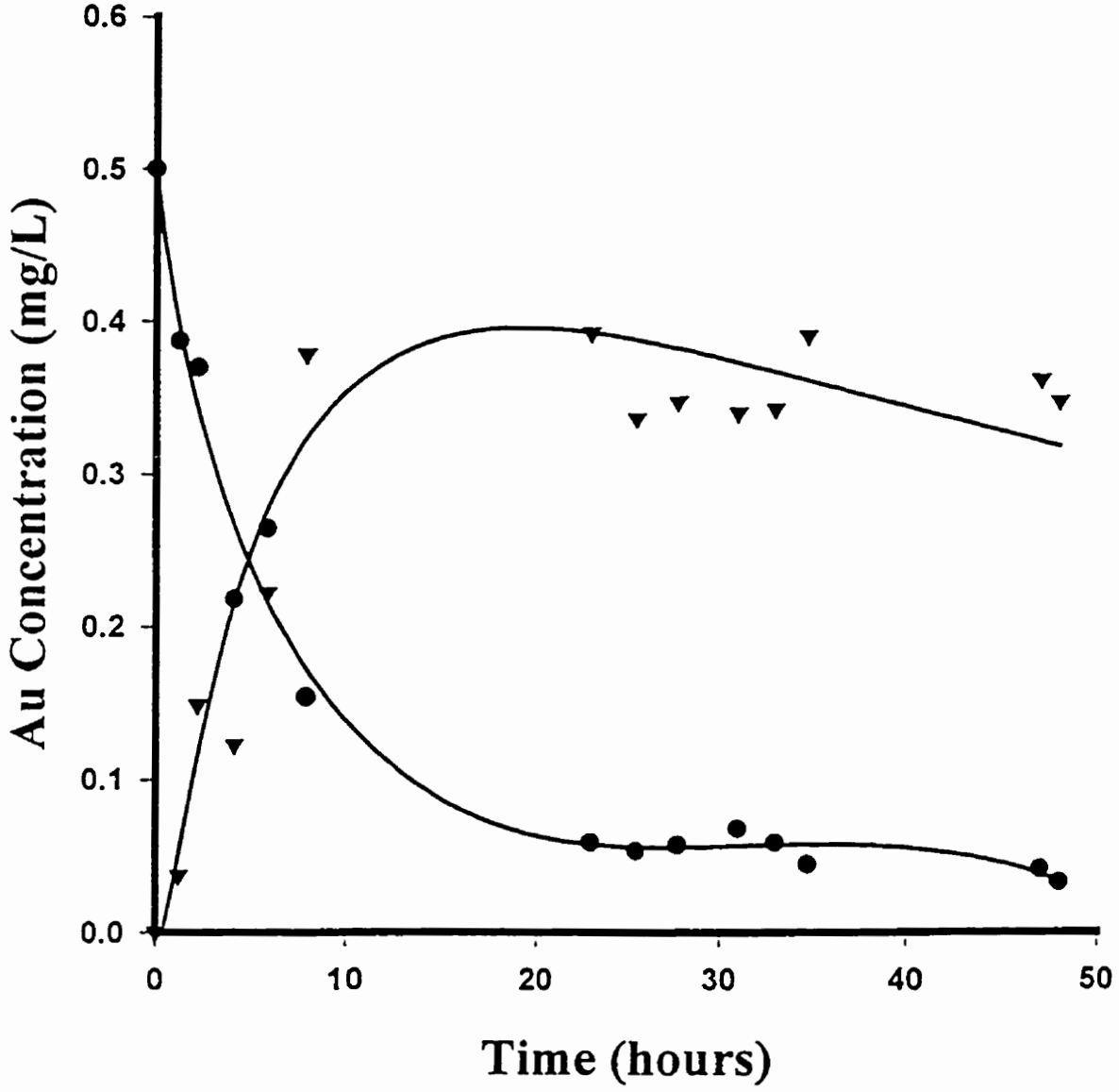

Figure 4-4a. The effect of using different cations in the starting cell on the extraction and transport of gold.

—●—Starting Cell, 10 mL of 2.0 M HCl
—▼—Receiving Cell, 30 mL of 0.05 M HCl

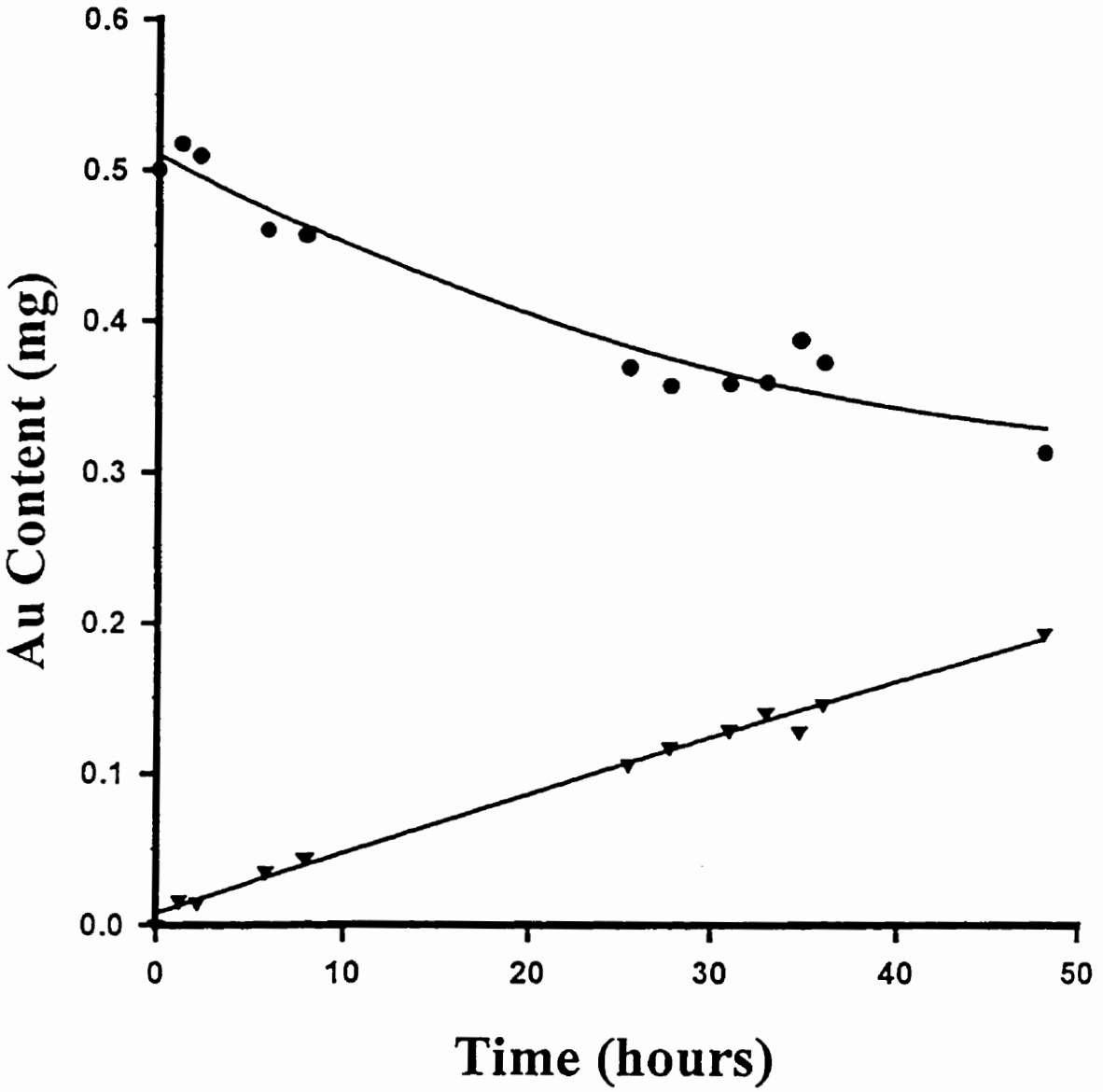

Figure 4-4b. The effect of using different cations in the starting cell on the extraction and transport of gold.

—●— Starting cell, 10 mL of 2.0 M NaCl
—▼—Receiving cell, 30 mL of 0.05 M HCl

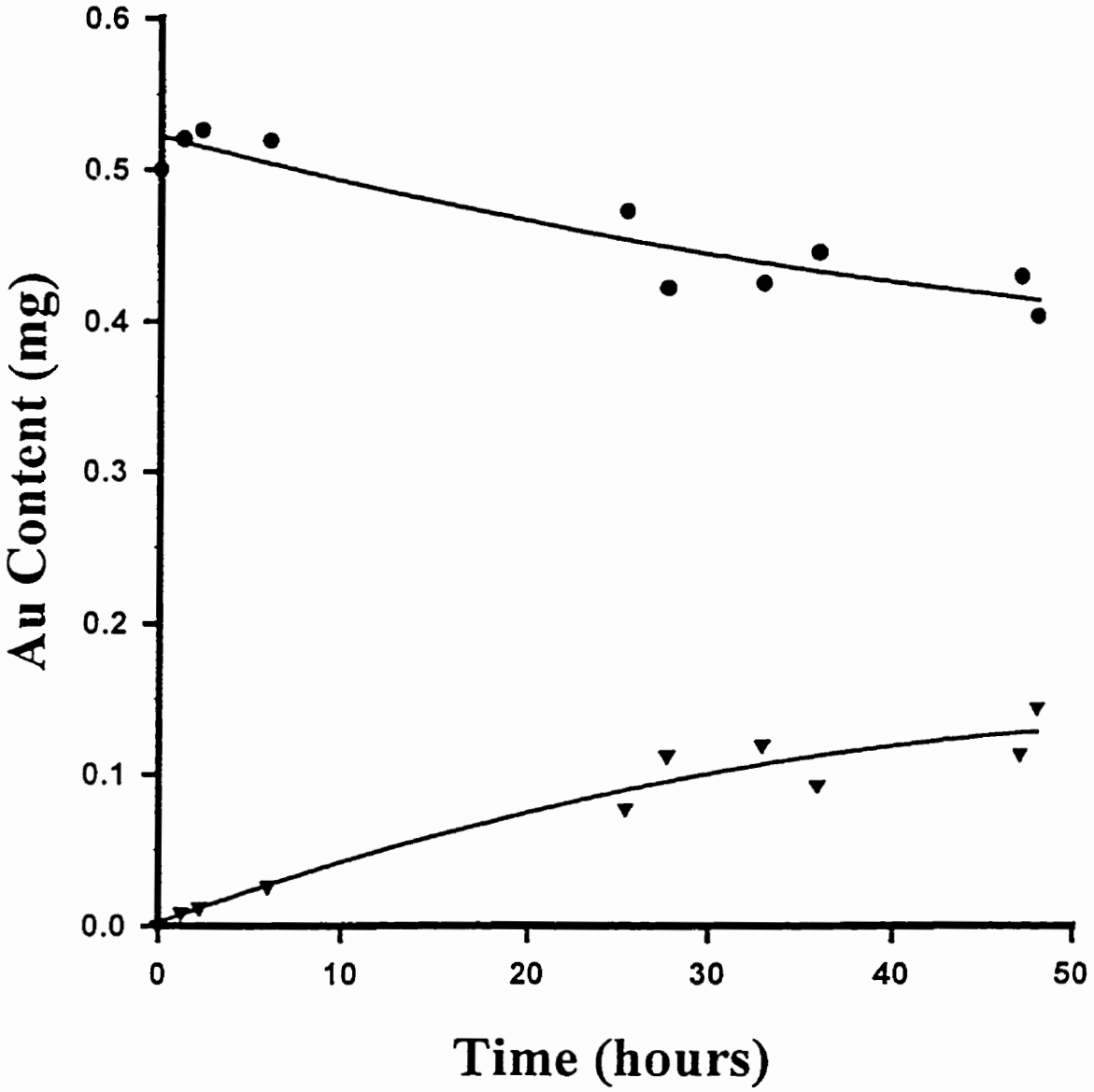

Figure 4-4c. The effect of using different cations in the starting cell on the extraction and transport of gold.

—●— Starting cell, 10 mL of 2.0 M KCl
—▼—Receiving cell, 30 mL of 0.05 M HCl

precipitation of the metal species. In addition, the solution must not allow for the sorption of the metal complex back into the membrane material.

Initially the receiving cell concentrations chosen for gold transport were similar to those used for the iron experiments (Chapter 3). Preliminary data showed that this composition was unsatisfactory for the quantitative recovery of the gold complex in the receiving cell. Different hydrochloric acid concentrations in the cell were tried ranging from no acid to 0.1 M HCl with little change in reproducibility and performance. In fact, when extremely low amounts of acid were used, the gold precipitated at the membrane/receiving cell solution interface. The identity of the precipitate was verified as gold using X-ray fluorescence spectroscopy (XRF). Later, the corresponding potassium salt was tried in the receiving cell and produced much better results, providing a better cell-to-cell reproducibility and a higher recovery of the gold species. After examining several salt concentrations as the receiving cell solution 0.5 M KCl was chosen for experiments where the $AuCl_4^-$ complex was used and 0.5 M KBr, for experiments where the $AuBr_4^-$ complex was desired. Examples of experiments performed with different receiving cell conditions are shown in Figures 4-5a - 4-5c. Figure 4-5a shows the results obtained using deionised water as the receiving cell solution. Although using deionised water led to the deprotonation of the gold complex once it was in the receiving cell, the complex was not stable in this environment and precipitated, leading to low recoveries and poor reproducibility. Figure 4-5b shows the use of 0.001M HCl as the receiving cell solution. In this case there was no precipitation but low recoveries and poor reproducibility still resulted. Using 0.5 M KCl as the receiving cell solution displayed a marked improvement over the other conditions used. The salt receiving cell

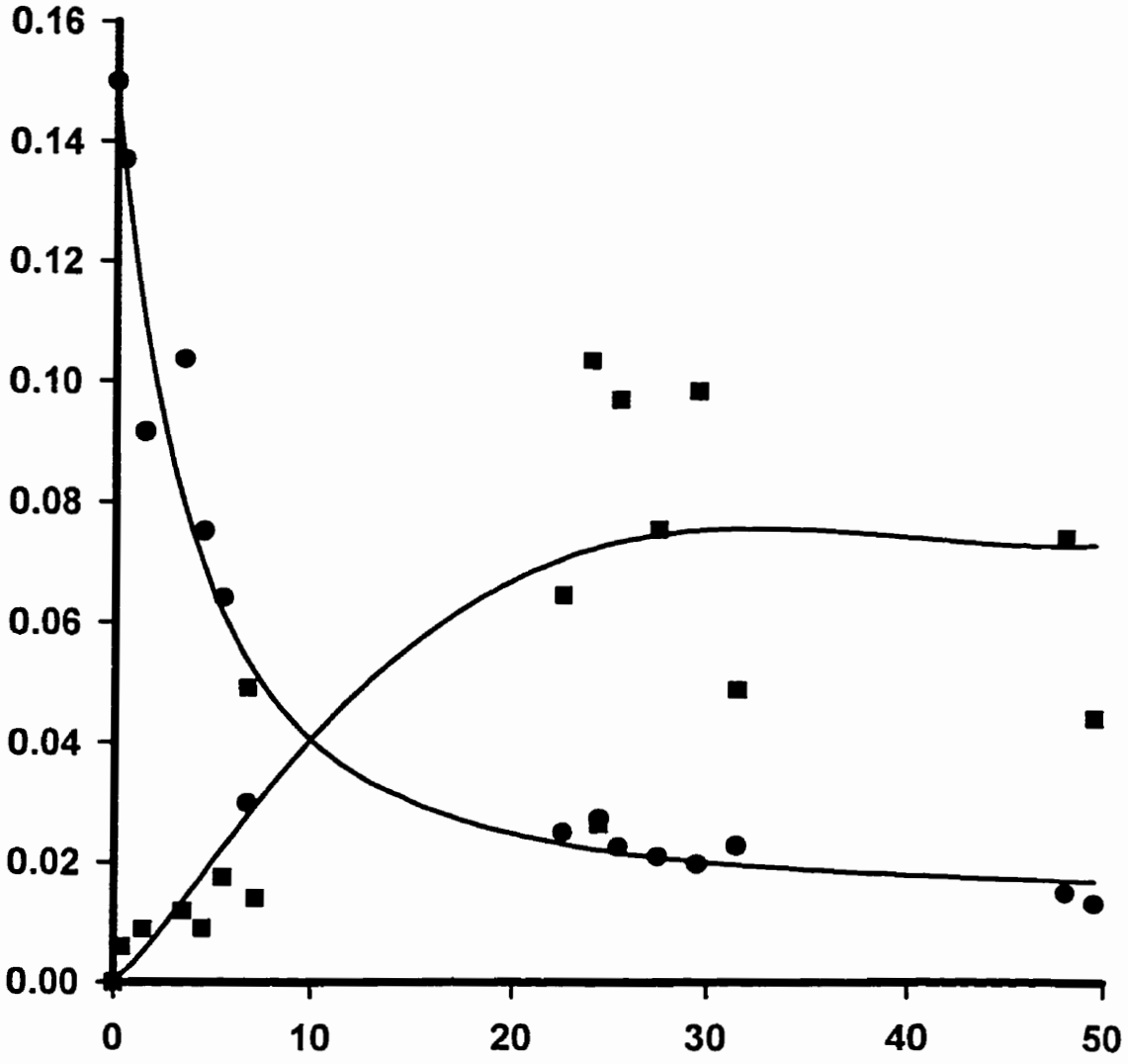

Figure 4-5a. The use of deionized water as the receiving cell solution

—●— Starting cell containing 10 mL of 15 mgL^{-1} Au/2.0 M HCl

—■— Receiving cell 30 mL of deionized water.

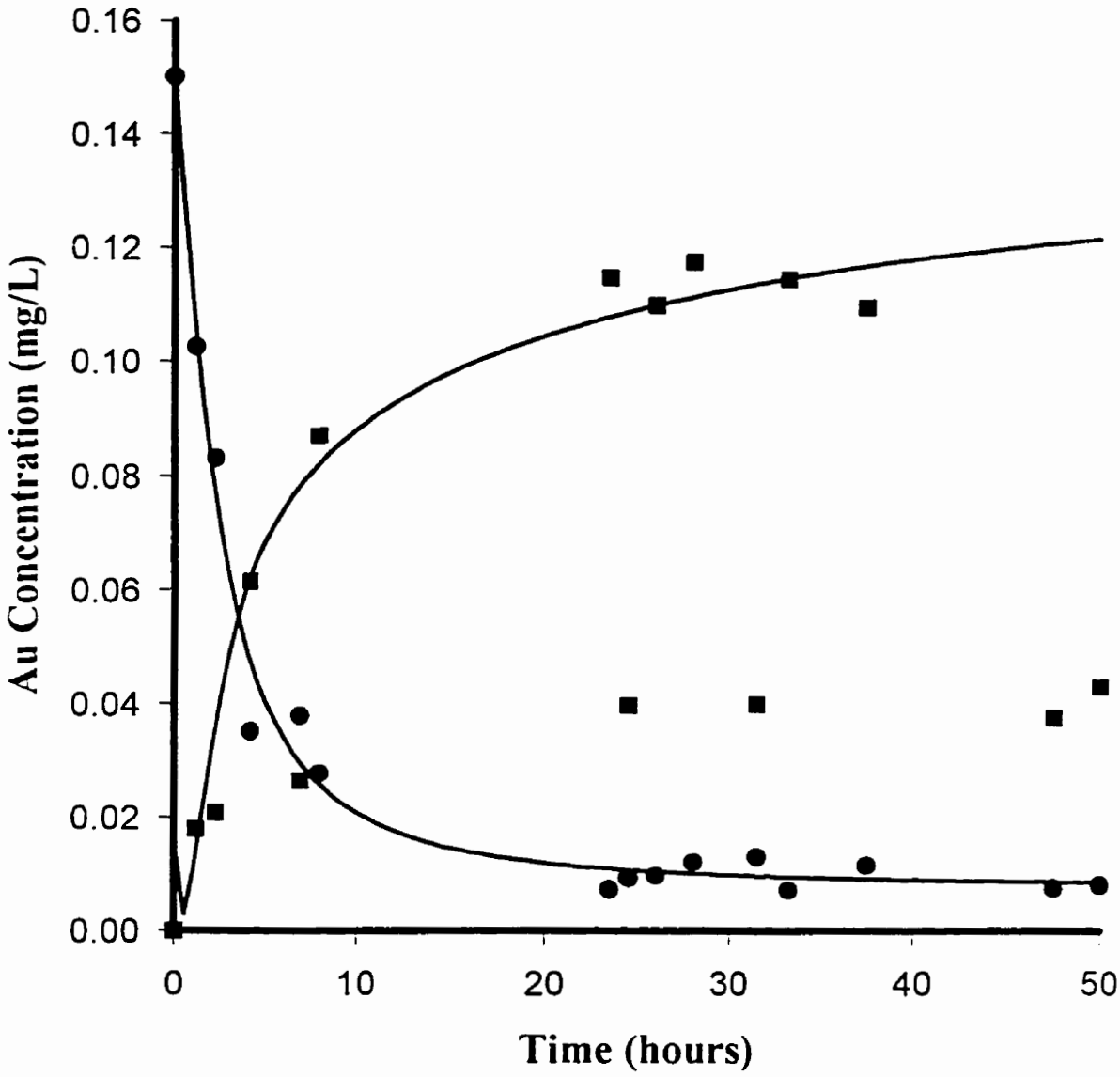

Figure 4-5b. The use of 0.001 M HCl as the receiving cell solution
— ●— Starting cell containing 10mL of 15 mgL^{-1} Au/2.0 M HCl
— ■— Receiving cell 30 mL of 0.001 M HCl

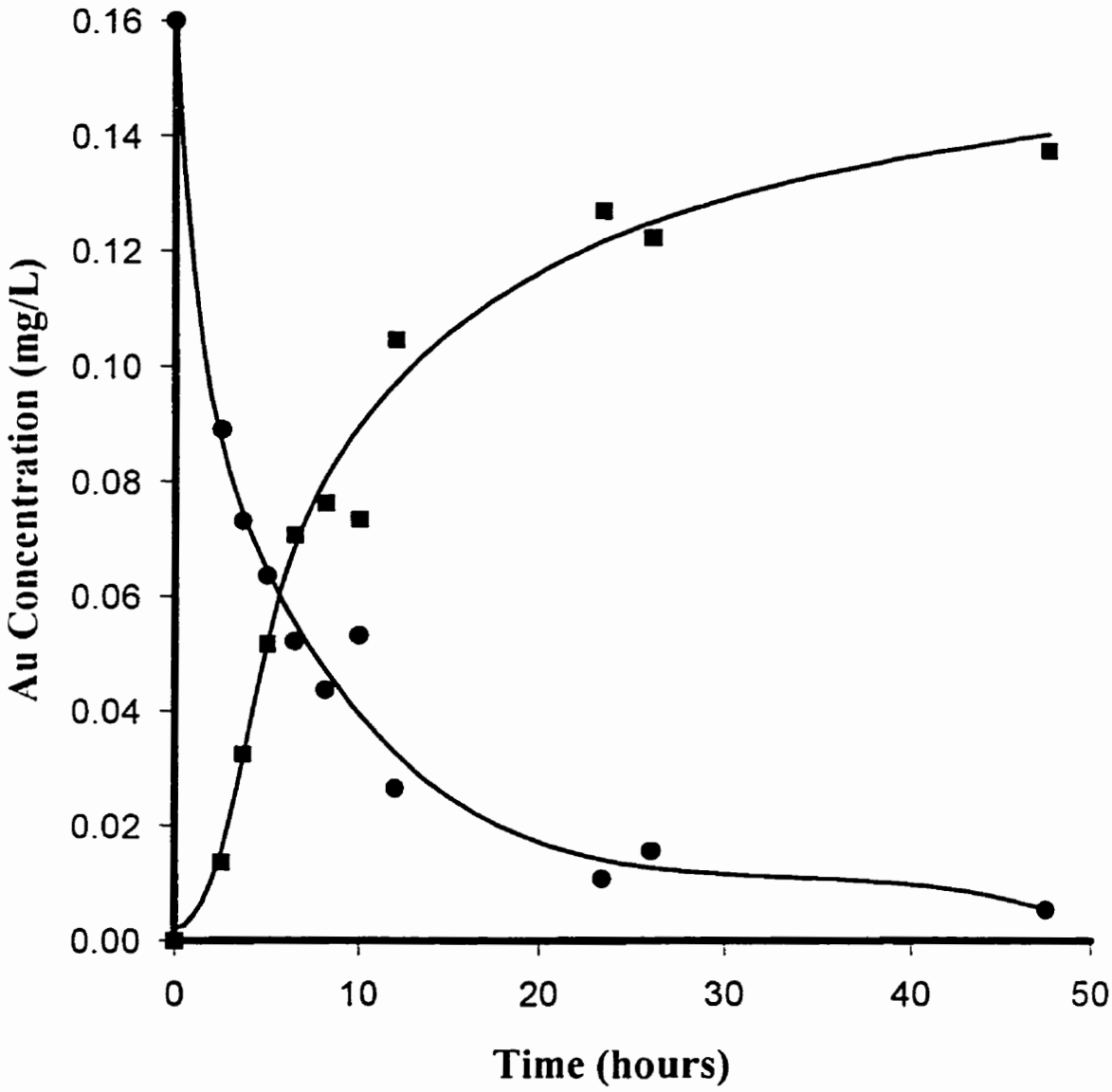

Figure 4-5c. The use of 0.5 M KCl as the receiving cell solution
—●—Starting cell containing 10 mL of 15 mg L^{-1} Au/2.0 M HCl
—■—Receiving cell 30 mL of 0.5 M KCl

solution produced high recoveries (>95%) and better cell-to-cell reproducibility. The relatively large salt concentration in the receiving cell provides a stable environment for the gold, preventing it from precipitating.

The quantitative recovery of the gold in the receiving cell is attributed to the pH of the receiving cell solution. The pH of the receiving cell solution favours the formation of the non-protonated gold complexes (ie. $AuCl_4^-$ and $AuBr_4^-$). The protonated neutral species are the only complexes that are extractable into the membrane material. Therefore, the protonated gold complexes diffuse through the membrane material and elute into the receiving cell solution where they form either the $AuCl_4^-$ or $AuBr_4^-$ non-protonated complexes, depending on the salt used. The non-protonated gold halide complexes are not extracted by the membrane, leaving the gold trapped in the receiving cell solution where it can be recovered. After the $HAuBr_4$ complex is eluted and deprotonated the pH of the receiving cell solution drops.

In addition to the gold complex, acid is also transported across the membrane independent of the gold complex, contributing to the lowering of the pH of the receiving cell. With small amounts of acid transported there is no adverse effects on the recovery of the gold complex. If the experiment is allowed to run for an extended period of time there is a build up of acid in the receiving cell solution causing the gold complex to re-protonate and re-enter the membrane. To try and prevent the lowering of the receiving cell pH we tried three different buffers in the receiving cell to neutralize the transported acid. The various buffers that were tried included: citrate, carbonate and acetate. The use of a buffer in the receiving cell prevented the pH from decreasing as expected, but also produced much lower recoveries

than expected. Recoveries without buffers were typically >95% while with buffers recoveries were typically around 60-70%. Results showing the use of an acetate buffer in the receiving cell are shown in Figure 4-6.

4.2.2 Determination of Transporting Complex

The identity of the transporting gold complex has been postulated as being the $HAuBr_4$ complex. To identify the complex that was being transported through the membrane material an experiment was performed using a large membrane diffusion cell. The large cell enables the facile determination of pH in the receiving cell of the membrane apparatus. By simultaneously monitoring the pH and gold concentration in the receiving cell and comparing that to a blank we can confirm the identity of the transported complex ($HAuBr_4$). An experiment was performed with a starting cell composition of 9L of 2.0 M HCl/ 0.25 M KBr/ 1 mg L^{-1} and 650 mL of 0.5 M KBr in the receiving cell. The pH and the gold concentration in the receiving cell were monitored throughout the experiment by pH electrode and by taking small aliquots of the receiving cell solution for atomic absorption analysis. The experiments yielded the data shown in Table 4-2 and 4-3. In the blank and gold experiments the pH of the receiving cell continually decreased for the duration of the experiment. Comparing the pH data from each experiment shows the pH of the experiment containing gold consistently has a lower pH in the receiving cell throughout the duration of the experiment. By subtracting the amount of acid transported at different times in the blank, $[H^+]_{blnk}$, from the experiment containing gold,$[H^+]_{Au}$, we can determine the amount of acid due solely to gold complex transport.

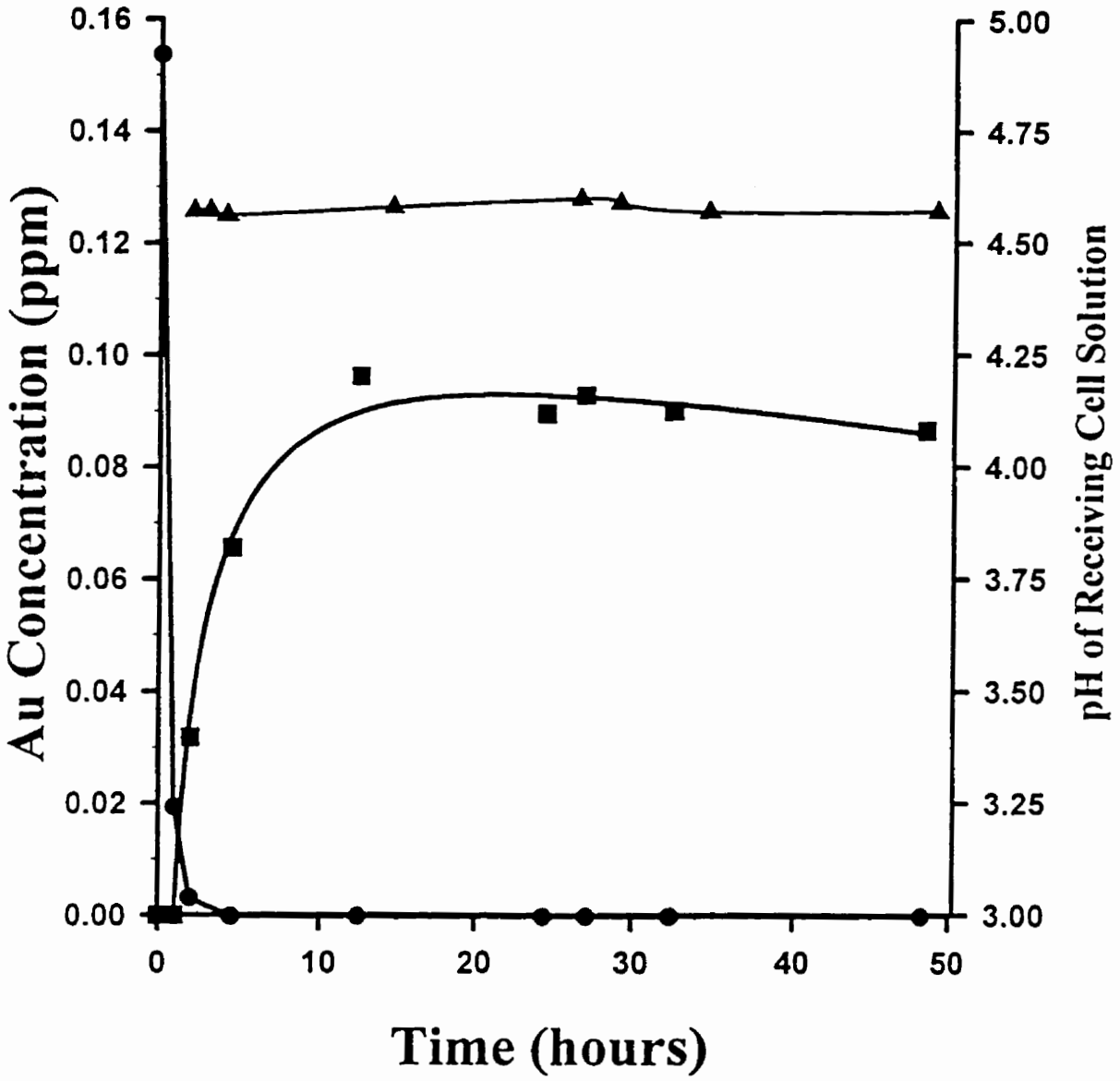

Figure 4-6. The use of 0.1 M acetate buffer in the receiving cell

—●— Starting cell, 30 mL of 5mg L^{-1} Au/ 2.0 M HBr(stirred)
—■— Receiving cell, 10 mL of 0.5 M KBr, 0.1 M Acetate Buffer, pH = 4.75
—▲— pH of the receiving cell solution

Table 4-2. The acid and gold concentrations within the receiving cell at different times

Time (hours)	$[H^+]$ M L^{-1}	[Au] M L^{-1}
0	2.08×10^{-5}	0
24	5.01×10^{-5}	1.45×10^{-5}
48	8.31×10^{-5}	2.88×10^{-5}
72	1.20×10^{-4}	4.20×10^{-5}
96	1.28×10^{-4}	5.38×10^{-5}
120	1.51×10^{-4}	5.84×10^{-5}
168	1.77×10^{-4}	6.80×10^{-5}

Table 4-3.The concentration of H^+ in the receiving cell solution during a blank experiment

Time (hours)	$[H^+]$ M L^{-1}
0	2.08×10^{-5}
25	3.89×10^{-5}
49	5.37×10^{-5}
97	9.33×10^{-5}
118	1.02×10^{-4}
166	1.25×10^{-4}

$$[H^+]_{Au} - [H^+]_{blank}$$

The data is shown in table 4-4 and Figure 4-7. Both Figure 4-7 and Table 4-4 show good agreement between the amount of acid due to gold transport and the gold concentration in the receiving cell showing that there is a stoichiometric amount of H^+ transported with the $AuBr_4^-$. This provides evidence that the $HAuBr_4$ complex is responsible for the gold extraction and transport under these conditions.

4.3 Membrane Thickness

To determine the effect of membrane thickness on the rate of transport, two different thicknesses of 0.025 mm and 0.05 mm were used. The solution conditions consisted of 2.0 M HBr/15 mg L^{-1} Au in the starting cell and 0.5 M KBr in the receiving cell. As expected the time required for the transport of the gold from the starting to receiving cells was faster for the thinner membrane. A transport profile for each thickness is shown in Figure 4-8. The quantitative recovery of the gold in the receiving cell required approximately 20 hours for the 0.025 mm membrane compared to approximately 40 hours for the 0.05 mm membrane.

Table 4-4. The difference in acid transport for the blank and gold experiment compared to the gold concentration in the receiving cell.

Time	$[H^+]_{blnk}$	$[H^+]_{Au}$	$[H^+]_{Au} - [H^+]_{blnk}$	[Au]
0	2.08×10^{-5} M	2.08×10^{-5} M	0	0
24	3.89×10^{-5}	5.01×10^{-5}	1.12×10^{-5}	1.45×10^{-5}
48	5.37×10^{-5}	8.31×10^{-5}	2.93×10^{-5}	2.88×10^{-5}
72	7.50×10^{-5}	1.20×10^{-4}	4.5×10^{-5}	4.20×10^{-5}
96	9.33×10^{-5}	1.34×10^{-4}	4.07×10^{-5}	5.38×10^{-5}
120	1.02×10^{-4}	1.51×10^{-4}	4.90×10^{-5}	5.84×10^{-5}
168	1.25×10^{-4}	1.77×10^{-4}	5.20×10^{-5}	6.8×10^{-5}

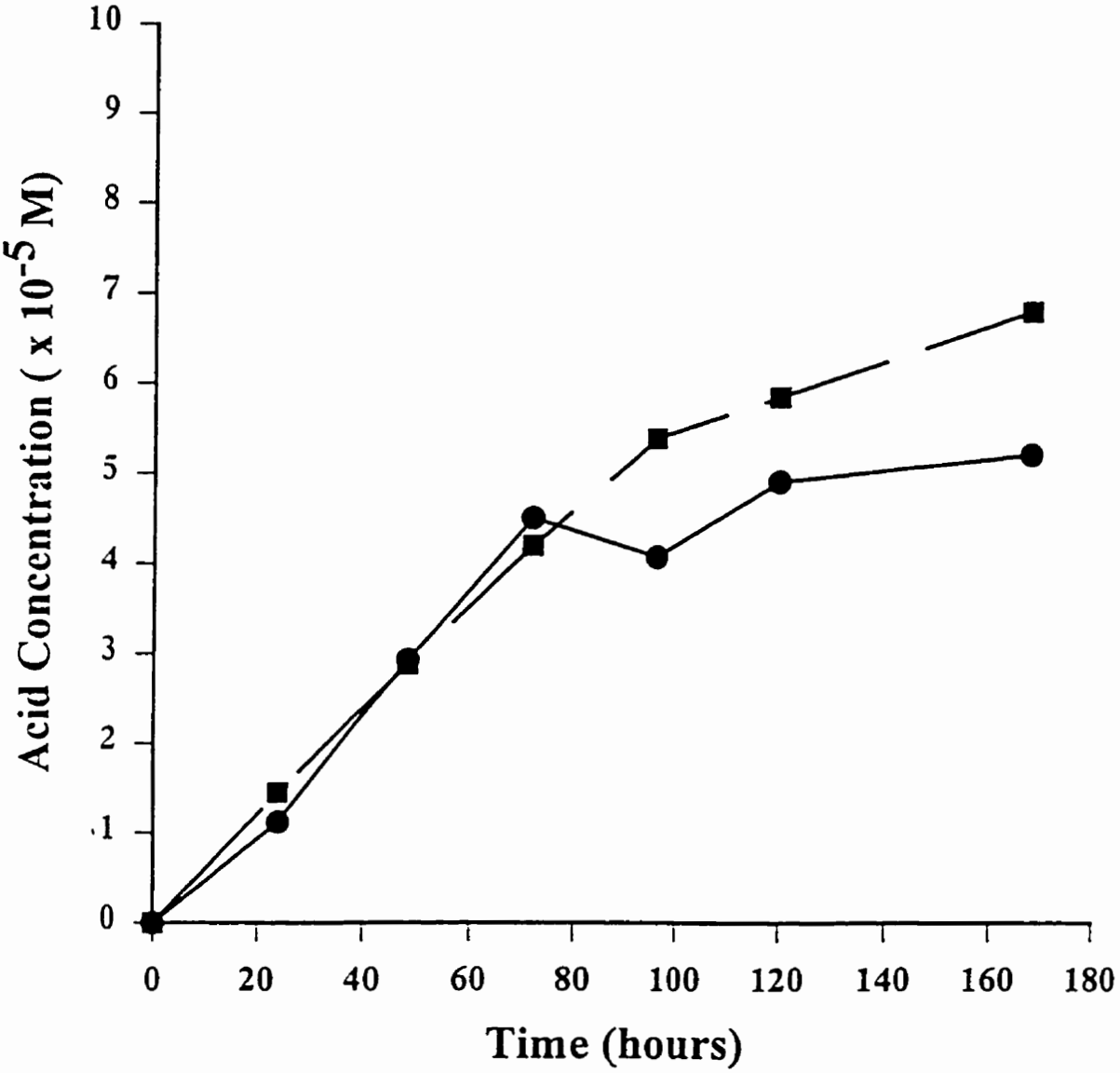

Figure 4-7. Comparison of the amount of acid transported and the amount of acid expected in receiving cell if species transported is $HAuBr_4$.

—●— **Acid concentration due to Au transport calculated by blank subtraction**

—■— **Acid concentration expected with 1:1 stoichiometric ratio for H^+ and $AuBr_4^-$**

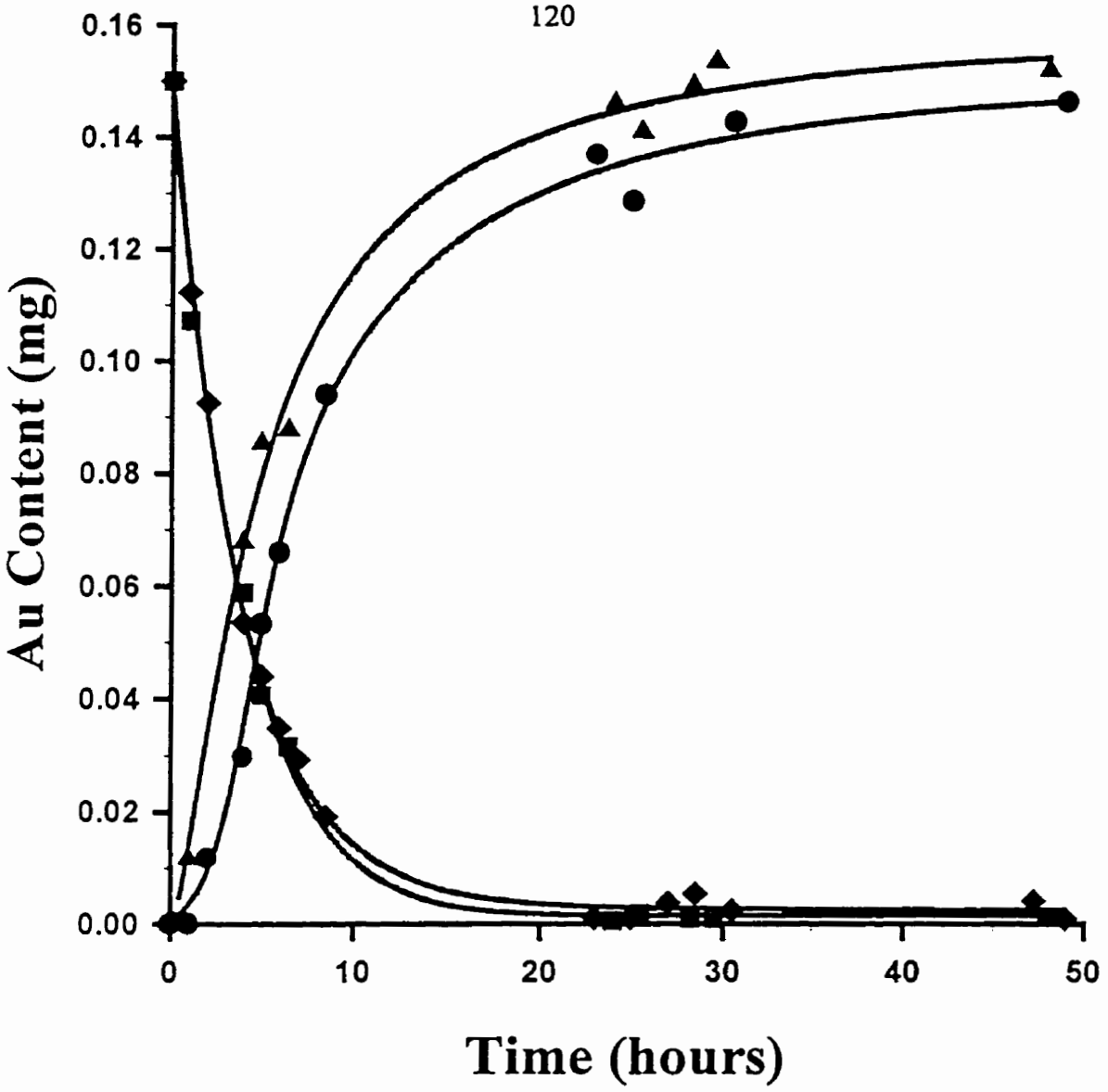

Figure 4-8. Extraction and transport of $HAuBr_4$ using two different membrane thicknesses. Starting cell contains 10 mL of 15 mg/L Au in 2.0 M HBr. Receiving cell contains 0.5 M KBr.

-▲- Starting cell using a 0.025 mm thick membrane
-◆- Receiving cell using a 0.025 mm thick membrane
-■- Starting cell using a 0.05 mm thick membrane
-●- Receiving cell using a 0.05 mm thick membrane

The flux is inversely proportional to the membrane thickness and is in accordance with Fick's law of diffusion (shown also in Chapter 3).

$$J_i = \frac{D_i \Delta c_i}{x_i}$$

where:

J_i – flux of penetrant "i"

D_i – diffusivity of penetrant "i"

Δc_i – the concentration difference between points "x" distance apart in the membrane

x_i – membrane thickness

The time required for the complete extraction of the gold complex from solution into the membrane was the same for both thicknesses demonstrating that the rate limiting step of the overall process is the diffusion of the gold complex through the membrane material following extraction. The amount of gold species present within the membrane can be calculated by subtracting the amount of gold present in both the starting and receiving cells from the initial amount of gold present in the starting cell.

$$Au_{mem} = Au_{tot} - (Au_{st} + Au_{rec})$$

where:

Au_{mem} – gold present within the membrane

Au_{tot} – tot amount of gold

Au_{st} – total amount of gold in starting cell

Au_{rec} – total amount of gold in receiving cell

Figure 4-9 shows the amount of gold complex present within two different thicknesses of membrane material under identical conditions. The figure shows that the amount of gold within the thicker membrane is always larger than that for the thinner membrane material. The increased rate of transport with a thinner membrane demonstrates that if an even thinner membrane was used, faster transport times could be obtained although this may lead to mechanical problems such as leakage, because of the fragile nature of extremely thin films.

4.4 Effect of Temperature

Experiments were carried out at four different temperatures (4, 22, 37 and 50 °C) with starting cell conditions being 2.0 M HBr /16 mg/L Au and receiving cells containing 0.5 M KBr. Results depicting the sorption of the gold into the membrane material at different temperatures are shown in Figure 4-10. With an increase in temperature an increase in the rate of sorption of the gold species into the membrane was observed. Also, an increase in the rate of diffusion in the membrane material and rate of recovery for gold in the receiving cell

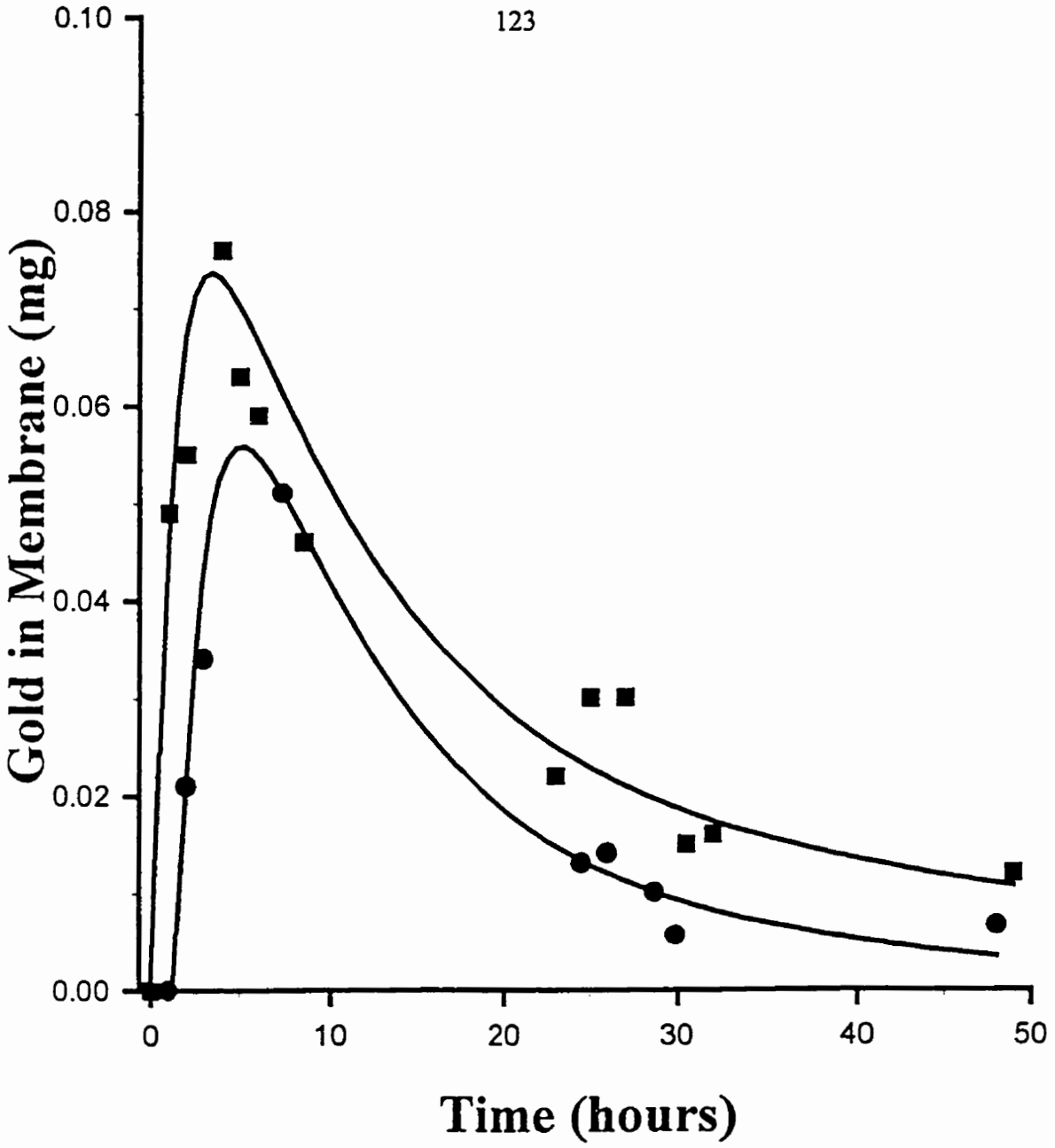

Figure 4-9. The amount of gold complex present within the membrane during transport with two membrane thicknesses. Starting cell contains 10 mL of 15 μg L^{-1} Au/ 2.0M HBr. Receiving cell contains 30 mL of 0.5 M KBr.

—●— 0.025 mm membrane
—■— 0.050 mm membrane

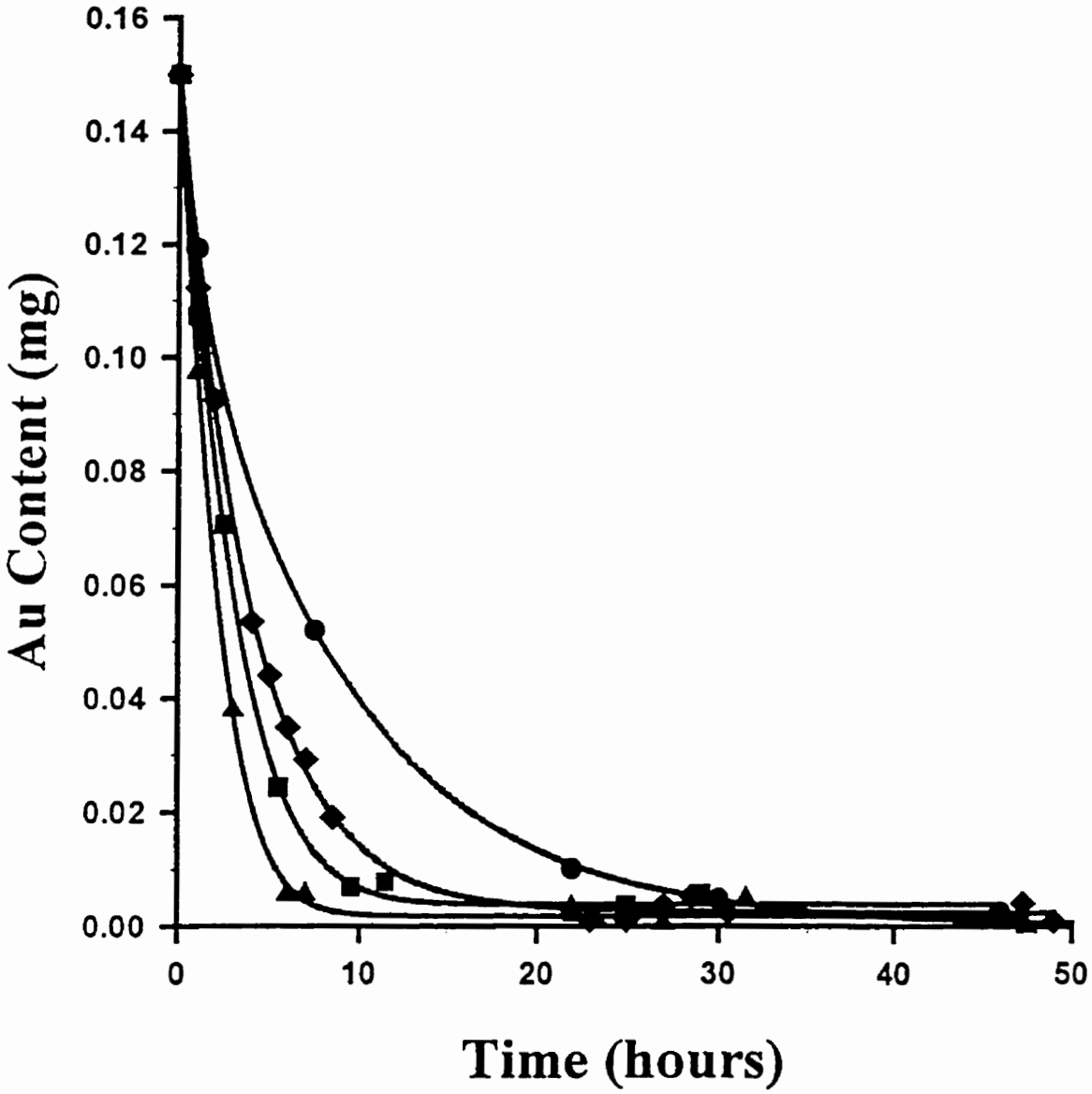

Figure 4-10. Extraction of gold into a polyurethane membrane at 5, 22, 37 and 50°C. Starting cell contains 10 mL of 15 mg/L Au in 2.0 M HBr. Receiving cell contains 0.5 M KBr.

- -●- Starting cell 5°C
- -◆- Starting cell 22°C
- -■- Starting cell 37°C
- -▲- Starting cell 50°C

was apparent. At 5 °C the complete extraction of the gold species required approximately 30 hours compared to 50 °C where it required under 10 hours. Conversely, the recovery of gold in the receiving cell at 50 °C required 11 hours while at 5 °C the recovery of the gold was not complete even after 200 hours.

The energy of activation for the extraction process was calculated to be 25 kJ mol^{-1} using an Arrhenius plot (see chapter 2 for calculation), as shown in Figure 4-11. This value is significantly lower than that found previously for iron (i.e. 50 kJ mol^{-1}). The lower value is probably due to the increased hydrophobicity of the gold complex compared to its iron analogue. The increased hydrophobicity of the gold complex allows easier sorption into the hydrophobic membrane material.

The harsh acid and temperature conditions did not appear to alter the performance of the membrane material but changed the physical appearance of the membrane from clear and translucent to slightly opaque. After the experiment had been stopped and the membranes dried, they returned to their initial physical appearance. The change in physical appearance is probably due to the swelling of the membrane from the absorption of water (discussed in Chapter 7). The effects of the high acid concentration (i.e. 2.0 M) on the membrane were not apparent; polyether-type polyurethane is quite resistant to acid hydrolysis owing to the stability of the ether linkages incorporated in this polymer compared to the polyester polyurethane analogue.

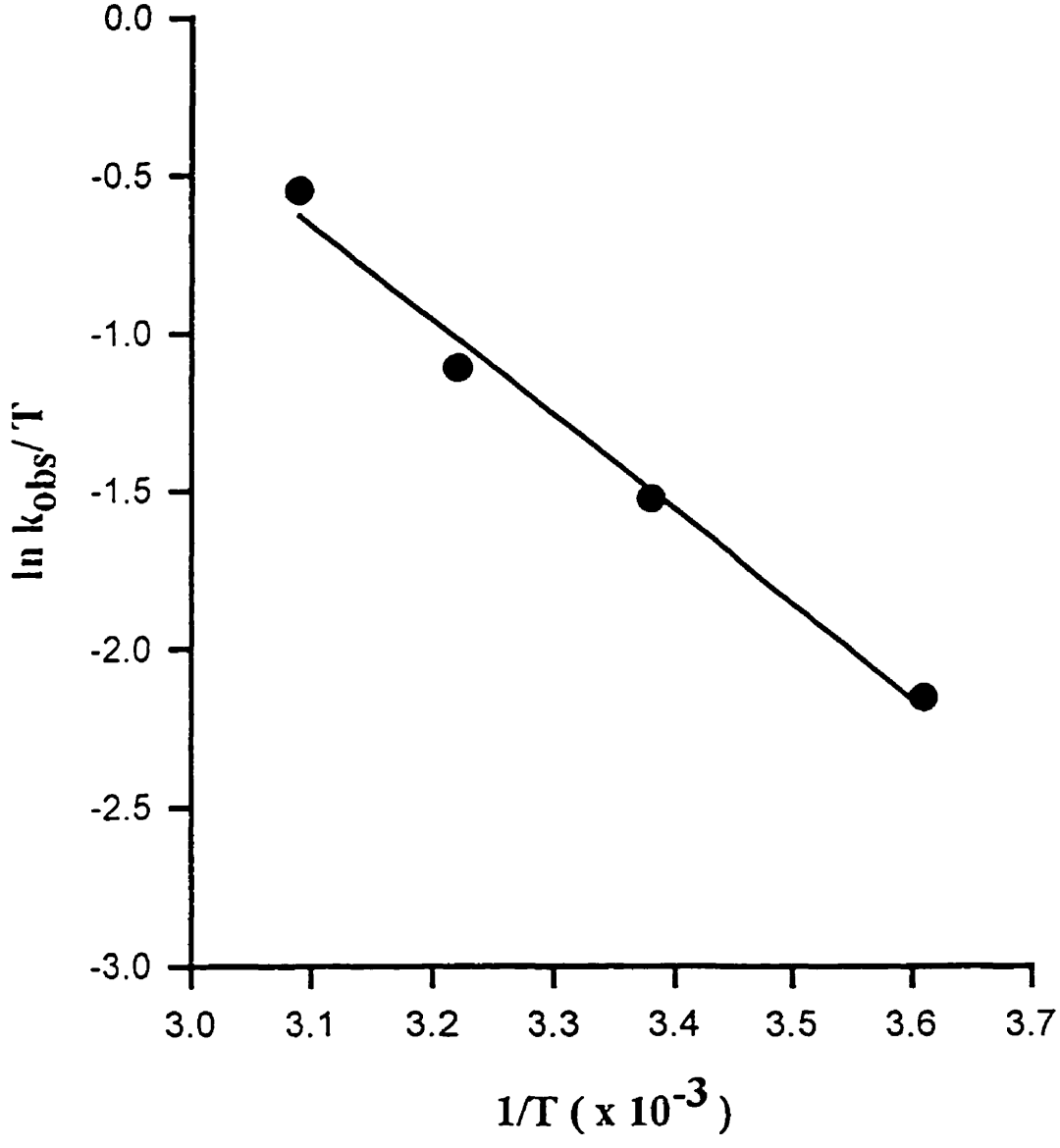

Figure 4-11. Arrhenius plot of the gold extraction into a polyurethane membrane. Starting cell contains 10 mL of 15 mg/L Au in 2.0 M HBr. Receiving cell contains 0.5 M KBr.

4.5 Effect of Stirring the Starting Cell

Often agitation of a chemical reaction enhances the speed at which it occurs. In membrane separations this same effect can be obtained by stirring the starting cell. Stirring enhances membrane transport by both reducing boundary layer effects at the membrane/starting cell solution interface and concentration polarization at the membrane surface. To determine the effect of stirring the starting cell on the rate at which gold complex is extracted, two sets of four cells were prepared with identical starting and receiving cell conditions. The starting cell contained 30 mL 16 mg L^{-1} Au/ 2.0 M HBr and the receiving cell contained 0.5 M KBr. One set had a stirring bar placed in the starting cell and was placed on a water stirrer, while the other set was unstirred, with diffusion providing the only means of "mixing" within the starting cell. The experiment was run over a period of six hours and the starting and receiving cell gold concentrations monitored. The results of this experiment are shown in Figure 4-12. The results show a marked difference between the "stirred" and "unstirred" cell sets. The stirring increases the extraction by an order of magnitude over the "unstirred". In two hours all of the gold was extracted from the starting cell solution while only 17% of the gold had been extracted in the "unstirred" experiment.

The increase in the rate of extraction and subsequent recovery for the stirred samples is important for the viability of the process in a practical setting. Although the increased rate due to stirring is an advantage in certain instances the inability of the stirrers to produce reproducible stirring speeds hampers it for cell to cell reproducibility. Other researchers[20] have shown that the stirring rate has a strong influence on the rate of membrane separation indicating precise control of stirring between cells is important for reproducibility. For most

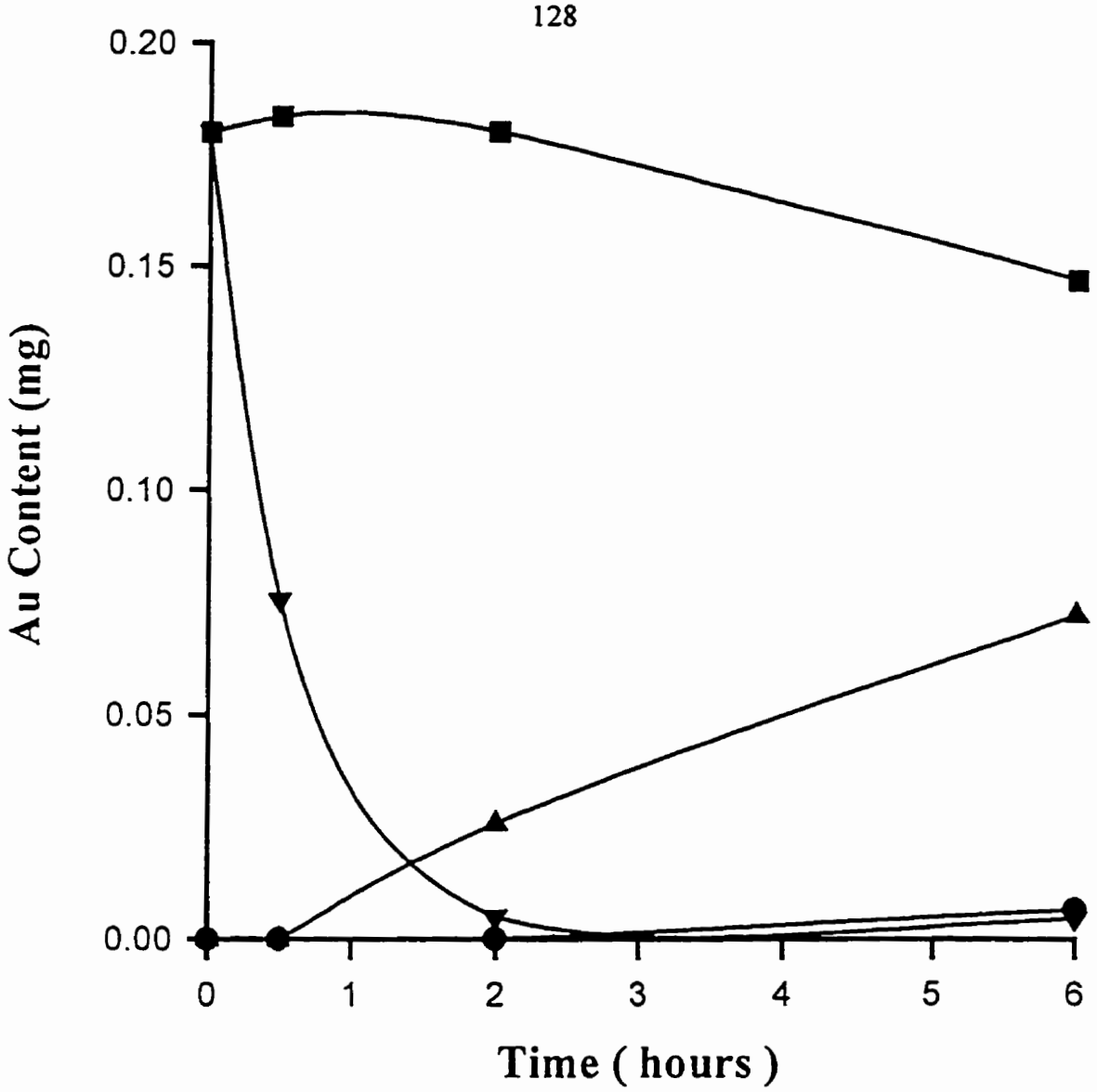

Figure 4-12. A comparison of extaction and transport rates between stirred and static starting cell solutions. Starting cell contains 30 mL of 6μg L^{-1} Au/2.0 M HBr. Receiving cell contains 10 mL of 0.5 M KBr.

—■— Static starting Cell

—●— Receiving cell (static starting cell)

—▼— Stirred starting cell

—▲— Receiving cell (stirred starting cell)

of the experiments performed stirring was not used to allow the direct comparison between experiments.

4.6 Metal Separations

The ability of gold to be transported under certain solution conditions using a polyether-type polyurethane membrane provides evidence that gold can be separated from other species using this process. Gold will preferentially form the extractable $HAuCl_4$ and $HAuBr_4$ complexes over other metals because of their higher stability constants. The separation of several binary metal systems has been achieved using this phenomenon. For example, in Figure 4-13 data is shown for the separation of gold from a 2.0 M HBr solution containing 16 mg/L Au and 16 mg/L Ni with the receiving cell containing 30 mL of 0.5 M KBr. The same transport profile is achieved for gold as was demonstrated in previous figures. However, the nickel is neither extracted into nor transported through the membrane material. The extraction and transport of nickel would be evident by the decrease or increase of the nickel concentration of either the starting or receiving cells respectively. The basis of this separation is that gold forms the extractable $HAuBr_4$ at 2.0 M HBr concentrations, while the nickel does not form an extractable complex and thus remains in the starting cell. Therefore the gold is able to pass into the receiving cell where it is quantitatively recovered. This type of separation would be possible for all metals not able to form extractable complexes at similar concentrations of the bromide ion.

There are some metals that are able to form extractable complexes with the bromide ion. It has previously been shown that iron can be quantitatively transported and recovered

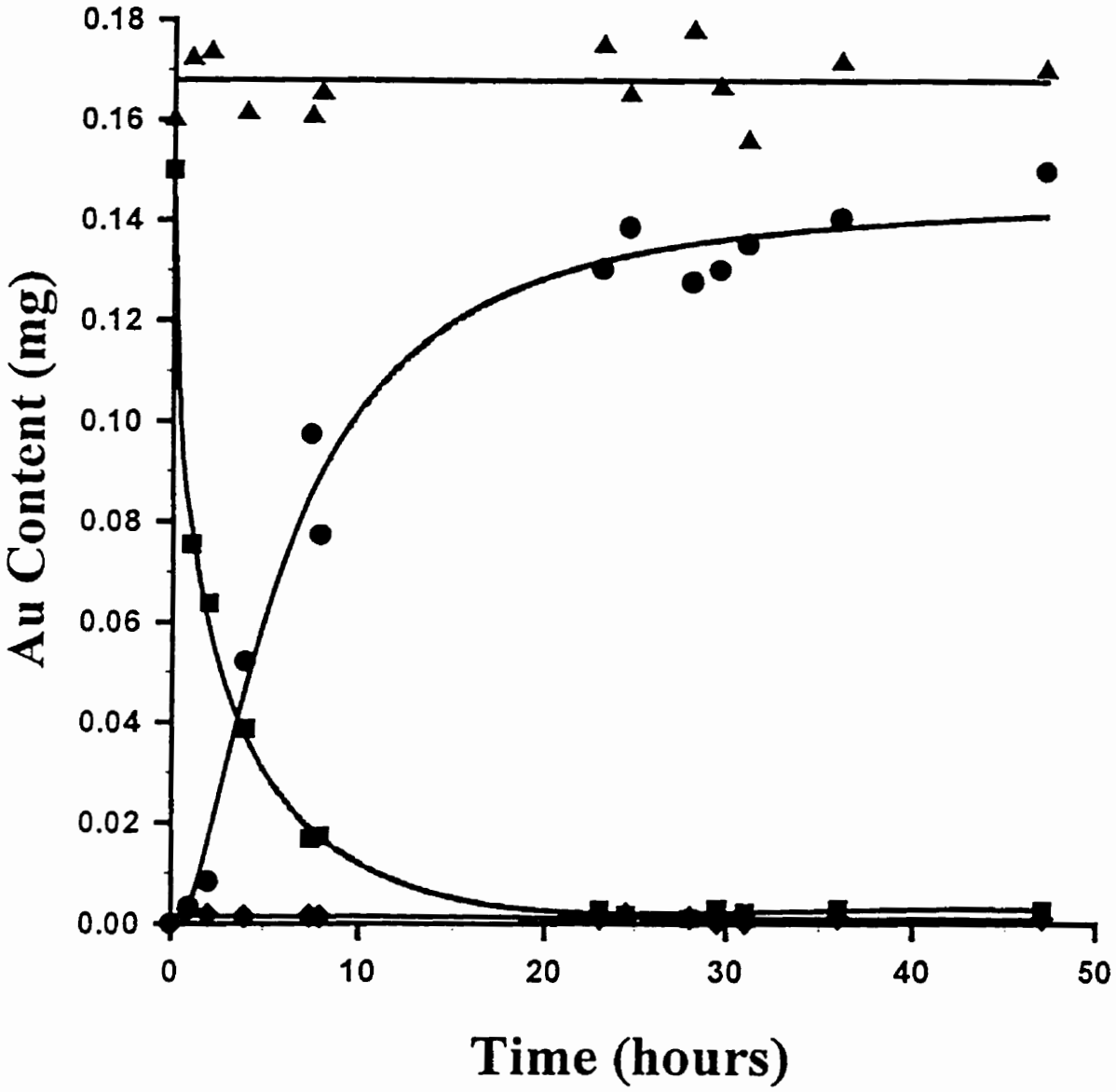

Figure 4-13. Separation of gold and nickel using a polyurethane membrane. Starting cell contains 15 mg/L Au and 15 mg/L Ni in 2.0 M HBr. Receiving cell contains 0.5 M KBr.

-■- Gold content in starting cell
-●- Gold content in receiving cell
-▲- Nickel content in starting cell
-◆- Nickel content in receiving cell

using an analogous process. At HBr concentrations of 5.0 M iron is present in the $HFeBr_4$ complex which is extractable into the polyurethane membrane material. A separation experiment involving gold and iron was performed with the results shown in Figure 4-14. The experiment was performed with a starting cell solution of 16 mg/L Au and 16 mg/L Fe in 2.0 M HBr and 0.5 M KBr in the receiving cell. The extraction and transport of the gold follows the same extraction/transport profile as previously shown, however the iron is neither extracted nor transported through the membrane material. The lack of iron extraction can be explained by the iron bromide stability constants. Iron(III) is a relatively hard acid requiring high bromide concentrations to from the $FeBr_4^-$ complex. At HBr concentrations of 2.0 M there is essentially no iron present as the $FeBr_4^-$ complex, thus none of the iron is extracted and ultimately transported through the membrane material. The iron remains in the starting cell while the gold is transported through the membrane and quantitatively in the receiving cell.

Several separations involving binary metal mixtures of gold and another metal have been successfully performed using HBr in the starting cell. These mixtures all involve gold with either nickel, zinc, iron, cadmium, tin or cobalt. In each case the extraction, transport and recovery of the gold species appears to unaffected by the presence of the other metal in solution. The shape of the separation profiles are all virtually identical.

In addition to using HBr in the starting cell we have found that HCl can also be used to facilitate the selective transport of gold. Several binary metal separations have been performed using hydrochloric acid (to form the $HAuCl_4$ complex) in place of hydrobromic acid (in the starting cell) and potassium chloride in place of potassium bromide (in the

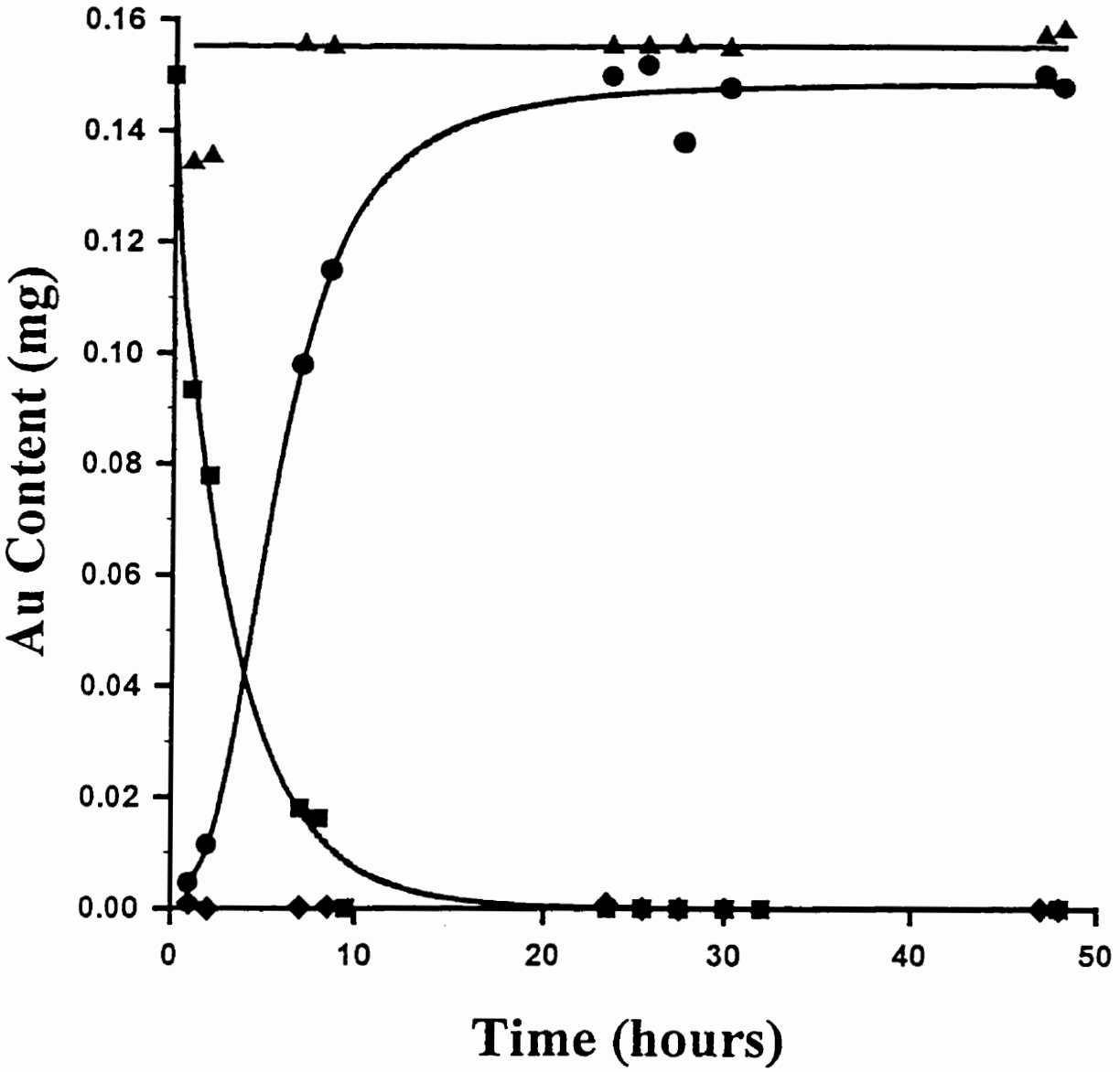

Figure 4-14. Separation of gold and iron using a polyurethane membrane. Starting cell contains 15 mg/L Au and 15 mg/L Fe in 2.0 M HBr. Receiving cell contains 0.5 M KBr

-■- Gold content in starting cell
-●- Gold content in receiving cell
-▲- Iron content in starting cell
-◆- Iron content in receiving cell

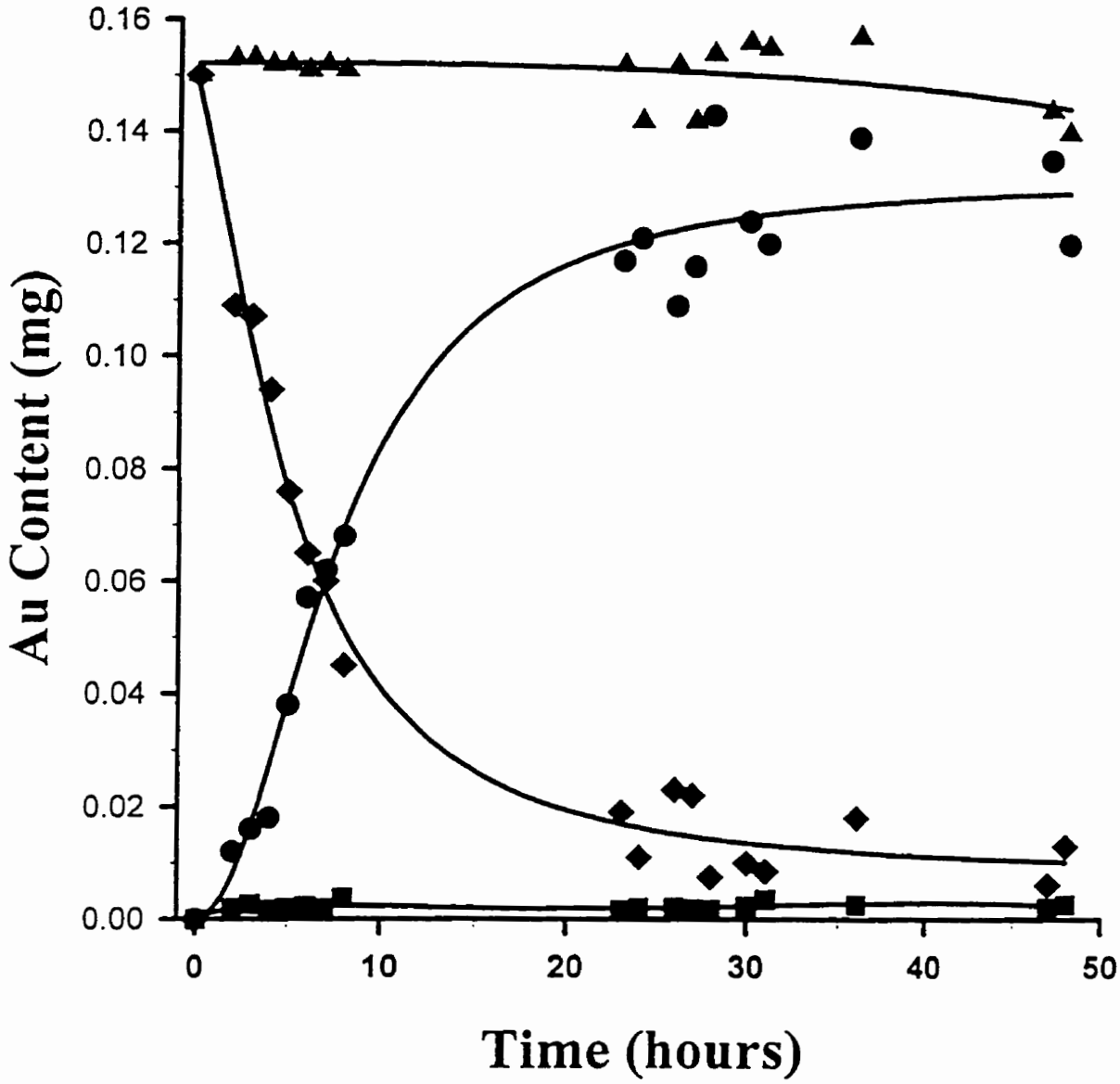

Figure 4-15. The spearation of gold from iron using a polyurethane ether-type membrane. Starting cell contains 10 mL of 15 mg L^{-1} Au, 15 mg L^{-1} Fe in 2.0 M HCl. Receiving cell contains 30 mL of 0.01M HCl

—◆— Au content, starting cell
—●— Au content receiving cell
—▲— Fe content starting cell
—■— Fe content receiving cell

receiving cell). An example of using the HCl/KCl combination s shown in Figure 4-15. These separations were successful but were slightly slower than those for the bromide analogue. The lower rate of extraction can again be attributed to the lower hydrophobicity of the chloride complex, $HAuCl_4$, relative to the bromide complex, $HAuBr_4$.

4.7 Preconcentration of Gold

Often metals are present at extremely low concentrations in the environment. These samples are usually subjected to sample pretreatment prior to being analysed. During pretreatment the sample is separated from interfering substances and concentrated making the analysis more facile. Using a polyurethane ether-type membrane we attempted concentrating gold by adjusting the solution volumes on either side of the membrane. Figure 4-16 shows a separation and preconcentration experiment involving 30 mL of 5 mg/L Au in 2.0 M HBr in the starting cell with 10 ml of 0.5 M KBr in the receiving cell. Using a smaller receiving cell volume with a comparatively large starting cell volume allows the concentration of the permeating species in the receiving cell. With these solution volumes the quantitative transport and recovery of gold in the starting cell should produce a 15 mg/L concentration of gold in the receiving cell, or a concentration factor of 3. The concentration factor is defined as the ratio of the initial concentration to the final concentration of the particular element of interest.

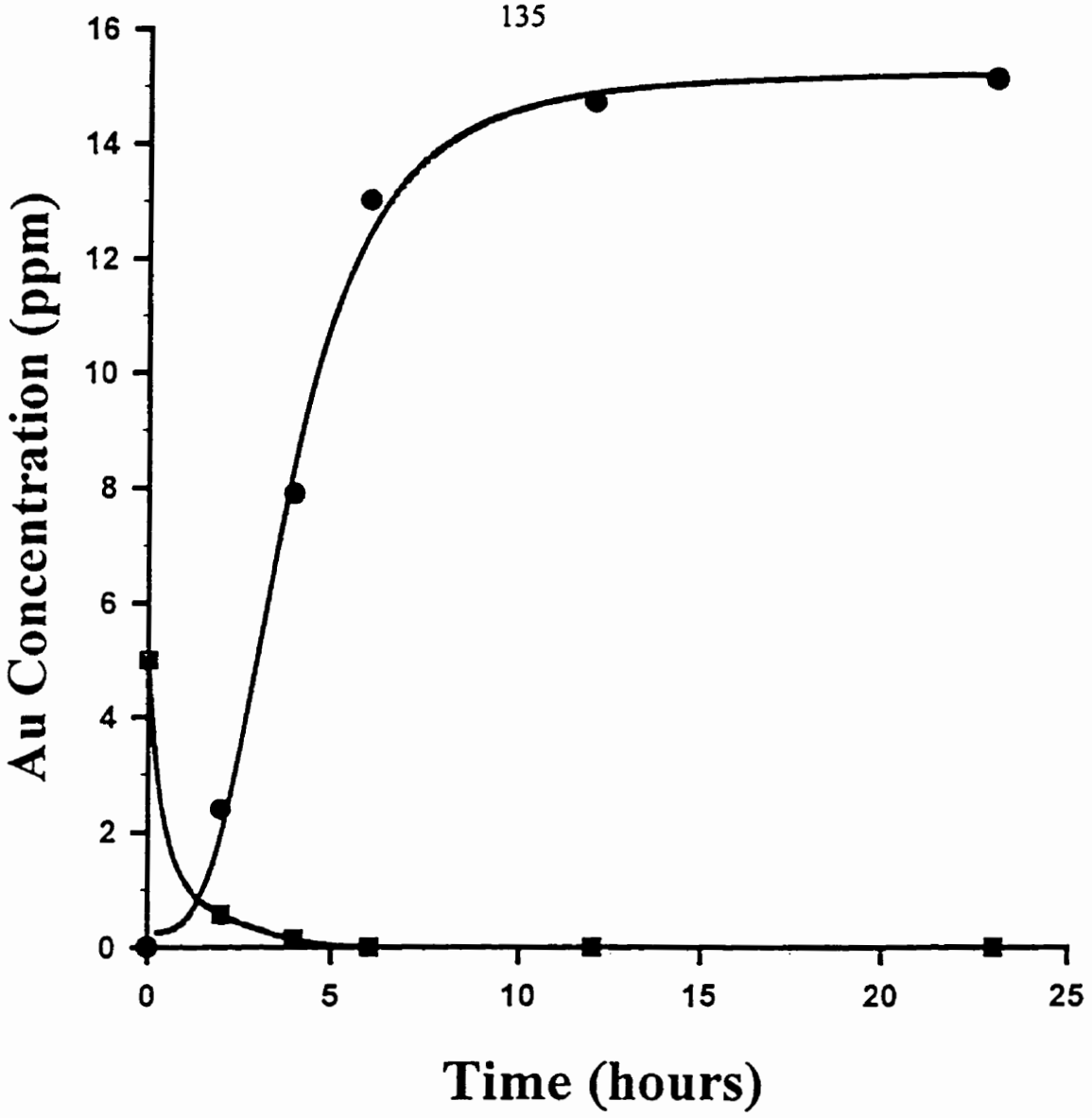

Figure 4-16. Preconcentration of gold using a polyether-type polyurethane membrane. Starting contains 30 mL of 5 μg L^{-1} Au/ 2.0 M HBr. Receiving cell contains 10 mL of 0.5 M KBr.

-■- Gold concentration in starting cell
-●- Gold concentration in receiving cell

$$C.F. = \frac{final\ concentration}{initial\ concentration}$$

In a membrane system incorporating different starting and receiving solution volumes the maximum concentration factor can be calculated by:

$$C_{A,R} = C_{A,S} \cdot (\frac{V_S}{V_R})$$

where:

$C_{A,R}$ – concentration of solute "a" in receiving cell

$C_{A,S}$ – concentration of solute "a" in starting cell

V_S – starting cell solution volume

V_R – receiving cell solution volume

The above equation provides the maximum preconcentration that can be achieved. Uphill transport, which by definition has the flux of an analyte against its concentration gradient, is required.

The experiment shown in Figure 4-16 clearly shows that gold can be transported and concentrated using the polyether-type polyurethane membrane material. The larger starting solution volume showed that the diffusion of the species through solution was hindering the extraction process to a significant degree. To minimize the effect of the larger solution volume the starting cell was stirred. This led to a greatly increased rate of extraction and

transport of the gold species. In most the experiments performed in this thesis the active surface area of the membrane has been kept at 5.3 cm^2 for the sake of comparison. If this area were increased the rate of extraction, and consequently the overall concentration factor, may be increased. In addition, all experiments with the exception of the concentration experiments were not stirred.

To determine if larger concentration factors could be obtained using this process several different membrane cells were used. In each case the receiving cell volume was a fraction of the starting cell volume. Schematic diagrams of the different preconcentration cells used are shown in Chapter 2. Using the different cell volumes a variety of preconcentration experiments were performed. Table 4-4 shows data from some of these experiments.

Table 4-5. Preconcentration of Gold Using Different Start Cell and Receiving Cell Volumes*

Starting Cell Volume	Receiving Cell Volume	Concentration Gold Starting Cell(start)	Concentration Gold Receiving Cell(end)	Theoretical Concentration Factor	Experimental Concentration Factor	Percent Recovery
30 mL	10 mL	5 mg L^{-1}	15 mg L^{-1}	3	3	100%
9000	700	1	11.34	12.8	11.34	89%
9000	55	0.027	3.802	164	141	86%

where:

$$Theoretical\ C.F. = \frac{Starting\ cell\ volume}{Receiving\ cell\ volume}$$

$$Experimental\ C.F. = \frac{Receiving\ cell\ concentration_{end}}{Starting\ cell\ concentration_{start}}$$

$$Percent\ Yield = \frac{Experimental\ concentration\ factor}{Theoretical\ concentration\ factor} \times 100$$

*Note: All experiments were performed with 2.0M HBr in the starting cell and 0.5M KBr in the receiving cell

4.8 Separation of Gold from Gold Ore

The ability of gold to be transported in the presence of other metals has already been shown in a previous section. Under these conditions the selective transport of gold could be achieved resulting in the quantitative separation of gold. Those separations were of relatively simple systems of a binary metal mixture. To demonstrate the ability of a polyurethane ether-type membrane to separate gold from a much more complicated medium we attempted the separation of gold from a gold ore solution. The gold ore solution was prepared as described in the experimental section (Chapter 2). The gold ore solutions were spiked with gold standard because the small amounts of gold in the ore (fire assay 3.06 oz / ton) would be difficult to analyse and quantitate. Each cell was spiked with 0.15 mg of gold. The starting cell consisted of 10 mL of gold ore solution while the receiving cell contained 30 mL of 0.5 M KBr. This experiment was performed at room temperature, carried out over a period of 48 hours and was unstirred. The results of the separation are presented in Figures 4-17a (starting cells) and 4-17b (receiving cells). The metals were analysed directly using AA and diluted before being analysed by ICP. The metals analysed were chosen by performing an initial scan of several metals suspected of being in the gold ore. If a metal was present in detectable concentrations it was further analysed for in each of the cells. The metals analysed in the gold ore samples consisted of Au, Fe, Co, Mn, Cu, Zn. The gold ore from the Kirkland Lake Mine is known to possess a large concentration of pyrite which is demonstrated by the very large iron concentrations in the samples. The iron concentration shown in Figure 4-17a was reduced by a factor of 50 in order to have it reasonably represented on the graph.

Examining the metal content of the starting cells we see that the gold content of the

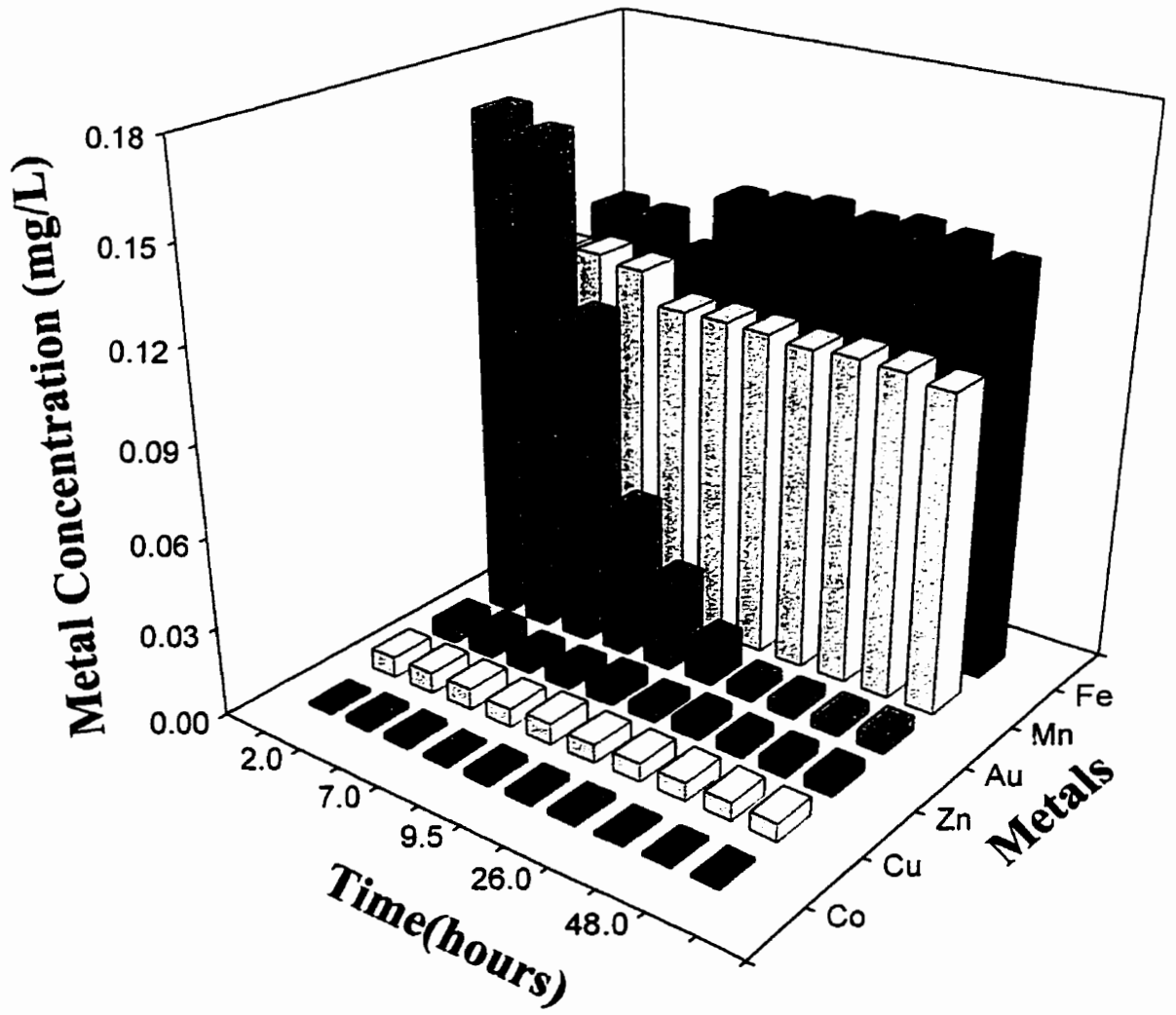

Figure 4-17a. The separation of gold from gold ore displaying metal concentrations in the starting cell. Starting cell contains10 mL of 2.0 M HBr.

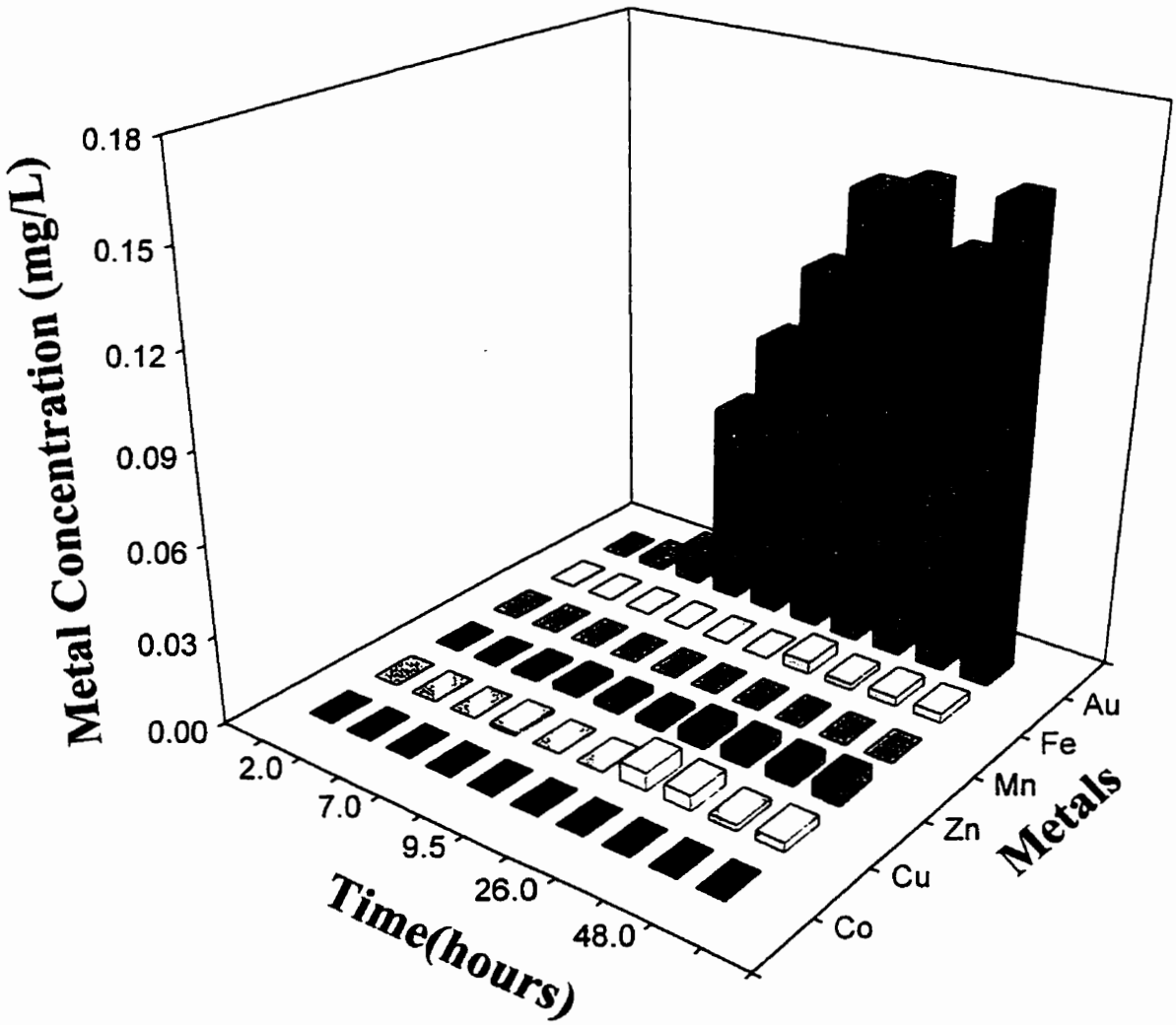

Figure 4-17b. The separation of gold from gold ore displaying metal concentrations in the receiving cell. Receiving cell contains 30 mL 0.5 M KBr.

top cell decreases as it is extracted into the membrane until it is almost quantitatively extracted after 26 hours. The amounts of the other metals in the starting cells did not change drastically over a 48 hour period. This indicates that very little of the other metals are extracted and transported into the receiving cell.

The analysis of the receiving cell once again shows the trend of the gold being transported through the membrane material and into the receiving cell solution. The initial gold content of zero at the start of the experiment gradually increases to 0.155 mg, a 92.3% recovery of the initial gold in the starting cell after 48 hours. Conversely, the analysis for the other metals in the receiving cells showed that there were no detectable amounts of either cobalt or manganese in any of the cells. Also the analysis of iron, zinc, and copper showed that only microgram quantities of these metals were present in the receiving cell solution after 48 hours. The small amounts of copper and zinc present approached the detection limits of the instrument and the concentrations of each in the receiving cell is not significant. The results of the gold ore separation again shows that there does not appear to be a competing ion effect between the other metals and gold even though some of those metals are present in much higher concentrations than gold. The rate of extraction and transport of the gold complexes is unchanged regardless of the concentrations of the other species in solution. By performing the separation of gold from gold ore we are not suggesting that this technique be used for this purpose as there are techniques already developed that are far more efficient for this process. We are suggesting however, that polyurethane ether-type membranes may be used for the separation of gold from complex matrices possessing a large number of species.

4.9 Use of Other Polyurethane Membrane Materials

4.9.1 Deerfield Urethane

Experiments investigating gold transport required the use of substantial amounts of membrane. It became difficult to obtain more material from Steven Elastomerics prompting us to try and find another source, or manufacturer of polyurethane membrane material. Our search led us to Deerfield Urethane (see experimental for details) who was willing to supply us large amounts of this material if necessary. From our membrane characterization studies (see Chapter 7) this material was judged to be almost identical to that of Stevens Elastomerics. Indeed after obtaining some of the Deerfield material, experiments were performed and showed that this material performed as well as the Stevens Elastomerics product. A few preliminary experiments were performed with the Deerfield membrane indicating that the membrane had a similar ability to extract and transport the gold species. In addition an experiment repeatedly replacing the gold in the receiving cell was tried using the Deerfield membrane. A piece of the membrane was placed in the membrane cell with 600 mL of 5 mg L^{-1} /2.0 M HBr in the starting cell and 600 mL of 0.5 M KBr in the receiving cell with both cells stirred. The experiment was run for two days and the pH of the receiving cell determined and an aliquot of both the starting cell and receiving cell solutions taken for gold analysis. After sampling both of the cells, more gold standard (1000 mg L^{-1}) was added to the starting cell to once again bring the starting cell gold concentration to 5 mg L^{-1}. The protocol was repeated roughly every two days and the experiment run for a 28 day duration. The data for the first nine days is shown in Figure 4-18. After two days the concentration of gold in the

starting cell has been depleted and the concentration of gold in the receiving cell is 5.0 mg L^{-1}. After adding more gold to the starting cell and then analysing the receiving cell concentration after an additional 48 hours, the starting cell gold concentration is again depleted, and the receiving cell concentration is now ≈ 10 mg L^{-1}. Repeating this procedure produces a concentration of 14 mg L^{-1} in the receiving cell. With repeated replenishment of the gold in the starting cell we see a continuous increase in the receiving cell gold concentration. This trend continues until the pH of the receiving cell becomes sufficiently low to begin protonating some of the gold complex. Once protonated the gold complex can be "re-extracted" into the membrane material. The change in pH throughout the experiment is shown in Figure 4-19.

Initially the pH of the receiving cell solution is ≈ 6.0. During the first day the pH begins to decreases quite rapidly until after 24 hours the pH is ≈ 4.2. and continues to decrease for the duration of the experiment. After nine days the lowered pH in the receiving cell becomes significant and re-protonation of the gold complex occurs, leading to the gold being "re-extracted" into the membrane material. The continual lowering of the pH in the receiving cell leads to a diminished recovery of gold in the receiving cell. Indeed the lowering of pH in the receiving cell solution could be controlled by titrating with a suitable base, maintaining a constant pH in the receiving cell, enabling the experiment to be run for much longer periods of time.

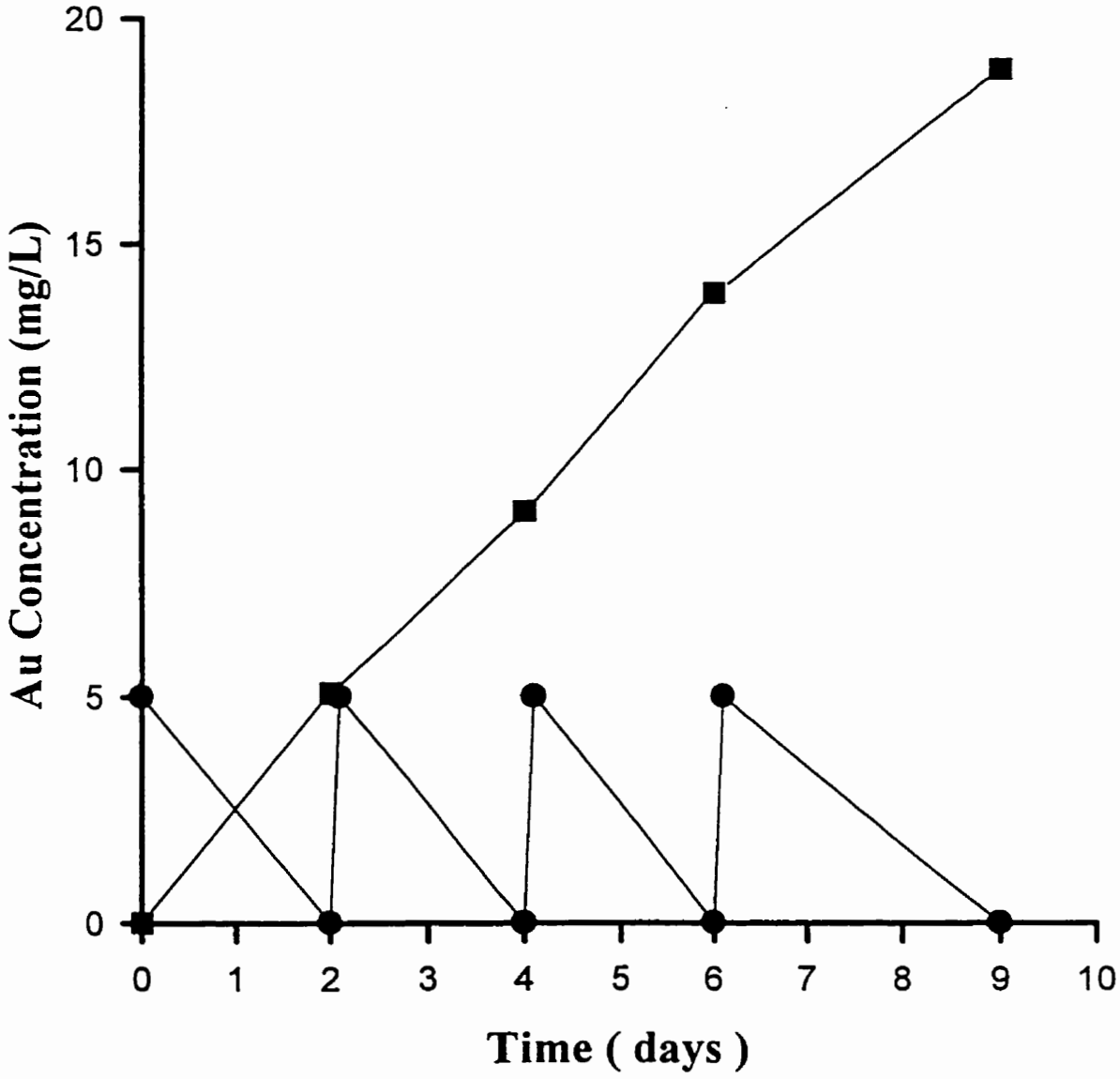

Figure 4-18. The transport of $HAuBr_4$ with multiple additions of gold to the starting cell.

Gold concentration in starting cell(stirred)

Gold concentration in receiving cell(stirred)

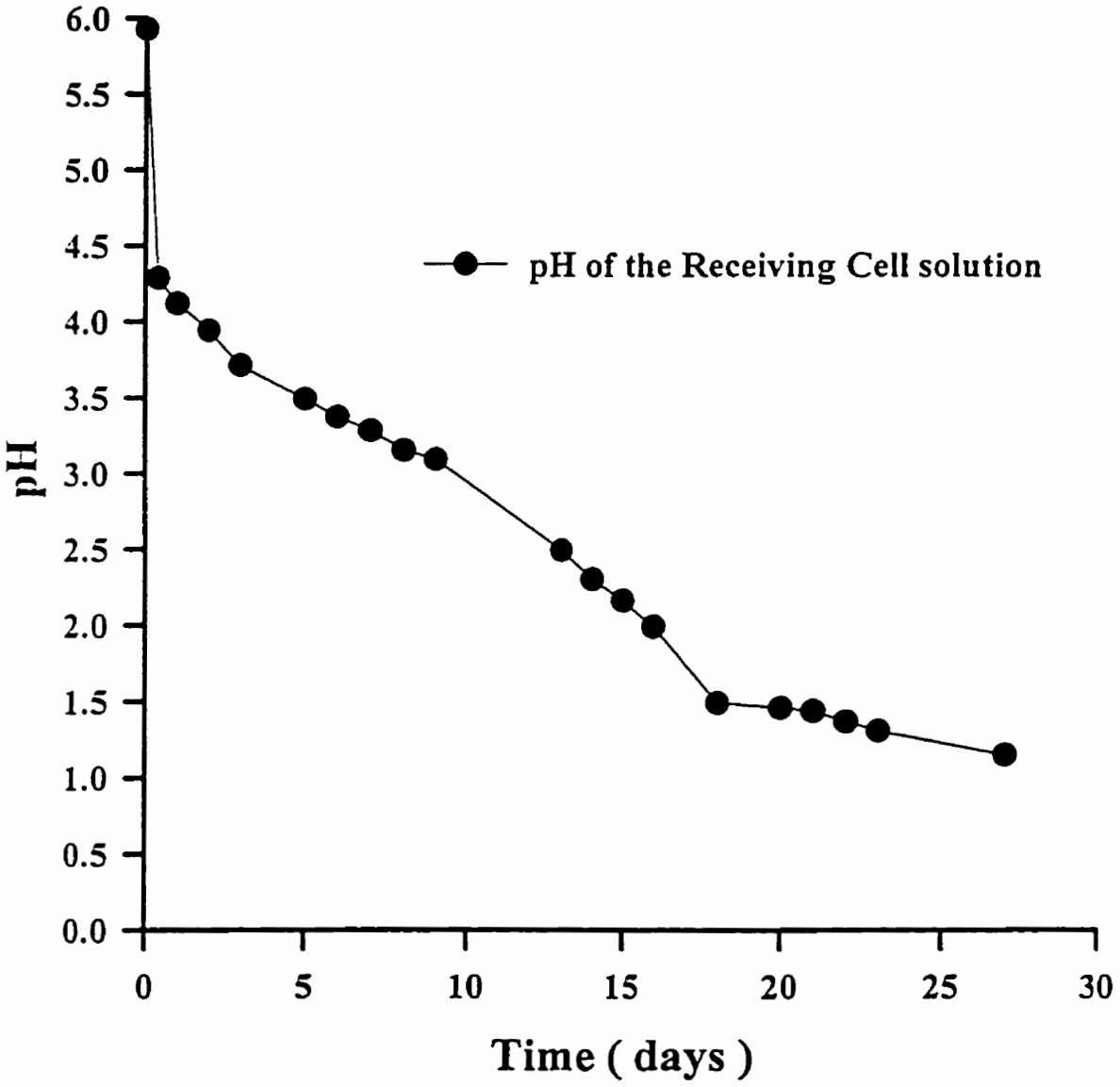

Figure 4-19. The decrease in the pH of the receiving cell with multiple additions of gold to the starting cell

4.9.2 Polyurethane Glove and Condoms

While performing the membrane experiments it was noted that a membrane in the form of a "bag" would be advantageous for a separation process. Attempts at forming a bag out of the Stevens and Deerfield membrane material using a heat sealing device were somewhat successful but prone to leakage. We then began looking for products composed of polyurethane that possessed our required physical form. We found two different products that fit this description. An article in Scientific American[21] described the development of a new polyurethane condom for people who were allergic to latex . A sample of these condoms was obtained from Suzanne Odell of Dow Chemical (condom specifics are presented in the experimental section). The condoms (thickness 127 μm) were then tested for their ability to extract and transport gold. Utilization of the condoms in a separation procedure first involved their cleaning. Condom cleaning involved the rinsing of the condom in methanol and then drying. The cleaning removed lubricant from the condom's surface. After cleaning the condom was used as a dialysis bag. Receiving cell solution (184 mL) was placed within the condom and the end of the condom sealed with a plastic clip. The condom was then immersed in the starting cell solution composed of 2.0L of 2 mg L^{-1} Au /2.0 M HBr. A schematic diagram of the condom testing device is shown in Figure 4-20. During the initial stages of the experiment the condom became yellow in colour consistent with the extraction of the $HAuBr_4$ complex. After 48 hours the experiment was stopped and the solution within the condom analysed for gold content. Analysis yielded a gold concentration of 14 mg L^{-1}. If quantitative recovery was achieved then a concentration of 22 mg L^{-1} is expected.

Figure 4-20. Schematic diagram of the condom testing apparatus.

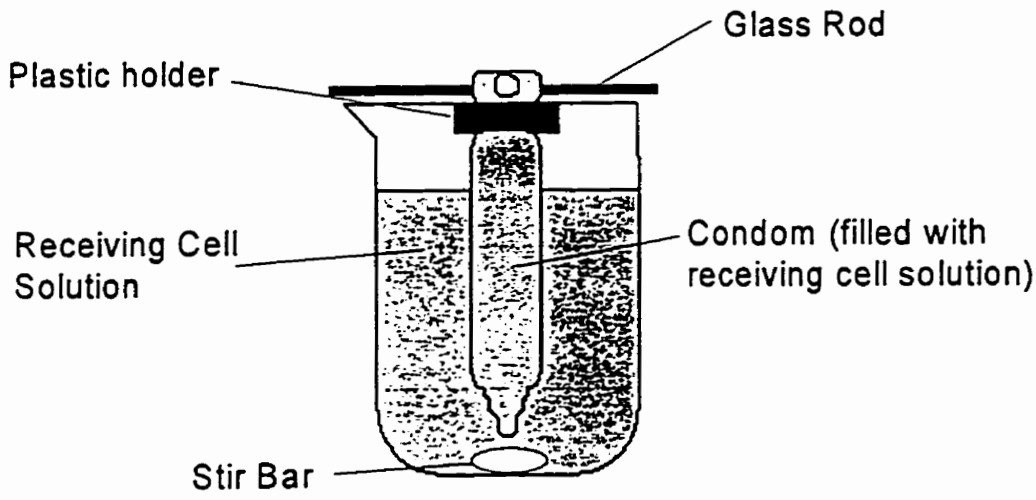

The lack of quantitative recovery was due to small holes formed in the condom material. The remaining gold was recovered by soaking the condom in fresh 0.5 M KBr suggesting the holes in the condom material led to the incomplete recovery of the gold species. Although this was a preliminary experiment it does show that the condom material behaves in a similar manner to that of the membrane material.

In addition to the polyurethane condoms we also found gloves (40 µm thickness) composed of polyurethane. Like the condoms, the gloves (see Chapter 2 for manufacturer details) also can be used as a "dialysis bag" for the isolation of gold species. An experiment similar to that of the condom was performed using the polyurethane glove. One of the gloves fingers was cut off and 14 mL of 0.5 M KBr placed within the finger. The filled finger was then placed in 600 mL of 100 µg L^{-1} Au/ 2.0M HBr. This experiment was run for two days and the solution in the finger analysed for gold content. The solution contained 3.9 mg L^{-1} Au corresponding to a 92% recovery and a concentration factor of 39. Again this demonstrates that this material behaves similar to the membrane material with respect to its ability to transport the $HAuBr_4$ complex. For both the condom and glove experiments we used the thicker materials (ie. 127 µm and 40 µm respectively). The thickness of the membrane material plays a significant role for the rate of separation. Using the thinner products will increase the speed of the separation.

4.10 Conclusion

A polyether-type polyurethane membrane can quantitatively transport gold from hydrochloric and hydrobromic acid solutions to KCl and KBr solutions, respectively. The transport process involves the extraction of the gold species, diffusion through the membrane material, and finally the quantitative elution of the gold species from the membrane. The extraction of the gold species is due to the two protonated gold halide complexes, $HAuBr_4$ and $HAuCl_4$, that predominate in high concentrations of either HCl or HBr. The diffusion through the membrane follows a Fickian diffusion model. The elution from the membrane is caused by the formation of the $AuCl_4^-$ and $AuBr_4^-$ complexes that are not extractable into the membrane.

The transport process is aided by the use of a thinner membrane and an increase in temperature. Also, with an increase in the surface area of the membrane we can expect that the overall rate of extraction and capacity of the membrane will be increased significantly so that it may be used in a practical setting. The rate limiting step for the transport and recovery of the gold is the diffusion through the membrane.

In this investigation all of the cells, with the exception of the preconcentration experiments, were unstirred. This allowed the direct comparison of experiments with no error associated with different rates of stirring. With the addition of stirring we see a tenfold increase in the rate of extraction into the membrane, but this does not allow direct comparison of separate experiments because of the lack of the ability for precise control of individual stirring rates. The membrane method is inexpensive and inherently simple compared to other

techniques available and so these methods may provide a useful alternative to other separation processes. Quantitative recovery of gold from the membrane into the receiving cell solution indicates that there is no permanent sorption of the complex, and further that there is no reduction of the complex to metal by the polymer.

The optimization of the process with stirring, an elevated temperature, and a thinner membrane material should lead to faster separation times such as less than one hour for quantitative separation.

The separation of gold from a number of other metals in binary metal systems shows that a polyurethane ether-type membrane can be used to separate gold from metals that do not form extractable complexes in the presence of either HBr or HCl. Even in cases where a metal does form extractable complexes in the presence of either of these acids (ie. iron), the membrane can still effectively separate the two metals based on the stability constants of those metal halide complexes.

Gold ore has large amounts of other metals besides gold which are not extracted and transported through the membrane into the receiving cell solution. The separation of gold from a gold ore solution demonstrates the ability of the membrane to separate gold from very complex matrices.

Chapter 5: The Separation of Gold by Selective Extraction of $HAuBr_4$ Using a Poly(tetramethylene) Ether Glycol-Impregnated Filter

5.1 Introduction

Classical solid phase extraction (SPE) is the selective partitioning of one or more components between a solid and liquid phase. Sorbent materials can be made for a specific analyte or analytes in order to extract only certain components in a mixture, or it can be modified so that only the compounds of interest are not sorbed. The extraction of metals is performed using either a chelating sorbent or by employing solution conditions to selectively form complexes that are extractable onto a sorbent material.

Extractable metal complexes can be formed using complexing agents such as crown ethers[1,2,3,4], or by attaching bulky ligands to a molecule followed by extraction onto a hydrophobic sorbent. The extent of formation of a complex is determined by the stability constant of the complex and the relative concentrations of the complexing agents present in solution. Gold(III) is a soft Pearson acid so it prefers to form complexes with bulky non-polar ligands. Gold(III) in the presence of sufficiently high chloride and bromide concentrations forms either the $AuCl_4^-$ or $AuBr_4^-$ (Figure 5-1) complex respectively (see Chapter 4). These complexes are stable in aqueous solutions[5,6] at a pH lower than 6. Both complexes are weak acids that become protonated at sufficiently low pH to form the extractable $HAuCl_4$ and $HAuBr_4$ complexes[7,8]. Gold has been shown to be extracted as either the $HAuCl_4$ or the $HAuBr_4$ complex by diethyl ether[9], isopropyl ether[10] and polyurethane

ether-type foams[11] and elastomers[12] . In particular, our work using a polyurethane membrane synthesized from polytetramethylene glycol and methylene bis-phenyldiisocyanate (see Chapter 7) has shown that gold can be separated from complex matrices by selectively extracting the $HAuBr_4$ complex. This has led us to believe that the portion of the polymer responsible for the gold extraction consists of the polytetramethylene ether glycol segments. We then decided to test polytetramethylene ether glycol individually for its ability to extract metal complexes.

The purpose of this investigation was to determine if polytetramethylene ether glycol could be substituted for the membrane material as a solid phase extractant using the gold bromide complex, $HAuBr_4$ as a probe. The investigation showed that the polytetramethylene glycol had similar extraction characteristics to the polyurethane membrane providing evidence that the portion of the polymer responsible for the gold extraction is the polytetramethylene glycol soft segments.

The study invetigated both the mechanism for the sorption and recovery processes in addition to demonstrating the ability of the OIF to selectively extract and isolate gold from complex matrices. Several factors affecting the rate of extraction were examined including: the effect of various amounts of HBr in the sample; the effects of different flow rates through the filter; the recovery of the metal complex following extraction; and the effect of using filters with different pore sizes, porosities and thicknesses.

Preliminary experiments using polytetramethylene ether glycol (polyTHF) (Figure 5-2) have shown that gold is also extracted from an HBr solution into the compound. By impregnating a porous polytetrafluoroethylene filter with polyTHF, the gold complex,

$HAuBr_4$ can be rapidly extracted from solution as it passes through the impregnated filter. This device is termed an organic-impregnated filter (OIF). The immobilization of polyglycols in the pores of a filter has also been used by Ho[13] to prepare supported liquid membranes for the removal of organics from aqueous solutions.

The rapid gold extraction is shown to be both selective and quantitative. Once extracted the gold can be recovered by an analogous process to the extraction. The gold complex is converted to the de-protonated $AuBr_4^-$ complex where it is stripped from the surface of the active layer and consequently removed from the filter. In this chapter, the use of an organic-impregnated filter for the selective removal of gold from solution is demonstrated. The effects of the HBr concentration, the flow rate, the filter pore size and the filter porosity on the extraction of gold from HBr solutions will be described.

Figure 5-1. Formation of the protonated tetrabromoaurate complex

$$Au^{3+} + 4Br^- \rightleftharpoons AuBr_4^-$$

$$AuBr_4^- \rightleftharpoons HAuBr_4$$

Figure 5-2. Structure of PolyTHF™

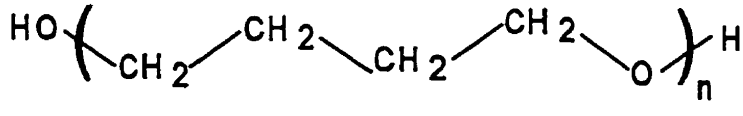

The recovery of the gold, and the ability of the OIF to preconcentrate and separate gold in simple binary metal mixtures and from gold ore will be investigated.

5.1.1 OIF Preparation

The preparation of the OIF was carried out as described in Chapter 2 (experimental). The preparation protocol leads to an average loading of 50 mg and 100 mg of PolyTHF on the 5.0 and 3.0 µm pore size material respectively. Scanning electron microscopy revealed that there are still holes visible on the surface of the OIF facilitating the passage of liquid through the filter. The polyTHF forms the active layer of the OIF providing a surface able to selectively extract the gold species as it passes through the filter. Figure 5-3 shows a schematic diagram of the fluorocarbon filter before and after impregnation with polyTHF.

5.2 Extraction of $HAuBr_4$ with an OIF

Gold in the presence of suitable HBr concentrations forms the $AuBr_4^-$ complex. The complex is a weak acid and at a low pH becomes protonated. We have shown previously using polyurethane ether-type membranes that, the $HAuBr_4$ complex is responsible for the extraction of gold. When using polyTHF as a sorbent material an equilibrium (Figure 5-4) is developed between the solution and the sorbent material. The equilibrium involves the extracted metal complex and the metal complex in solution.

Figure 5-5 shows the extraction of gold from several solutions containing 5 µg/mL Au with increasing HBr concentrations. The solutions were each passed through

Figure 5-3. Schematic diagram of the polytetrafluoroethylene filter before and after impregnation.

Before impregnation:

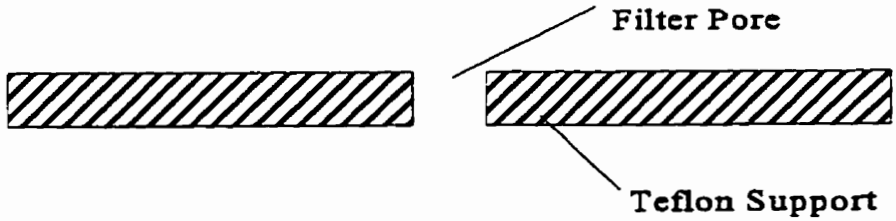

After Impregnation:

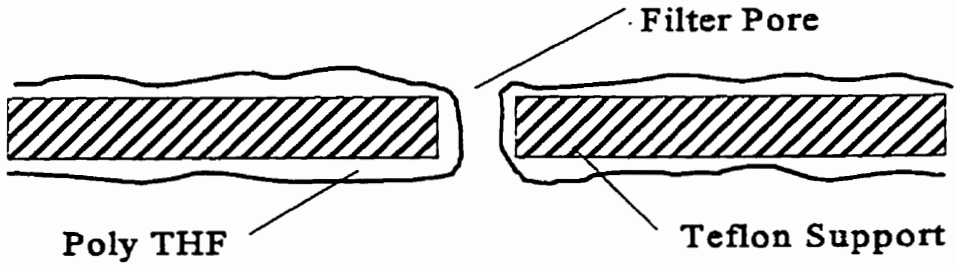

Figure 5-4. Equilibrium between the extractable gold complex in solution and in the membrane material.

$$HAuBr_4 \rightleftharpoons \overline{HAuBr_4}$$

*overline indicates the species present in the polyTHF layer of the OIF

the filter at 100 mL/min. The extraction of the solution containing 0.01 M HBr showed that 50 % of the gold still remained in the filtrate after one pass through the filter. Conversely, the extraction of gold from the solution containing 1.0 M HBr showed that the gold is quantitatively removed from the solution after only one pass through the OIF. The larger the HBr concentration, the greater the percentage of gold present in the extractable form leading to more of the gold being removed after one pass through the filter. The extraction of gold can be followed both by the development, and loss, of an orange hue (λ_{max} = 374 nm) on the filter, and in the gold solution respectively.

The effect of flow rate on the extraction of gold was tested using the 5.0 µm filter (Figure 5-6). Several 100 mL solutions of 5 mg/L Au in 2.0 M HBr were passed through a 5.0 µm filter at different flow rates ranging from 22 to 277 mL/min. At flow rates of approximately 200-300 mL/min, 85-90 % of the Au is removed from solution after one pass, and is quantitatively removed after 2 passes through the OIF. At flow rates of 92 mL/min and below the gold is quantitatively removed after only one pass through the OIF. The faster flow rates do not allow sufficient contact time for all of the gold to be extracted from solution. A comparison of the effect of flow rate on the extraction of gold for both the 5.0 µm and 3.0 µm filters is shown in Figure 5-7. The 3.0 µm filter (thickness 200 µm, 85% porosity) has a greater thickness and porosity than the 5.0 µm filter, (thickness 125 µm, 60 % porosity). The larger thickness and porosity leads to a greater loading of polyTHF on the surface of the filter which gives improved extraction performance. Even at a flow rate of 600 mL/min, the 3.0 µm OIF quantitatively removes the gold from solution. The extraction of gold is an extremely fast process as the actual contact time for the solution on the filter is

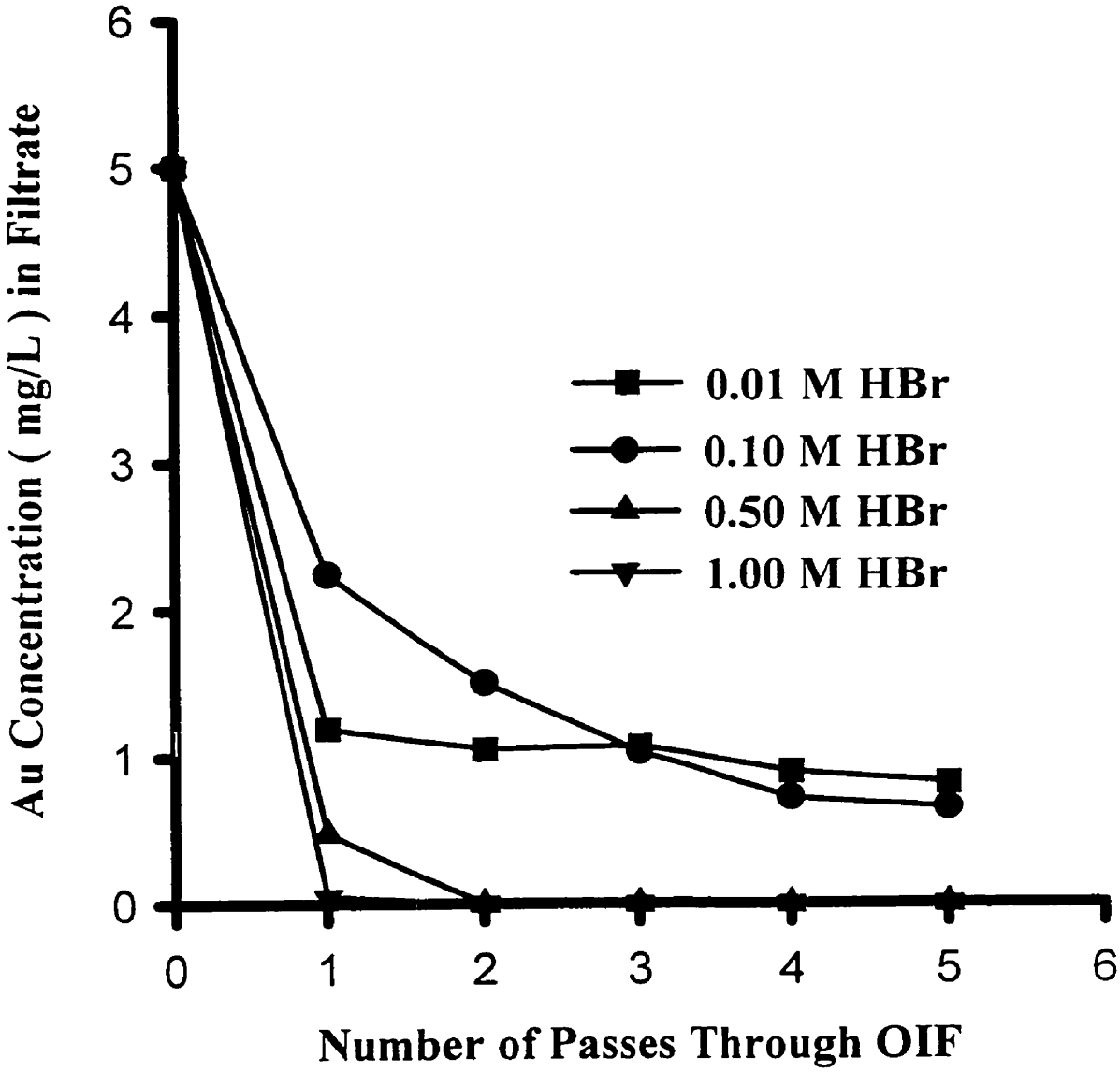

Figure 5-5. The extraction of gold from solutions containing increasing HBr concentrations. Experiments were performed on 100 mL of solution at a flow rate of 100 mL/min through a 5.0 μm OIF.

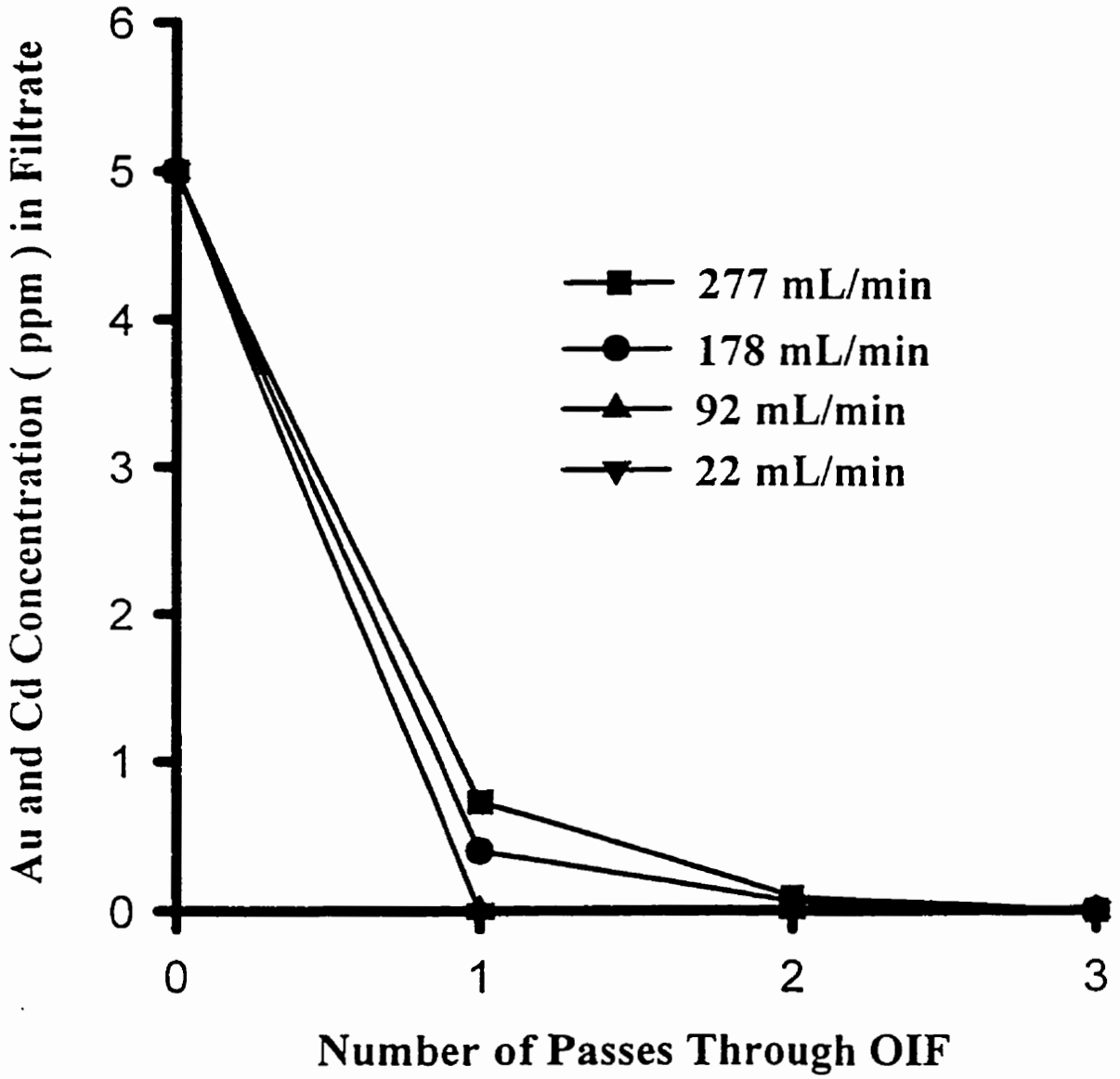

Figure 5-6. The extraction of gold from 2.0 M HBr solutions using different flow rates with a 5.0 μm OIF.

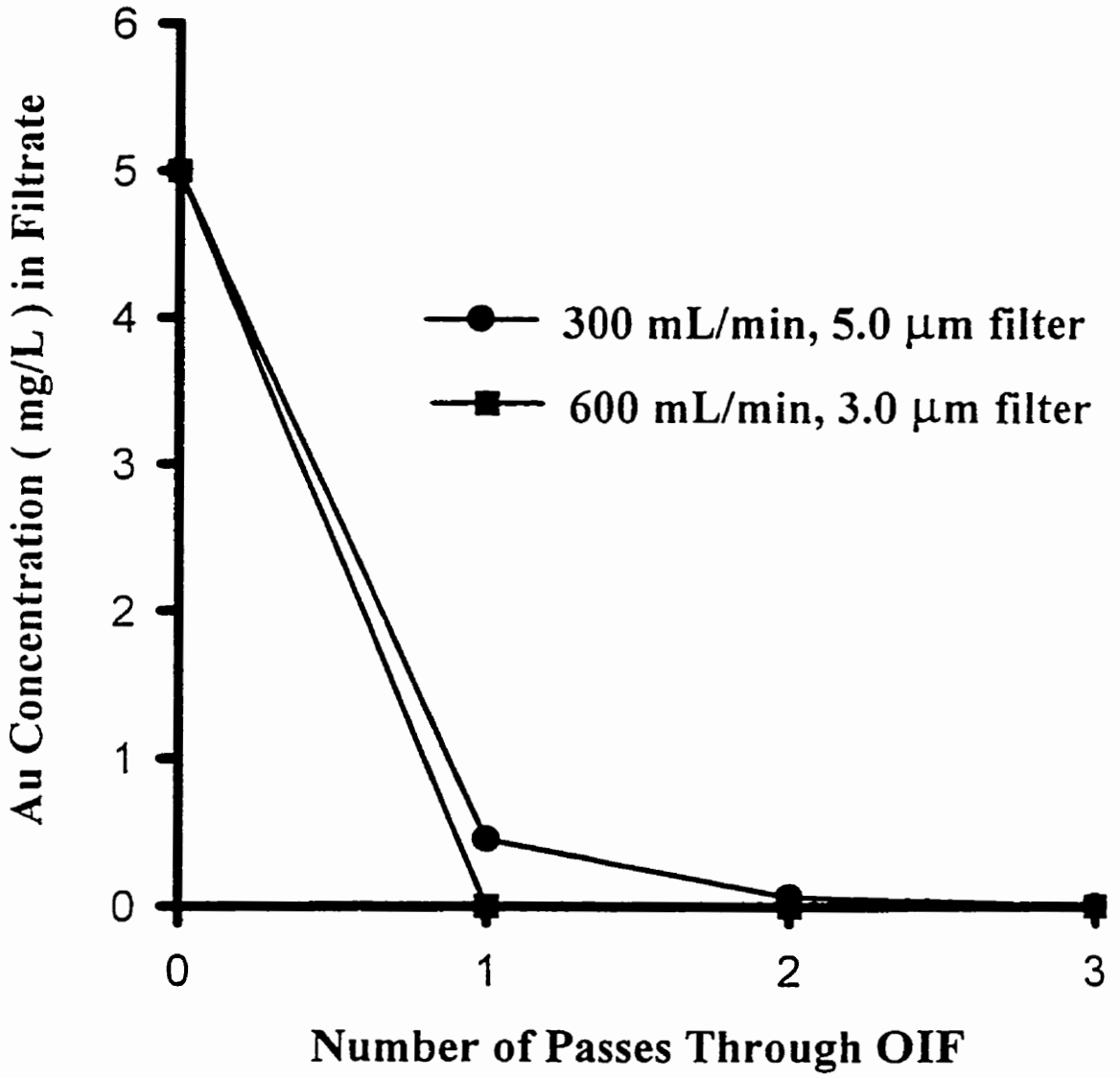

Figure 5-7. The effect of using filters with different physical characteristics : ■ pore size 3.0 μm, porosity 85% and thickness 200 μm, ● pore size 5.0 μm, porosity 60% and thickness 125 μm

extremely short. Filters with smaller pore sizes (i.e. 0.5 and 0.2 μm) could be made but they usually became plugged after coating with polyTHF and did not allow sufficient solution flow.

Different molecular weights of polyTHF were tested ranging from 650- 2000 g/mol. There appears to be no difference in extraction efficiency between the different molecular weights. However, although there was no difference in the extraction efficiencies, the larger molecular weights had the advantage of being more viscous and more resistant to creep. Creep is the process by which a polymer undergoes a slow change of shape or a flowing action when subjected to a constant force. For the experiments performed in this chapter, the polyTHF (M.W. 1000) used showed very little creep as measured by the slight weight loss incurred by an OIF for the duration of an experiment.

The capacity of the OIF was determined by passing several 100 mL solutions of 100 mg/L Au in 2.0 M HBr through the OIF until no further gold was extracted from solution. It was determined that greater than 0.5 mg of gold could be extracted for every mg of polyTHF loaded onto the filter, translating into 2.5 moles of Au for every mole of polyTHF.

5.3 Recovery of Gold from the OIF

In solid phase extraction the recovery of an extracted analyte is important to the final analysis of a particular species. In this case the gold can be recovered from the OIF in a similar manner to which it was extracted. The extraction of the gold into the active layer of the OIF is dependent on the formation of the $HAuBr_4$ complex which is readily extractable into the active polyTHF layer held on the surface of the OIF. If the complex is not protonated it is not extracted into the organic layer. Furthermore, conversion of the protonated complex at the surface of the polymer layer, to the deprotonated complex, leads to the elution of gold

from the OIF.

The gold can be recovered with efficiencies of 95-100 percent at flow rate of 10 mL/min using a solution of 0.5 M KBr adjusted to pH 10. The recovery of gold requires a flow rate that is substantially slower than that used for the extraction step. Once the $HAuBr_4$ is extracted, the complex is able to diffuse throughout the polyTHF layer. Elution from the OIF requires the deprotonation of the gold complex. Only complexes present at the surface of the polymer layer are deprotonated by the change in elution solution and then subsequently removed, which induces a concentration gradient within the polyTHF layer. This gradient causes more gold complex to diffuse to the surface of the polyTHF layer where it can deprotonate and subsequently be removed. The recovery process is diffusion-limited, requiring flow rates of approximately 10 mL/min, roughly 10 % of that of the extraction step. Eventually all of the gold on the filter is removed by the constant deprotonation of complexes that were formerly deeper within the polymer layer. The thin layer of polyTHF on the OIF is preferential to a disk made entirely of polyTHF. The thin layer allows faster elution of the extracted species. If the filter were made entirely of polyTHF or the applied layer made extremely thick, the filter would possess a greater capacity for the gold species, but would suffer from the extremely long elution times required to allow the complexes to diffuse to the surface.

The eluting solvent was adjusted to a pH of 10 to neutralize any residual acid that was present on the filter. If this pH adjustment is not made then gold recoveries are not quantitative. The residual acid present on the filter and filter equipment lowers the pH of the

Figure 5-8. Deprotonation of the gold complex leading to the elution of the gold species.

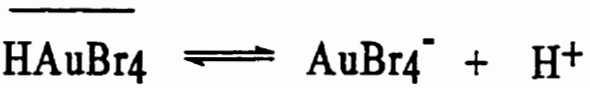

* over line indicates species present in the polyTHF layer on the OIF

eluting solution enough to inhibit the deprotonation of the $HAuBr_4$ complex. Consequently some of the gold will remain in the polyTHF layer.

The gold can also be removed from the filter by removing the entire polymer layer from the filter. Washing the filter with acetone will dissolve the polyTHF layer and remove it from the polytetrafluoroethylene filter. The filter can then be reused by impregnating it again with polyTHF.

5.4 Preconcentration Using the OIF

Gold is usually found in low concentrations (µg/L) in natural waters and gold ore. Therefore it is often valuable to concentrate as well as separate gold from other species prior to analysis. The OIF can be employed to concentrate gold by extracting gold present at low concentrations in a large volume of solution, and then eluting the gold using a relatively small volume of solution. A 2.0 L solution of 125 µg/L Au in 2.0 M HBr was passed through a 5.0 µm OIF at a flow rate of 100 mL/min. The gold complex was then eluted from the filter using 100 mL of 0.5 M KBr adjusted to pH 10. Under these conditions the quantitative recovery of the gold should produce a gold concentration of 2.5 µg/ mL in the eluting solvent. The concentration of the gold in the eluting solvent was found to be 2.4 µg/mL. This corresponds with a 96 % recovery of the gold and a 20 fold increase in concentration compared to the original solution. The experiment shows that gold can be concentrated from solution onto the OIF even when initial concentrations are quite low.

5.5 Extraction of Gold in the Presence of Other Metals

Acyclic polyethers are relatively weak and unselective at complexing metal ions[14]. Only metals that can be made hydrophobic by either attaching hydrophobic ligands or by complexation can be extracted. The separation of gold from other metals in solution is possible if gold is the only metal that can form an extractable complex with the HBr. Gold was shown to be quantitatively and selectively extracted from binary metal mixtures. An example of a binary mixture separation is gold from cadmium shown in Figure 5-9, which demonstrates the effectiveness of the OIF as a separation device for the separation of gold from other metals. A 100 mL solution containing 5 mg/L Au, 5 mg/L Cd in 2.0 M HBr was passed through a 5.0 μm OIF at a flow rate of 100 mL/min. After one pass through the filter all of the gold was quantitatively removed from the solution and extracted onto the OIF, while none of the cadmium was extracted and it remained in the filtrate even after several passes of the solution through the OIF. The slight variation in cadmium concentration between each pass can be attributed to analytical errors. In this case gold is the only one of the two metals that is able to form an extractable complex under these conditions. In Figure 5-10 the separation of gold from iron is shown. A 100 mL solution of 5 mg/L Au and 5 mg/L Fe in 2.0 M HBr was passed through a 5.0 μm OIF at a flow rate of 100 mL/min. In this case >95% of the gold is removed from solution after one pass through the OIF while the iron is left in the solution. In this binary metal mixture both Au and Fe are able to form hydrophobic extractable complexes in HBr. The stability constants of the $HFeBr_4$ complex

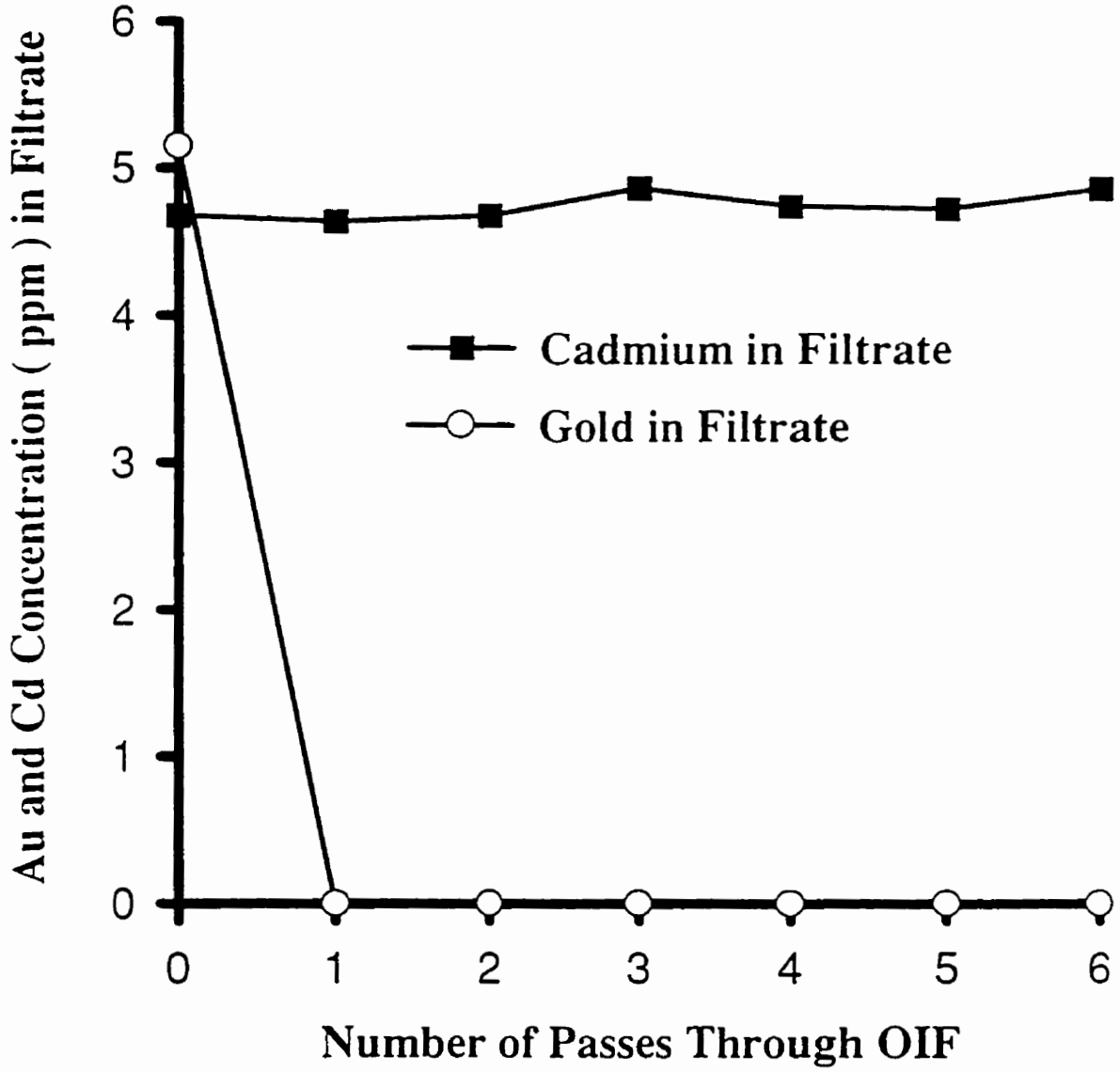

Figure 5-9. The separation of gold from cadmium using an OIF. Experiment was performed on 100 mL of solution at a flow rate of 100 mL/min through a 5.0 µm OIF.

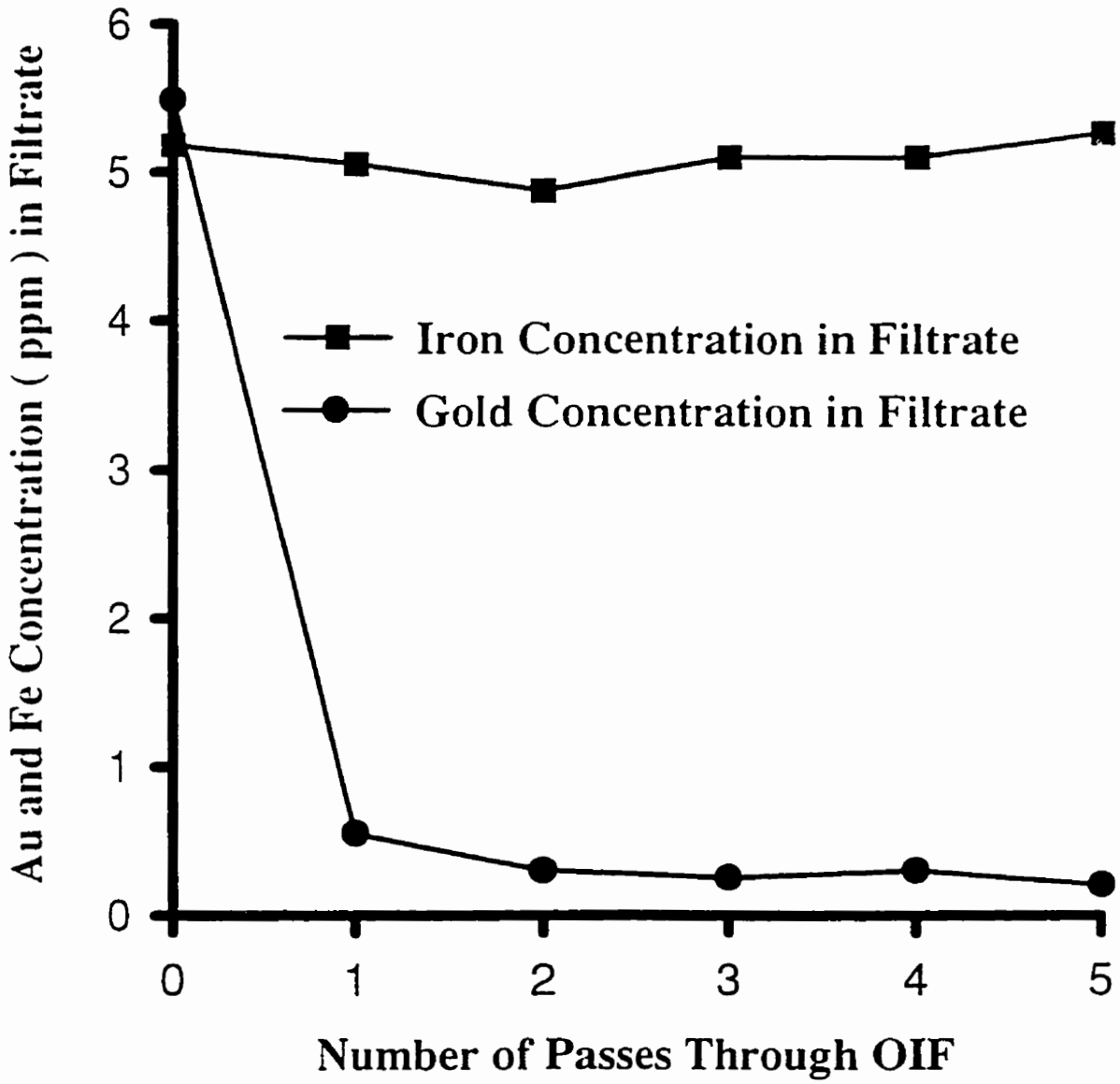

Figure 5-10. The separation of gold from iron using an OIF. Experiment was performed on 100 mL of solution at a flow rate of 100 mL/min through a 5.0 μm OIF.

dictate that much higher HBr concentrations[15] than those used would be required in order to form the extractable $HFeBr_4$ complex. Under these conditions gold is the only metal that can be extracted.

5.6 Separation of Gold from Gold Ore

The ability to extract gold quantitatively and selectively in the presence of other metals has been demonstrated for relatively simple systems with binary metal mixtures. To demonstrate the ability of an OIF to separate gold from a more complicated matrix we attempted the separation of gold from a gold ore solution. The gold ore solution was prepared as described in the experimental section (Chapter 2). The results of the separation of gold from a gold ore solution spiked with 1 µg/mL Au are shown in Table 5-1 and Figure 5-11. The metals analysed were chosen by performing an initial scan of several metals suspected of being present in the gold ore. If a metal was present in detectable concentrations it was further analysed for in the resulting samples. The gold ore from the Kirkland Lake Mine is known to possess a large concentration of pyrite which is indicated by the very large iron concentrations in the samples.

Figure 5-12 shows the concentrations of gold and iron present in the spiked gold ore sample at different stages of the separation. Even though iron was present in concentrations 300 times as large as gold, the gold was still selectively extracted and removed from solution to the point where it was below the detection limits (calculated as in Chapter 2) of the ICP after one pass through the filter. This indicates that the OIF can separate gold from solutions where large concentrations of possible interfering ions are present. The concentrations of the

other metals do not change even after several passes through the OIF which demonstrates that none of these are extracted under the experimental conditions used. None of the metals present in the Canadian ore sample were co-extracted with the gold complex. Ore samples from different areas possess different metal and mineral compositions which may lead to interferences.

The analysis of the eluting solution showed a 93 % recovery of the extracted gold from the filter and virtually undetectable amounts of other metals present. The separation results of other gold ore solutions were similar. In each of the separations the gold was removed from solution by the OIF and the gold recovered using an eluting solution. The results of the gold ore separation indicates that there does not appear to be a competing ion effect between the other metals and gold, even though some of the metals are present in significantly higher and lower concentrations than gold.

Table 5-1. Concentrations of metals present in the filtrate at different stages of the gold ore separation.

Number of Times Through OIF	Metal Concentration (mg/L)					
	Au	Mn	Cu	Fe	Cd	Zn
stock	**4.2**	26.78	1.03	1112	0.27	1.41
1	**0.36**	26.45	1.05	1111	0.30	1.40
2	**0.30**	27.36	1.15	1140	0.30	1.48
3	**0.03**	26.58	1.13	1135	0.27	1.49

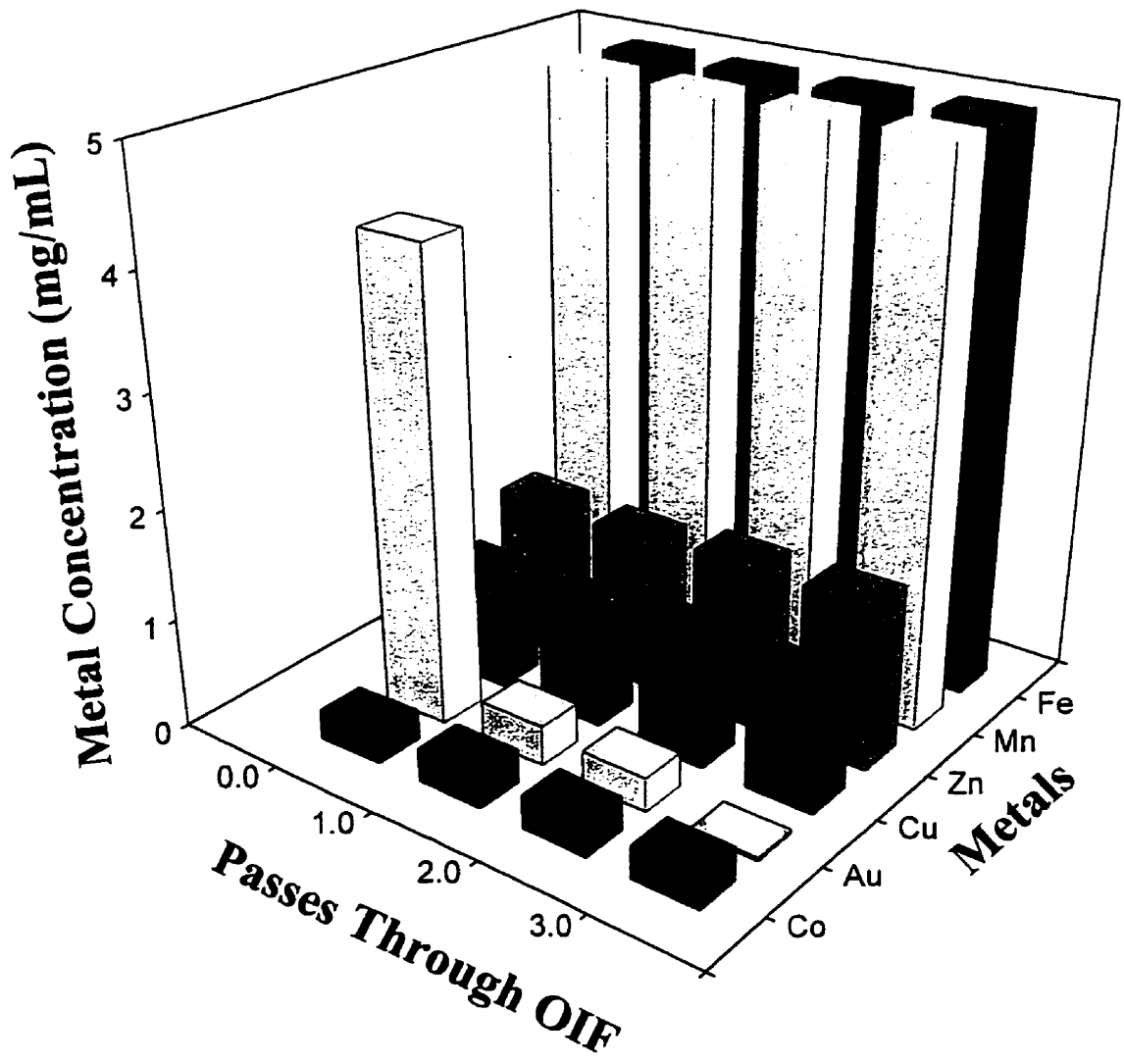

Figure 5-11. The separation of gold from gold ore displaying metal concentrations in the starting cell. Starting cell contains10 mL of 2.0 M HBr.

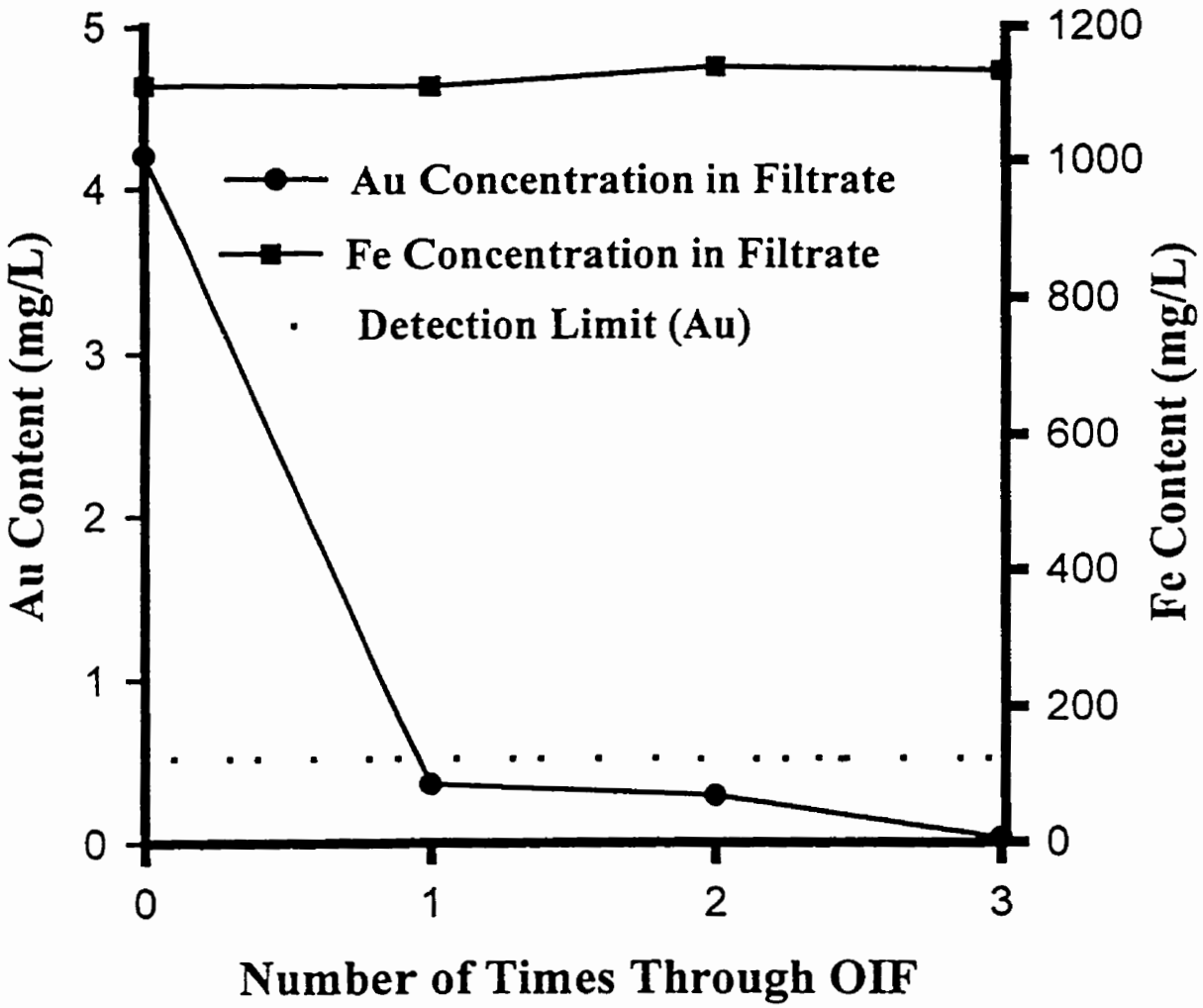

Figure 5-12. The concentration of gold and iron present in the filtrate for the separation of gold from gold ore solution. Experiment was performed on 100 mL of solution at a flow rate of 100 mL/min.

5.7 Conclusions

A polytetrafluoroethylene filter impregnated with polyTHF can rapidly and quantitatively separate gold from HBr solutions that flow through it. The separation is due to the formation of the $HAuBr_4$ complex in HBr solutions, and subsequent extraction into the PolyTHF layer on the OIF. The rate of extraction was found to increase with an increase in HBr concentration because of increased formation of the extractable species. The filter type effects the performance of the OIF with filters having larger porosity and greater thickness performing better because of the increased surface area and loading of PolyTHF.

The extracted gold can be removed from the OIF using an analogous process to the extraction. The protonated complex, $HAuBr_4$, can be eluted from the filter by converting it to the anionic, $AuBr_4^-$ complex using a 0.5 M KBr solution; the deprotonated form of the complex is not soluble in PolyTHF. Since only those complexes at the surface of the organic layer can be deprotonated, the elution process is diffusion-limited and requires reduced solution flow rates compared to the extraction to obtain recoveries greater than 95%.

The separation of gold from a number of other metals shows that the OIF can be used to separate gold from metals that cannot form extractable complexes in the presence of HBr. The separation of gold from gold ore solution demonstrates the ability of the OIF to separate gold from matrices that are quite complex. This method is inherently simple and rapid compared to other techniques currently available and can be expanded to include other metals.

References for Chapter 5

1. S. Tsurubou; *Anal. Chem.*, 67 (1995) 1465.

2. S.Fang, L. Fu; *Indian J. Chem.*, 33A (1994) 885.

3. Y. Hongwu, Z. Zhixian, Z.Mingrui, Z. Xianxin, R. Boyang; *Polyhedron*, 10 (1991) 1025.

4. R. Izatt, G.Clark, J. Bradshaw, J. Lamb, J. Christensen; *Sep. Purif. Methods*, 15 (1986) 21-72.

5. F. Fry, G. Hamilton, J. Turkevich; *Inorg. Chem.*, 5 (1966) 1943.

6. N. Bjerrum, *Bull. Soc. Chim.* Belg., 57 (1948) 432.

7. S. Martínez, A. Sastre, N. Miralles, F. Alguacil; *Hydrometallurgy*, 40 (1996) 77.

8. I. Villaescusa, N. Miralles, J. de Pablo, V. Salvadó, A. Sastre; *Solvent Extr. Ion Exch.*, 11 (1993) 613.

9. E. Souaya, M. Ramsis, S. Tobia; *Microchemical Journal*, 39 (1989) 194.

10. D. Maljković, D. Maljković, A. Paulin; *Solvent Extr. Ion Exch.*, 10 (1992) 477.

11. R. Caletka, R. Hausbeck, V. Krivan; *Anal. Chim. Acta*, 229 (1990) 127.

12. R. Oleschuk, A. Chow; *Talanta*, 43 (1996) 1545.

13. S. Ho, P. Sheridan, E. Krupetsky; *J. Membr. Sci.*, 112 (1996) 13.

14. T. Okada; *Analyst*, 118 (1993) 959.

15. R. Oleschuk, A. Chow; *Talanta*, 43, (1995) 957.

Chapter 6: The Separation of Platinum and Palladium by Selective Extraction of $H_2Pt(SCN)_6$ and $H_2Pd(SCN)_4$ Using a PolyTHF-Impregnated Filter

6.1 Introduction

The value of platinum and palladium as precious metals has prompted several investigations into their separation and concentration. Most methods involve the complexation of the metals followed by either solvent extraction or ion exchange of the complexes[1-13]. Solvent extraction is one of the most widely used methods for the separation of platinum and palladium from aqueous solutions because of its inherent simplicity. Platinum(IV) and palladium(II) form a number of complexes that are soluble in organic solvents because of the labile character of their chloro complexes, $PtCl_6^{2-}$ and $PdCl_4^{2-}$, towards several hydrophobic ligands. This leads to the formation of several highly extractable complexes at room temperature.

Although both metals undergo substitution reactions, the rates of the reactions for palladium(II) are faster by a factor of 10^5 to 10^6 than those for platinum(IV)[14]. Both metals prefer to coordinate most strongly with polarizable atoms which has focussed the development of extracting agents on those with donor atoms such as sulphur, phosphorous and nitrogen. Such ligands are termed "soft" by the empirical Pearson classification.

Thiocyanate (SCN^-) has long been known to form extractable complexes with both

platinum and palladium. The SCN^- ligand can coordinate through either the "hard" nitrogen atom, or "softer" sulphur atom. Both platinum(IV) and palladium(II) form complexes coordinating with the sulphur atom, leading to the formation of $Pt(SCN)_6^{2-}$ and $Pd(SCN)_4^{2-}$ complexes (shown in Figure 6-1) under appropriate solution conditions. Both complexes have been shown to be extractable into oxygen-containing organic solvents[15]. The relative rates of complex formation for each of these metals are quite different. Palladium(II) in the presence of SCN^-, undergoes a substitution reaction almost instantaneously while the formation of the platinum(IV) thiocyanate complex is highly dependent on SCN^- and acid concentrations, although formation can be accelerated photochemically or with heating[16,17]. The difference in the formation of the platinum(IV) and palladium(II) thiocyanate complexes was first exploited for the separation of the metals by Ishida et al[18] on an anion exchanger and later by Al-Bazi et al. on polyurethane foam[19].

Although linear polyethers such as polyTHF are weaker cation chelators than their cyclic analogues, they are effective extractants for some metal complexes. By impregnating a porous polytetrafluoroethylene filter with polyTHF, the platinum(IV) and palladium(II) thiocyanate complexes can be rapidly extracted from a solution as it passes through the impregnated filter. This device is termed an organic-impregnated filter (OIF)[20].

The intent was this investigation was to demonstrate the application of a polyTHF impregnated filter for the separation and isolation of platinum and palladium. The extraction of platinum(IV) and palladium(II) from acidic thiocyanate solutions is demonstrated using a fluorocarbon filter impregnated with α- hydro -ω hydroxypoly(oxy -1,4 -butanediyl), (polyTHF), shown in Figure 6-2. The effect of various concentrations of NH_4SCN on the rate

of metal extraction was investigated in addition to the effects of solution flow rate and acidity. Following extraction an eluting solution was used to recover the metals by deprotonating the metal complexes. The separation of platinum and palladium was investigated by exploiting the difference in the length of time required to form the extractable complexes (H_2PtSCN_6 and H_2PdSCN_4).

Figure 6-1. Formation of $Pt(SCN)_6^{2-}$ and $Pd(SCN)_4^{2-}$

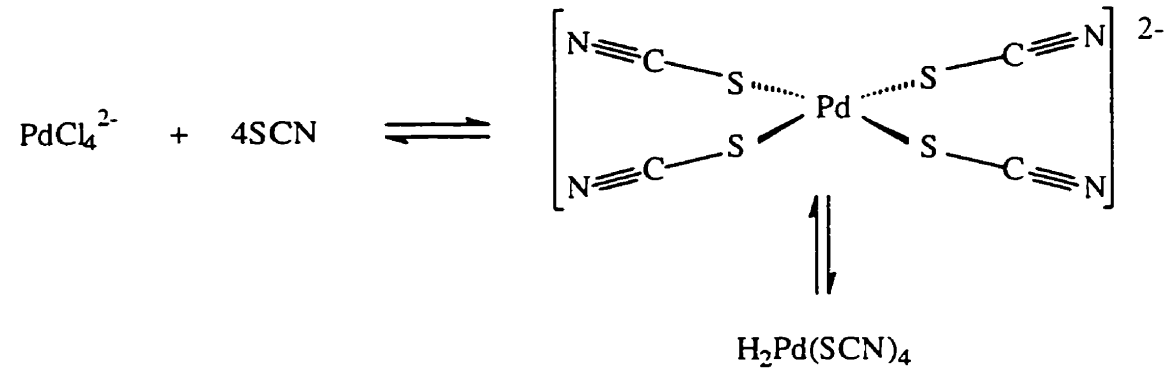

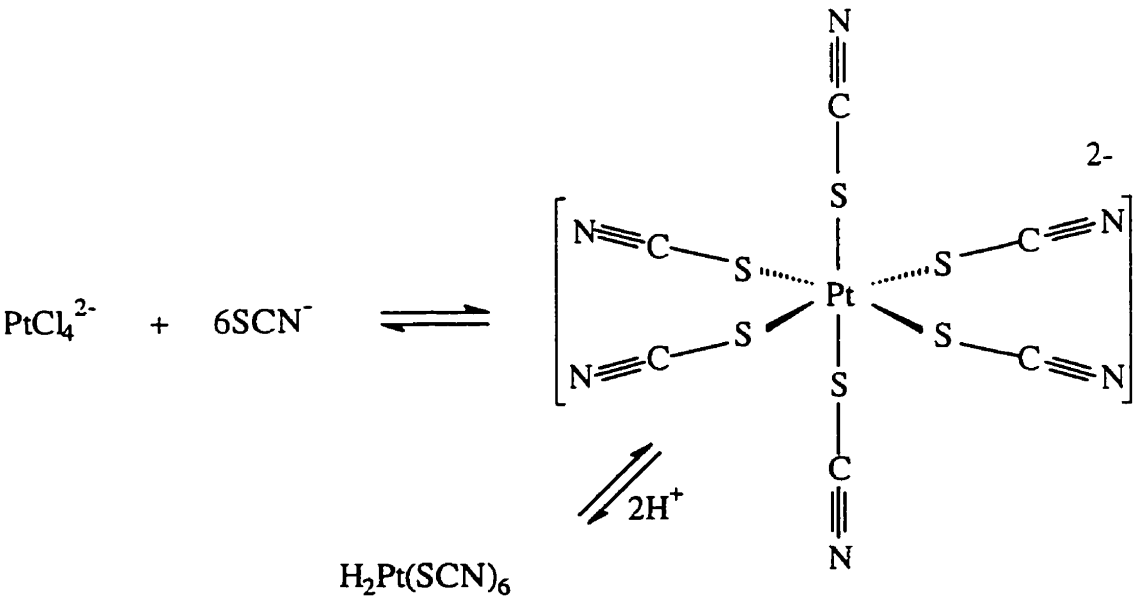

Figure 6-2. Structure of Poly THF

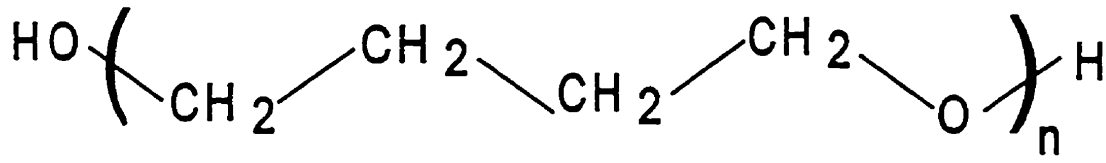

6.2 Extraction of $H_2Pd(SCN)_4$ with an OIF

Palladium in the presence of suitable HCl and NH_4SCN concentrations forms the $(Pd(SCN)_4)^{2-}$ complex. This complex is a weak acid and at a low pH becomes protonated to form the neutral species $H_2Pd(SCN)_4$ as shown in Figure 6-1. This complex has been shown to be extracted into polyurethane foam[21]. The formation of the orange/brown $(Pd(SCN)_4)^{2-}$ complex occurs almost instantaneously upon the addition of sufficient amounts of thiocyanate ligand.

Several different solutions were prepared with different concentrations of ammonium thiocyanate while maintaining a constant HCl concentration. Solutions of 4.7×10^{-5} M Pd and 0.73 M HCl were prepared with ammonium thiocyanate concentrations ranging from 1×10^{-4} to 0.1 M. The formation of the $(Pd(SCN)_4)^{2-}$ was observed at 308 nm[22].

The results of passing each of these solutions through an OIF at 40 mL min^{-1} are shown in Figure 6-3. The extraction of the $H_2Pd(SCN)_4$ complex could be monitored visually by the development of an orange/brown hue on the surface of the OIF due to the sorption of the complex into the active layer of the filter.

At a concentration of 1.0×10^{-4} M NH_4SCN only 20 % of the initial Pd is removed even after five passes through the OIF. The stoichiometric amount of thiocyanate ligand needed to form the complex is 1.9×10^{-4} M. By increasing the NH_4SCN concentration to 0.001 M and 0.01 M, the amount of the $H_2Pd(SCN)_4$ complex extracted is increased. In these cases there is an adequate SCN^- concentration to form the $Pd(SCN)_4^{2-}$ complex and subsequently >96 % of the Pd is extracted after five passes through the OIF.

Figure 6-3

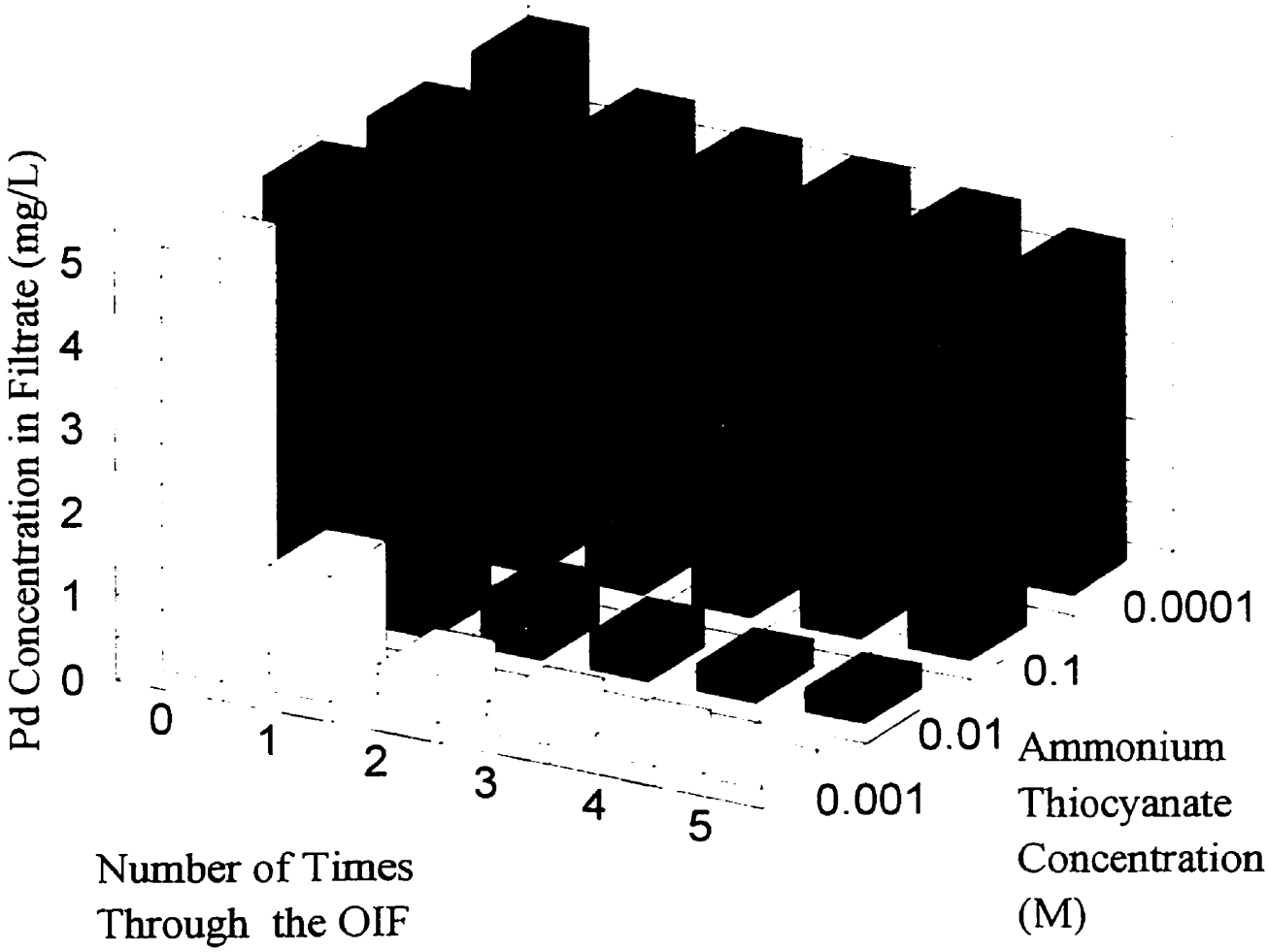
Pd Concentration in Filtrate (mg/L)
0
1
2
3
4
5
0
1
2
3
4
5
Number of Times Through the OIF
0.0001
0.1
0.01
0.001
Ammonium Thiocyanate Concentration (M)

A further increase in the NH_4SCN concentration to 0.1 M decreases the amount of Pd extracted from 99 % to 70 %. Figure 6-4 shows the spectra of three solutions containing 5 $\mu g\ mL^{-1}$ Pd concentrations and NH_4SCN concentrations ranging from 1 x 10^{-4} to 0.1 M. In spectra "A" there is no significant peak at 308 nm indicating that very little of the $Pd(SCN)_4^{2-}$ complex has formed. Increasing the NH_4SCN concentration to 0.001 M produces a peak at 308 nm in addition to a peak at 280 nm. The peak at 280 nm is presumed to be mixed Pd complexes with the general formula, $PdCl_{4-n}(SCN)_n^{2-}$ (n = 1,2,3). Further increasing the NH_4SCN to > 0.01 M and produces solely the $Pd(SCN)_4^{2-}$ complex. Experimental results suggest optimum extraction takes place when sufficient ligand is available to form the extractable complex. Although this explains the lack of extraction at low thiocyanate concentrations it does not account for the poorer extraction at higher thiocyanate concentrations.

The smaller extraction at higher complexing agent concentrations can be attributed to an increase in the amount of free SCN^- ion present in solution. In sufficiently acidic solutions the free thiocyanate becomes protonated to form thiocyanic acid (HSCN) with a $pK_a \approx -1.0 - -2.0$[23,24]. The metal acid equilibrium is shown in Figure 6-5. It has been suggested[25] that HSCN is also extracted from solution into organic solvents. The thiocyanic acid forms hydrogen bonds[26] with the ether oxygens present in the active layer shown in Figure 6-6. Hydrogen bonding with the ether oxygen blocks the possible sorption sites on the surface of the OIF preventing the metal complex from being sorbed by the active layer of the OIF. The effects of the thiocyanic acid can be controlled by minimizing the amount of free acid and free thiocyanate that is present in solution. For the extraction of platinum

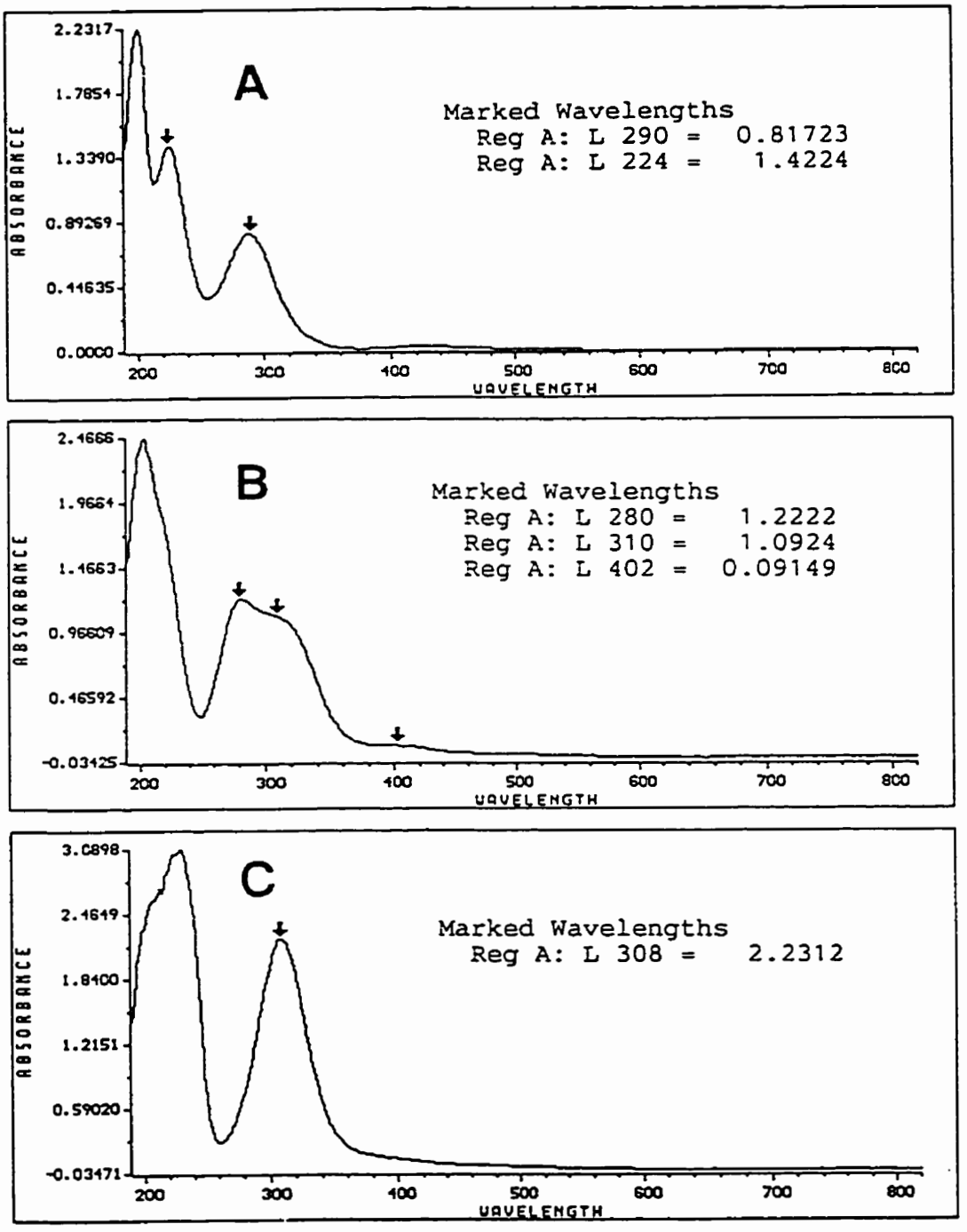

Figure 6-4. The UV/Vis spectra of solutions containing 5 μg mL^{-1} Pd and 0.73 M HCl and various concentrations of NH_4SCN. A: 1 x 10^{-4} M NH_4SCN, B:1 x 10^{-3} NH_4SCN, C: 0.1 M NH_4SCN

Figure 6-5. Formation of the neutral palladium(II) thiocyanate complex

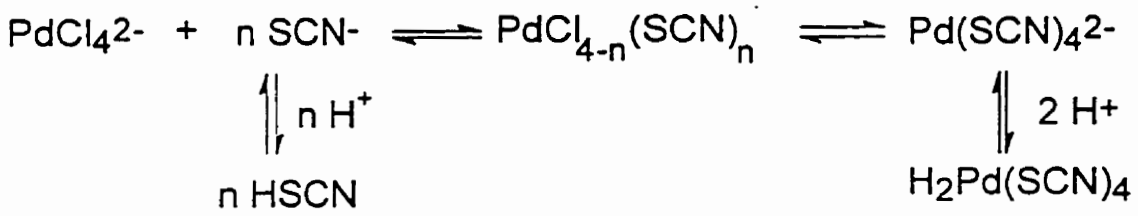

Figure 6-6. Hydrogen Bonding of Thiocyanic Acid (HSCN) to polyTHF layer

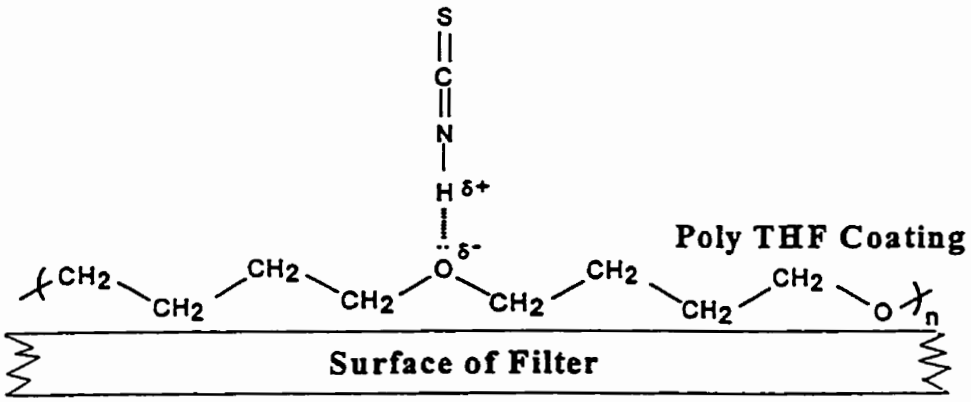

and palladium complexes this is best achieved by controlling the thiocyanate concentration because a relatively high acid concentration is required to produce the extractable metal complexes.

The effect of solution flow rate on the extraction of $H_2Pd(SCN)_4$ was examined using the best extraction conditions from Figure 6-4 consisting of 100 mL of 5 μg mL^{-1} Pd in 0.001 M NH_4SCN/0.73 M HCl. Several different flow rates were tested ranging from 2 to 600 mL min^{-1} and the results are shown in Figure 6-7. At a relatively low flow rate of 2 mL min^{-1}, the palladium complex is 98 % removed from solution after only one pass through the OIF. In comparison, only 32 % of the palladium complex is removed at a flow rate of 600 mL min^{-1} after one pass. The poor extraction can be improved by passing the solution through the OIF several times. Five passes through the OIF at 20, 40 and 600 mL min^{-1} led to recoveries of 96, 95 and 84 % respectively.

The flow rate required for quantitative recovery can be increased using a "stacked" OIF consisting of two OIF's placed on top of one another. This doubles the amount material available to sorb the metal complexes and allows flow rates of up to 10 mL/min while still quantitatively removing the $H_2Pd(SCN)_4$ from solution in a single pass through the OIF.

6.3 Extraction of $H_2Pt(SCN)_6$ with an OIF

Platinum(IV) also forms an extractable complex in the presence of suitable concentrations of NH_4SCN and HCl (Figure 6-8), although at a much slower rate than

Figure 6-7

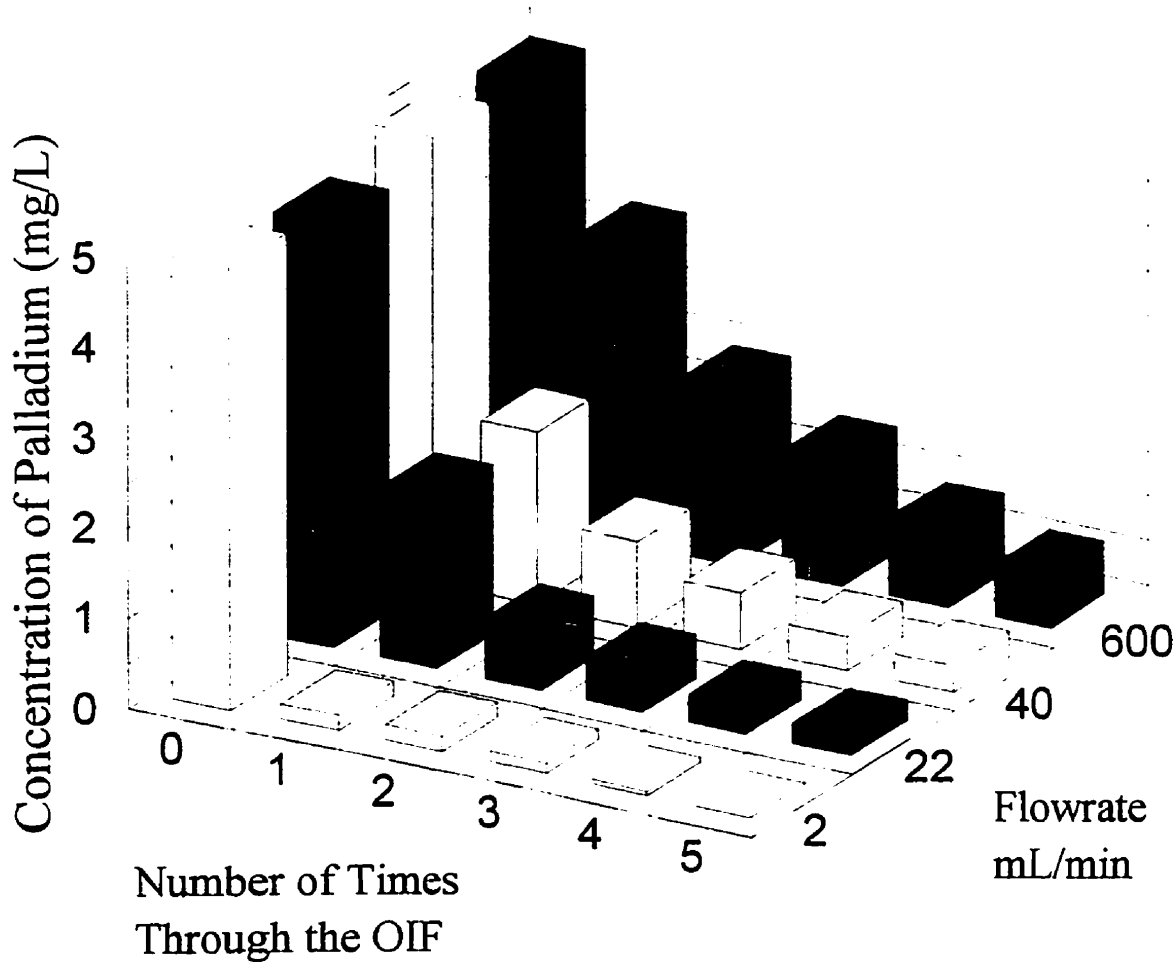
Concentration of Palladium (mg/L)
0
1
2
3
4
5
0
1
2
3
4
5
Number of Times
Through the OIF
2
22
40
600
Flowrate
mL/min

Figure 6-8. Formation of the neutral platinum(IV) thiocyanate complex

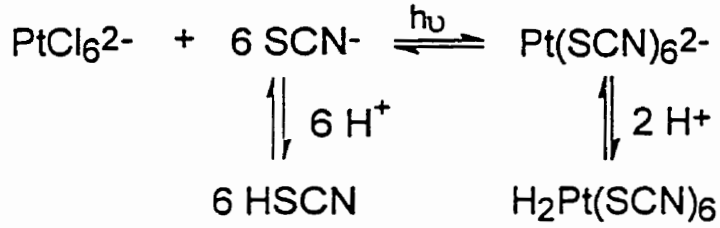

palladium(II). Platinum forms the complex $Pt(SCN)_6^{2-}$, which like $Pd(SCN)_4^{2-}$, is a relatively weak acid that can become protonated at a sufficiently low pH. The protonated neutral complex has been shown to be responsible for the extraction of platinum from aqueous solutions into various organic solvents. The substitution reaction of $PtCl_6^{2-}$ and SCN^- to develop $Pt(SCN)_6^{2-}$ is slow requiring several hours to form at room temperature and in the absence of strong light. The rate of formation of the $Pt(SCN)_6^{2-}$ complex can be accelerated by exposing the solution to either UV light or heat. The formation of the $Pt(SCN)_6^{2-}$ was observed at 286 and 360 nm [27,28]

Figure 6-9 shows the passage of two solutions, identical in composition, through the OIF. One solution was passed through the OIF 5 minutes after being prepared while the other was exposed to sunlight for 1 hour and then passed through the filter. Analysis of the freshly prepared solution showed only one peak (λ_{max} = 262 nm) due to the presence of the $PtCl_6^{2-}$ complex. The freshly prepared solution showed very little extraction even after 5 passes through the OIF at a flow rate of 100 mL min^{-1}. Conversely, the solution that was exposed to UV light for 1 hour showed >99 % extraction after only one pass through the OIF with the same flow rate. The spectrum of this solution prior to passing it through the OIF revealed a large peak at 286 nm indicating the presence of the $Pt(SCN)_6^{2-}$ complex. The platinum extraction can be followed visually by the appearance of a yellow hue on the surface of the OIF that becomes darker with increasing amounts of $H_2Pt(SCN)_6$ sorbed into the active layer of the OIF.

The effect of flow rates from 15 – 600 mL min^{-1} on the extraction of the $H_2Pt(SCN)_6$ was tested. Even at a flow rate of 600 mL min^{-1} > 99% of the $H_2Pt(SCN)_6$ is removed from

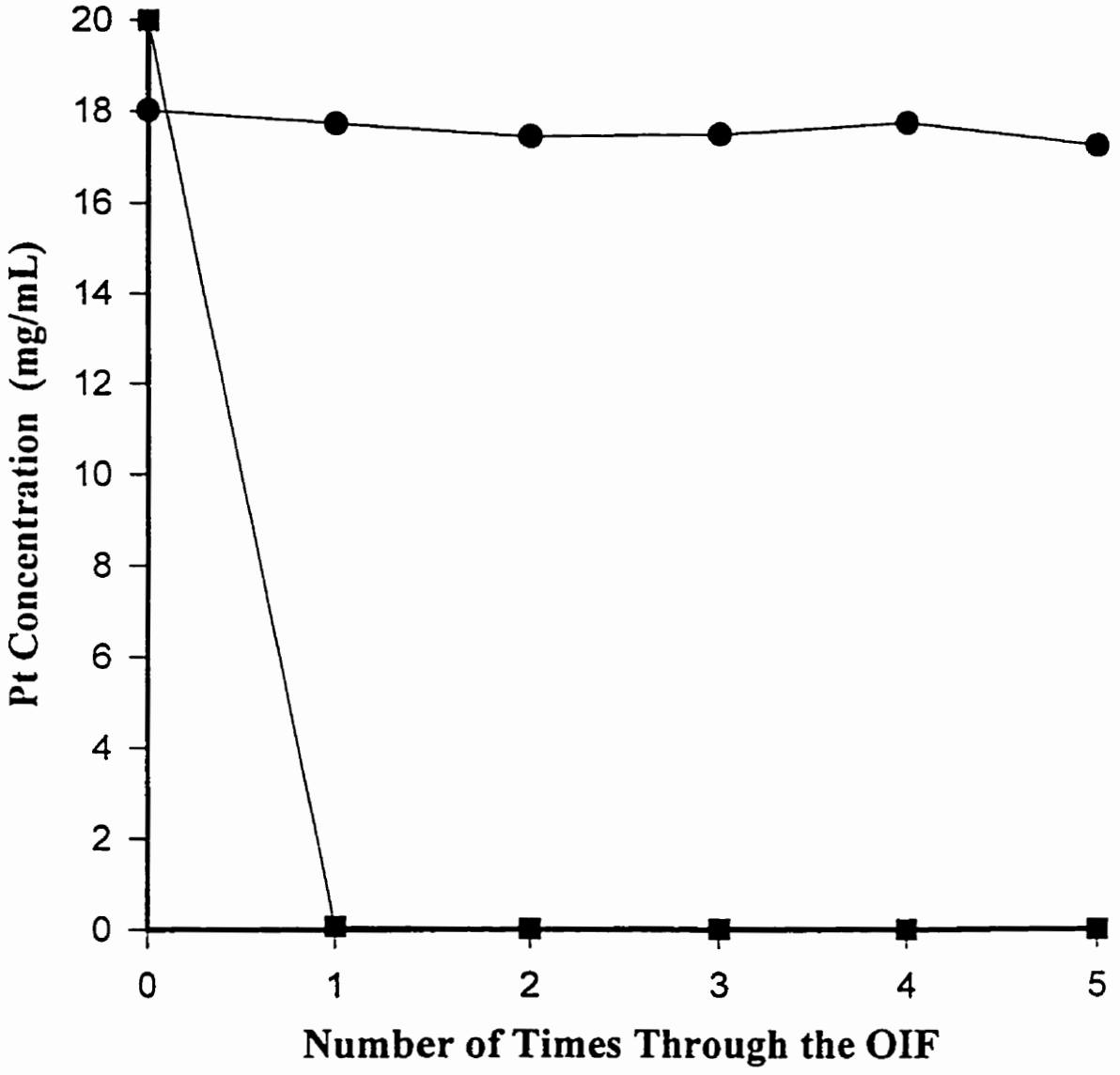

Figure 6-9. The extraction of two solutions of 15 μg mL^{-1} Pt(IV)/ 1 x 10^{-3} M NH_4SCN/ 0.73 M HCl at a flow rate of 100 mL min^{-1} : ●Pt (IV) concentration present in the filtrate for a freshly prepared solution; ■Pt (IV) concentration in the filtrate for a solution exposed to UV light to form the extractable complex.

solution. These results are markedly different from those for $H_2Pd(SCN)_4$ which showed a much poorer extraction at a flow rate of 600 mL min^{-1}. The difference in the relative rates of extraction for each of the metal complexes is probably due to two reasons. Platinum(IV) has a larger ionic radius and a higher oxidation state than palladium(II). Both factors contribute to the formation of a stable six coordinate platinum thiocyanate complex compared to a four coordinate complex for palladium(II). The increased number of hydrophobic ligands and larger size of the complex makes the platinum species much more hydrophobic than that of the palladium. Consequently, the extraction into the hydrophobic layer of the OIF is much faster for $H_2Pt(SCN)_6$ than for $H_2Pd(SCN)_4$. The second factor affecting the rate of extraction concerns the equilibria of the complexes. Analysis of optimum solution conditions shows that all of the platinum is in the form of the extractable complex while palladium is an equilibrium between several complexes.

6.4 Recovery of Platinum(IV) and Palladium(II) from the OIF

Once the platinum(IV) or palladium(II) complexes have been extracted onto the filter they can be removed by converting either of the complexes from an extractable to a non-extractable form. Al-Bazi et al. have shown[29] that converting both the $H_2Pt(SCN)_6$ and $H_2Pd(SCN)_4$ complexes to their ammonia analogues allows the recovery of these metals from polyurethane foam. Also we have shown that a metal complex can be eluted from an OIF by simply using conditions that favour deprotonation of the metal complex as shown in Figure 6-10.

Figure 6-10. Elution of Platinum and Palladium from the OIF with Different Eluting Solutions

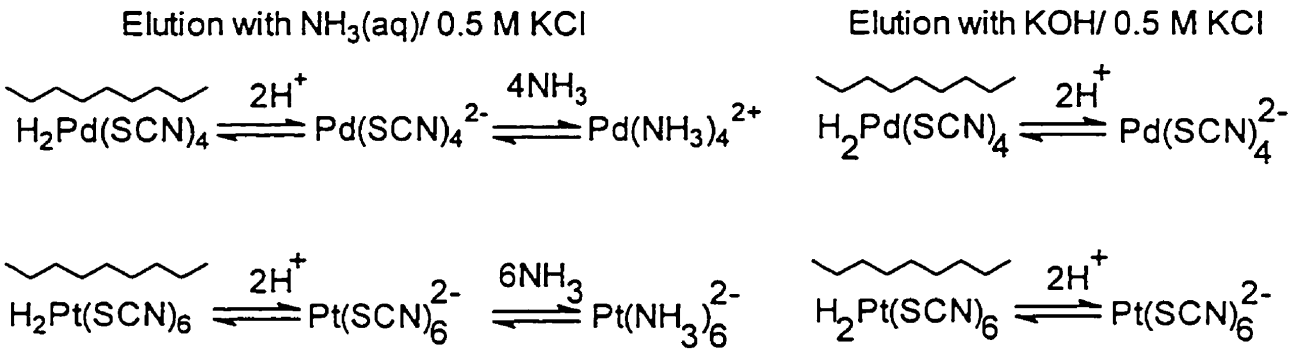

Note: Overline indicates species in the organic layer of the OIF

The recovery of each of the metals from the OIF was attempted using eluting solutions composed of 0.1 M NH_3(aq)/0.5 M KCl. As the eluting solution is added to the OIF for both the recovery of platinum and palladium, the filter changes from coloured to colourless because the thiocyanate complexes undergo a substitution reaction to form their ammonia analogues. Consequently each of the metals is removed from the OIF into the eluting solution with recoveries of between 95 - 100 %. The eluting process is rapid requiring only 20 seconds of contact time for the conversion of the complexes and their removal from the filter.

The elution of the metals from the OIF may be due to either the deprotonation of the complexes or the change to the ammonia complex. To determine which process is responsible for elution, a different eluting solution was used composed of 0.1 M KOH/ 0.5 M KCl. Potassium hydroxide was chosen because it does not develop an alternative complex with either platinum(IV) or palladium(II) but maintains a high pH favouring the deprotonation of the thiocyanate complexes. Eluting the platinum and palladium complexes with KOH solution showed that both are removed from the OIF with >95% recoveries. The high recovery indicates that the deprotonation step is responsible for the elution of the complexes from the filter, rather than conversion to another complex. Although both eluting solutions lead to excellent recoveries, their stabilities on standing are quite different. The metals are stable in the ammonium hydroxide eluting solution indefinitely, while those in the potassium hydroxide solution precipitate in a matter of hours.

6.5 Simultaneous Extraction of $H_2Pd(SCN)_4$ and $H_2Pt(SCN)_6$

In the previous two sections we have described the extraction of platinum(IV) and palladium(II) individually. To determine the ability of the OIF to simultaneously extract both $H_2Pt(SCN)_6$ and $H_2Pd(SCN)_4$ a solution containing both metals in their extractable forms was passed through the OIF. A solution containing both 15 $\mu g\ mL^{-1}$ Pd(II) and 15 $\mu g\ mL^{-1}$ Pt(IV) in 0.01 M NH_4SCN/ 0.73 M HCl was prepared and exposed to sunlight for 5 hours. The thiocyanate concentration was increased by an order of magnitude to provide sufficient ligand for the formation of the extractable complexes for both metals. In cases where inadequate amounts of thiocyanate were present, both metals suffered poor extraction. The solution containing the two metals was passed through an OIF and fractions collected after each pass for analysis. The results of the experiment are shown in Figure 6-11. The platinum and palladium complexes were both extracted into the OIF simultaneously. The platinum complex was quantitatively extracted from the solution after two passes through the OIF at 70 mL/min while the palladium was 95 % removed from solution after the third pass through the OIF. The results show that both metals can be simultaneously removed from solution as their thiocyanate complexes if both are in an extractable form.

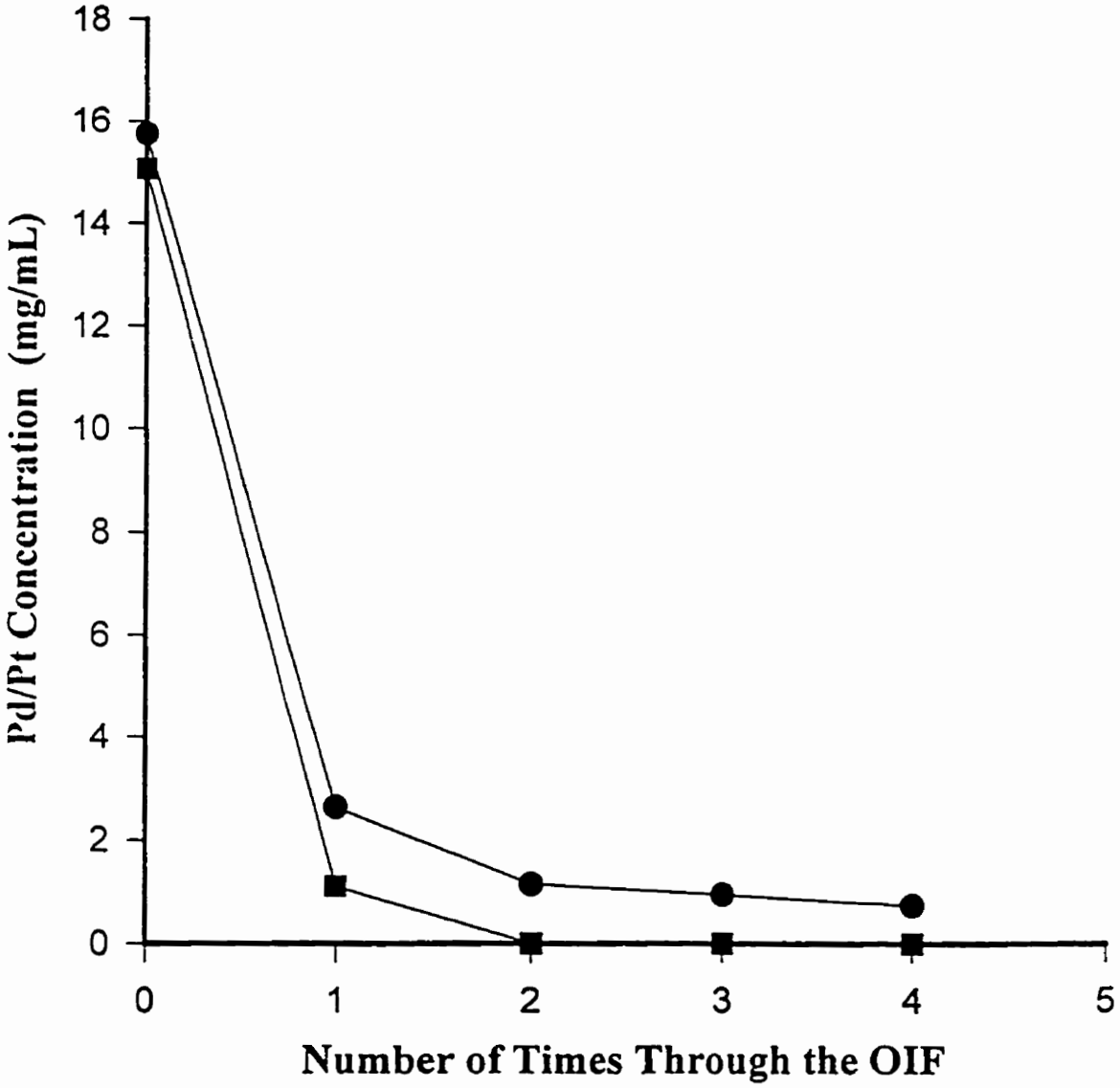

Figure 6-11. Simultaneous extraction of both Pt(IV) and Pd(II) from a solution of 0.01 M NH_4SCN/ 0.73 M HCl at a flow rate of 70 mL min^{-1}: ● Pd (II) concentration in filtrate; ■ Pt (IV) concentration in filtrate.

6.6 Separation of $H_2Pd(SCN)_4$ and $H_2Pt(SCN)_6$ with an OIF

We have shown that both the platinum(IV) and the palladium(II) thiocyanate complexes can be extracted either individually or simultaneously. The separation of these two complexes can be achieved using the same solution chemistry and conditions as described. The $H_2Pd(SCN)_4$ complex is formed at a much faster rate than that of the $H_2Pt(SCN)_6$ and therefore the palladium(II) complex can be removed prior to the development of the extractable platinum(IV) complex separating the two metal complexes from one another. A solution containing 15 μg mL^{-1} palladium(II) and 15 μg mL^{-1} platinum(IV) in 0.01 M NH_4SCN/ 0.726 M HCl was freshly prepared and passed through the OIF three times at a flow rate of 20 mL min^{-1}. The results are shown in Figure 6-12.

After only one pass, 98 % of the palladium was removed from solution while the platinum concentration remained at 15 μg mL^{-1} throughout. After the third pass through the OIF the remaining filtrate was exposed to sunlight for 3 hours to allow the extractable platinum complex to develop. The irradiated solution was then passed through the OIF at 20 mL min^{-1}. After one pass through the filter 98% of the platinum was extracted from the irradiated solution and remained on the filter throughout the final two passes. This demonstrates that these two metals can be separated with high recoveries and excellent selectivity using the OIF process.

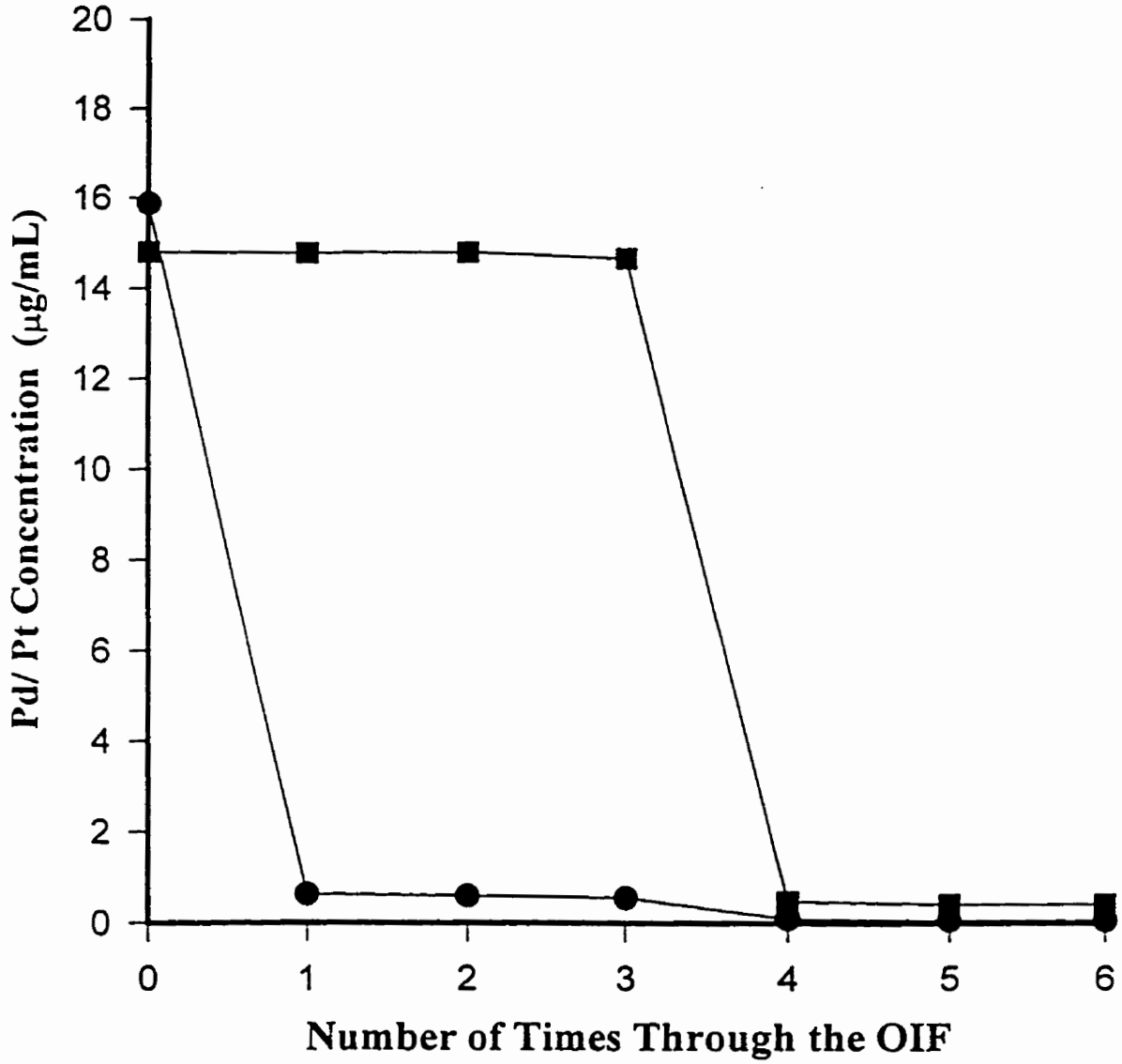

Figure 6-12. Separation of Pt (IV) and Pd (II) using an OIF from a solution of 0.01 M NH_4SCN/ 0.73 M HCl at a flow rate of 20 mL min^{-1}. After the third pass through the filter the filtrate was exposed to UV light : ● Pd (II) concentration in filtrate; ■ Pt (IV) concentration in filtrate.

6.7 Preconcentration of Platinum and Palladium Using the OIF

Platinum and palladium are often present a low levels below the 5 ng/L level[30] in marine and natural waters. At low concentrations platinum and palladium are difficult to separate, recover and determine. Several tests were performed to determine the suitability of the OIF for use as a preconcentration device. One litre solutions were prepared containing various concentration levels of palladium ranging from 1 to 100 ng/mL in 0.001 M NH_4SCN/ 0.73 M HCl. Each of the solutions was passed through a freshly prepared OIF at a flow rate of 20 mL min^{-1}. The palladium complex was then washed from the filter using 10 mL of an eluting solution of 0.1 M $NH_3(aq)$/0.5 M KCl. The amount of palladium recovered did not exceed 20% of what was present in solution even though favourable extraction conditions were used. The poor extraction suggests that either the increased amount of thiocyanic acid coming in contact with the OIF from the larger sample size or the lower concentration of palladium is interfering with the extraction process. To determine which factor was responsible for the poor recoveries a smaller volume of sample with the same palladium concentration was passed through the OIF. A solution consisting of 100 ng mL^{-1} was passed through the OIF three times at a flow rate of 20 mL min^{-1}. After eluting the palladium with 10 mL of the ammonium hydroxide eluting solution, a 98 % palladium recovery was obtained producing a 10 fold increase in concentration in the eluting solution compared to the initial sample. This result shows that even at low palladium concentrations the extraction is effective and that the poor recoveries can again be attributed to the presence of thiocyanic acid in solution. The lower palladium concentrations and larger sample volume contributes to increased amounts of total thiocyanic acid in the sample which interferes with the extraction

of the palladium complex. The overall extraction is limited by the exchange capacity of the OIF for the thiocyanic acid present in solution. Once the available sorption sites are blocked by the thiocyanic acid, the metal complexes are no longer extracted from solution.

To eliminate the problem of excess thiocyanic acid two routes can be taken. The first method involves changing the concentration of NH_4SCN present in solution. The results of changing the SCN^- concentrations are shown in Table 6-1 where 10 mL of eluting solution were used to recover the palladium. If quantitative recovery was obtained a concentration factor of 100 would result. The results show that the optimum NH_4SCN concentration for the recovery of palladium from 1 L solutions is approximately 1.9×10^{-4} M, although the recovery is still quite low. The recovery of palladium in 10 mL of eluting solution results in an increase in concentration of 20-30 x from the original 1 L starting solution.

The amount of acid present in solution can also be varied to try to minimize the effect of HSCN in the solution although sufficient acid is required to protonate the metal thiocyanate complexes. Hydrochloric acid concentrations ranging from 0.73 M to 0.073 M were tested with resulting recoveries ranging from 32 to 40 % for one pass through the filter.

The interference caused by the presence of HSCN is a considerable problem when trying to obtain large preconcentration factors with the OIF. By carefully controlling the ammonium thiocyanate and hydrochloric acid concentration the effects of the interference can be somewhat minimized. The OIF process has been shown to be unsuitable for large volume preconcentration (ie. > 1 L) because of the relatively poor recoveries, but is suitable for smaller volume preconcentration where the effect of thiocyanic acid is not as prevalent.

Table 6-1. The effect of varying NH_4SCN concentration on the recovery of palladium

Concentration			Solution	% Recovery
Pd ng/mL	**NH_4SCN (M)**	**HCl (M)**	**Volume (mL)**	
100	1.0×10^{-2}	0.73	1000	20
100	1.0×10^{-3}	0.73	1000	17
100	1.9×10^{-4}	0.73	1000	32

$$Note: \%\ Recovery = \frac{Mass\ of\ metal(eluting\ solution)}{Mass\ of\ metal(original\ sample)}\ X\ 100$$

6.8 Conclusions

A polytetrafluoroethylene filter impregnated with poly(tetramethylene) ether glycol can selectively extract platinum and palladium from NH_4SCN/HCl solutions that flow through it. The extraction is due to the formation of the $H_2Pd(SCN)_4$ and $H_2Pt(SCN)_6$ complexes and their subsequent extraction into the polyTHF layer on the OIF. The rate of extraction was found to be optimum in solutions containing between 0.01 and 0.001 M NH_4SCN. Extraction efficiencies decreased with increasing amounts of thiocyanic acid present in the sample.

Once extracted, the protonated complexes, $H_2Pd(SCN)_4$ and $H_2Pt(SCN)_6$, can be eluted from the filter by converting them to the anionic, $Pd(SCN)_4^{2-}$ and $Pt(SCN)_6^{2-}$ complexes using a basic solution. The deprotonated forms of the complexes are no longer soluble in polyTHF layer and are eluted.

Platinum(IV) and palladium(II) can be extracted individually or simultaneously depending on the different solution conditions used for the extraction. Separation of the two metals can be achieved by exploiting the difference in the rate of formation of their thiocyanate complexes. Palladium develops the extractable complex almost instantaneously in the presence of the SCN^- ligand, while platinum requires several hours under "normal" conditions to develop the extractable complex. The separation of palladium from platinum demonstrates the ability of the OIF to separate metals from one another in solution but interferences from HSCN limit analytical applications.

References for Chapter 6

1. M. Lee, G. Tölg; *Analytica Chimica Acta*, 272 (1993) 193.

2. R. Gaita, S. Al-Bazi; *Talanta*, 42 (1995) 249.

3. P. Di, D. Davey; *Talanta*, 42 (1995) 685.

4. J. Enzweiler, P. Potts; *Talanta* (1995) 1411.

5. Y. Baba, T. Fukumoto; *Chemistry Letters* (1992) 727.

6. G. Lee, K. Chung; *Analyst*, 115 (1990) 965.

7. E. Basova, V. Ivanov, T. Bol'shova, N. Babkova; *Zhurnal Analiticheskoi Khimii*, 45 (1990) 671.

8. S. Kumar, R. Verma, B. Venkataramani, V. Raju, S. Gangadhara; *Solvent Extraction and Ion Exchange*, 13 (1995) 1097.

9. Z. Su, Q. Pu, X. Luo, X. Chang, G. Zhan, F. Ren; *Talanta*, 42 (1995) 1127.

10. Fu, J.; Nakamura, S.; Akiba, K.; *Analytical Sciences*, 11 (1995) 149.

11. C. Gavino, G. Marangoni, B. Pitteri, N. Stevanato, A. Vavasori; *Reactive Polymers*, 14 (1991) 143.

12. G. Hall, J. Pelchat; *Analytical Atomic Spectrometry*, 8 (1993) 1059.

13. S. Al-Bazi, A. Chow; *Talanta*, 31 (1984) 815.

14.A. Yordanov, J. Mague, D. Maxhill; *Inorg. Chim. Acta.*, 240 (1995) 441.

15. Forsythe, J. H.; Magee, R. J.; Wilson, C. L.; *Talanta*, 3 (1960) 330.

16. J. Forsythe, R. Magee, C. Wilson; *Talanta*, 3 (1960) 330.

17. P. Senise, L. Pitombo; *Talanta*, 11(1964) 1185.

18. K. Ishida, T. Kiriyama, R. Kuroda; *Anal. Chim. Acta.*, 41 (1968) 537.

19. S. Al-Bazi, A. Chow; *Anal. Chem.*, 55 (1983) 1094.

20. R. Oleschuk, A. Chow; *Talanta*, in press.

21. S. Al-Bazi, A. Chow; *Talanta*, 29 (1982) 507.

22. R. Magee, M. Khattak; *Microchem. J.*, 8 (1964) 285.

23. T. Morgan, G. Stedman, P. Whincup; *J. Chem. Soc.*, (1965) 4813.

24. T. Crowell, M. Hankins; *J. Phys. Chem.*, 73 (1969) 1380.

25. A. Jurriaanse, D. Kemp; *Talanta*, 15 (1968) 1287.

26. T. Barakat, N. Legge; Pullin. A.D.E.; *Trans. Faraday Soc.*, 5 (1963) 1773.

27. P. Senise, L. Pitombo; *Talanta*, 11 (1964) 1185.

28. D. Swihart, W. Mason; *Inorg. Chem.*, 9 (1970) 1749.

29. S. Al-Bazi, A. Chow; *Talanta*, 30 (1983) 487.

30. G. Hall, J. Pelchat; *J. Anal. At. Spectrom.*, 8 (1993) 1059.

Chapter 7: Membrane Characterization and Degradation

7.1 Introduction

Polyurethanes have been of considerable interest to our research group for a number of years as they possess the ability to preferentially extract and separate a variety of analytes from several different media. Manufacturers of polyurethane are often reluctant to release information pertaining to the formulation of their polymers. This is due to the trade secrets involved and the intense competition between polymer manufacturers. The lack of information about the polymer composition combined with a large number of possible compounds used in polyurethane synthesis, makes mechanistic information on the polyurethane extraction process extremely difficult to obtain. In addition during experiments using the membrane materials to separate metals, the membranes are subjected to a harsh acid gradient. This gradient led to the eventual degradation of the membrane material. For this reason a variety of analytical methods were used to characterize the molecular structure of the two polymers involved in our research and to attempt to determine the nature of the degradation process occurring when the membranes are subjected to strong acid conditions.

The most common methods used for polymer analysis include gel permeation chromatography (GPC), Fourier transform infra-red spectroscopy (FTIR), attenuated total reflectance infra-red spectroscopy (FTIR-ATR), differential scanning calorimetry (DSC) , electron spectroscopy for chemical analysis (ESCA) and gas chromatography/mass spectrometry (GC/MS).

7.2 Polymer Information

Both polymers tested in this investigation were produced by J.P. Stevens & Co., Inc. Stevens Elastomerics/Urethane Products, Northhampton. Polymers were tested in the form of a thin film with thicknesses of 50 µm (0.002") and 25 µm (0.001").

XPR625-FS - an ether based polyurethane film

MP1495-SL - an ester based polyurethane film

7.3 Infrared Analysis

The use of infrared spectroscopy for polymer analysis is based on the excitation of polymer vibrations by the absorption of photons in specific spectral regions. Characteristic absorbencies of specific wavelengths of infra-red radiation can be used to elucidate polyurethane structure[1,2,3].

In the following section we describe the elucidation of various portions of the polyurethane structure using both FTIR (direct transmission) and FTIR-ATR (attenuated total reflectance).

Infrared ATR analyses were performed using a Nicolet 550 Fourier transform infrared spectrometer (Laval University). Spectra were obtained with angles of incidence being 30, 45 and 60°. The refractive index of the polymer was found to be 1.5, leading to a sampling depth of 0.5 µm to 3.0 µm over the wavelengths 4000 - 700 cm^{-1} at 45°. Spectra were collected for 100 scans at a resolution of two wavenumbers. The different ATR angles were used to probe the change of chemical composition with increasing depth in the polymer

matrix. Direct transmittance measurements were performed using a Bomem MB series FTIR (University of Manitoba).

The direct transmittance spectra for both polymer films are shown in Figure 7-1 and the peak assignments are shown in Tables 7-1 and 7-2. The spectra of the XPR625-FS film showed a strong absorption at 1102 cm^{-1}, indicating the C-O-C etheral asymmetric vibration stretching derived from the polyether soft segment. The spectra of the MP1495-SL demonstrated a strong absorption bands at 1170 and 1140 cm^{-1} which is characteristic of the ester group present in the ester soft segment. Absorption bands of 1597 and 1413 cm^{-1} in each of the samples indicated the presence of aromaticity, most likely in the hard segment. Also the absence of an absorbance band in the region of 1640 cm^{-1} showed that there were no urea linkages present in either of the samples. This indicates that the chain extenders used in synthesizing the polyurethanes were diol rather than diamine.

Further analysis of the infrared spectra focussed on three spectral regions: the N-H stretching region (3450-3300cm^{-1}); the carbonyl stretching region (1740-1690cm^{-1}); and the combination C-N + N-H stretching and bending region (1250-1050cm^{-1}). In both of the ATR spectra the N-H stretch consists mainly of a band located at 3322 or 3333 cm^{-1}. Therefore almost all of the N-H group on both surfaces of the polymers were hydrogen bonded. Two overlapping and well separated shoulders at 1733, 1700 cm^{-1} or 1728, 1701 cm^{-1} represent non-bonded carbonyl groups and hydrogen bonded carbonyls respectively. The intensity of peaks in these regions was higher for the MP1495-SL than the XPR625-FS because of the ester soft segment incorporated in the MP1495-SL polymer. The presence of a larger peak at (1701 and 1700 cm^{-1}) then at (1733 and 1728 cm^{-1}) indicates that most of the carbonyl

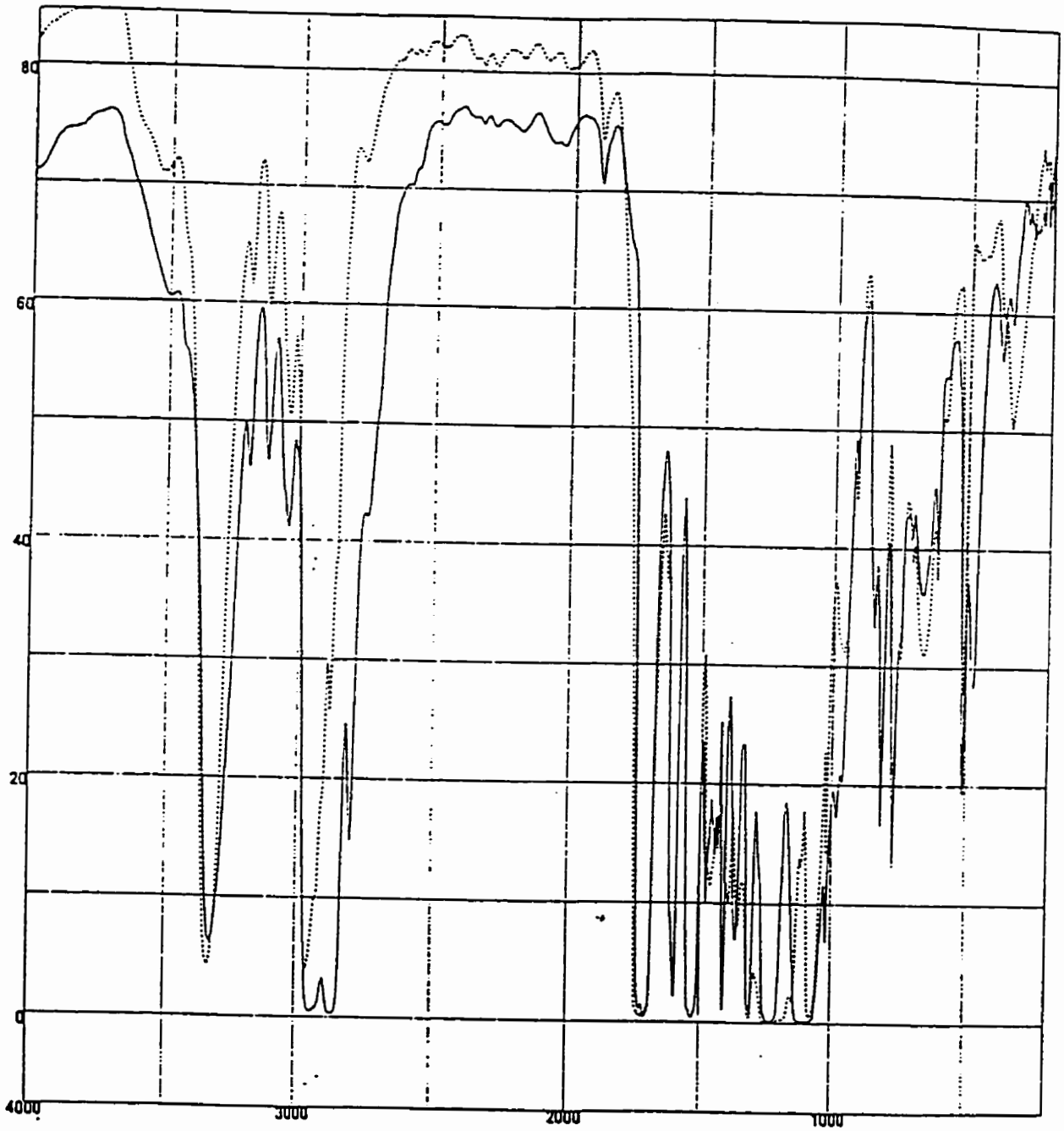

Figure 7-1. Direct transmittance FTIR spectra for the polyether-type (dashed) and polyester-type (solid) polyurethane.

Table 7-1. Peak assignments for the FTIR of the XPR625-FS and MP1495-SL.

XPR-625FS(ether type)		MP1495SL(ester type)		Assignment
Wave number(cm-1)	Relative intensity	Wave number(cm-1)	Relative intensity	
3322	M	3333	M	v(N-H),H-bond
2918	M	2957	M	va(C-H) in CH2
2850	S	2873	M	or vs(C-H) in CH2
2796	M	••		vs(C-H) in CH2
1733	S	1728	VS	v(C=O) urethane amide I,nonbonded
1700	S	1701	VS	v(C=O) urethane amide I,H-bonded
1596	S	1597	S	v(C=C) aromatic ring
1528	VS	1528	VS	v(C-N)+r(N-H) amideII
1413	S	1413	S	v(C-C) aromatic ring
1363	M	1361	M	w(C-H) in CH2
1309	S	1310	S	v(C-N)+r(N-H) amideIII
1219	VS	1219	VS	v(C-N)+r(N-H)
••		1170	VS	v(C-O-C)in ester
••		1140	VS	v(C-O-C)in ester
1102	VS	••		va(C-O-C) aliphatic ether
1072	VS,sh	1064	VS	vs(O=C-O)
1017	S	1018	S,sh	i(C-H) in plane,aromatic ring+vs(C-O-C)
982	M	••	M	vs(C-O-C) aliphatic ether
961	M	960		w(C-H) out of plane,aromatic ring
816	S	817	S	w(C-H) aromatic ring
770	S	771	S	(O=C-O)

Table 7-2. Changes in absorbance of some peaks with different ATR angles.

Assignment	ATR30°		ATR45°		ATR60°	
	Position	Abs.	Position	Abs.	Position	Abs.
vs(C-H) in CH2	2793cm-1	0.2030	2795cm-1	0.0313	2797cm-1	0.0104
v(C=O),nonbonded	1728cm-1	0.3032	1733cm-1	0.1248	1730cm-1	0.0503
v(C=O),H-bonded	1697cm-1	0.5304	1701cm-1	0.2766	1703cm-1	0.0928

groups in each of the samples are hydrogen bonded. The third region included an overlap absorption band due to the amide(III) combination band and C-O stretching vibration of the ester in the hard segment or ester and ether in the soft segments. The features and positions of these peaks were used to identify the type of polyurethane (i.e. ester or ether) mentioned earlier and will not be discussed further.

The ATR spectra of the XPR625-FS polymer were examined at the 30, 45 and 60° angles of incidence shown in Figure 7-2. There were some small changes in the spectral features, peak position and /or relative absorbances. A gradual decrease in the intensity of a peak at 2796 cm^{-1} (the stretching vibration associated with methylene in the soft segment) indicated that the concentration of soft segment near the surface was higher than deeper inside the polymer matrix. The carbonyl group concentration (including both hydrogen and non hydrogen-bonded) was also higher near the surface shown by a decrease in the absorbance at 1733 and 1700 cm^{-1}.

A dramatic increase in absorbance at the 1018, 982 and 962 cm^{-1} peaks in the ATR 30° spectrum were also noted. However, several absorption bands overlap in this region making it difficult to determine the absorbance of the individual bands. Therefore confirmation on the changes in composition responsible for the change in absorption could not determined.

In summary, FTIR analysis indicated that both of the polymer samples possessed aromatic segments. The XPR625-FS and MP1495-SL were confirmed as ether and ester respectively. These spectra were in general agreement with spectra from the literature[4, 5, 6], and previous work[7], with some minor shifts in peak position.

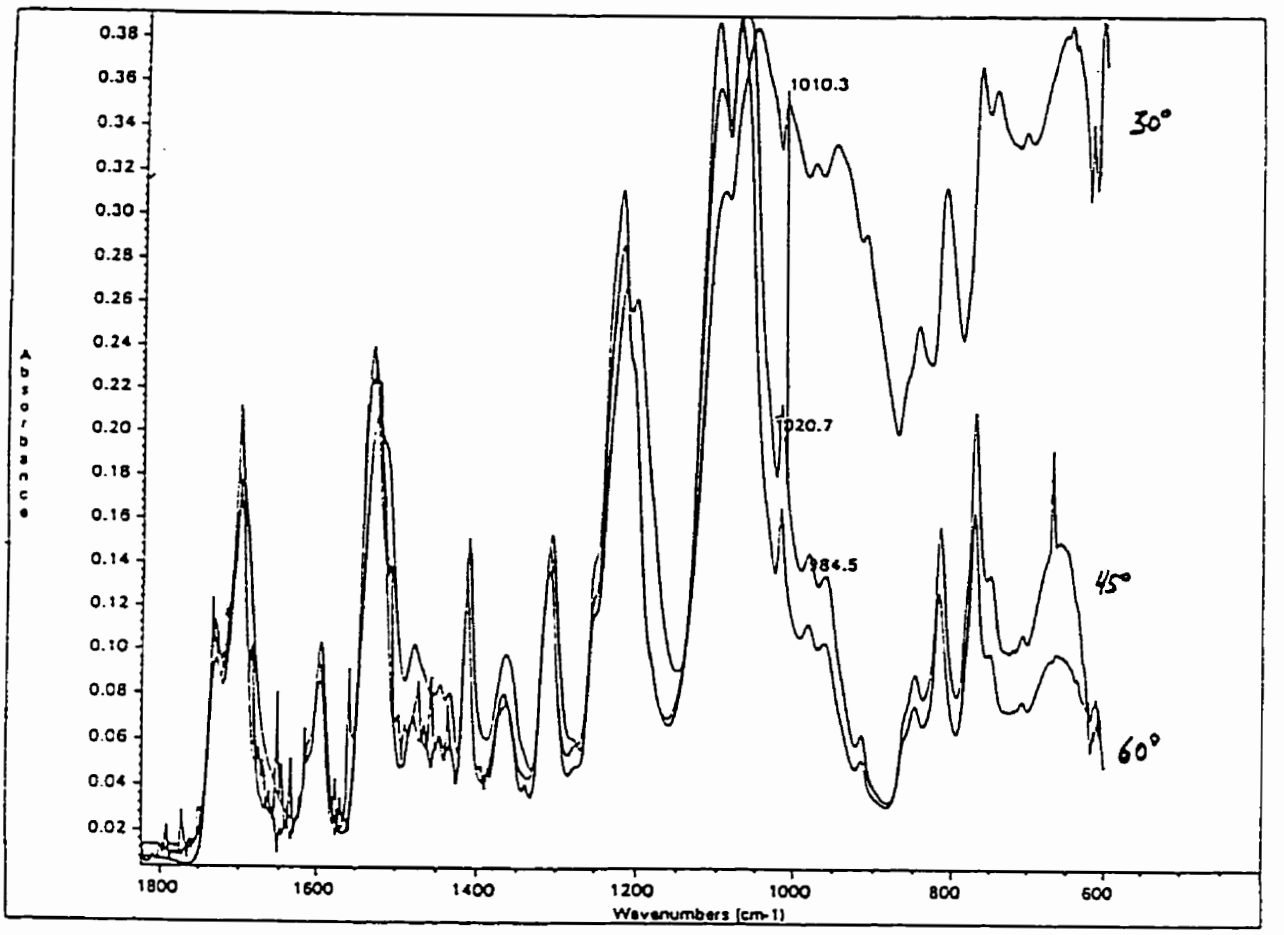

Figure 7-2. ATR-FTIR spectra recorded at different angles of the XPR625-FS polyurethane membrane.

7.4 Electron Spectroscopy for Chemical Analysis (ESCA)

ESCA, also known as X-ray photoelectron spectroscopy (XPS) uses x-ray radiation to remove an electron from the inner core of atoms within the sample. Once the electrons have been ejected the kinetic energy of the electron is measured. The difference in energy between the exciting photons and the removed electrons is equal to the binding energy of the electron. The ESCA spectrum is therefore a map of the binding energies of the various atoms in the sample structure[8]. ESCA has been used extensively for the elucidation of polyurethane structure.[9,10]

ESCA analyses were carried out by Jean François Paget (Institut des Biomateriaux) using a Perkin-Elmer PHI model 5600 (Physical Electronic Division), which applied a monochromatic Al K_{α} X-ray source. The X-ray gun was operated at 14 kV and 18 mA with the pressure of the sample chamber below 10^{-8} Torr. The take-off angle was 45°. The analysis included a survey of scans (0-1100 eV) to determine the elemental composition on both surfaces of the film as well as performing a high resolution scan of the carbon C1s peak. All data was processed using the standard software attached with the instrument, and C1s spectra were deconvoluted by assuming it contained a mixture of Gauss-Lorentz components.

The results of the survey scans showed that the surface of the XPR625-FS only contained the elements C and O, whereas the surface of MP1495-SL contained C, N and O, shown in Figures 7-3 and 7-4. The quantitative analysis for the elemental composition for the two surfaces suggested that the carbon element was dominant on both of the surfaces (94.5% for the XPR625-FS and 90.98% for the MP1495-SL) shown in Tables 7-3 and 7-4.

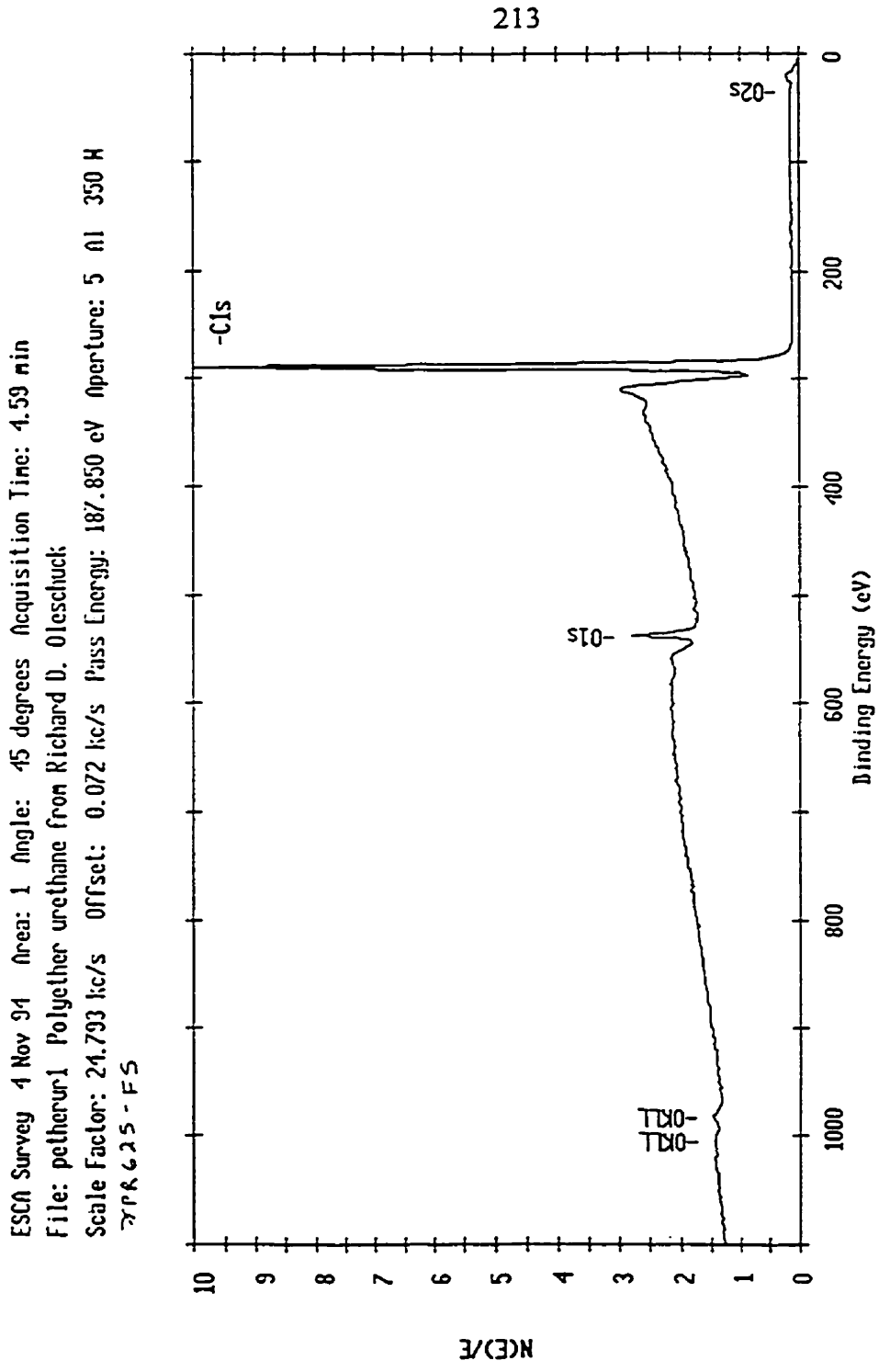

Figure 7-3. ESCA spectrum of the XPR625-FS polyurethane membrane

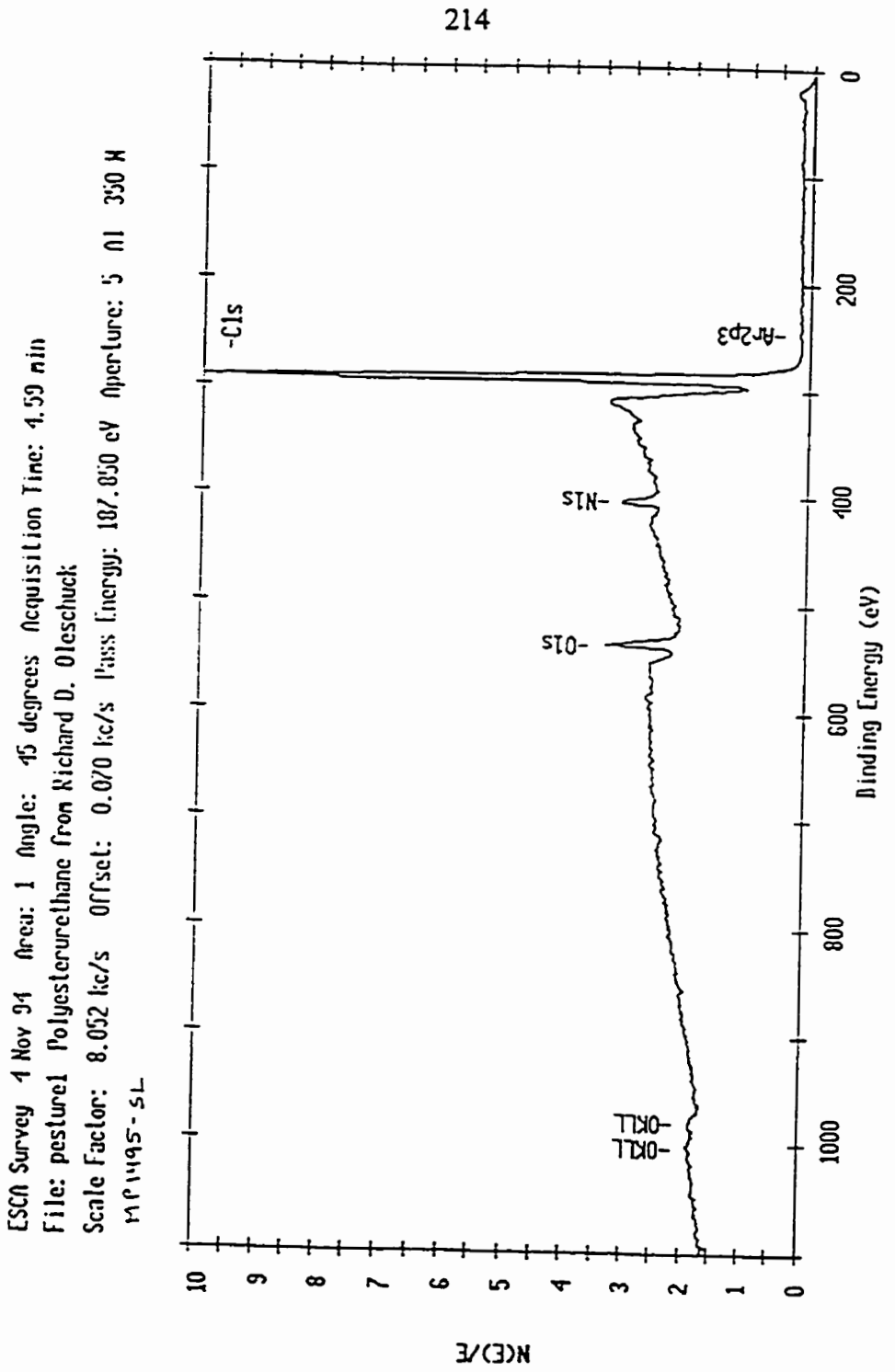

Figure 7-4. ESCA spectrum of the MP1495-SL polyurethane ester-type membrane

Table 7-3. Atomic concentration table for the XPR625-FS determined by ESCA analysis

Atomic Concentration Table
Polyether urethane from Richard D. Oleschuck
Minimum Area Omni-Focus Source: Monochromated

Element	Area (cts-eV/s)	Sensitivity Factor	Concentration (%)
C1s	1057075	58.185	94.95
O1s	132002	136.496	5.05

Table 7-4. Atomic concentration table for the MP1495-SL determined by ESCA analysis

Atomic Concentration Table
Polyesterurethane from Richard D. Oleschuck
Minimum Area Omni-Focus Source: Monochromated

Element	Area (cts-eV/s)	Sensitivity Factor	Concentration (%)
C1s	394495	58.185	90.98
N1s	27330	92.694	3.96
O1s	51480	136.496	5.06
Ar2p	0	199.376	0.00

High resolution spectra of the C1s peak of the two samples were obtained and are shown in Figures 7-5 and 7-6. Four peaks were assigned for the XPR625-FS at 285.20 eV, 286.64 eV, 288.25 eV and 291.46 eV. The major C1s peak located at 288.25 eV is probably due to presence of the C=O or -O-C-O- functional groups, while the peaks at 286.64 eV and 285.2 EV correspond to the ether and aliphatic carbons. The peak at 291.46 eV is probably related to the carbonate group. Five peaks were identified for the MP1495-SL sample. The peaks were located at 285.11, 286.58, 287.82, 288.99 and 291.42 eV. (Figure 7-6) where the peak at 288.99 eV corresponds to the carboxylic acid/ester (-COOR) group and urethane linkage: while the peak at 287.82 corresponds to the C=O group. The other peaks are assigned in the same manner as the XPR625-FS sample. The carbon functionality assignments are listed in Table 7-5 and percent compositions for each polymer are presented in Table 7-6 and 7-7. The results of the high resolution scans of the C1s peaks demonstrated that the majority of carbon situated on the surface was not aliphatic carbon. The XPR625-FS sample had a aliphatic carbon concentration of 12.95 %. This is similar to the MP1495-SL, that possessed an aliphatic carbon concentration of 17.79%.

As a result of no trace of nitrogen on the surface of the XPR625-FS in the survey scans, the chemical component on the surface may be composed entirely of soft segment in the depth range measured by ESCA. The presence of nitrogen in the survey scans of the surface of the MP1495-SL sample indicates the presence of hard segments near the surface of the polymer.

Unlike most typical polyurethanes which possesses an oxygen element concentration

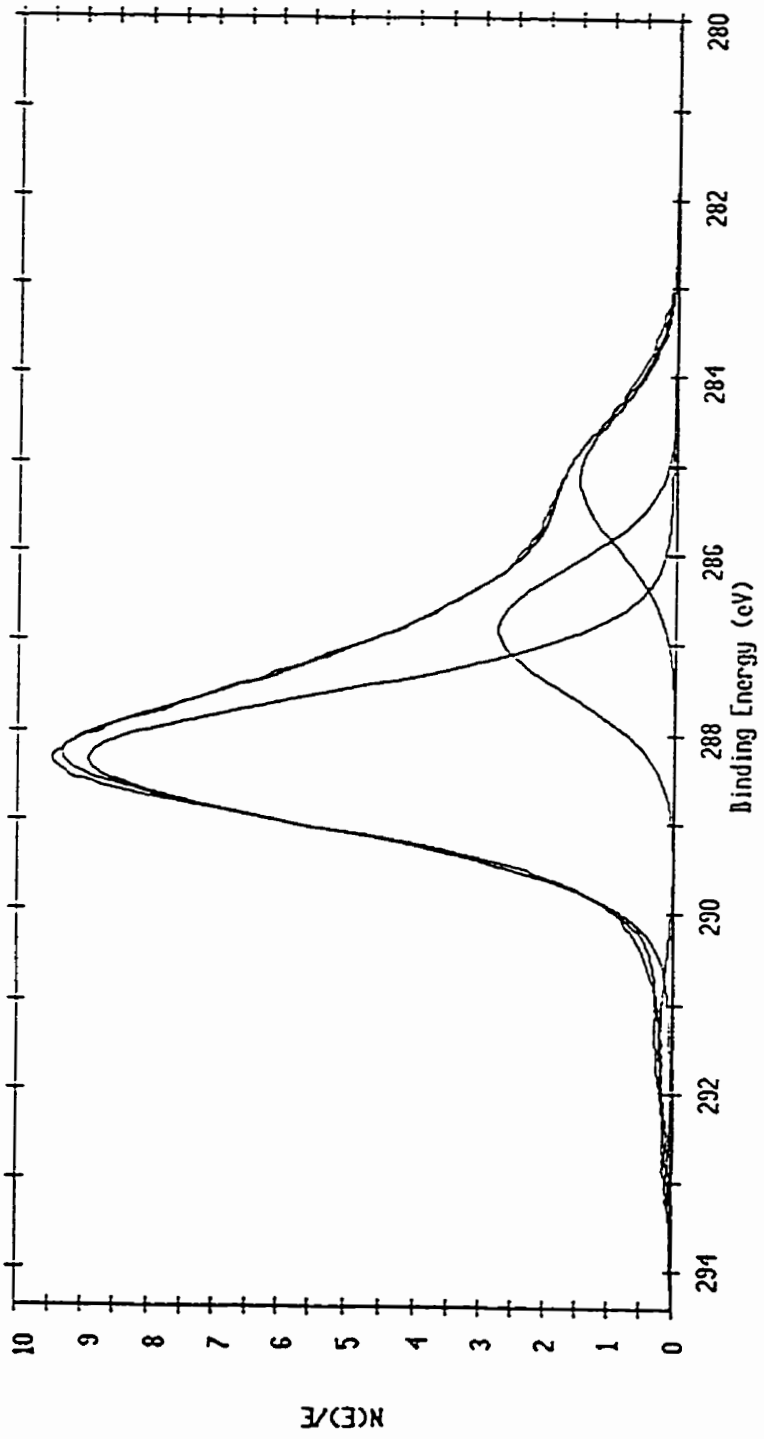

Figure 7-5. High resolution ESCA scan of the carbon peak for the XPR625-FS polyurethane ether-type membrane

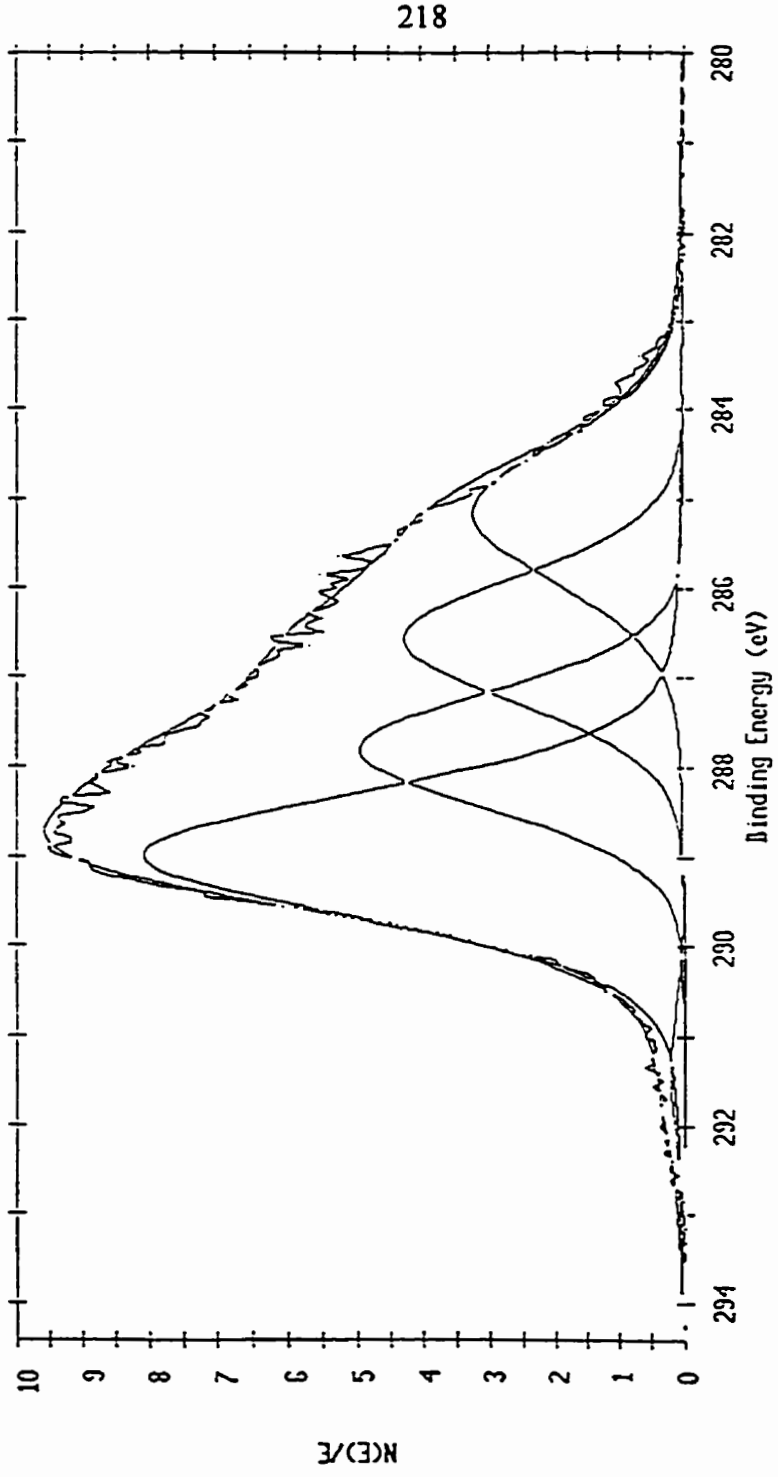

Figure 7-6. High resolution ESCA scan of the carbon peak for the MP1495-SL polyurethane ester-type membrane

Table 7-5. Carbon 1s peak assignment for the XPR625-FS and MP1495-SL polyurethane membranes

XPS-625FS PEAK POSITION(eV)	MP1495SL PEAK POSITION(eV)	ASSIGNMENT
285.20	285.11	C-C OR C-H BACKBOND HYDROCARBON
286.64	286.58	C-O OR C-N
	287.82	C=O OR -O-C-O-
288.25		C=O OR -O-C-O-
	288.99	O=C-O OR O=C-N
291.46	291.42	OCOO,CARBONATE GROUP?

Table 7-6. Percent concentrations of the various carbon 1s peak assignments for the XPR625-FS polyurethane ether-type membrane.

Band No.	Peak Pos.	Delta	Height	FWHM	% Gauss	Area	% of Total Area
4	291.46	6.26	590	2.25	91	1475	1.33
2	288.25	3.05	39002	1.86	91	80682	72.99
3	286.64	1.44	8736	1.45	91	14071	12.73
1	285.20	0.00	6755	1.91	91	14316	12.95

Table 7-7. Percent concentrations of the various carbon 1s peak assignments for the MP1495-SL polyurethane ester-type membrane.

Band No.	Peak Pos.	Delta	Height	FWHM	% Gauss	Area	% of Total Area
5	291.42	6.26	209	1.85	91	430	1.13
2	288.99	3.82	7747	1.67	80	15051	39.53
4	287.82	2.65	4754	1.55	91	8184	21.49
3	286.58	1.41	4103	1.68	91	7636	20.06
1	285.17	0.00	3114	1.87	80	6773	17.79

on the surface of around 20 %, the XPR625-FS sample has a concentration of only 5.05 %. The carbon element concentration whose binding energy was shifted is up to 85.72 %. Most of these carbon atoms need to combine with oxygen in the double bond or two oxygens directly to generate the 3 eV shift.

In summary, the chemical structure and aggregation state of each of the polymers appears unique and extraordinary. A high concentration of carbon atoms with a chemical shift existed on both films accompanied by only a small concentration of oxygen atoms leading to a surface that is actually electropositive. Compared to ESCA results for polyurethanes from other investigators some of the assignments of the peaks are unsatisfactory. Peaks such as 291.40 eV were even higher than that of the carbonate group at 290.5 eV. We failed to determine the component and structure of the moiety leading to this peak. In addition, as the binding energy of the functional groups is shifted various secondary induced effects became apparent, thus the identity position and magnitude of the peaks may contain a significant degree of uncertainty.

7.5 Gel Permeation Chromatography (GPC)

Gel permeation chromatography was performed using a Waters™ Linear Ultrastyragel Column (7.8 x 300 mm, part # 10681), with a Spectra Physics SP8700 HPLC system coupled with a Spectra Physics SP8450 UV/Vis detector. The multi-wavelength detector was set on 294 nm. The mobile phase was 100% HPLC grade THF at a flow rate of 1.0 mL/min

and a pressure of 174 psi. Ten molecular weight polystyrene standards from Showa Denko (Shodex Standard , SM-105, #41201) ranging from 1.28 x 10^3 to 3.15 x 10^6 Daltons, were used to calibrate the column. Each of the samples and standards were made to 0.01 % wv in HPLC grade THF and dissolved over a period of 6 hours with gentle agitation.

Each standard was run individually and the elution volume recorded. The elution volume was then plotted against the log of the molecular weight producing a calibration curve. The calibration curve obtained from the ten molecular weight standards is shown in Figure 7-7. A sample chromatogram of both the virgin ether and ester-type polyurethane membranes is shown in Figures 7-8 and 7-9 respectively. The GPC analysis of the two polymers led to the results shown in Table 7-8.

Table 7-8. Elution volumes for the two polyurethane samples tested.

Polymer	Elution Volume (mL)
XPR625-FS	8.56
MP1495-SL	8.86

These elution volumes translate into the XPR625-FS having a molecular weight of 1.6 x10^5 mass units and the MP1495-SL having a molecular weight of 6.5 x10^4 mass units.

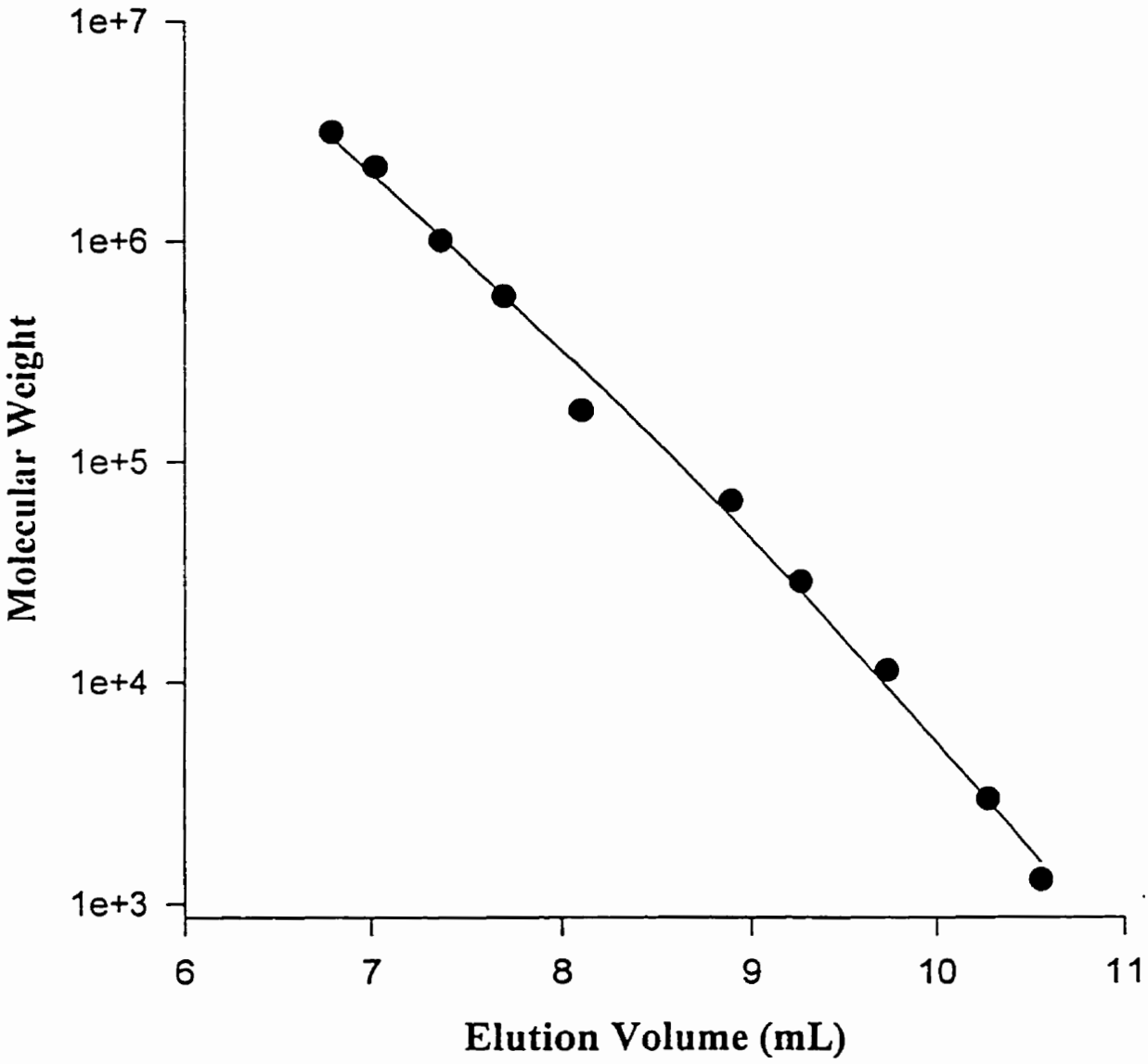

Figure 7-7. Calibration curve for the GPC analysis of polyurethane membrane materials

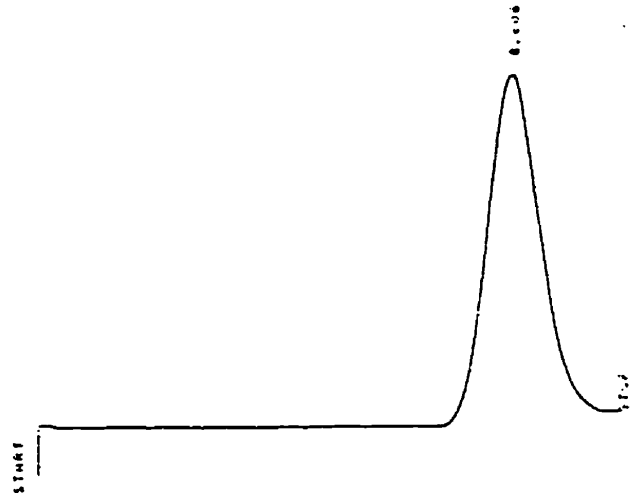

Figure 7-8.Gel permeation chromatogram of the XPR625-FS polyether- type polyurethane membrane

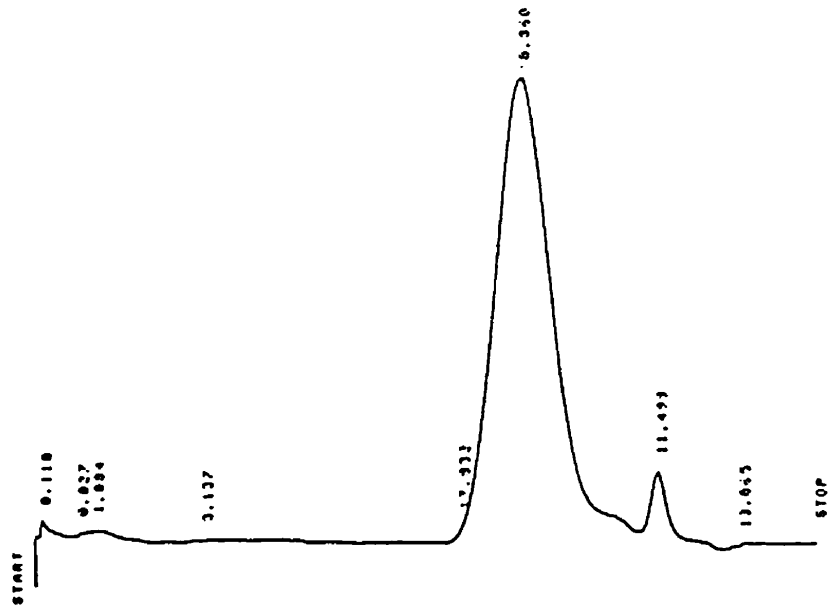

Figure 7-9. Gel permeation chromatogram of the MP1495-SL polyester- type polyurethane membrane

7.6 Differential Scanning Calorimetry

Differential scanning calorimetry is the most popular technique for the measurement of glass transition temperatures.[11] The glass transition temperature of a polymer can be used to determine the amount of crystallinity within a polymer. Polyurethanes are somewhat unusual in that they possess a two phase structure consisting of hard crystalline domains and soft amorphous domains. The relative size of these domains can be determined by the different transitions a polymer undergoes as it is heated.[12]

Differential scanning calorimetry (DSC) thermograms were collected by Ming Jing Yang (Institut des Biomatériaux) over a range of -100 °C to 250 °C using a Perkin-Elmer Model 7 DSC. The temperature was increased at a rate of 20 °C/min. Liquid nitrogen was chosen as the coolant to start the scans below room temperature. Calibration was performed with indium and pure water standards. The data was processed and analysed using software attached to this instrument. The weight of the samples used for the DSC analysis of the XPR625-FS and MP1495-SL were 1.32 mg and 1.60 mg respectively.

The thermograms for the two samples are shown in Figures 7-10 and 7-11. The gradual distinct transitions indicating the glass transition temperature (T_g) for both samples are located at -72.44 °C (XPR625-FS) and -67.55 °C (MP1495-SL). Polyurethanes often possess two melting points corresponding to the melting of the soft segments and the melting of the hard segments. Small shallow endotherms were visible from 4.13 to 44.36 °C (XPR625-FS) and from 3.73 to 17.56 °C (MP1495-SL) corresponding to the melting of the soft segments. This area was followed by a very broad transition corresponding to the melting of the hard segments. The endotherm representing the melting of the hard segment

Figure 7-10. DSC Thermogram for the XPR625-FS Membrane Material

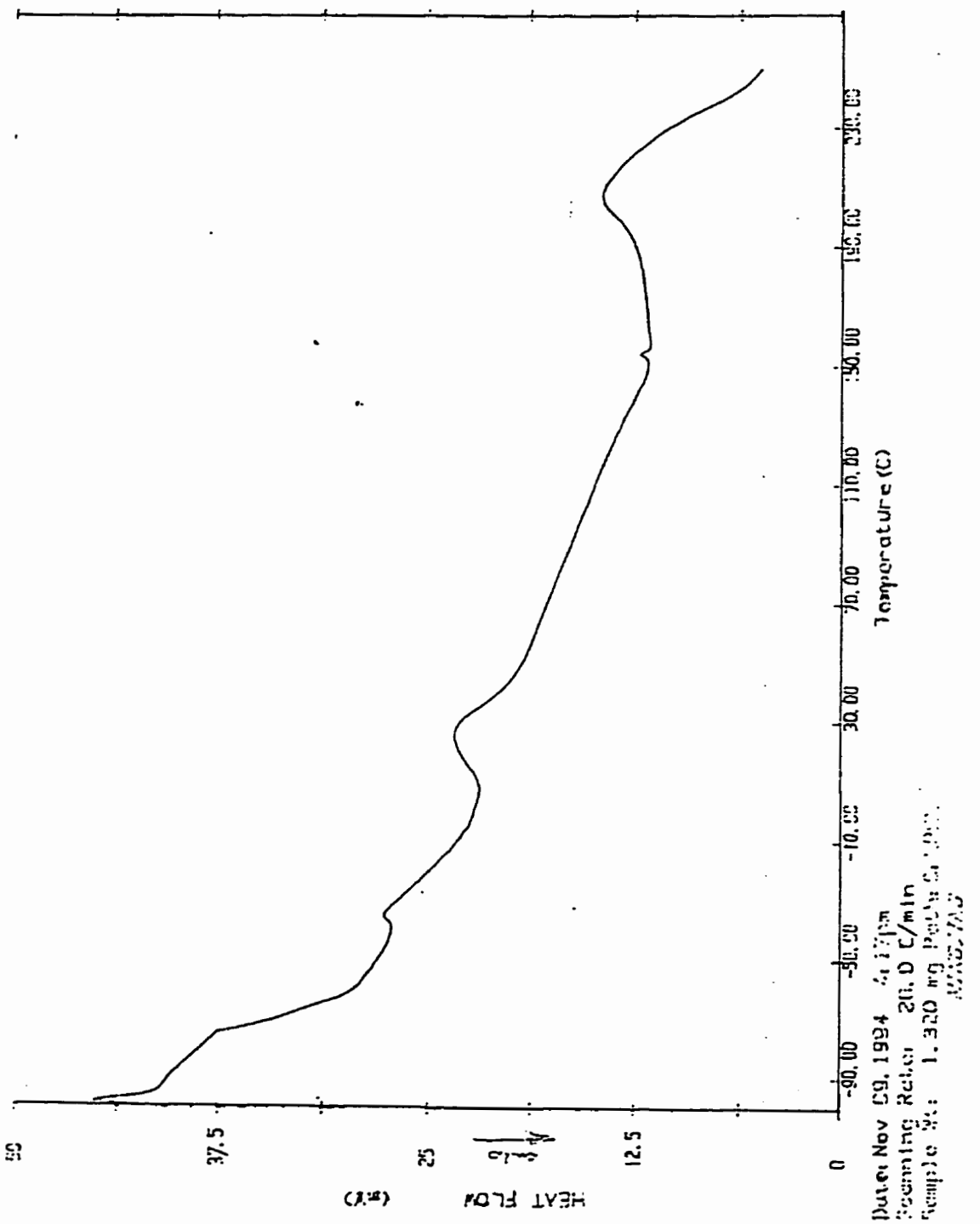

Figure 7-11. DSC Thermogram for the MP1495-SL Membrane Material

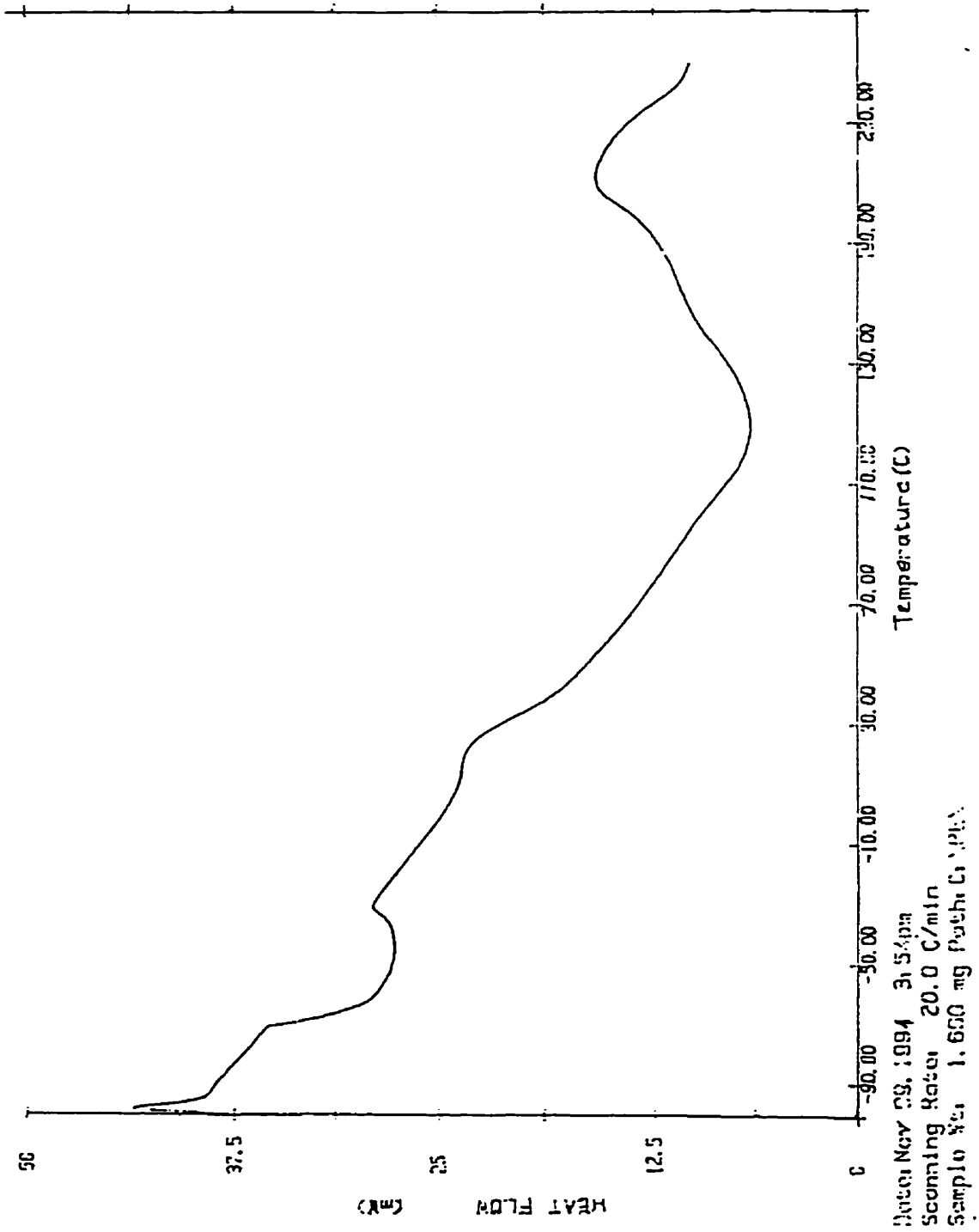

was much shallower for the XPR625-FS as compared to that of the MP1495-SL. Data from the thermograms is presented in Table 7-9. The thermograms of each of the samples indicated that the molecular chains of the two polymers were quite flexible. The relatively low T_g for both of the samples implies that the degree of phase separation between the hard and soft segments may not be extensive. This may also be attributable to the relative lack of hard segment in the bulk polymer itself. The small endotherm defined as soft segment melt showed that the soft segment of the polymer material may exist in an amorphous rather than crystalline (some degree of order/structure) state. The broader melt point range of the hard segment for the XPR625-FS suggests many small hard domains while the broader deeper melting point range of the MP1495-SL suggests that the size of the hard segments is larger than those in the XPR625-FS sample. The rigid aromatic structure of the hard segments leads to hydrogen bonding between the carbonyl in the urethane linkage and the N-H group of the urethane group on adjacent polymer chains. Considering the aromatic nature of the hard segments in both samples the majority of the hard segment should exist in a crystalline or semi-crystalline form.

7.7 Gas Chromatography/ Mass Spectrometric Analysis

GC/MS is used to characterize relatively low molecular weight compounds.This feature precludes its use for the analysis of long chain polymers. Polymer analysis by GC/MS is usually performed by either breaking up the polymer and running the fragments or by extracting components from within the polymer matrix with a suitable solvent and analysing

Table 7-9. Glass transition temperatures calculated from the DSC curves of the polyether and polyester-type polyurethane membranes

Polymer Type	Glass Transition Temperature (T_g)
XPR625-FS	-67.55 °C
MP1495-SL	-72.44

the extract. In our case we chose to extract the membrane material followed by the analysis of the extract. A membrane sample (2 cm x 2 cm) was immersed in CH_2Cl_2 (5 mL) for a period of 11 days to extract as many possible components from the membrane. The resulting extract was then analysed using GC/MS. The GC program was as follows:

Initial column temperature	80 °C
Hold time	5 min.
Final column temperature	250 °C
Rate °C/min	5
Final hold time	8 min.

The resulting chromatogram is shown in Figure 7-12. The chromatogram exhibited several peaks labelled 1 to 6 . In our case we were only able to identify one of the compounds that was extracted. Peak "2" was identified by first performing a background subtraction and then performing a library search on the residual spectrum. The search yielded a very good match with the compound methylene bis(p-phenyl diisocyanate) shown below.

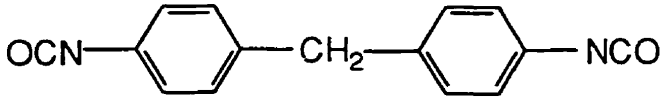

methylene bis(p-phenyl diisocyanate)
(MDI)

The experimental spectrum and the matching library spectrum are shown in Figure 7-13.

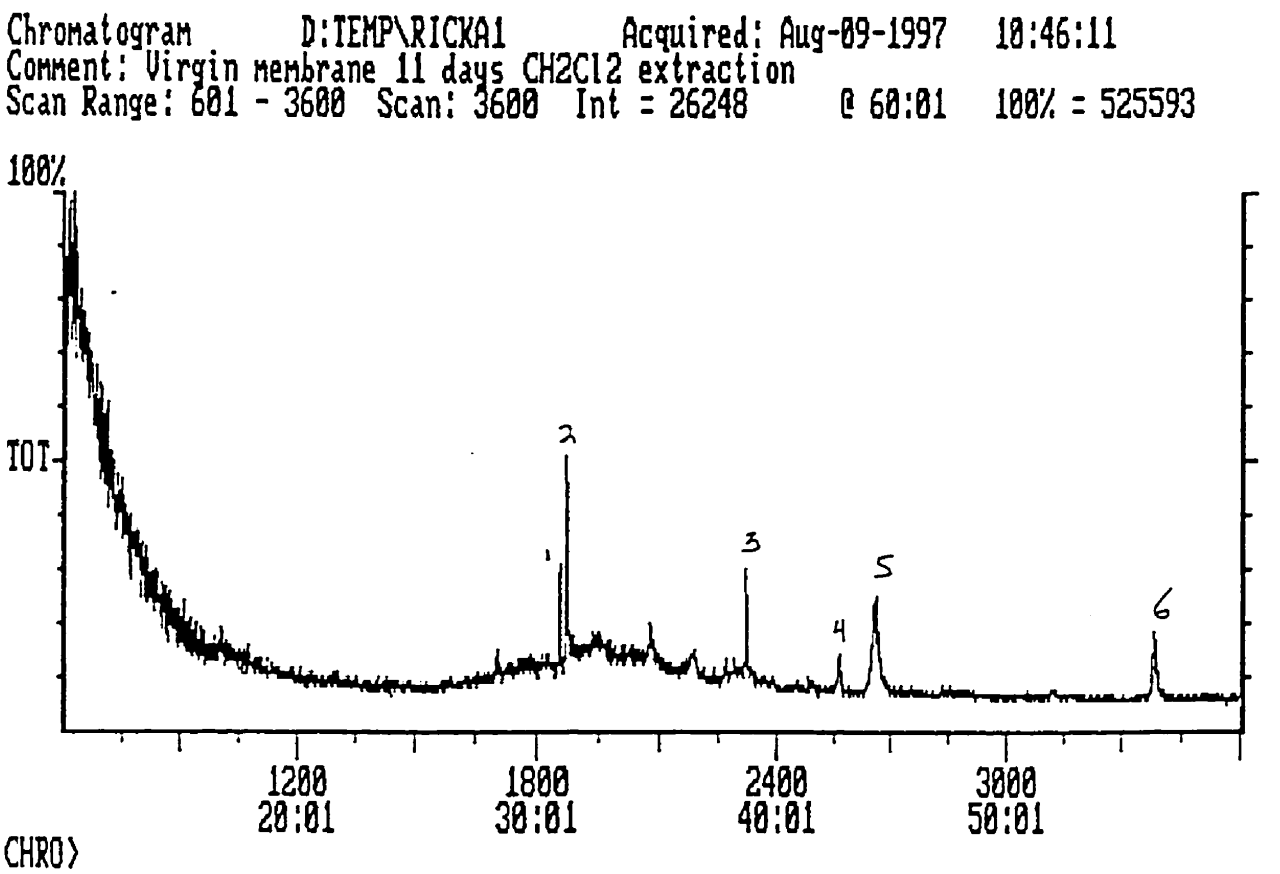

Figure 7-12.GC/MS chromatogram of the dichloromethane extract of the polyurethane ether-type membrane.

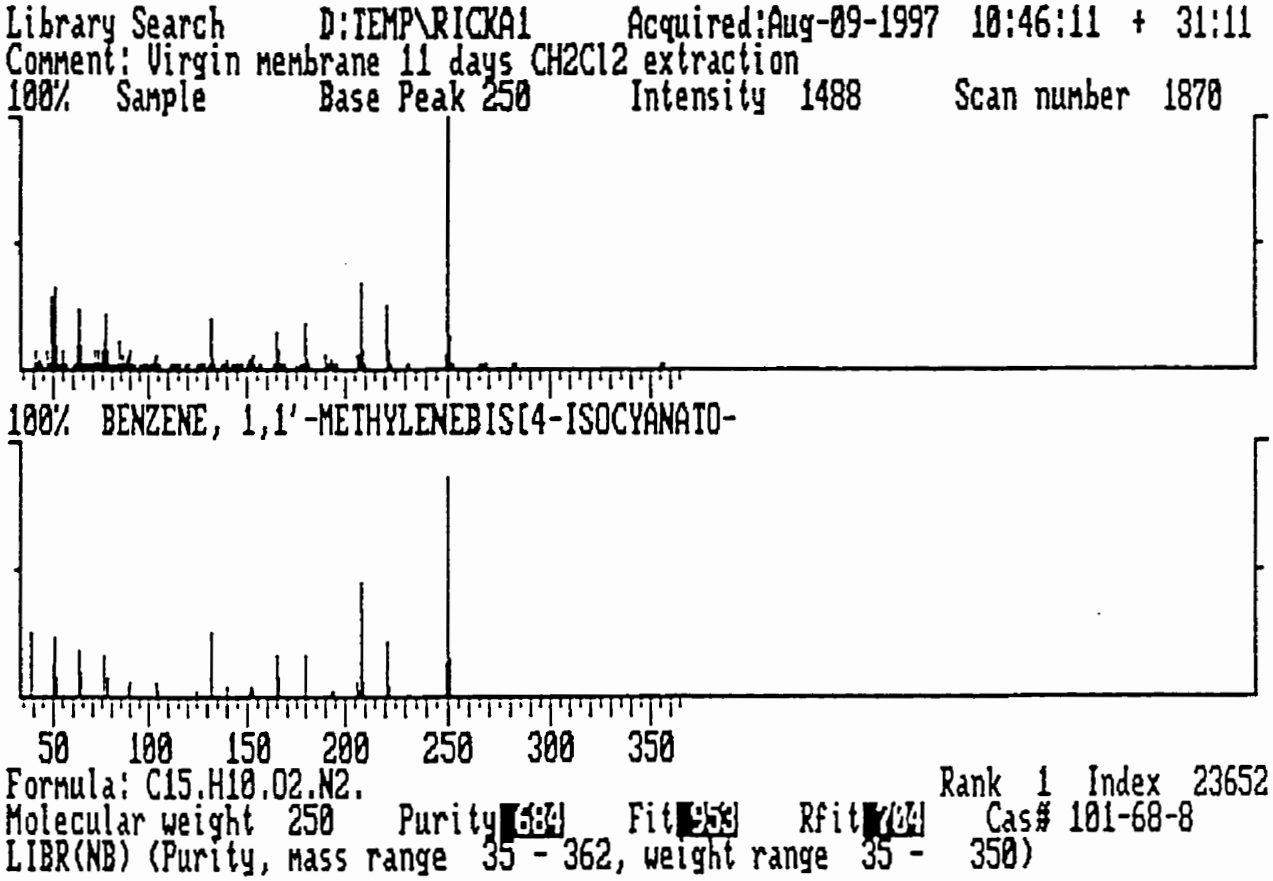

Figure 7-13. Comparison of the sample spectrum and the library spectrum for MDI

The presence of this compound in the extract shows that the polymer was probably synthesized with MDI as the di-isocyanate. MDI is commonly used for polyurethane synthesis. This data correlates well with the infra-red data which suggested an aromatic isocyanate. This technique was also used to identify degradation products from the exposure of the membrane to high concentrations of acid.

7.8 Elucidation of Polymer Structure

One difficulty that was encountered for the elucidation of the polymer's structure was the identification of the polymer used as the ether polyol, and as the chain extender. From the ESCA and FTIR data we knew that the soft segments were polyethers with a relatively large ratio of carbons to oxygen atoms. Later when talking to a representative from Dow Chemical, which supplies Stevens Elastomerics with polyurethane precursors, we learned that they use a large amount of polytetramethylene ether glycol(PTMG) for polyurethane synthesis. Tests performed by Dow Chemical suggested that the polyol they have used is PTMG. In addition, several studies using X-ray diffraction[13,14] for conformational analysis, have been performed on polyurethane elastomers synthesized with MDI and PTMG. These yielded similar results helping to confirm the identity of our polymer. Polyurethanes based on PTMG soft segments have been shown to exhibit soft segment enrichment at the air-polymer surface.[15,16] The enrichment of the soft segments of the polyurethane at the surface helps explain the atypical amount of oxygen present at the polymer surface. Using the data from the various techniques the following polymer structure shown in Figure 7-14 is proposed.

Although we are fairly certain of the both the structure and the overall molecular weight of the polymer, the molecular weight of certain components of the polymer can not be precisely determined (ie. the value of "n" in Figure 7-14).

The characterization of the two polyurethanes showed that both were prepared from aromatically based diisocyanates and chain extended with diols rather than diamines. The ESCA analysis showed that there was no nitrogen present on the surface of the XPR625-FS. This suggests that there is only soft segment present at the polymers surface. This is interesting because the degradation of an ether-based polyurethane such as the XPR625-FS occurs at the hard segments containing urethane and urea linkages. In the case of this polymer these segments appear to be protected by the resistant soft segments. This structure may lead to the increased stability of polyurethanes in harsh environments. The gel permeation chromatography showed that the XPR625-FS had a molecular weight of approximately 1.6 x 10^5 and the MP1495-SL had a molecular weight of approximately 6.5 x 10^4 mass units. The DSC demonstrated that there appeared to be a general lack of phase separation in both of the samples. The broader melt point range of the hard segments for the XPR625-FS suggests that there are many small hard domains compared to that of the MP1495-SL which possessed larger hard segments.

Figure 7-14. Structure of the Stevens Elastomerics XPR625-FS polyurethane elastomer

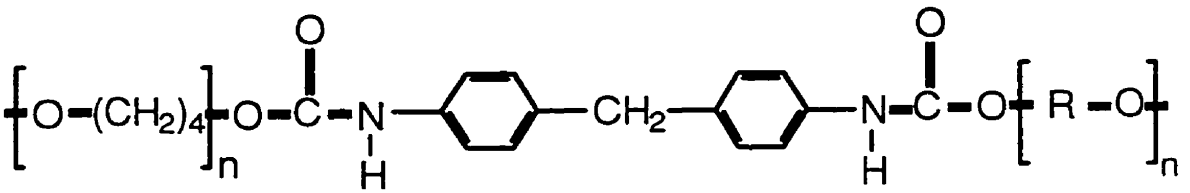

7.9 Polyurethane Degradation

Polyurethanes can be made extremely tough, but like most polymers polyurethanes are susceptible to different types of degradation[17,18]. Degradation has come to encompass a variety of meanings concerning the decrease in physical and mechanical properties, as well as changes in the physical appearance of a polymer. The physical effects of degradation can take on many forms. They can consist of the cracking or the pitting of the surface or interior of the polymer, as well as changes in the polymer's mechanical properties such as strength and elasticity. Figure 7-15 shows the degradation of polyether and polyester type polyurethane membranes[19] subjected to a strong acid gradient environment. The extent of pitting for the ether and cracking for the ester-type can be readily seen. The extent of degradation can be determined using qualitative techniques such as optical microscopy (OM) and scanning electron microscopy (SEM) or quantitative techniques such as gel permeation chromatography (GPC), Fourier transform infra-red spectroscopy (FTIR), electron scanning for chemical analysis (ESCA), and mechanical testing.

In the past, the extent of degradation has often been found by testing the mechanical properties of a polymer, before and after being subjected to a degrading media. Mechanical testing is highly insensitive to the early stages of degradation because substantial amounts of chain scission are needed to observe measurable changes in mechanical properties of the polymer. Researchers[20] have found the existence of cracks and decreased molecular weights where degradation was obviously present, yet without a measurable change in mechanical properties.

Degradation can occur as a result of a variety of processes. Processes such as

Figure 7-15. Scanning electron micrographs of polyether and polyester-type polyurethanes before and after being used as a membrane with 5.0 M HCl/0.1 M HCl conditions.

Polyether (before)

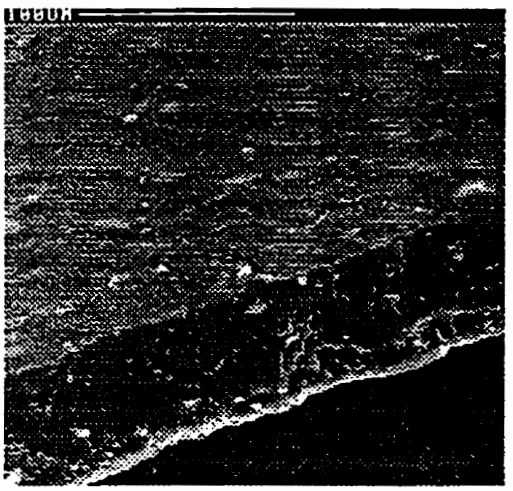

Polyether (after)

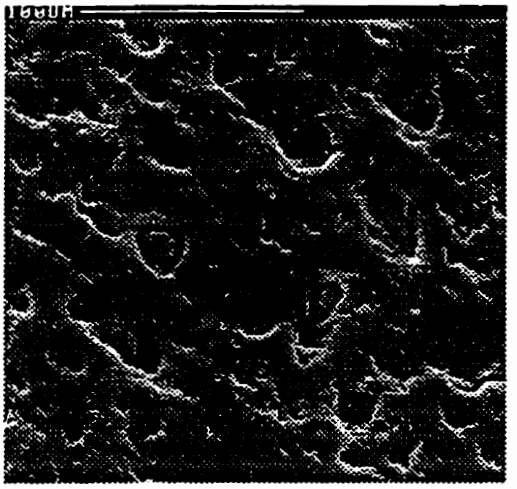

Polyester (before)

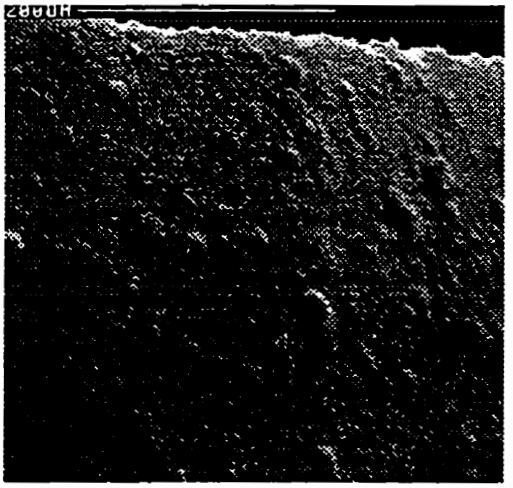

Polyester (after)

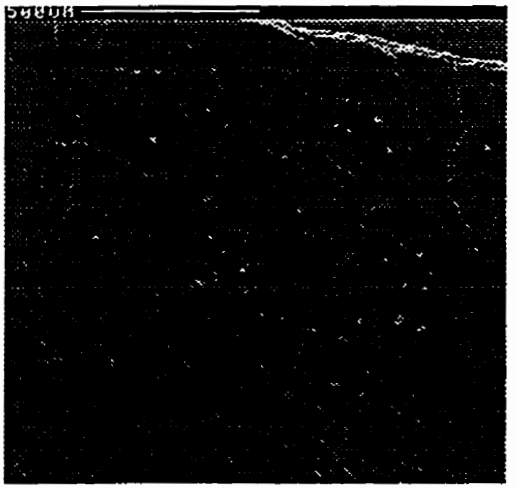

oxidation, photolysis, thermolysis, and hydrolysis as well as others. The degradation pathway most often associated with the use of polyurethanes in harsh chemical environments is hydrolysis.

7.10 Degradation of a Polyurethane Membrane Exposed to an Acid Gradient

The application of a polyurethane membrane for the separation and isolation of metals subjects the membrane to extremely harsh conditions (ie. 5.0 M HCl). During a separation experiment with 5.0 M HCl in the starting cell and 0.1 M HCl in the receiving cell the membrane swells and develops extremely small holes on its surface. These holes continue to become larger until the membrane ultimately becomes osmotic. Normally one would attribute this degradation to the hydrolysis of the polymer from the harsh acid conditions. This may in fact be partly true however we have found that the holes first develop on the side in contact with the low acid concentration and once formed the holes continue to grow, changing an initially non-porous membrane material into a osmotic porous membrane. The phenomenon of swelling and degradation has not yet been characterized in the literature. To try and understand the mechanism of the degradation a number of experiments were performed utilizing SEM, GPC, FTIR and ESCA. Figures 7-16 shows the degradation and swelling of the membrane over the course of five days of exposure. The larger membrane cell was used to allow easier observation of the degree of swelling. The

Figure 7-16(continued). The degradation and swelling of the polyurethane ether-type membrane over the course of five days of exposure to an acid gradient of 0.1 M HCl/ 5.0 M HCl.

4 Days

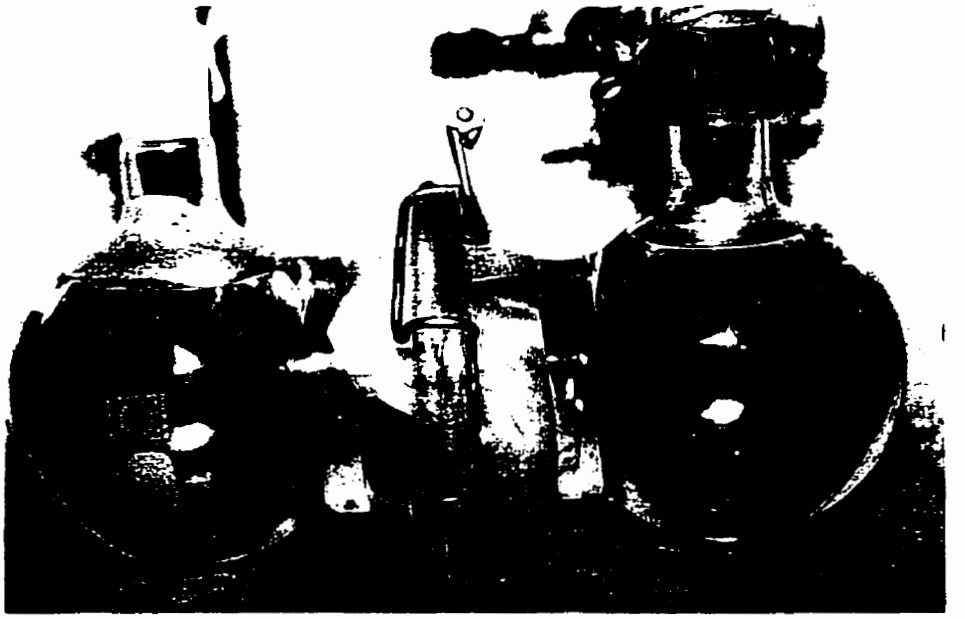

5 Days

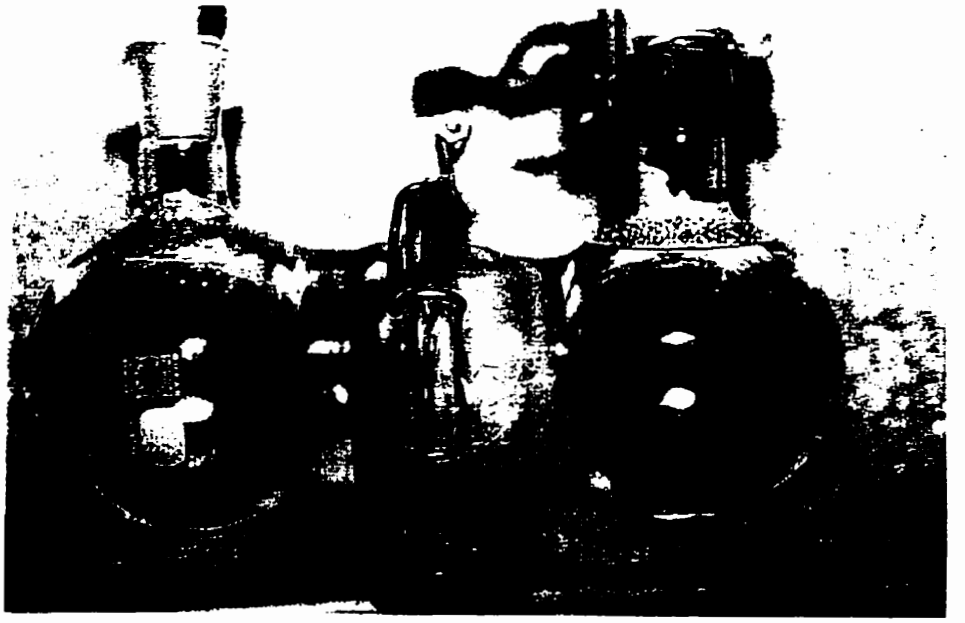

membrane used was the XPR625-FS (0.025 mm thickness) with 5.0 M HCl in the starting cell and 0.1 M HCl in the receiving cell. After one day of exposure we do not see any membrane swelling but the membrane has become noticeably cloudy compared to the original material. After the second day of exposure there is only a small amount of swelling, noticeable by the membrane becoming slightly puckered. After three days of exposure the membrane swelling becomes quite obvious and the membrane begins to protrude in both of the cells. Later, after four days of exposure, the membrane begins to bulge more noticeably toward the lower acid cell while still continuing to swell. Finally, on the fifth day the membrane no longer bulges towards the high acid side at all and is fully extended towards the low acid side. At this point the membrane ceases to swell any further. Presumably the acid gradient induces the membrane to swell and develop small pores within the polymer. After the pores are all the way through the membrane it becomes osmotic and water flows from the low acid cell into the high acid cell to relieve the osmotic pressure. The increase in the volume of solution in the high acid cell causes the swollen membrane to bulge towards the low acid cell. The solution volume change in the starting cell is quite substantial. Over a two week period the volume may increase by more than 40%.

7.11 Scanning Electron Microscopy of Degraded Membrane

The technique of scanning electron microscopy (SEM) was used in this investigation because it is highly sensitive to the early stages of degradation (i.e. the formation of holes on

the polymer surface)

To examine the degradation of a polyurethane ether-type membrane a modified Donnan dialysis cell (shown in Chapter 2) was used. For this experiment 10 identical cells were prepared and stopped at different times to obtain samples at different stages of degradation. The top flask contained 10 mL of 5.0 M HCl and the bottom cell contained 30 mL of 0.1 M HCl. The cells were run over a period of 6 days stopping one or two cells each day. Each side of the membrane was labelled as either high acid or low acid depending what solution the side was in contact with. Also the length of exposure time for each membrane was noted. Each of the membranes were rinsed in de-ionised water and stored in a desiccator prior to being analysed on the SEM.

The membrane used was a polyurethane ether-type produced by Stevens Elastomerics (XPR625-FS). Chemical testing on the membrane material has shown that it is prepared from an aromatic isocyanate (MDI) and polytetramethylene glycol. The thickness of the membrane material is 0.002" or 0.050 mm. The membrane was received in the form of large sheets and was cut into 5.0 cm x 5.0 cm pieces prior to being used in experiments.

7.11.1 SEM Analysis

Two portions of each degraded membrane were cut using a two hole punch for SEM analysis. One portion was placed on a specimen mount with the highly acid side facing up while the other was placed with the low acid side was facing up. The samples were anchored to the specimen holder using conductive carbon paint. Each of the samples were then coated with Au/Pd using an Edwards Sputter Coater #5150B to make them conductive. The

degraded membrane samples were placed in the sample compartment of the Cambridge Instruments Stereoscan 120 scanning electron microscope and viewed. Representative images of each sample were taken and stored for image analysis. Image analysis was performed with an IBAS Kontron Electronik Image Analyser with its accompanying software. For the determination of the % area, number and size of holes, the backscattering images of the membrane surfaces were used because they provided superior contrast to that of the secondary emission image. The superior contrast was needed to aid the imaging software in distinguishing the holes on the polymer surface. To make measurements the backscattering images were first converted to a binary map where they were then subjected to several software corrections such as "erosion", "dilation" and "scrapping" to get a best fit for the representation of holes. The holes were counted and measured and the total area covered by the holes determined. The data was converted into ASCII form and imported into Quattro Pro™ for manipulation and Sigma Plot™ for graphing.

The degradation of the membrane material can readily be seen using the scanning electron microscope. Figure 7-17 shows the scanning electron micrographs of the membrane material in contact with low acid concentration (0.1 M HCl). During the first day of exposure there are no visible forms of degradation. However, the analysis of the membrane material after subsequent days displayed considerable degradation in the form of holes on the surface of the polymer material. These holes continued to get larger and cover a greater area of the polymer surface. Figure 7-18 displays the edge-on view of a cross section of the membrane exposed for six and eight days showing the formation of holes within the polymer as well as on the surface. Figure 7-19 shows the degradation of the membrane surface in contact with

Figure 7-17. Scanning electron micrographs of the membrane material in contact with the 0.1 M HCl.

1 day of exposure

2 days of exposure

3 days of exposure

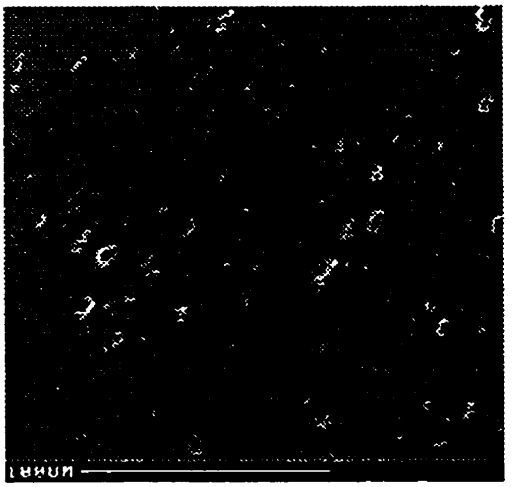

5 days of exposure

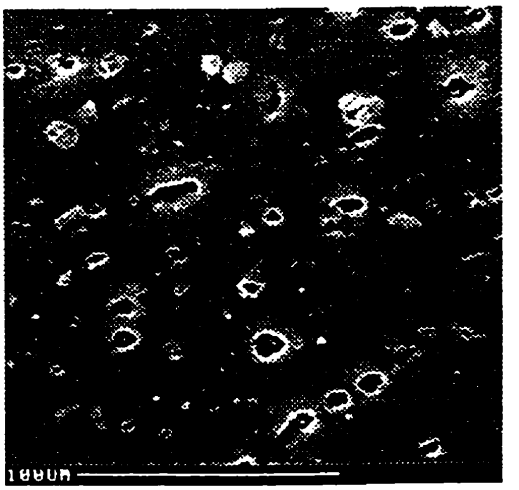

Figure 7-17(continued). Scanning electron micrographs of the membrane material in contact with the 0.1 M HCl.

6 days of exposure **8 days of exposure**

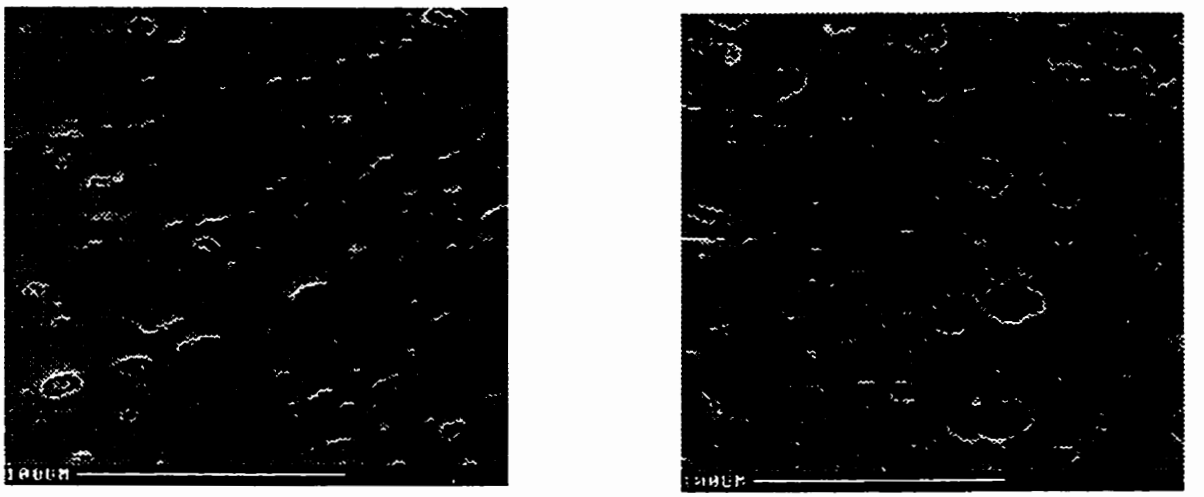

Figure 7-18. Scanning electron micrograph of an "edge on" view of the membrane at six and eight days of exposure. Side "A" was in contact with 0.1 M HCl, while side "B" was in contact with 5.0 M HCl.

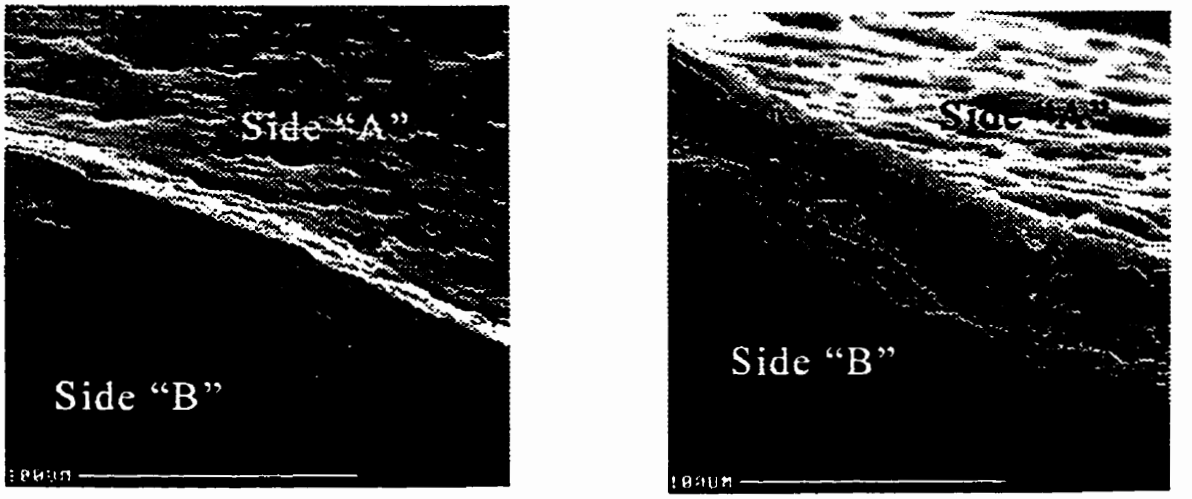

Figure 7-19. Scanning electron micrographs of the membrane material in contact with 5.0 M HCl.

1 day of exposure

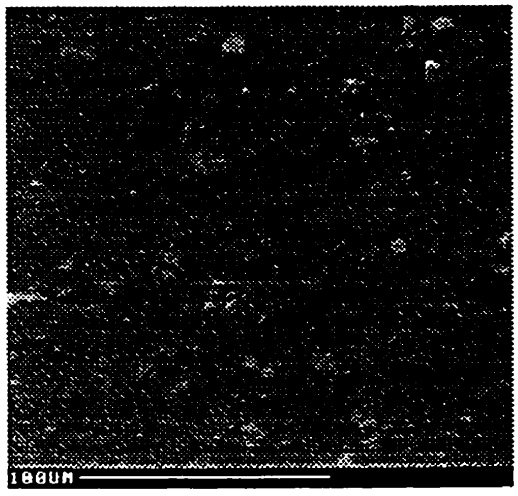

2 days of exposure

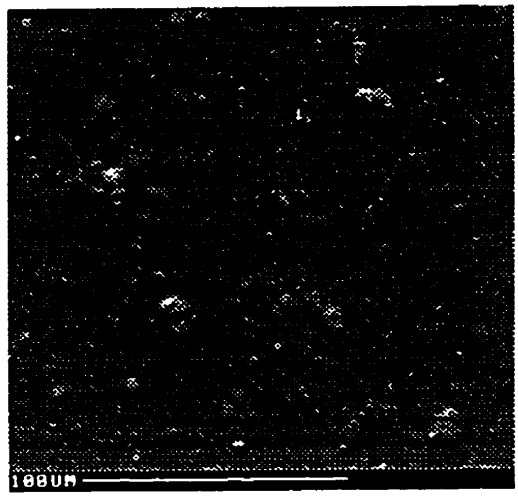

3 days of exposure

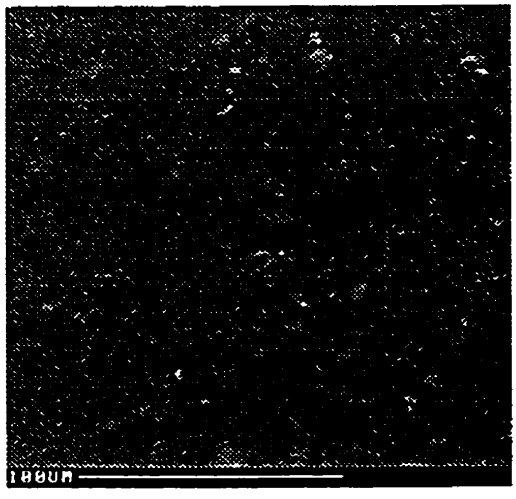

5 days of exposure

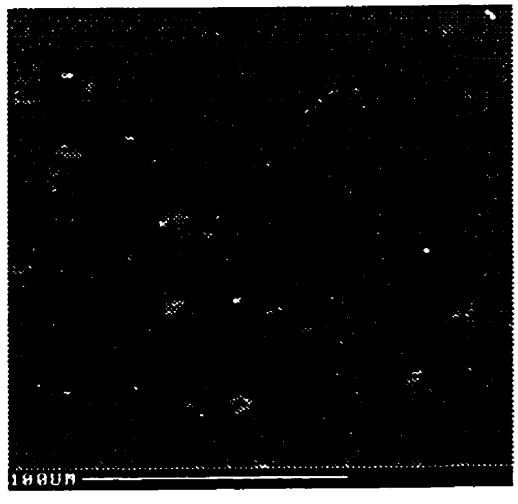

Figure 7-19(continued). Scanning electron micrographs of the membrane material in contact with 5.0 M HCl

6 Days of exposure **8 days of exposure**

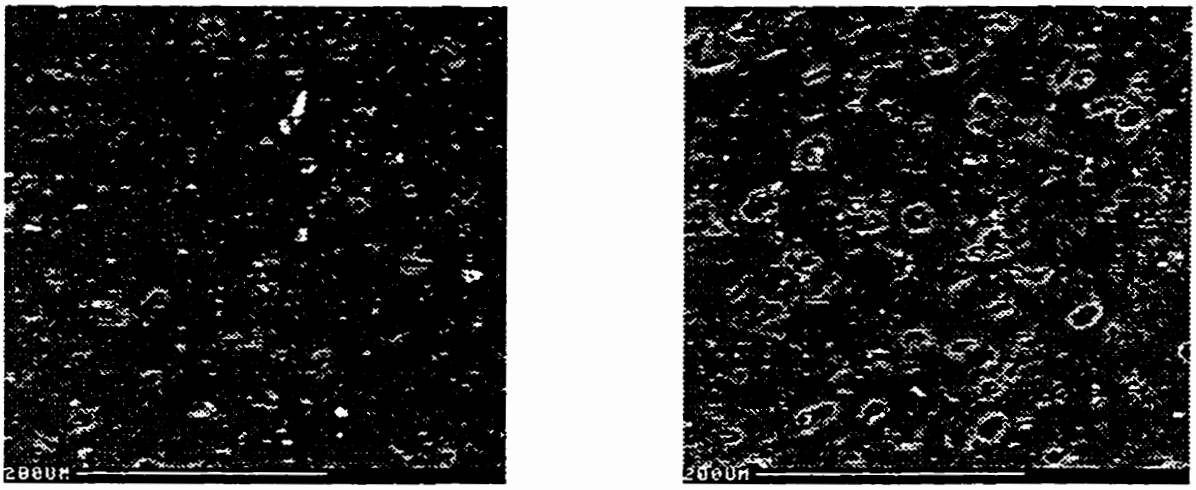

Figure 7-20. Scanning electron micrograph of an "edge on" view of the membrane at 6 and 8 days of exposure. Side "A" was in contact with 0.1 M HCl, while side "B" was in contact with 5.0 M HCl

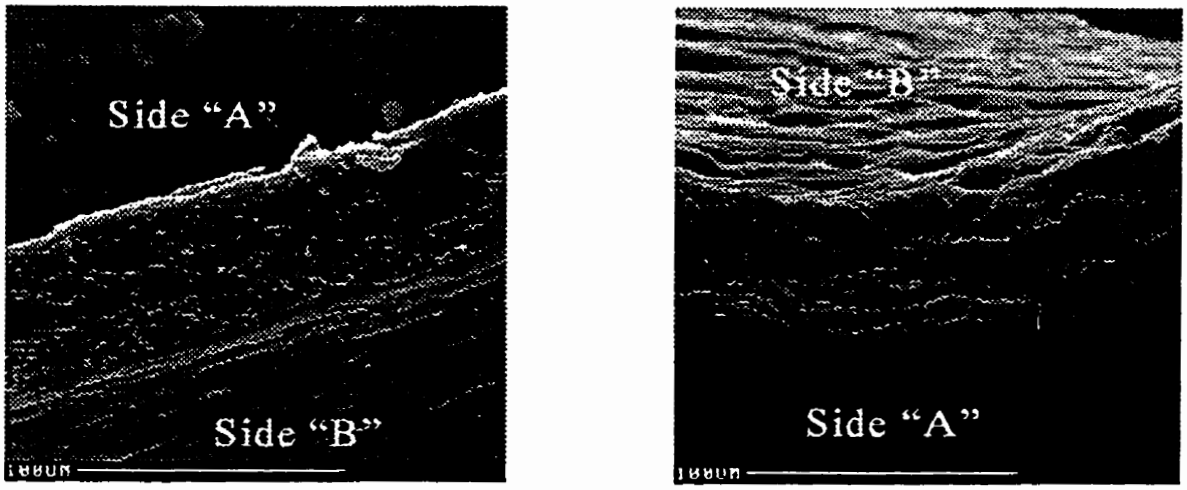

the high concentration of acid. Looking at the scanning electron micrographs of the surface of the polymer we see a similar trend to the membrane in contact with the 0.1 M HCl. Interestingly, the holes take longer to form on the high acid side than they do on the low acid side. On the low acid side the development of holes begins to occur after 2 days of exposure, while the high acid side requires 5 days of exposure for the first appearance of holes. Figure 7-20 shows the edge-on view of the polymer after six and eight days exposure, again showing that the degradation is occurring on the surface and deeper within the polymer. In addition, the figure shows more holes closer to the lower acid side than the higher acid side which again shows that degradation occurs on the low acid first.

Each of the scanning electron micrographs was stored and used for image analysis. Image analysis yielded information on the number of holes, average size of the holes, and the percentage of the area covered by holes, on the surface of the polymer.

7.11.2 Number of Holes in Membrane

Prior to being subjected to an acid gradient, both surfaces of the XPR625-FS (thickness 0.025 mm) membrane are smooth and devoid of any noticeable topography at the a magnification of 300 times. After just one day of being exposed to the acid gradient we begin to see the formation and appearance of holes on the surface of the membrane in contact with 0.1 M HCl. Conversely on the high acid side there is no degradation present. The results of the degradation are quite surprising. One would expect that the degradation of the membrane surface in contact with the high acid solution would occur first, and more rapidly. In fact, initially the holes appear only on the low acid solution side. Only, after three days of

degradation, do small holes begin to develop on the high acid side. This phenomenon is shown graphically in Figure 7-21.

7.11.3 Size of Holes in Membrane

Using the IBAS imaging software we were not only able to count the number of holes and calculate the area of each individual hole, but determine the average size of the individual holes as well. With an increase in exposure time we observe both an increase in the number and size of the holes. At early stages of degradation (i.e. 1-2 days) the holes all had roughly the same dimension. With increased exposure the standard deviation in hole sizes increased dramatically. This is mainly due to two reasons. Firstly, the holes formed at early stages of degradation continue to grow throughout the duration of the experiment. Secondly, new holes are continually being formed throughout the entire degradation process. The overall result is a large range of hole sizes on the surface of the polymer. The average size of the holes in the membrane for each period degradation is shown in Figure 7-22.

7.11.4 Total Area Covered by Holes

Using the size of each of the holes we can calculate the total area covered by holes in each of the SEM views. As expected, the longer the exposure of the membrane, the larger the percentage of the area covered by the holes (Figure 7-23). The percentage of the area covered by holes appears to be increasing at a geometric rate. This rate will eventually have

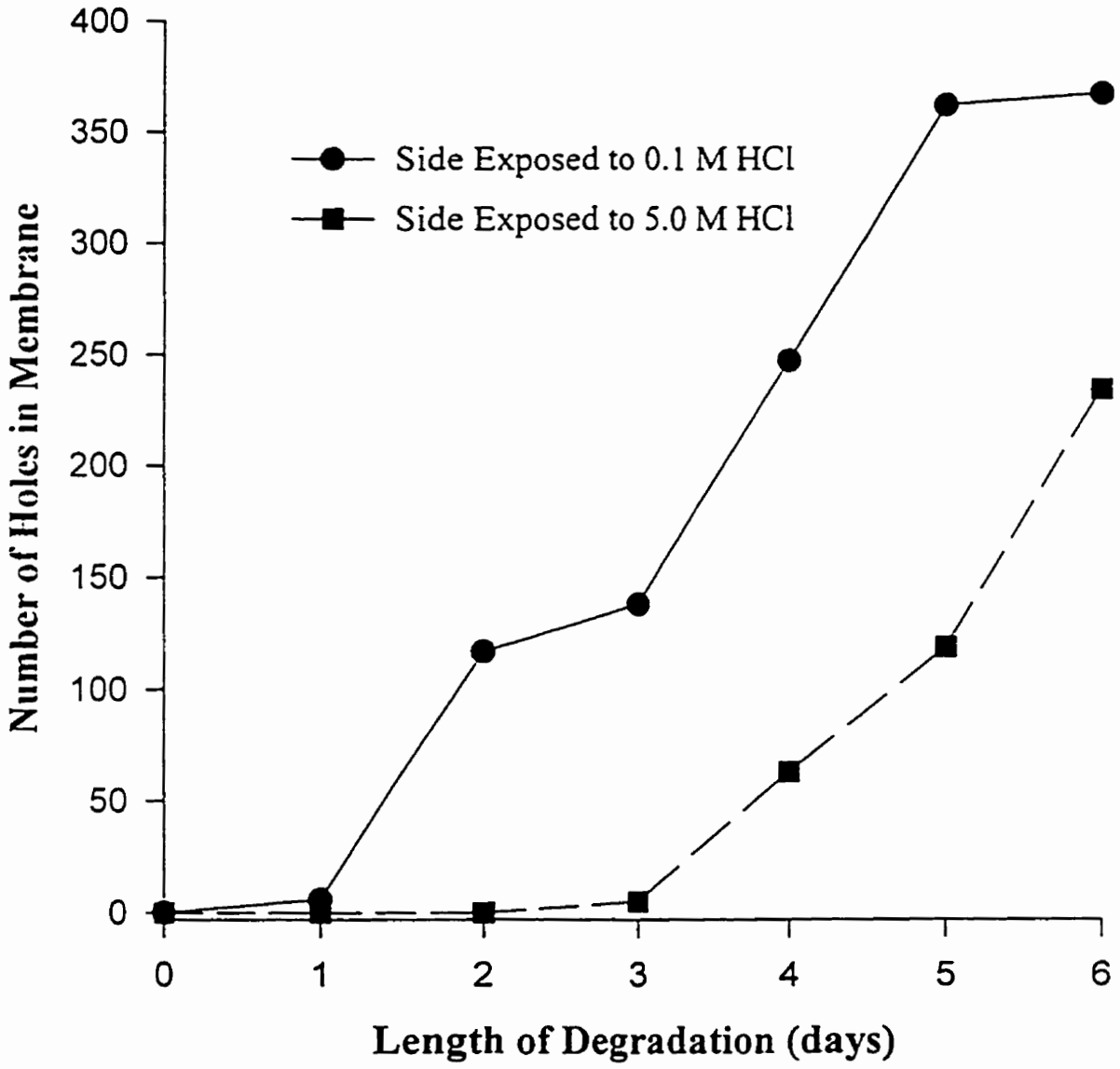

Figure 7-21. Number of holes on the surface of the membrane with difference lengths of exposure to an acid gradient

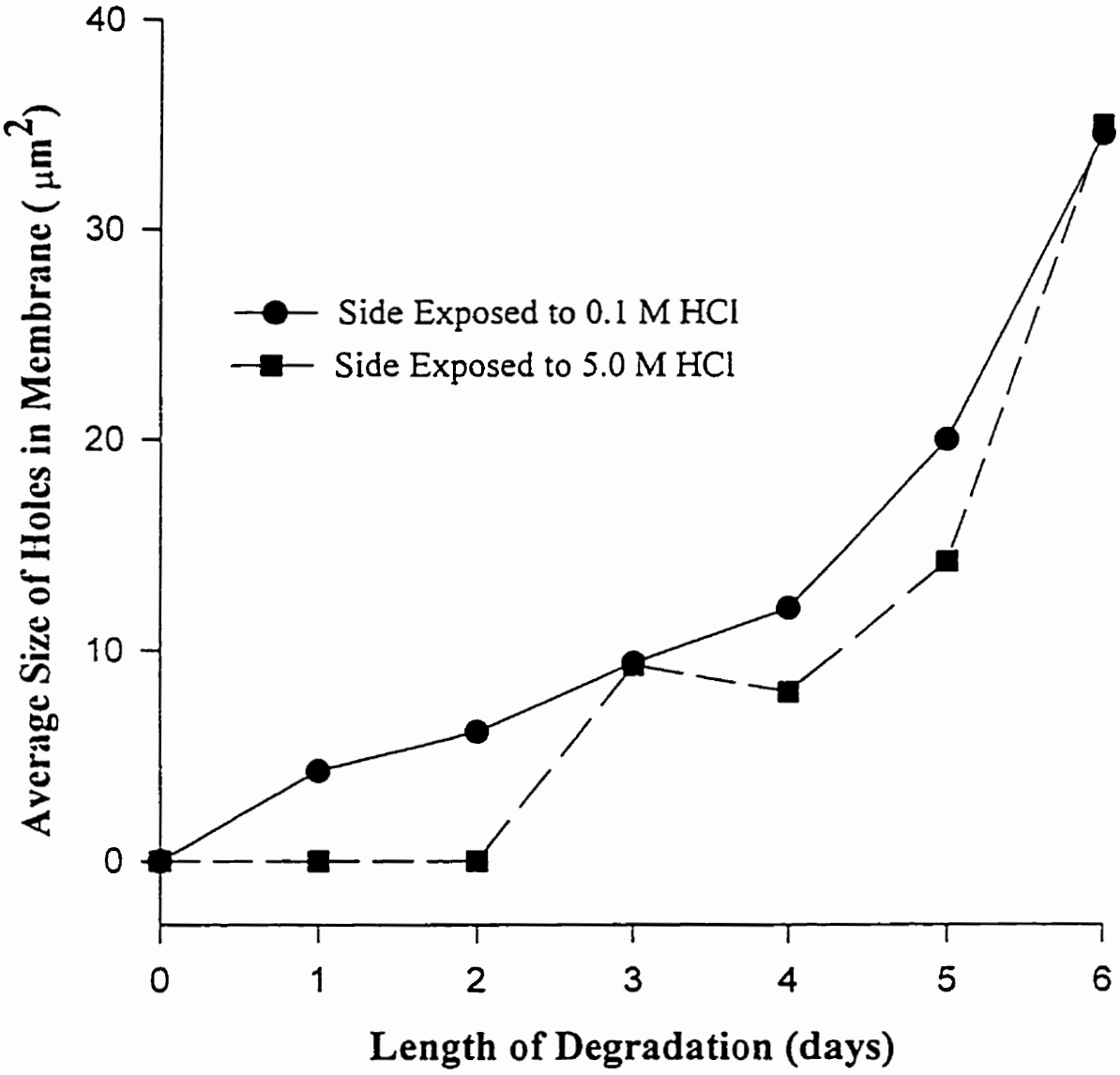

Figure7-22. Average size of holes on the surface of the membrane with different lengths of exposure

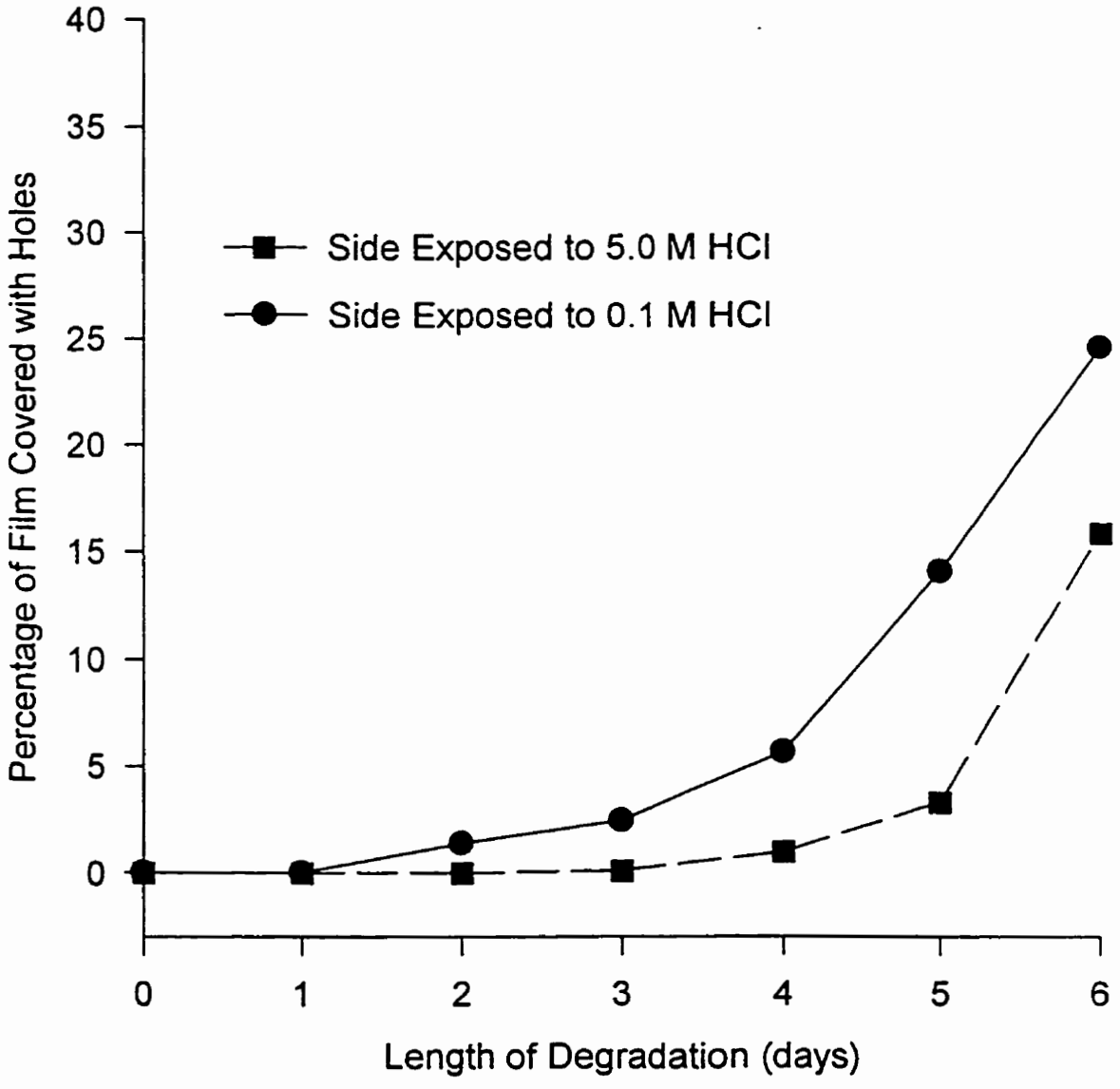

Figure 7-23. Percentage of membrane covered with holes on the surface of the membrane with difference lengths of exposure to an acid gradient

to decrease because the total surface of the membrane will become saturated with holes. We did not see this decrease in rate because the samples were degraded for only 6 days. The time required to saturate the surface with holes may be considerably longer than 6 days.

Looking at the shape of the holes that develop on either side of the membrane we see that they are markedly different. On the low acid side the holes appear circular and as they continue to degrade they remain circular. Conversely, on the strong acid side we see holes that are small and more random in shape with "channels" emanating from the hole along the polymer surface. The reason for the difference is not readily apparent. The holes on the high acid side may be from the holes on the lower acid side coming through the membrane to the other side. The mechanism for this is not obvious and requires further investigation.

Using the SEM we could also take a "peek" inside some of the larger holes in the membrane material. By looking in the holes we could establish that they did not perforate right through the material. The inside of each hole looked as if there were "off shoots" leading from the original hole to other areas inside the polymer matrix. The depth of the holes and length of the "off shoots" has not been determined. These "off shoots" may lead to the osmotic behaviour of the membrane at later stages of degradation.

Using the SEM it is impossible to determine where the hard and soft segments begin and end in the polymer. If we knew the position of these segments we might be able to determine which linkages are responsible for the degradation observed. If the hard segments were degrading we could conclude that the urea or urethane bonds were being cleaved. If it were the soft segment being degraded we could conclude it was the ether linkages being hydrolysed. This may explain why the holes start to form in certain positions along the

polymer surface. If for example it is the urethane or urea linkages that are being broken as other researchers have suggested, the holes may be forming only in hard segment regions on the polymer surface and vice versa for the soft segments (see diagram of polyurethane phase separation Chapter 1). The cleavage of polymer chains in the hard or soft segment region may lead to the segment becoming solubilized and from where it is subsequently eliminated from the polymer leaving a hole. Knowledge of the location of the hard and soft domains may provide insight into the identity of the bonds being broken.

7.12 GPC Analysis of the Degraded Membrane

The degradation of the membrane material is readily apparent using SEM analysis. If the degradation is due to the hydrolytic cleavage of the polymer chains then a decrease in the molecular weight of the polymer should be apparent[21]. To determine the molecular average molecular weight at different stages of the degradation we performed GPC analysis on a number of samples subjected to different conditions

Gel permeation chromatography was performed using a Waters™ linear Ultrastyragel Column (7.8 x 300 mm, part # 10681), with a Spectra Physics SP8700 HPLC system coupled with a Spectra Physics SP8450 UV/Vis detector. The variable-wavelength detector was set on 294 nm. The mobile phase was 100% HPLC grade THF at a flow rate of 1.0 mL/min and a pressure of 174 psi. To calibrate the column, ten molecular weight polystyrene standards were used. Each of the standards were prepared depending on the molecular weight of each standard. The appropriate %w/v was determined using Table 7-10. The standards were then dissolved in 10 mL of HPLC grade THF and dissolved over a period of hours with gentle agitation.

The effect of the applied acid gradient was tested using a modified Donnan dialysis cell. To examine whether physically restricting the membrane while it is subjected to the various conditions plays a part in the degradation process, membranes were also freely soaked in vials containing the same acid conditions as those in the cells.

After every 24 hours of exposure time one cell representing each of the conditions was halted by taking the membranes and rinsing them to neutrality with deionized water. The membranes were then dried by dabbing them with a paper towel and labelled accordingly. The membranes were then placed in a desiccator to dry thoroughly prior to GPC analysis. The exposure lengths and conditions for each of the samples are shown in Tables 7-11 and 7-12.

After exposure the samples that had a gradient of 5.0 HCl/0.1 M HCl were the only samples that appeared to have had some physical damage to them as shown by the change from clear and colourless to white and opaque. No physical change was noticed in any of the other samples including those that were freely soaked in 5.0 M acid solutions. We had expected to find a large change in the molecular weight distribution of the polymers where a change in physical appearance had been noticed. In fact, all of the samples had roughly the same elution volume and virtually identical curve shapes demonstrating that the average molecular weight did not change significantly. The molecular weight of the original material was established to be roughly 1.6×10^5 Daltons with an elution volume of 8.56 mL. All of the samples in this investigation were close to this same elution volume ($\pm$ 0 .1 mL). This was surprising because we had expected at least a slight change in the molecular weight distribution. The lack of change could be due to two factors: the number of polymer

Table 7-10. Preparation of molecular weight standards for GPC analysis

Molecular Weight	Concentration	Injection Volume
500 - 700,000	0.05 %	20 -200 µL
1,000,000 and above	0.01 %	20 -200 µL

Table 7-11. Gradient Exposure Conditions for the Membrane Material

Cell #	Gradient	Exposure Time	Observations
1	5.0MHCl/1.0MHCl	24 h	membrane cloudy
2	"	42 h	membrane cloudy/white
3	"	72 h	"
4	"	96 h	"
5	1.0MHCl/0.1MHCl	24 h	no change
6	"	42 h	--
7	"	72 h	--
8	"	96 h	--
9	5.0MHCl/5.0MHCl	24 h	no change
10	"	42 h	--
11	"	72 h	--
12	"	96 h	--
13	1.0MHCl/1.0MHCl	24 h	no change
14	"	42 h	--
15	"	72 h	--
16	"	96 h	--
17	0.1MHCl/0.1MHCl	24 h	no change
18	"	42 h	--
19	"	72 h	--
20	"	96 h	--

Table 7-12. Soaking Exposure Conditions for Membrane Material

Cell #	Soaking Medium	Exposure Time	Observations
1s	5.0 M HCl	24 h	no change
2s	"	42 h	"
3s	"	72 h	"
4s	"	96 h	"
5s	1.0 M HCl	24 h	no change
6s	"	42 h	"
7s	"	72 h	"
8s	"	96 h	"
9s	0.1 M HCl	24 h	no change
10s	"	42 h	"
11s	"	72 h	"
12s	"	96 h	"

chains hydrolysed was too small to detect (this factor might be elucidated by a longer term experiment to allow more of the polymer chains to be hydrolysed); the changes that are occurring to the polymer are not due to the hydrolysis of the polymer chains, but to another degradation process that does not effect the molecular weight of the polymer.

The fact that no observable physical change was noted for any of the polymer that had been soaked in acid (even those subjected to 5.0 M HCl) indicates that this particular polymer is quite resistant to hydrolysis. The physical changes that occur when the membrane has an acid gradient of 5.0M HCl /0.1M HCl applied across it are intriguing The cause of these physical changes should be investigated further by using other analytical techniques such as ESCA, ATR FT-IR and DSC. More than likely the polymer is being hydrolysed. Hydrolysis of polyurethanes has been extensively studied.

Hydrolysis in the most general sense, is the reaction of the polymer with water. This reaction can occur via several different mechanisms depending on the type of conditions and environment to which the polymer is exposed. In aqueous solution there are mainly two types of environments, acidic (pH < 7) and basic (pH > 7). In these two environments, degradation is due either to the reaction of H^+ (acidic solution) or the reaction of OH^- (basic solution) with the polymer because of the breaking of individual chemical bonds in the polymer. When enough of the bonds in a polymer are broken, the physical properties will change.

There are four types of bonds that are particularly susceptible to hydrolysis in polyurethanes. These are the ester, ether, urea, and urethane linkages. These bonds are shown in Figure 7-24.

Figure 7-24. Bonds and Linkages Susceptible to Hydrolysis

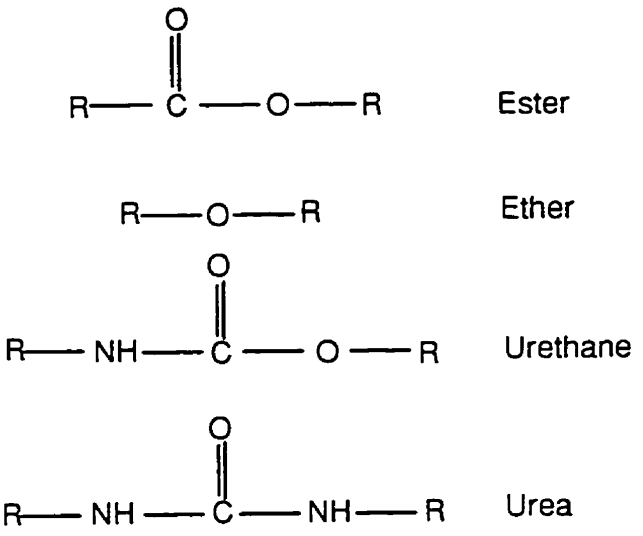

The hydrolytic cleavage of the ester, urea and urethane linkages is acid/base catalysed. In fact the degradation of the ester linkage is autocatalytic (ie. the reaction can start and then catalyze itself independent of the addition of a catalyst). The degradation of the ester linkage produces a carboxylic acid, which can then go on to catalyse the hydrolysis of other ester linkages. The urea and urethane linkages follow a similar mechanism but they are not autocatalytic as they require the presence of an acid or a base to initiate the catalytic process. In the presence of either harsh acid or base conditions, these reactions proceed quite rapidly leading to the failure of the polymer. The ether linkage is only susceptible to acid catalyzed hydrolysis and only in strong acid environments (> 1*M*). The hydrolysis of the ether follows a mechanism where the ether oxygen is first protonated. This is followed by an S$_N$1 reaction: the ether bond is first cleaved followed by nucleophilic attack on the carbocation by water which results in the formation of two alcohols.

The hydrolytic stability of the two major types of polyols has been ranked in a review by Schollenberger et al.[22] as ether > ester. Skrabal and Zahorka[23] determined the half life of diethyl ether in a strong acid (0.5 *M* H_2SO_4) solution to be 18.8 years. Originally, hydrolytic degradation of polyether type polyurethanes was thought to be caused by the hydrolysis and subsequent cleavage of the ether linkages. Recently, Chapman[24] found that the hydrolysis of the urethane linkage rather than the ether linkage was responsible for the degradation. This led to the stabilities of the possible sites for degradation to be ranked as follows:

ether > urea > urethane > ester

The hydrolytic degradation pathways described earlier lead to a decrease in the average molecular weight of the bulk polymer. When sufficient linkages are hydrolysed the bulk properties of the polymer such as tensile strength and elasticity begin to suffer and ultimately lead to the failure of the polymer.

7.13 Acid Transport Through The Membrane

During experiments studying the transport of metal complexes through a polyurethane ether-type membrane it was noticed that "free" acid is transported in addition to acid due to the metal complex (see Chapter 4). The acid transport is due to an acid gradient that is applied across the membrane material. In addition degradation only occurred when a gradient was applied across the membrane material. This prompted an investigation into the acid transport across the membrane material to determine if it played a role in the degradation of the polymer. Three different concentrations of acid (1.0, 2.0 and 5.0 M HCl) were placed in the starting cell along with deionised water in the receiving cell. The pH of the receiving cell was then monitored for several days. The results of these experiments are shown in Figure 7-25. With a concentration of 1.0 M HCl in the starting cell we did not observe any acid transport through the membrane as evidenced by no change in pH of the receiving cell solution. There was also no change in polymer appearance. A concentration of 2.0 M HCl in the starting cell leads to some acid transport and the polymer becomes slightly translucent in appearance. When using 5.0 M HCl in the starting cell we get much more acid transport accompanied by significantly more degradation. The results of these experiments suggest that acid transport plays a significant role in the degradation process.

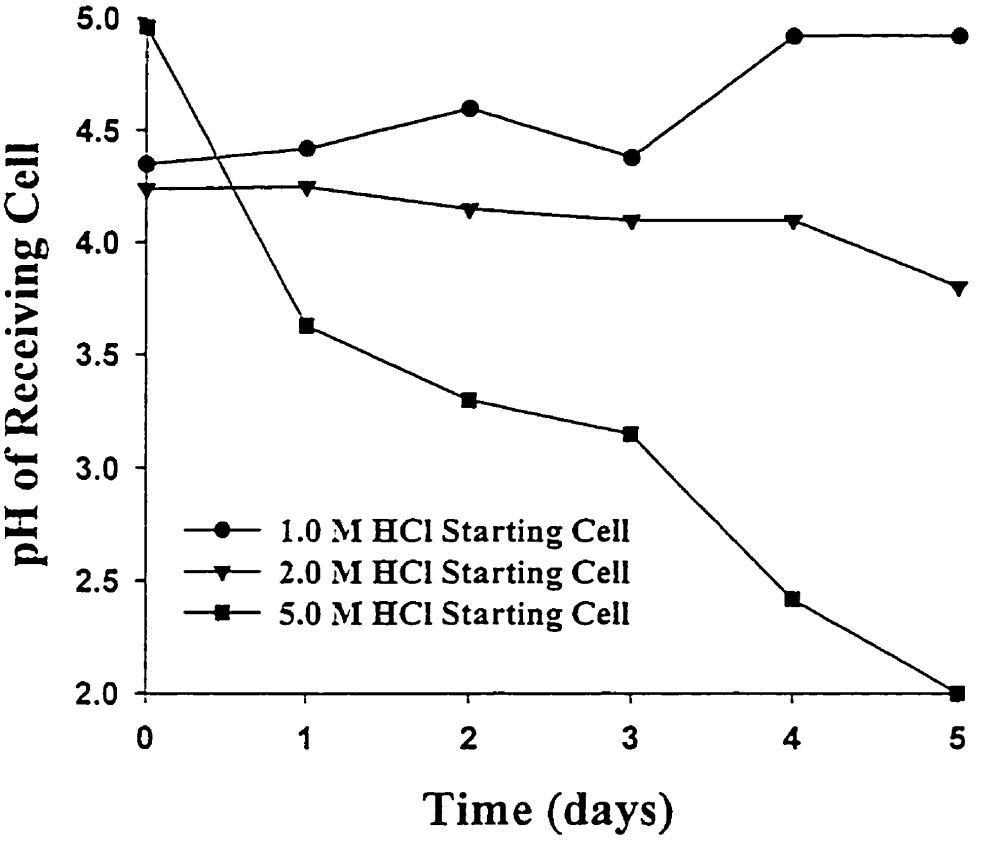

Figure 7-25. The transport of acid through a polyurethane ether-type membrane with different concentrations of HCl in the starting cell. Starting cell volume 650 mL and receiving cell volume 650 mL

7.14 Conclusion

The degradation of a polyether-type polyurethane by an acid gradient has been studied using several analytical techniques. The degradation of the membrane had the physical appearance of holes which were observed to increase in size and number with longer periods of degradation. The formation of holes was observed first on the side in contact with low acidity with observable holes being formed after only one day which we found surprising. Interestingly, the formation of holes on the high acid side did not occur until three days into the degradation experiment. The shape of the holes formed on the two sides of the membrane were markedly different.

The formation of holes in the membrane material only appeared when using high concentrations (i.e. 5.0 M) of HCl on one side of the membrane with low concentrations (i.e. 0.1 M) of HCl on the other side. Most membrane applications we have studied in this thesis required far less harsh conditions that did not lead to such extensive degradation.

The degradation of the membrane material caused an initially non-porous membrane to become porous and osmotic. This phenomenon has not yet been reported in the literature. The ability to develop a microporous polyurethane membrane may be attractive for other applications.

The degradation process is believed to be due to a combination of acid transport and hydrolysis, although the identity of the bonds being broken is questionable. Further investigation into the nature and mechanism of the degradation process is required not only

for our application, but for any situation where a polyurethane elastomer is used in a harsh chemical environment.

Figure 7-26. Summary of Hydrolysis Reactions

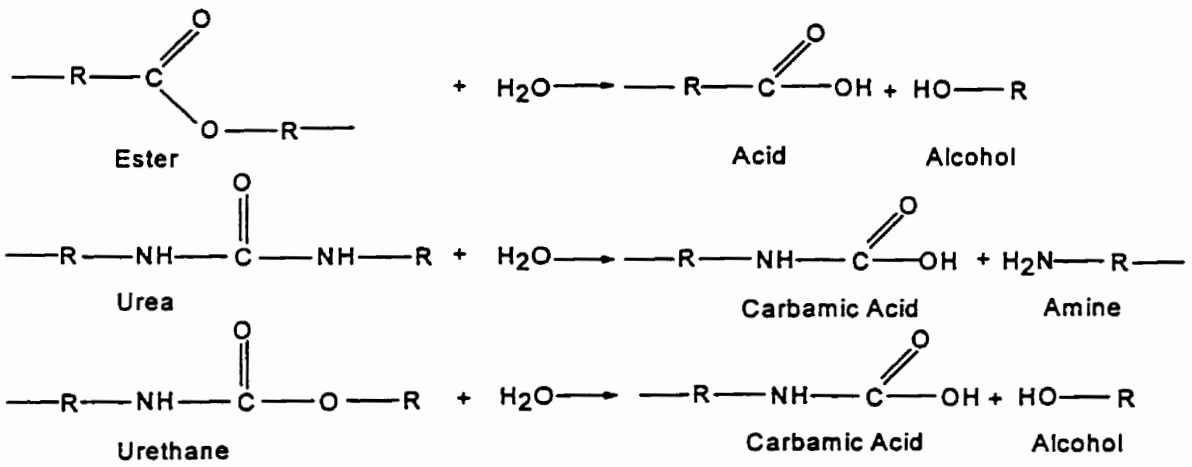

References for Chapter 7

1. W. Klopffer; Introduction to Polymer Spectroscopy, Chapter 7, Springer-Verlag, 1984.

2. K. Kole, P. Van Gheluwe; *J. Appl. Polym. Sci.*, 34 (1987) 395.

3. J. Lambert, H. Shurvell, D. Lightner, R. Cooks; Introduction to Organic Spectroscopy, Macmillan (1987).

4. W. Srichatrapimuk, S. Cooper; *J Macromol Sci Phys*, B15 (1978) 267.

5. M. Coleman, K. Lee, D. Skrovanek, P. Painter; *Macromolecules*, 19 (1986) 2149.

6. L. Bellamy; The Infra-red Spectra of Complex Molecules, London: Chapman & Hall. 1975.

7. Z. Zhang, M. King, R. Guidoin, M. Therrien, M. Pezolet, A. Adnot, P. Ukpabi. M. Vantal; *Biomaterials*, 15 (1994) 483.

8. W. Klopffer; Introduction to Polymer Spectroscopy, Chapter 2, Springer-Verlag, 1984.

9. H. Lin, K. Lewis, D. Leach-Scampavia, B. Ratner, S. Cooper; *J. Biomater. Sci. Polymer Edn.*, 4 (1993) 183.

10. B. Ratner, S. Yoon, N. Mateo; Polymer Surfaces and Interfaces, Chapter 12, John Wiley and Sons Ltd ,1987.

11. H. Allcock, F. Lampe; Contemporary Polymer Chemistry, Prentice Hall, 1990.

12. Z. Petrovic , J. Ferguson, *Prog. Polym; Sci.*, 16 (1991) 695.

13. J. Blackwell, M. Nagarajan, T. Hoitink; *Polymer*, 23 (1982) 950.

14. J. Blackwell, K. Gardner; *Polymer*, 20 (1979) 13.

15. A. Takahara, J. Tashita, T. Kajiyama, M. Takayanagi, W. MacKnight; *Polymer*, 26 (1985) 978.

16. A. Takahara, J. Tashita, T. Kajiyama, M. Takayanagi, W. MacKnight; *Polymer*, 26 (1985) 987.

17. V. Gajewski; *Rubberworld*, September (1990) 15.

18. H. Shintani, A. Nakamura; J. Appl. Polym. Sci., 42 (1991) 1979.

19. R. Oleschuk and A. Chow, Scanning Electon Microscope Data, presently unpublished.

20. W. Lemm , *Progress in Biomedical Engineering, Vol. 3 , Polyurethanes in Biomedical Engineering II ed.*,H. Planck, I. Syre, C. Egbers, Elsevier, 103, 1984.

21. D. Brown, R. Lowry, L. Smith; *Macromolecules*, Mar.-Apr. (1980) 248.

22. C. Schollenberger and F. Stewart," Thermoplastic polyurethane hydrolysis stability ", *J. Elastoplast.* 2 (1971) 28.

23. A. Skrabal and A. Zahorka; *Montash. Chem.*, 63 (1933) 1.

24. T . Chapman; *J. Polymer Sci.*, 27 (1989) 1993.

Chapter 8: Conclusions and Future Work

8.1 Extraction and Transport of Metal Complexes

Throughout this thesis we have demonstrated the use of polyurethane membrane materials for a number of metal extractions and separations. The extraction of the metal species was found to be dependent on several factors including the formation of the metal-ligand complex which can be used to facilitate separation. For example, we have performed the separation of gold from a mixture of gold and iron in solution using both a polyurethane ether-type membrane and an organically-impregnated filter (OIF). In each case both the iron and gold can form extractable complexes in an HBr solution but because the extractable gold complex forms at lower bromide concentration, we can control which species is extracted. The gold complex is extracted leaving the iron in solution. Another example involves the separation of platinum and palladium. The length of the time required to form the extractable thiocyanate complexes is vastly different. Palladium forms the extractable complex 10^5 times faster than does the platinum, thus the palladium is removed before the extractable platinum complex is formed, separating the metals.

In addition to the formation, the hydrophobicity/hydrophilicity of the metal-ligand complex plays an important role in the extraction process. We have shown that the larger, more hydrophobic complexes are more readily extracted than their more hydrophilic analogues. This was shown for the extraction of $HFeMX_4$ (where: X= Cl, Br) metal complexes. The ferric chloride ($HFeCl_4$) complex forms more readily than the ferric bromide ($HFeBr_4$) complex but the bromide complex is extracted/transported fives times as fast as the

chloride. Also when looking at the extraction/transport of the gold halide complexes the gold bromide ($HAuBr_4$) complex is extracted and transported twice as fast as the chloride ($HAuCl_4$) complex. This is also shown for the extraction of platinum and palladium thiocyanate. The platinum(IV) thiocyanate ($H_2Pt(SCN)_6$) complex is more readily extractable in to the polyTHF layer of the OIF than the palladium(II) thiocyanate $H_2Pd(SCN)_4$ complex. In each case it is the hydrophobic/hydrophillic character of the complex that dictates the rate at which the complex is extracted and ultimately transported, in addition to its ability to be formed.

Throughout the thesis we have shown that metal separations are possible using the polyurethane membrane material. Although the separations are not extremely fast they require very little energy to perform. In certain cases where the speed of a separation is not an issue then the membrane separation process may be well suited. In some cases more drastic conditions than were necessary for simply a separation were used to facilitate metal transport. For example the HBr conditions used for the majority of the gold experiments were larger than required. Stability constant data showed that the extractable gold complex forms at HBr concentrations much lower than 2.0 M. The lower amount of acid required makes the separation more attractive from both a cost and environmental standpoint. The separation of gold from gold ore demonstrated that the membrane can be used to separate gold from a complex matrix made up of a number of metals in concentrations much greater than that of gold.

During the membrane transport studies the separation conditions were not optimized to determine the maximum rate of that could be achieved. With proper alterations to the

procedure the length of time required may be significantly reduced. Optimizing the temperature, membrane thickness, stirring rate and the type of metal complex as well as using a more favorable membrane configuration (ie. larger surface area) should increase the rate of separation substantially. More work is needed in this area to fully determine the potential of the separation process.

The rate-determining step of the membrane separation process was determined to be the diffusion of the metal species through the membrane following extraction. Utilizing the fact that the extraction is due to the PTMG portions of the polymer material, a supported liquid membrane (see Chapter 1) could be prepared with PTMG as the liquid membrane phase. The use of a liquid phase would provide a significant increase in the rate of transport through the membrane because of faster diffusion rates within liquid membranes compared to solid membranes. The use of glycols in SLM applications has recently been reported[1] for the separation of organic compounds.

8.2 Membrane Degradation

The degradation of the polyurethane ether-type membrane during the study of the transport of iron halides led to further studies on the nature of the degradation. The degradation was shown only to occur when an acid gradient was applied to it and not when the membrane was just soaked in high acid concentrations. In addition, the membrane did not degrade as significantly at acid gradients lower than 3 M HCl/0.1M HCl. The degradation process caused an initially non-porous material to become porous and osmotic. The membrane degrades when it is exposed to an acid gradient of 5.0 M on one side and 0.1 M

on the other side but does not degrade when soaked in either of the solutions alone. Surprisingly the holes created by the degradation process form on the low acid side after two days of exposure and appear only after 5 days of exposure on the high acid side. From our study we have determined that the degradation is probably due to a combination of the high acid conditions and the transport of acid through the membrane material.

8.3 Other Analytical Applications of PolyTHF and Polyurethane Membrane Materials

8.3.1 Use of PolyTHF as a Stationary Phase for Column Chromatography

PolyTHF has been used a solid phase extractant for gold bromide as well as platinum and palladium thiocyanate complexes. The utility of the polyTHF suggests its use as a stationary phase for column chromatography and HPLC. We have performed some initial experiments coating Chromosorb G non-acid washed packing material with polyTHF molecular weight 4000. The resulting particles were packed into a glass column and tested by running solutions of gold, platinum and palladium in their extractable forms through the column. Preliminary experiments suggested that the stationary phase could be used to separate metals based on the affinity of the metal for the stationary phase and the pH of the solution. The metal complexes when protonated were sorbed to the column material. By then running successively higher pH eluents through the column the metals are eluted in the order of increasing proton affinity. Preliminary results suggest that this material may be well suited

as a stationary phase for column chromatography and HPLC but continued research is necessary to determine its potential.

8.3.2 Use of a Polyurethane Ether-type Membrane as a Sample Support for MALDI-MS

In addition to the uses of the membrane for the separation and isolation of metals we have found that the membrane material is useful for another analytical application. In a project initiated by myself and Mark McComb of Professor Hélène Perreault's research laboratory, we investigated the use of a polyurethane membrane as a sample support for matrix assisted laser desorption ionization mass spectrometry (MALDI-MS). MALDI-MS[2,3,4] provides a rapid means of determining the molecular weight of proteins and peptides. The method involves ablating a sample of protein co-crystallized with a matrix, such as sinnipinic acid, resulting in the formation of singly and doubly charged protein ions. The molecular weight of the ions can then be measured by a time-of-flight mass spectrometric detector. One difficulty with using MALDI for the analysis of high molecular weight compounds is that the technique is affected by the amount of impurities in a sample. Impurities lead to the development of adducts in the mass spectrum and can suppress the MALDI process. Several methods have been developed for the preparation of MALDI samples to remove impurities including chromatography and dialysis methods[5]. Both methods are time consuming and require MALDI samples to be transported to the laboratory by conventional means (ie. in solution and on ice).

The use of membrane supports has recently been adopted for both sample preparation and delivery into the mass spectrometer. There have been several different membranes

investigated in the literature including: poly(vinylidene difluoride)[6,7], (PVDF); nitocellulose[8]; and polyether[9].

During membrane sample preparation methods the protein is adsorbed to a hydrophobic membrane material and can then be inserted into the mass spectrometer. In addition the membrane allows the incorporation of a washing step into the sample preparation protocol. The membrane can be washed removing the hydrophilic impurities within the sample. Preliminary experiments performed with the polyurethane membrane showed that the membrane was effective for MALDI-MS analysis. Further investigations yielded that use of the membrane provided sensitivity equivalent to the metal target. Comparing the polyurethane membrane to PVDF showed that the sensitivity with the polyurethane membrane was much improved. This improved sensitivity was in part attributed to the non-porous nature of the polyurethane membrane material and its ability to bind protein less strongly than PVDF. Spectra showing the comparison of the metal target, PVDF membrane and polyurethane membrane is shown in Figure 8-1. The figure shows the MALDI-MS spectrum of bovine insulin on three different sample supports. The membrane showed greater sensitivity than the PVDF target and equivalent sensitivity to the silver target. Also, once the protein was adsorbed onto the membrane it was stable in excess of one month[10].

Protein digests were also performed directly on the membrane and the resulting protein fragments then analyzed by MALDI-MS. Recently the use of the polyurethane membrane material for MALDI-MS has been undertaken by another research group in the Department of Chemistry for routine protein analysis.

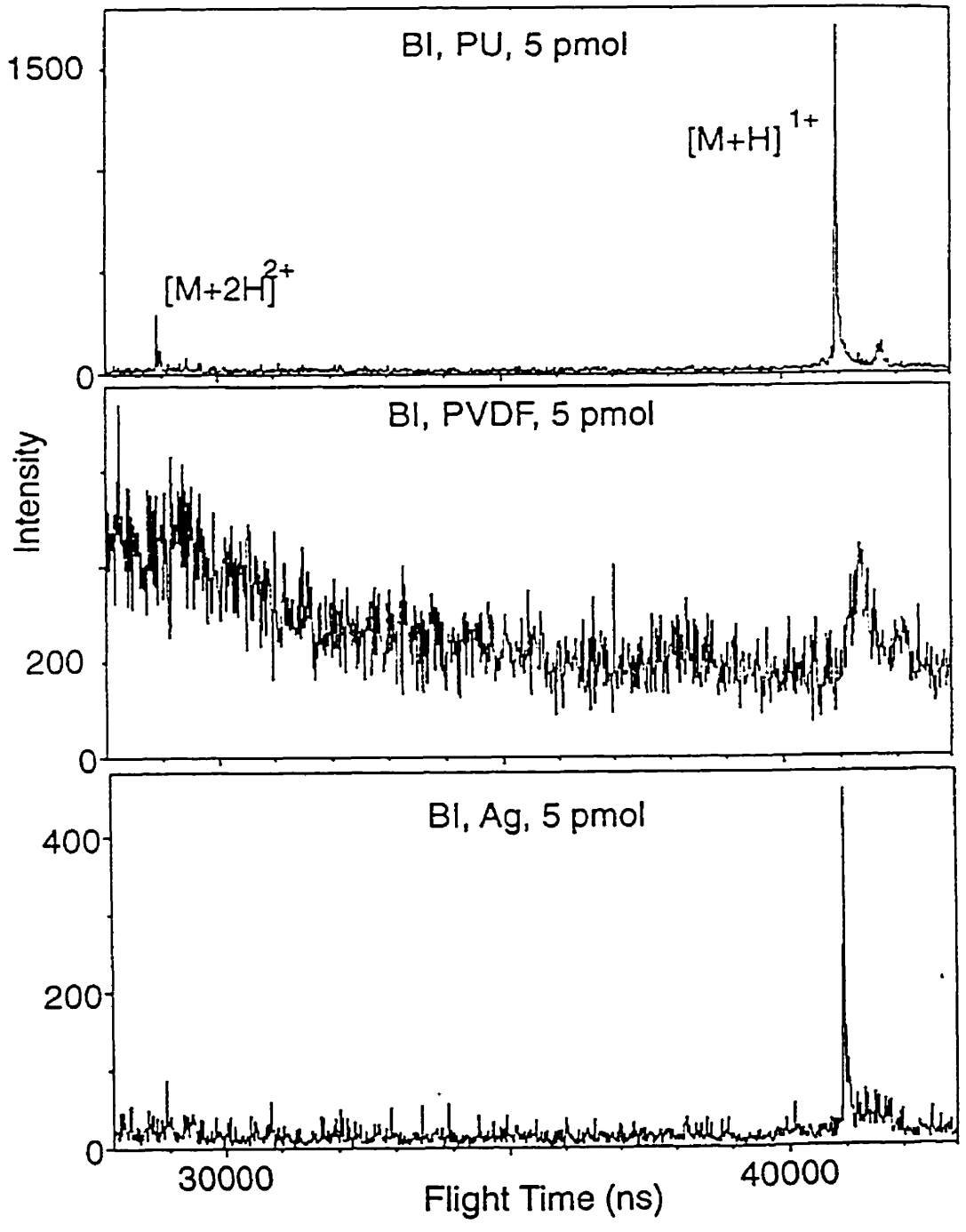

Figure 8-1. Comparison between using polyurethane, PVDF and silver targets for MALDI-MS. Spectra are of 5 picomoles of bovine insulin (M.W. 5733).

We have continued to research the use of polyurethane for a variety of novel MALDI-MS applications. Polyurethane has been shown to bind both hemoglobin and plasma proteins from blood. Following adsorption, these proteins can then be analyzed by MALDI-MS with the possibility of characterizing protein abnormalities. A patent[11] is currently being sought for the use of a non-porous polyurethane membrane material for blood analysis by MALDI-MS. In addition we have initiated a research project with Dr. M. King at the Institut des Biomateriaux in Quebec city for the direct analysis of proteins adsorbed onto bio-implant devices. Polyurethanes have been used as materials for bio-implants for a number of years. Surfaces of medical devices made of biomaterials such as polyurethane are often susceptible to protein sorption which may initiate a physiological response and the eventual degradation or rejection on an implanted material. The determination of protein sorption has typically involved the in-vitro study of protein binding using radio-labeled proteins. This method is sensitive but can only be used in a single component system. Our initial studies using polyurethane for MALDI-MS demonstrate that the direct analysis of a bio-implanted device should be possible offering several advantages over conventional analysis techniques. MALDI-MS does not require the proteins to be radio-labeled which enables the analysis of sample that we exposed in vivo. In addition MALDI-MS is not limited to analyzing only one component at a time, as the technique allows the routine determination of protein mixtures.

The use of polyurethane as a sample support has been shown to be effective for MALDI-MS. Future work will include the use of the polyurethane membrane for the analysis of whole blood and blood components in addition to proteins adsorbed to biomedical implant devices.

References for Chapter 8

1. Ho, S.; Sheridan, P; Krupetsky, E; *J.Membr. Sci.*, 112 (1996) 13.

2. M. Karas, U. Bahr, U. Giessman, *Mass Spectrom. Rev.*, 10 (1991) 335.

3. F. Hillenkamp, M. Karas; *Meth. Enzym.*, 193 (1990) 280.

4. E. J. Zaluzec, D. A. Gage, J. Watson, *Prot. Exp. Purification*, 6 (1995) 109.

5. M. Kussmann, E. Nordhoff, H. Rahebeb-Nielson, S. Haebel, M. Rossel-Larson, L. Jakobsen, J. Gobom, E. Mirgorodskaya, A. Kroll-Krisensen, L. Palm, P. Roepstorff; *J. Mass Spectrom.*, 32 (1997) 593.

6. M. Vestling, C. Fenselau; *Anal. Chem.*, 66 (1994) 4371.

7. K. Strupat, M. Karas, F. Hillenkamp; *Anal Chem.*, 66 (1994) 464.

8. Y. Liu, J. Bai, D. Lubman, *Anal. Chem.*, 67 (1995) 3482.

9. J. Blackledge, A. Alexander, *Anal. Chem.*, 67 (1995) 843.

10. M. E. McComb, R. D. Oleschuk, D. M. Manley, L. Donald, A. Chow, J. O'Neil, W. Ens, K. G. Standing and H. Perreault, *Rapid Communications in Mass Spectrometry*, 11 (1997) 1716-1722.

11. M. McComb, R. Oleschuk, D.Manley, L. Donald, H. Duckworth, A. Chow, J. O'Neil, W. Ens, K. Standing, H. Perreault, Use of Polyurethane for MALDI-TOFMS Analysis of Whole Blood, Patent Application (1998).

IMAGE EVALUATION
TEST TARGET (QA-3)

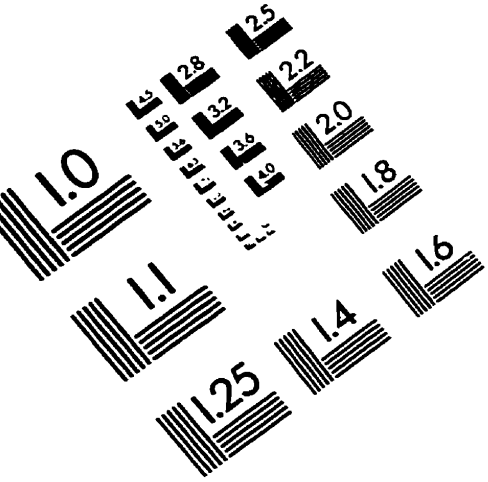

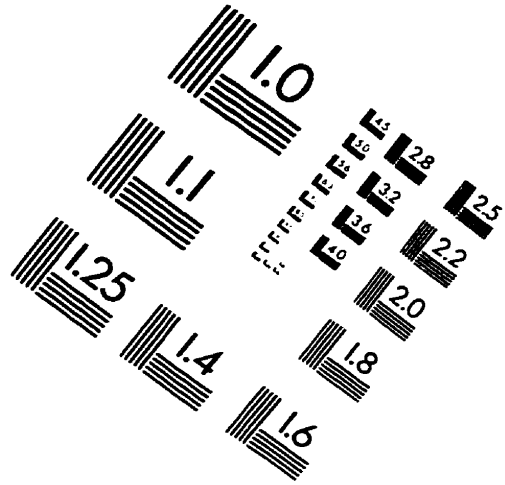

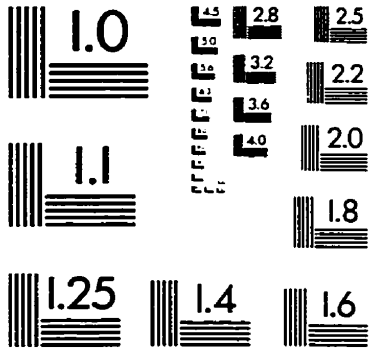

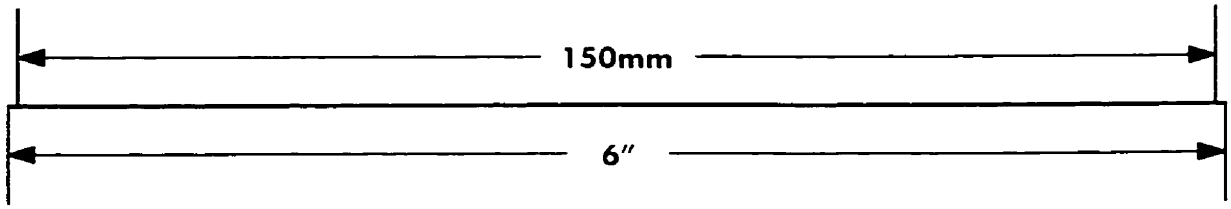

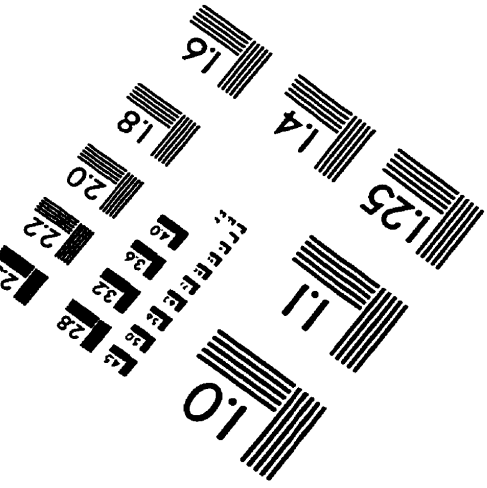

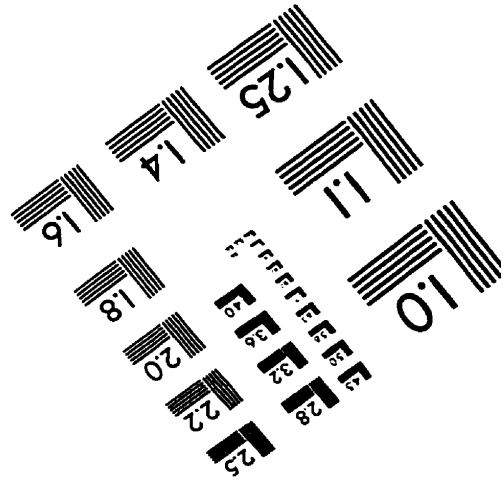

APPLIED IMAGE, Inc
1653 East Main Street
Rochester, NY 14609 USA
Phone: 716/482-0300
Fax: 716/288-5989